

AD-A112 533

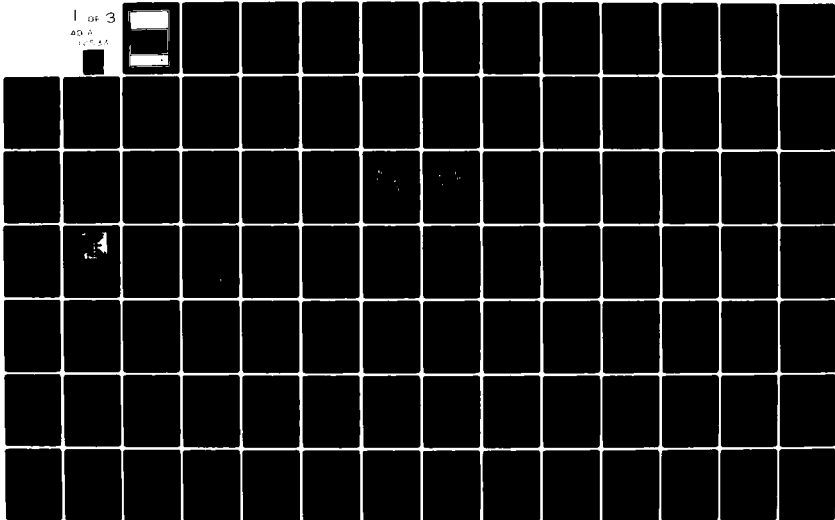
ADVISORY GROUP FOR AEROSPACE RESEARCH AND DEVELOPMENT--ETC F/6 1/3
DYNAMIC ENVIRONMENTAL QUALIFICATION TECHNIQUES.(U)
DEC 81

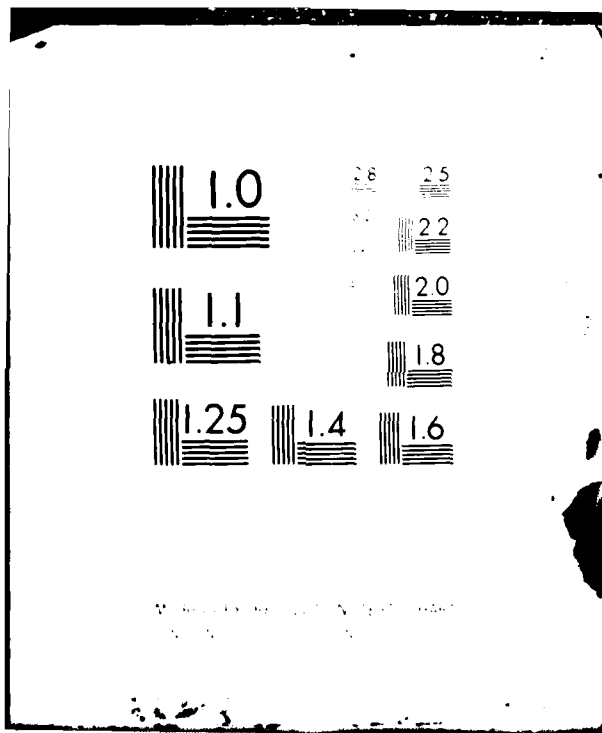
UNCLASSIFIED

AGARD-CP-318

NL

1 OF 3
40 A
1/1/81





Resolution Test Chart
1.0 1.1 1.25 1.4 1.6 1.8 2.0 2.2 2.5 2.8



AGARD-CP-318

AGARD-CP-318

AGARD

ADVISORY GROUP FOR AEROSPACE RESEARCH & DEVELOPMENT

7 RUE ANCELLE 92200 NEUILLY SUR SEINE FRANCE

AGARD CONFERENCE PROCEEDINGS No. 318

Dynamic Environmental Qualification Techniques

A

NORTH ATLANTIC TREATY ORGANIZATION



DISTRIBUTION AND AVAILABILITY
ON BACK COVER

82 03 26 007

DTIC FILE COPY
14-2590

NORTH ATLANTIC TREATY ORGANIZATION
ADVISORY GROUP FOR AEROSPACE RESEARCH AND DEVELOPMENT
(ORGANISATION DU TRAITE DE L'ATLANTIQUE NORD)

AGARD Conference Proceedings No.318
DYNAMIC ENVIRONMENTAL QUALIFICATION TECHNIQUES

A

Papers presented at the 53rd Meeting of the AGARD Structures and Materials Panel
in Noordwijkerhout, the Netherlands on 27 September-2 October 1981.

THE MISSION OF AGARD

The mission of AGARD is to bring together the leading personalities of the NATO nations in the fields of science and technology relating to aerospace for the following purposes:

- Exchanging of scientific and technical information;
- Continuously stimulating advances in the aerospace sciences relevant to strengthening the common defence posture;
- Improving the co-operation among member nations in aerospace research and development;
- Providing scientific and technical advice and assistance to the North Atlantic Military Committee in the field of aerospace research and development;
- Rendering scientific and technical assistance, as requested, to other NATO bodies and to member nations in connection with research and development problems in the aerospace field;
- Providing assistance to member nations for the purpose of increasing their scientific and technical potential;
- Recommending effective ways for the member nations to use their research and development capabilities for the common benefit of the NATO community.

The highest authority within AGARD is the National Delegates Board consisting of officially appointed senior representatives from each member nation. The mission of AGARD is carried out through the Panels which are composed of experts appointed by the National Delegates, the Consultant and Exchange Programme and the Aerospace Applications Studies Programme. The results of AGARD work are reported to the member nations and the NATO Authorities through the AGARD series of publications of which this is one.

Participation in AGARD activities is by invitation only and is normally limited to citizens of the NATO nations.

The content of this publication has been reproduced directly from material supplied by AGARD or the authors.

Published December 1981

Copyright © AGARD 1981
All Rights Reserved

ISBN 92-835-0306-6



Printed by *Technical Editing and Reproduction Ltd*
Harford House, 7-9 Charlotte St, London, W1P 1HD

PREFACE

For the proof of the safety and reliability of modern aircraft with respect to the effects of natural and induced dynamic environments peculiar to military operations and requirements, numerous dynamic qualification test methods have been established. It was the purpose of this Specialists' Meeting

- To review the state of the art of dynamic qualification techniques and test methods presently applied for military aircraft and helicopters, particularly when carrying external stores;
- To exchange technical information in this field between all AGARD countries;
- To review the background and intentions of related Military Standards publications;
- To try to formulate a common basis for dynamic structural requirements and substantiation procedures.

The Specialists' Meeting revealed that considerable progress has been made on this subject in recent years. Thus a general review is quite overdue. However, the way in which new findings can be brought together in improved standards remained an open question and deserves further common activities.

H.FORSCHING
Chairman, Sub-Committee on
Dynamic Environmental
Qualification Techniques

CONTENTS

	Page
PREFACE by H.Försching	iii
	Reference
<u>SESSION I – OVERVIEWS</u>	
DEVELOPMENT AND USE OF DYNAMIC QUALIFICATION STANDARDS FOR AIR FORCE STORES by A.H.Burkhard and O.F.Maurer	1
PROBLEMS IN THE GROUND SIMULATION OF DYNAMIC RESPONSES INDUCED IN EXTERNALLY CARRIED STORES DURING FLIGHT by J.Homfray	2
PROGRES DANS L'ELABORATION DES PROGRAMMES D'ESSAIS D'ENVIRONNEMENT MECANIQUE par M.Coquelet	3
QUALIFICATION OF EQUIPMENT FOR GUNFIRE INDUCED VIBRATION by A.Peacock	4
<u>SESSION II – APPLICATIONS – Part 1</u>	
DYNAMIC QUALIFICATION TESTING OF F-16 EQUIPMENT by H.E.Nevius and W.J.Brignac	5
DEVELOPMENT OF VIBRATION QUALIFICATION TEST SPECTRA FOR THE F-15 AIRCRAFT by G.R.Waymon	6
EQUIPMENT VIBRATION QUALIFICATION FOR HARRIER AND HAWK AIRCRAFT by D.C.Thorby	7
ACOUSTIC NOISE TEST AS PART OF THE DYNAMIC QUALIFICATION PROGRAM IN AEROSPACE by G.Bayerdörfer	8
<u>SESSION III – APPLICATIONS – Part 2</u>	
VIBRATION QUALIFICATION OF EXTERNAL AIRCRAFT STORES AND EQUIPMENT by M.Steininger and G.Haidl	9
AIRCRAFT FUEL TANK SLOSH AND VIBRATION TEST by H.Zimmermann	10
<u>SESSION IV – HELICOPTER</u>	
THE STRUCTURAL DYNAMIC INTERFACE REQUIRED FOR DEVELOPING HELICOPTER TARGET ACQUISITION SYSTEMS by S.T.Crews	11
APPROACH IN DYNAMIC QUALIFICATION OF LIGHT HELICOPTER STORES AND EQUIPMENTS by D.Braun and J.Stoppel	12
THE DYNAMIC QUALIFICATION OF EQUIPMENT AND EXTERNAL STORES FOR USE WITH ROTARY WINGED AIRCRAFT by G.M.Venn	13

SESSION V – DEVELOPMENT

APPLICATION OF MODAL SYNTHESIS TECHNIQUES FOR THE DYNAMIC QUALIFICATION OF WINGS WITH STORES by E.Breitbach	14
STOL AIRCRAFT STRUCTURAL VIBRATION PREDICTION FROM ACOUSTIC EXCITATION by B.F.Dotson and J.Pearson	15
GUNFIRE BLAST PRESSURE PREDICTIONS by R.Munt, A.J.Perry and S.A.Moorse	16
DEVELOPMENT OF A TAPED RANDOM VIBRATION TECHNIQUE FOR ACCEPTANCE TESTING by J.Devitt, R.Pokallus, J.Popolo and E.Baird	17

DEVELOPMENT AND USE OF DYNAMIC QUALIFICATION
STANDARDS FOR AIR FORCE STORES

by

ALAN H. BURKHARD
Combined Environments Test Group
Wright Aeronautical Laboratories
AFWAL/FIEE Wright-Patterson AFB OH 45433

OTTO F. MAURER
Structural Vibration Branch
Wright Aeronautical Laboratories
AFWAL/FIBG Wright-Patterson AFB OH 45433

INTRODUCTION

The Cataloging and Standardization Act, (originally enacted by the U.S. Congress in 1952), requires the achievement of the highest practicable degree in the standardization of items, materials and engineering practices within the Department of Defense. This legislation was implemented by the Department through the Defense Standardization and Specification Program (DSSP) [1] which formed the basis for the procedural process and application of most of the presently applicable Military Specifications and Standards. Military Specifications existed before this legislation and its implementation, however formal procedures were now available for generating, updating and utilizing these documents.

At this point it may be the time to introduce some definitions of terms as they are delineated in Reference 1. In this connection, a standard is described as "A document that established engineering and technical requirements for processes, procedures, practices and methods that have been adopted as a standard. Standards may also establish requirements for selection, application and design criteria for material". A specification is delineated as -- "A document prepared specifically to support acquisition which clearly and accurately describes the essential technical requirements for purchased material. Procedures necessary to determine that the requirements for the purchased material covered by the specification have been met shall be included".

The advantages of this standardization are obvious in that it leads to simplification of the procurement, development, and production processes by fostering uniformity, direct comparability, interchangeability of the standardized objects and procedures and a concomitant reduction in acquisition and maintenance costs. On the other hand, standardization may lead to stagnation of technological progress if standards are not continuously revised, updated or replaced or if existing standards are interpreted and applied in a rigid manner. The latter consideration under certain conditions may even negate some of the advantages expected from standardization. This is particularly true with respect to acceptance and qualification testing. Recognition of this fact has paved the way in which qualification test standards are now being perceived and utilized.

Traditionally, a procedure or test method contained in a standard was considered the only way to accomplish the desired test. The test standards were considered the "Tester's Bible". If it is in the standard, it must be right or there is some valid reason why it is done this way.

When test standards are viewed in this manner, their procedures become dogmatic. In this environment, common sense, cost effectiveness, and good engineering practice are ignored and the consideration of passing the test becomes paramount. The reasons for, or the technical objective of the test become secondary or are disregarded. The technical discipline of test engineering becomes pejorated to selecting a curve from a figure and conducting a test by rote.

This was the climate which still prevailed in the 1960's even though some test standards contained abrogative statements as for example MIL-STD-810 [2] carried the following sentence on page one:

"When it is known that the equipment will encounter conditions more severe or less severe than the environmental levels stated herein, the test may be modified by the equipment specification."

The obvious question is why did the qualification testing standard evolve in this manner? To answer this question, the state-of-the-art of test techniques and procedures has to be considered.

HISTORICAL PERSPECTIVE

Prior to 1940, environmental testing as we know it today was practically non-existent. With World War II came the requirement for world wide operations under a wide variety of environmental conditions. There were few standard procedures for performing tests and most testing within the Army Air Corps or its successor the Air Force was done at Wright Field, Ohio (now called Wright-Patterson Air Force Base). As the workload increased, especially for qualification of new equipments, Wright Field

began to assign tests to industry. Almost immediately, industry laboratories performing tests in accordance with the multitude of military individual equipment specifications were faced with varying requirements for the same type test and inconsistencies in specifying like requirements from one test program to the next [3].

The lack of uniformity in test programs and the lack of knowledgeable and experienced environmental personnel in industry resulted in a need for the issuance of written standard test methods. The test methods included in such documents were those test levels and techniques that seemed to accomplish their intended purpose with the available test equipments. War time priorities resulted in giving little consideration if a test level or method was cost effective or caused equipments to be over-designed for environmental effects.

A prime example is the much assaulted temperature -51°C (-65°F). Worldwide weather does show that the probability of occurrence of surface air temperature below -51°C is quite low [4]. Likewise, there is historical information accumulated over many years found in cold weather testing, that if equipment could withstand and operate under -51°C air temperature, it would be suitable for arctic usage.

The key thought is suitability for arctic usage. The arctic environment is not always -51°C and at times it can be even colder. Even so it was found that those equipment that satisfactorily passed a -51°C laboratory test would perform adequately in the arctic environment. Thus, the requirement for -51°C was stated in military requirement documents.

Under dates of 14 and 22 March 1943, the Director of Military Requirements stated [5]:

"...in the future all combat aircraft and cargo airplanes, C-60 or larger, for the Army Air Force (AAF) will be so constructed that all parts thereof will function normally at all temperatures down to -65°F outside air temperature...the Material Command would be held responsible that all such aircraft produced would be capable of operating under extreme conditions of cold temperatures of -65°F ... thus, -51°C (-65°F) was written into almost every environmental design and test specification.

The institutionalization of this low temperature limit is typical of most environmental test conditions including vibration tests. Technical judgments made under or during war time conditions were promulgated and became the way to test. This was natural because the test conditions were familiar to the technical community. Why change something that works?

Unfortunately, since the technical judgments which formed the basis for environmental testing were made during a war time environment, cost and technical effectiveness of such testing were not seriously considered. The judgments were focused on how to rapidly evaluate equipment items so they could be quickly deployed to the field. Cost of testing and how much overdesign was precipitated by the selected approaches were not seriously considered.

Another contributor to this problem is that once a test method appears in the standard, specialized facilities are developed to perform that test. Because these facilities exist, there is a propensity to perpetuate these test methods. Thus, there develops an inertia to any change in test method.

Over the past 20 years, the cost of operating and maintaining equipment in the field has been growing to where it is an unacceptable percentage of the entire Department of Defense budget [6, 7]. Because specifications and standards were perceived as causing poor performance, goldplating, delivery delays, or excessive costs, a study task force examined specifications and standards [8]. It was found, that instead of a problem with a specification per se it was misinterpretation or misapplication.

"In general, the documents contain much more flexibility than appears to be used in practice. Most of the instances of 'excessive cost' examined by the Task Force resulted from a failure to utilize this flexibility in a reasonable way, rather than a fundamental problem with the specification itself."

A detailed study of one aircraft found that over 50 percent of equipment field failures were environmentally induced by those environmental stresses included in an environmental qualification testing program [9]. Furthermore, 55 percent of the equipment studied had failure modes that could be correlated with test level waivers, deviations or complete elimination of a test.

What appeared to have occurred was a climate developed in which it was perceived that standards were overly conservative, therefore waivers, deviations and the elimination of requirements were routinely approved. The net result of this climate was that testing lost credibility and many equipments were not effectively evaluated for the real field conditions. As a result, equipment performance degraded and maintenance costs increased. The situation became so acute during 1965-1970 that a major effort was initiated to understand and hopefully reduce these problems for externally carried stores.

EXTERNALLY CARRIED STORES

In order to approach the actual subject of this presentation, it is considered opportune at this point to mention that there exists no unified standardization of structural store testing, neither static nor for that matter dynamic. The main reason for this can be found in the large diversity of devices which are summarized under the designation of stores and which range from fuel tanks, to bombs, air-launched missiles, ECM pods, dispensers, etc. Requirements for dynamic or vibration design criteria and tests are distributed throughout several Military Specifications and Standards. The major specifications and standards directed toward stores are given in Reference [10] through [13]. While Reference [10] (MIL-A-8591F) is an up-to-date documentation of general criteria applicable to the design, test and development of airborne stores, in contrast Reference [11] (MIL-T-7378A) (USAF) which establishes requirements for External Fuel Tanks, has been revised last in 1958 and must be considered obsolete by the technology of today, particularly in its dynamic test requirements. This specification, regardless of the structural dynamic properties of a tank, required a sinusoidal vibration test to be conducted at a frequency of $2000 \pm 0, -6$, cycles per minute. Reference [12] (MIL-T-7743E) is a test specification for store suspension and release equipment and the requirements of its current version concerning vibration qualification, to some extent parallels those of an older issue of Reference [2] (MIL-STD-810). Environmental criteria for Air Launched Weapons are given in Reference [13] (MIL-STD-1670) which is intended to provide a method for the definition of the total service environment and its translation into design and qualification criteria. This standard also refers frequently to MIL-STD-810 for environmental data and excitation and vibration level calculation techniques. From the frequent citation of MIL-STD-810 in store testing, it can be inferred that it assumes a central role in the environmental qualification of stores. Although this test standard is basically intended for application to military aircraft equipment only, its role appears to have expanded to include also structural implications. This seems to be confirmed by the introductory sentence to store vibration testing:

"This vibration test is performed to determine that the assembled store as a system is constructed to withstand and perform in the expected dynamic environment".

However, if the store system is considered as a piece of aircraft equipment, the structural dynamic implication is partially reconciled and the store structure for dynamic qualification purposes can be considered separate from the aircraft. For aeroelastic qualification, panel flutter excluded, the store still will have to be considered within the compound of the aircraft structure. Because of this importance of MIL-STD-810 for store qualification, the development and application of this aspect of the standard will be discussed in the rest of this paper.

In the past, the recommended procedure for vibration testing of an assembled externally carried aircraft store was to suspend and vibrate the entire store via its normal mounting lugs. The vibration levels were usually specified in terms of 5 to 10G sinusoidal input. Both resonance dwells and sinusoidal sweeps were employed [15].

This type of vibration test had the testing levels specified in terms of an input, so it is commonly called a controlled input test. The input vibration levels are rigidly established regardless of how the store responds. The response of the whole store at its natural frequencies can be several times the input levels. The large amplitude of store vibration associated with a controlled input test has caused numerous failures in the laboratory which do not occur in the field, and vice versa [14].

A controlled input test on large stores requires the development of significant dynamic forces for the 5 or 10G input levels. Elaborate fixtures have been built for the express purpose of testing assembled stores to these levels [16]. The cost of these large fixtures for a controlled input assembled store vibration test usually is prohibitive, so only a few facilities have built such equipment.

To improve the realism in the assembled store vibration test, necessitates an understanding of the dynamic environment to which a store is exposed in captive flight. Dreher, Lakin, and Tolle [14] have extensively analyzed the captive flight environment of externally carried aircraft stores. They found that the store vibration environment was basically random over the entire frequency range and was primarily caused by two distinct sources -- aerodynamic effects (turbulent boundary layer, buffeting, etc.) and aircraft motion (maneuvers, ground roughness during take-off, air gusts).

The aerodynamic effects cause random pressure fluctuations on the surface of the store. The surface panels of the store are randomly excited but respond most at their natural frequencies. The surface panels, in turn, excite the internal structure and equipment in a store. Therefore, the aerodynamically induced captive flight vibration response of a store is a function of the surface panel's acceptance of the forcing environment, mass distribution, and the structure's mechanical impedance. Aerodynamically excited store vibrations tend to be in the higher frequency range since the structure of a store is driven by the store surface panels which have their natural frequencies in the higher frequency range.

Aircraft motion excites the store through its lugs since they are the primary physical interface between an aircraft and a store. Typical store suspension equipment tends to have low natural frequencies so that a store is effectively isolated from the aircraft in terms of higher frequency vibrations [17].

These revelations by this extensive analysis of the captive flight vibration response of a store resulted in the reformulation of thinking about the nature of assembled store testing. It was concluded that the assembled store test should be in terms of random instead of sinusoidal vibration, and another or new testing procedure is required since all significant store vibration does not occur at those frequencies associated with the fundamental modes of the whole store.

DUAL ENVIRONMENT TEST CRITERIA

The analysis of measured flight data clearly showed that two distinct sources of vibration existed for externally carried aircraft stores. Thus, it was proposed that a realistic assembled store vibration test should utilize acoustic noise for higher frequencies of vibration and a vibration shaker for the lower frequencies [16]. This approach was quite novel so that experimental programs were proposed to identify the limits of this approach.

Measured captive flight data was collected on 30 different stores. This data was analyzed to determine a prediction criteria for the store vibration environment [17]. Six of these instrumented stores were positioned in a reverberant acoustic chamber. The acoustic chamber conditions were adjusted until the store responded in the higher frequency range to the measured captive flight vibration environment [18].

Three of the six stores used in acoustic evaluation were used to evaluate vibration shaker techniques for assembled store testing. Two test techniques were evaluated. One approach was to hold and excite the store via its normal mounting lugs. The other approach was to suspend the store by its normal mounting lugs off a low frequency isolation system. Vibration excitation is applied via a mechanical connection to the store at an appropriate location.

It was found that in general a vibration shaker could not practically excite the entire frequency range of interest. Therefore, vibration shaker testing was only recommended for simulation of a portion of the entire store vibration spectrum. To properly control such an assembled store test, it was found desirable to use a controlled response approach. The controlled response approach is to specify the test requirement in terms of the level and spectrum the test item must be vibrated to rather than the level and spectrum to be inputted to the test article.

In general, it was found that both acoustic and shaker vibration testing techniques were necessary to have realistic assembled stores vibration testing [18]. The shaker covered frequencies where an acoustic test was ineffective and vice versa. Therefore, a dual environment test is recommended in MIL-STD-810C. This approach has been used on several recent store programs [19, 20].

Currently, the only vibration test for localized acoustic effects is the proposed cavity resonance test to be in MIL-STD-810D.

STORE CAVITY RESONANCE

Many stores are used as dispensers which have open cavities that are exposed to the air stream. Such cavities can have intense acoustic standing waves which result in very intense but highly localized acoustic noise. Extensive windtunnel and flight test measurements of this phenomenon for typical store cavity conditions have been made [23, 24]. MIL-STD-810D will include a recommended test for this condition using sinusoidal acoustic excitation.

INTERMITTENT DYNAMIC EFFECTS

In addition to the always present flight induced store vibration, externally carried stores can be exposed to dynamics effects that occur intermittently during flight. The most significant of these are caused by the following sources: firing on-board guns, store buffet, store launch, and open weapon bays. The dynamic environment caused by each source will be discussed separately in the next few sections. In general, the method for testing for these environments is not fully developed.

GUNFIRE INDUCED VIBRATION

The primary source of store vibration, because of the firing of on-board guns, is the over-pressure pulses that are emitted from the front of the gun muzzle [21]. These pulses impinge directly on the surface of the store. Thus, the relative location of the gun and store, whether or not any other structure exists between the gun and store that would block or attenuate these pressure pulses, and the gun characteristics are all important factors in determining the vibration of a store caused by the firing of on-board guns.

Measured gunfire vibration is broadband with well-defined vibration peaks which can be related to the firing rate of the gun and the natural frequencies of the major store structural components that are most susceptible to acoustic excitation. The currently available gunfire vibration prediction method in MIL-STD-810D is not directly applicable to store vibration induced by gunfire. In general, the prediction method will predict a more severe vibration condition because it does not take into account any potential attenuation of the pressure pulses by aircraft wings, fuselage or adjacent stores.

STORE BUFFETING

Modern high performance aircraft have thrust-to-weight ratios greater than one so that it is possible to sustain very high angles of attack. Also these aircraft can establish very severe yaw conditions. These conditions can occur under maneuver and combat which result in highly separated turbulent airflow around the aircraft [22]. Available flight measurements do not show conclusively that buffet induced vibration is always caused by the direct impingement of this highly disturbed air or indirectly by the shaking of the store through the host aircraft.

It is hypothesized that, depending upon the maneuver and the location of the store on the aircraft, a store could be excited both directly and indirectly during the same captive flight. The direct impingement of separated flow would induce broadband vibration with noticeable vibration peaks at the characteristic frequencies of the pressure fluctuation in the air and the natural frequency of the surface structure of the store. Indirect excitation would cause broadband vibration with noticeable vibration peaks at the natural frequency of the aircraft, pylon, store rack and major store structural elements excited. In general, these frequencies are different. Therefore, a generalized dynamics test needs to be developed that would cover both types of excitation.

One approach to this problem is outlined in Reference 22. This approach developed a composite envelope of vibration peaks. This approach generally will overtest the test item because all of the vibration peaks do not occur simultaneously during captive flight.

STORE LAUNCH

The store launch environment for a store that is not being launched can be very significant. Consider a cluster of stores being carried on a single pylon. One of these stores is released by an explosive charge used to eject the store away from the aircraft. The remaining stores may experience this intense shock repeatedly until they are released.

Likewise missiles that are launched off a rail can experience intense high frequency vibration. The missile sliding down the rail can be like drawing a bow across violin strings. Intense vibrations can be excited that influence both the store being launched and those remaining. These environments need to be understood and appropriate tests developed.

STORES IN OPEN WEAPON BAYS

Stores carried in the weapon bays of an aircraft normally experience a much reduced vibration environment when the weapon bay doors are closed as compared to externally carried stores. However, with open bay doors, the aeroacoustic environment will be extremely severe. The flow induce pressure oscillations which consist of discrete cavity modes superimposed on a random turbulence pressure field under certain circumstances will be able to cause damage or malfunction even during the short duration of the bay doors open position [25]. In general, only the lowest frequency cavity resonances will reach extreme spectral levels with magnitude ratios between maximum discrete tones and random noise depending on the length to depth ratio of the weapon bay. Usually long and shallow bays will be dominated by random noise while the deeper bays will exhibit the higher cavity resonance pressures. Approaches to reduce these pressure oscillations during the development of an aircraft are not always successful to the point where a completely safe environment for the store can be generated. Therefore, qualification of a store for the particular environment of an aircraft will be necessary. A proposed method to simulate the oscillating pressure distribution over the store surface for qualification purposes was presented in [26]. This work is based on measurements of the pressure distributions on a store located in a very shallow cavity. Further measurements of this type are required to make this proposed approach more generally applicable.

FUTURE DIRECTION OF DYNAMIC QUALIFICATION TESTING

The trend in the Air Force store dynamic qualification standards is toward a tailored testing approach. The format of the standard will be such that the test levels cannot easily become dogmatic. The testing standards will give guidance as to what would be a good test but the decision will rest with the equipment acquisition community to determine test levels and duration. The tester will have to make a mission/life analysis to identify these parameters for each particular application [27].

This approach necessitates further updating of operational environmental information and improvements in the capabilities to predict the environments to which the stores are exposed and for which they have to be qualified. In addition, further refinements of test techniques will have to evolve to render the test simulation closer to realism. Work in these areas is presently being performed by the U.S. Air Force and Navy.

Since it has to be expected that stores qualified to the standards of one country will be carried by aircraft of different nations, cooperation should be invited to further commonality in the practices and procedures to which the stores are qualified.

REFERENCES

- [1] DoD Manual 4120.3-M Defense Standardization and Specifications Program, Policies, Procedures, and Instructions, August 1978
- [2] MIL-STD-810C Environmental Test Methods, March 10, 1975
- [3] V. J. Junker "The Evaluation of USAF Environmental Testing", AFFDL-TR-65-197, October 1965
- [4] Norman Sissenwine
Rene' V. Cormier "Synopsis of Background Material for MIL-STD-210B Climatic Extremes for Military Equipment", AFCRL-TR-74-0052, 24 January 1974
- [5] Army Air Force Report ATSC Cold Weather Tests Winter 1944-1945, AAF Technical Report 5230, 31 May 1945
- [6] Howard Gates
et al "Electronic X: A Study of Military Electronics with Particular Reference to Cost and Reliability", Director of Defense Research and Engineering Report R-195, January 1974
- [7] Workshop Proceedings "Summary Report of the Joint Logistics Commanders Electronics Systems Reliability Workshop", available from National Technical Information Service, order number AD016826, 1 August 1975
- [8] Joseph Shea
et al "Report of the Task Group on Specifications and Standards" Office of the Director of Defense Research and Engineering, available from National Technical Information Service, Order Number ADA040455, April 1977
- [9] Allan Dantowitz
George Hirschberger
David Pravidlo "Analysis of Aeronautical Equipment Environmental Failures" AFFDL-TR-71-32, May 1971
- [10] MIL-A-8591F Military Specification Airborne Stores, Associated Suspension Lugs and Aircraft-Store Interphase (carriage phase) General Design Criteria for, January 30, 1979
- [11] MIL-T-7378A MIL-T-7378A (USAF) Military Specification Tanks, Fuel, Aircraft, External Auxiliary, Removable, October 20, 1958
- [12] MIL-T-7743E MIL-T-7743E Military Specification Testing Store Suspension and Release Equipment, General Specification for, October 8, 1976
- [13] MIL-STD-1670 Military Standard Environmental Criteria and Guidelines for Air-Launched Weapons, July 30, 1976
- [14] J. F. Dreher
et al "Vibracoustic Environment and Test Criteria for Aircraft Stores During Captive Flight", Shock and Vibration Bulletin, No. 39, Supplement (April 1969), pp 15-40
- [15] J. F. Dreher "Effects of Vibration and Noise on Aircraft Stores Compatibility", Proceedings Aircraft Stores Compatibility Symposium, Vol VI, pp 245-271, November 1969
- [16] Alan Burkhard "Simulation of Captive Flight Aircraft Store Vibration", Proceedings of National Aerospace Engineering and Manufacturing Meeting, Los Angeles, 16-18 October 1973, SAE Paper No. 730938
- [17] Allan Piersol "Vibration and Acoustic Test Criteria for Captive Flight of Externally Carried Aircraft Stores", AFFDL-TR-71-158, December 1971
- [18] Alan Burkhard "Acoustic Testing to Simulate the Flight Vibration Environment of Aircraft Stores", AFFDL-TR-73-110, April 1974
- [19] Alan Burkhard "Dynamic Structural Integrity Testing of Guided Glide Bomb Using General Store Test Criteria", AFFDL-TM-75-60, April 1975
- [20] D. B. Meeker
W. D. Everett "U.S. Navy Experience on the Effects of Carried-Aircraft Environment on Guided Missiles", NATO AGARD Conference Proceedings, CP270, 1980

REFERENCES (Continued)

- [21] R. W. Sevy
J. Clark "Aircraft Gunfire Vibration The Development of Prediction Methods and the Synthesis of Equipment Vibration Techniques", AFFDL-TR-70-31, November 1970
- [22] W. G. Frost
P. B. Tucker
G. R. Wayman "Captive Carriage Vibration of Air to Air Missiles on Fighter Aircraft", Journal of Institute of Environmental Sciences, September/October 1978, pp 11-16
- [23] R. N. Bingman "Aero-Acoustically Excited Vibration of External Stores on Fighter Aircraft" Proceedings Aircraft/Stores Compatibility Symposium, Vol VI, pp 281-321, November 1969
- [24] K. A. Herzing and
S. N. Schwantes "Design Philosophy and Wind Tunnel Test of an External Store with Cavity Resonance", Proceedings Aircraft/Stores Compatibility Symposium, Vol VI, pp 322-370, November 1969
- [25] O. F. Maurer "Investigation and Reduction of Open Weapon Bay Pressure Oscillations Expected in the B-1 Aircraft", AFFDL-TM-74-101-FYA, January 1974
- [26] L. L. Shaw and
D. L. Smith "Aeroacoustic Environment of a Store in an Aircraft Weapons Bay", AFFDL-TR-77-18, March 1977
- [27] H. W. Egbert MIL-STD-810D, A Progress Report Proceedings of the 27th Annual Technical Meeting of the Institute of Environmental Sciences, Los Angeles, May 5-7, 1981, pp 218-221

Problems in the ground
simulation of dynamic responses
induced in externally carried
stores during flight

J. Homfray

Cape Warwick Limited
Environmental Engineering Division
Cape Road
Warwick CV34 5DL
England

Summary

The need for ground testing is assumed and consideration is limited to complete stores. Guided missiles are not specifically included but some of the arguments must apply equally to this type of store.

The difficulties encountered in testing stores over a wide frequency band are described. This wide frequency range has led to vibration tests using single point excitation with an electrodynamic shaker, to cover the low frequency regime, and tests using distributed acoustic excitation to cover the middle and high frequency regimes. Both types of test are discussed in some detail with emphasis on the particular difficulties encountered with large, comparatively low density thin-skinned stores.

Shortcomings inherent in the current techniques are highlighted and the validity of MIL-STD-810C as a means of determining test levels in the absence of flight data is examined.

It is concluded that the current two part test technique is not particularly realistic when applied to the large thin-skinned stores.

Tentative suggestions are made for a more realistic test method.

1. Introduction

Cape Warwick Limited (CWL) is an independent environmental test house supported by MOD (PE) and has, over the past few years, been required to carry out ground vibration tests on complete, large stores to simulate the external flight carriage environment. For stores flown on low level high speed missions this is often the most severe environment they experience, except in the case of some guided weapons where the air launch or powered free flight phase may be more severe.

A growing understanding of the flight carriage environment has led to more elaborate test procedures than those used hitherto for this purpose. Such procedures applied to large low density thin-skinned stores of the kind currently under development raise considerable difficulties. The tests represent a fairly radical departure from the earlier practice of qualifying the store almost entirely by static strength tests, with separate vibration tests on internal components. A final shake of the complete store was undertaken but this was little better than a simple ruggedness test.

The difficulties encountered with this new breed of store has prompted CWL to examine the test procedures and the philosophy behind them more closely.

The new stores are large and complex and the internal equipment is such that it is believed that representative testing of the complete store must be carried out as well as component and sub-assembly testing. However the difficulties with the complete store are such that it may be pertinent to ask whether these tests really are necessary. By analogy with aircraft practice and experience there are arguments to suggest that they are not, at least in the form currently employed

Nevertheless, the ability to test complete stores realistically, if this could be done, has considerable potential. It offers, in principle, the possibility of addressing both the structural and functioning aspects in one test under representative conditions. Such testing may also be advantageous in the validation of advanced mathematical modelling techniques.

However, current testing, a major item in the store development programme, is costly, time consuming and not particularly realistic, as this paper hopes to illustrate. Tests on the large thin-skinned stores at CWL have been useful, and have shown up potential failures in particular cases but there is room for improvement in several areas.

In what follows below guided weapons are not specifically included, since CWL has little experience of these, but some of the arguments must apply equally to this type of store.

2. The external carriage environment and the implications for ground testing

The environment itself is not properly understood in detail, but the main characteristics are generally agreed.

Store acceleration responses in this environment show broad band random and stationary characteristics in general, with substantially gaussian amplitude distribution. The frequency range is wide; typically from a few Hz to 2500 Hz or more.

Basically there are two sources of excitation; the aircraft itself, with all its associated inputs acting through the store suspension points, and unsteady aerodynamic processes in the air flow around the store, acting directly on, and distributed over, the surface of the store. Several mechanisms are involved in the two sources, some common to both.

Because the aircraft structure is comparatively large and flexible with many joints the input to the store from this source tends to be confined to the low frequency region. The aerodynamic input is broad band but is virtually the only source of high frequency excitation.

Any ground simulation of this environment must recognise the essential nature of the two sources; the very localised predominantly low frequency input, and the distributed broad band input extending to high frequencies.

These arguments have led to the adoption of a two part vibration test technique. Tests using single point excitation with an electrodynamic shaker are intended to cover the low frequency regime and tests using acoustic excitation, which by its nature is distributed, to cover the middle and high frequency regimes. Note that this high frequency test is not an acoustic test as such.

For convenience the two types of test are referred to as low frequency (LF) and high frequency (HF) respectively, although they overlap.

It is comparatively easy to excite small stores through their suspension equipment for the LF test (though not necessarily realistic) but it becomes difficult to do this with large heavy stores (typically 5 metres long weighing up to 1400 Kg), which require large shakers. This is particularly true if they are required to be tested the right way up, that is with the suspension lugs on top.

Acoustic excitation for these large stores requires fairly extensive test facilities consuming up to $\frac{1}{2}$ MW or so of power to raise the currently required highest input levels.

Even if appropriate facilities are available there are considerable problems in some areas.

This sets the background to the two part test technique as used at CWL to simulate the flight carriage environment for large low density (but heavy) thin-skinned stores.

There is a lack of flight data for these stores and the only other source of information for testing purposes is the American Standard MIL-STD-810C, 10 March 1975 which sets out a procedure for the two-part test and a means for deriving the test levels.

3. Outline of the two part test procedure as defined by MIL-STD-810C 10 March 1975

3.1. The low frequency (LF) test

This is covered by Method 514.2, Procedure II B, Table 514.2 - IV and Figure 514.2 - 4A, which define a controlled response test based on acceleration power spectral density. A method is provided for determining acceleration response envelopes for each of two strong points, one at the forward and one at the aft end of the store. This is based on the store geometry - in particular the skin thickness and store cross-sectional radius - the number of missions and the flight conditions.

The input spectrum is set to the shape of the forward response envelope but minus 6dB, then this basic shape is notched or peaked according to information gained on an initial low level resonance search. This is intended to position the response peaks at the forward and aft ends of the store such that they correspond to the derived response spectrum shapes.

There is a choice of mounting arrangements for the store. It can either be mounted directly onto the shaker table using a suitable fixture, or suspended from a suitable structural frame. In either case its normal mounting lugs are to be used. The shaker table fixture "shall be such that its induced resonant frequencies are as high as possible but none below one-third of any f_0 frequency" (the maximum LF test frequency). With the structural frame: "The test setup shall be such that the rigid body modes (translation and rotation) of vibration for the store; frame; suspension system are between 5 - 20 Hz. Vibration shall be applied to the store by means of a rod or other suitable mounting device running from

a vibration shaker to a relatively hard structurally supported point on the surface of the store." Different input locations may be tried to determine a position which allows both ends of the store to be raised to the required acceleration levels simultaneously.

Separate tests are to be carried out in the vertical and lateral directions unless it can be shown that the specified levels in each plane can be raised simultaneously in one test.

Two test levels are required; a functioning level and an endurance level. The levels derived are weakly dependent on number of missions to be flown N , and test time T , or, more specifically, on $(N/3T)^{1/4}$.

3.2. The high frequency (HF) Test

This is called up as additional to the low frequency test and is covered by Method 515.2, Procedure II, Table 515.2-II and Figure 515.2-4. It is not required if the highest frequency of the LF test is greater than 1200 Hz.

This test is an acoustically excited controlled input test based on one third octave band sound pressure level spectra.

The store is required to be mounted on a soft suspension, the natural frequency of which must be less than 25 Hz. A jet engine on an open air test stand or in a test cell, or an acoustic chamber are suggested as suitable noise sources, and baffles are to be provided for shaping the noise spectra to the required profiles.

Three reference planes are defined, at $1/6$, $1/2$, and $5/6$ of the store length, with three microphones, 120° apart, in each plane. Each microphone must be positioned within 460 mm (18 in) of the store surface or at one half the distance between the store and the nearest baffle surface, whichever is less.

A method is given for determining the required noise spectrum profiles at each reference plane, based on the store geometry, the mission profile and the flight conditions.

Two test levels are required; a functioning level and an endurance level. Again there is the same dependence on number of missions and testing time as in the LF test.

4. The problem areas

Two particular examples of large low density thin skinned stores, and the tests carried out on them, are used to illustrate the difficulties described in this section and they are referred to throughout, as necessary.

Both stores have basic structures of light alloy, comprising thin skins with frames, bulkheads and longitudinal stiffeners, similar to traditional aircraft practice. They have structure weights of approximately one half of the total weight in each case. They are shown in outline in Fig. 1 and 2 where overall dimensions and weights are given, and are chosen to represent two main types.

Store No. 1 is of medium size, has no fins and contains a comparatively large open cavity. Store No. 2 is large, enclosed and has two horizontal fins. Fig. 3 to 6 show the test arrangements used for the stores and Fig. 7 to 16 show the results obtained, including comparison with flight in some cases. They are presented in the form of store acceleration response power spectral density plots. Only the vertical components of the responses are given and only vertical excitation is considered in the LF tests. This gives a very much simplified picture but, hopefully, illustrates the points adequately.

Further details on the testing of these stores and the results are given elsewhere in this paper as necessary.

4.1. Store support rig for the LF test

Of the two alternatives allowed by MIL-STD-810C the only practicable test arrangement for large heavy stores is the flexible store support rig. Such a rig must provide adequate constraint to allow coupling of the shaker to the store without damage to the shaker due to side loads. The shaker should not support any of the store weight in the static condition. Out of plane responses should be minimised, since, although it would be convenient to raise the required levels in both planes simultaneously in one test this is, at best, uncontrolled.

MIL-STD-810C specifies only that the rigid body modes shall be between 5 and 20 Hz.

The rig used for store No. 1 is shown in Fig. 3 together with the frequencies. Identification of the modes by the words 'vertical', 'lateral', 'pitch', 'roll' etc. is misleading since the mode shapes are complex. However the behaviour of the store in each mode approximated to the descriptions given in the figure.

For store No. 2 the rig was designed using finite element techniques. The resulting 'X' shaped layout evolved from the finite element work as an arrangement which allowed adjustment of the frequency of each mode fairly independently of the other modes. The rig is shown in Fig. 4, together with the measured rigid body frequencies, and the shaker arrangement in Fig. 5. The descriptions of the mode shapes given in Fig. 4 are representative of the motion at the store.

The two rigs have quite different characteristics. The spring rig has more damping than the X-frame and it exhibits a behaviour in vertical translation (of the store) which approximates to a single degree of freedom system, because of the springs. The finite element analysis indicated that the X-frame rig has 47 normal modes in the frequency range 3.5 to 680 Hz. In this analysis information for modes above the 20th is not reliable but does give an indication of the modal density.

Rig behaviour at frequencies above the rigid body mode values influences the excitation force required to raise a given response in the store. In particular, if the excitation is applied close to the store supports the force required may be comparatively large at some frequencies; sufficient in some cases to cause unrepresentative local damage to the store. Such damage has occurred with store No. 2 though at much higher test levels than those reported here. This is a particularly difficult problem when the store has no accessible strong points. In this case local strengthening is required to accept the input. If this is excessive the store structure becomes unrepresentative.

The difficulty of finding the optimum position for the input, to raise the required level at both ends of the store simultaneously, is aggravated by the lack of strong areas. Fixtures, both internal to the store and external, had to be manufactured to allow the shaker to be attached. Under these circumstances there is a reluctance to experiment with input position since a new fixture has to be provided almost every time.

When local damage occurs at the input point this could be due to insufficient support of the store structure at this point, test levels which are too high or a rig impedance which is too high. Under the pressure of time prevailing in project work it is usually not possible to decide which of these effects is most relevant.

It is apparent that, so far as unrepresentative damage is concerned, and so long as the excitation is applied directly to the store, the behaviour of the rig at frequencies above those of the rigid body modes is important; as important as the necessity to keep the rigid body frequencies low.

Under these circumstances what criteria should be used for acceptable rig dynamic behaviour? The design, manufacture and commissioning of a rig of this kind is a very significant item in the test programme.

Regarding the requirement to test in both the vertical and lateral planes, separately, experience with the spring and X-frame rigs has shown that the out-of-plane responses were indeed low enough to necessitate the separate tests.

4.2. Acoustic simulation of aerodynamic inputs

The arrangement used for the HF test is shown in Fig. 6. A large reverberant chamber was used employing two acoustic horns driven by up to 6 electropneumatic noise transducers. To raise the high noise levels required by MIL-STD-810C at the store aft reference plane it was necessary, in the case of store No. 1, to position the aft end inside the mouth of the horn. This could not be done with store No. 2 because of its length; in this case the fins were removed and the aft end positioned as near to the horn as possible.

MIL-STD-810C suggests a jet engine on an open air test stand, or in a test cell, as a suitable noise source. These alternatives were examined but the required high levels could not be raised in an engine test cell, and could only be raised just inside the jet noise cone in the open air. The open air test is inconvenient because of weather and security problems. The cost of running an engine solely for such tests is prohibitive and consequently there is a heavy dependence on the engine running programme.

Acoustic excitation is distributed and does come closer to simulating the aerodynamic input than is possible with a single mechanical shaker; even if the shaker has an adequate high frequency performance. However the mechanisms involved in acoustic processes are not the same as those involved in aerodynamic processes. The spatial correlation of the pressure fluctuations is different in each case. In addition aerodynamic damping is generated when air flows over a vibrating body; greater than that which is generated when the body is in stationary air. In the acoustic test the specimen is essentially in still air so that there is no aerodynamic damping present.

These differences mean, in effect, that the acoustic field is more efficient at producing vibration in a structure than the aerodynamic processes are. The effect is enhanced or diminished depending upon the correlation length relative to skin panel dimensions; that is, whether or not panel resonances are induced.

There is evidence from tests on a thick-shell store having a sheet metal tail that fin vibration inputs to the store are not simulated in the acoustic tests. This may be because unsteady lift is generated in flight which cannot be present in the test, or because of the inherent symmetry of the pressure fluctuations on each side of a thin fin in a reverberant field.

The noise levels required by MIL-STD-810C and the degree to which they were achieved are shown in Fig. 7 for store No. 1. These were the best that could be achieved in terms of both overall sound pressure level and spectrum shape and were on the limits of the acoustic facility used.

An estimate of the sound pressure level spectrum in an attached turbulent boundary layer, calculated (from Ref. 1) for the aft end of the store, is shown in Fig. 7 for comparison. However it must be remembered that the test levels are intended to encompass effects from flow separation and buffet as well as the contribution from the attached boundary layer. In the case of store No. 2 the MIL-STD-810C levels, as such, were not used (see section 4.3.). The required and achieved levels for this store are shown in Fig. 8.

4.3. Initial derivation of test levels

Having accepted the two-part test procedure it is still necessary to determine the excitation levels and test durations. The levels depend upon the flight conditions and the store configuration, and the durations depend upon the purpose of the test (which involves the store mission profile) and on the acceptability, or otherwise, of accelerated testing.

At CWL, in the absence of any directly relevant flight data for the large low density stores, it was required that MIL-STD-810C, 10 March 1975 was used as a starting point. It was initially applied to the testing of store No. 1 but several interpretations were possible. It became apparent that this store was outside the scope of the Standard. In particular the cross-sectional shape did not readily fit the alternatives given. It was difficult to allocate appropriate values for the number of missions and testing time for this store, which was a development item and not representative of the final vehicle. The dependence of the MIL-STD-810C derived levels on $(N/3T)^{1/4}$ caused arguments about the exchange between test level and test time.

The minimum average store weight density allowed by MIL-STD-810C was 40 lb/ft³ (640 kg/m³) whereas the calculated value for store No. 1 was only 20 lb/ft³ (320 kg/m³). The lower limiting value for the parameter t/R^2 was 0.001 in⁻¹ (0.000039 mm⁻¹) and the calculated value only 0.0004 in⁻¹ (0.000016 mm⁻¹).

In such cases the standard requires that the limiting values be used. Consequently there was doubt about the validity of the levels derived from these values when the actual ones were so far out of range.

It was decided that alterations to the test levels should be made as necessary, in the light of experience, and when flight evidence became available from the stores themselves.

The result of applying the MIL-STD-810C procedure for setting up the input spectrum in the LF test (section 3.1.) is illustrated in Fig. 9. for store No. 1. In this case there was virtually no choice about the input location. The nose cone was removed and the exposed front bulkhead stiffened to accept the input (Fig. 3). The mass and stiffening effect of the fixture was compensated for, to a limited degree, by the absence of the nose cone. It is notable that in spite of the 8 dB notch in the drive spectrum there is still a strong response at the same frequency at the aft bulkhead. The input was controlled using a closed loop digital system.

Similar arguments applied to store No. 2 but this came later in the programme when some experience had been gained with store No. 1. The levels used for store No. 2 were derived from engineering judgement coloured by results from earlier tests.

With store No. 2 a central excitation point was used (Fig. 5) for a comparatively low level input, with adequate transmission to each end of the store. The input was controlled on the mean of the responses at the forward and aft bulkheads, using the digital system.

Derivation of the noise level for use in the HF acoustically excited tests was relatively straightforward except for the problems associated with number of missions and testing time, mentioned above. In the case of store No. 1 the MIL-STD-810C derived noise spectra were used without alteration, but for store No. 2 the spectra were modified and the levels reduced slightly.

4.4. Validity of the tests

The realism of the tests can only be assessed by a comparison of the store acceleration responses resulting from ground and flight tests. Such comparisons are shown in Fig. 10 to 13 for store No. 1 and Fig. 14 to 16 for store No. 2. Only limited comparisons are available for store No. 2 due to accelerometer failures.

The 10⁻⁴g²/Hz line is reinforced in all figures to aid the eye in making comparisons. No particular significance attaches to the 10⁻⁴ level; it is merely an arbitrary reference.

In general the responses raised in the ground tests are greater than those from flight; by orders of magnitude in some cases. Clearly the stores were overtested for the particular flights on the aircraft used for the tests. However, this does not necessarily imply an overttest in terms of the store development programme. Worst case test levels would be expected to be higher than average flight levels; also the aircraft used for the test flights may have given a comparatively smooth ride. There are doubts as to whether these flight levels can be applied to other aircraft or to different store positions on the same aircraft.

Bearing these arguments in mind the following broad conclusions can be drawn from the comparisons.

4.4.1. Store No. 1

The LF regime

The ground response spectrum levels at the forward bulkhead are roughly the same as those from flight although the shapes are not in agreement (the response is forced at this position because the input was located there), as seen from Fig. 10. The ground test levels at the aft bulkhead rise to about 3 times the flight levels (Fig. 11). However the lug pocket levels are considerably higher than flight; conspicuously so at the aft pocket where the ground levels are around 100 times the flight levels.

The HF regime

In general the ground response levels are the same as those in flight (Fig. 12 and 13) except for the forward bulkhead values which are approximately 10 times the flight values. This anomalously high level cannot be explained at present.

The spectrum shapes compare fairly well except that the sharp narrow peaks raised in flight do not appear in the ground responses.

A possible reason for the good agreement between ground and flight responses in this case is given in section 4.5.

4.4.2. Store No. 2

The LF regime

The peaks in the ground test responses are of the order of 10 times the flight levels at the bulkhead. They are up to 100 times the flight levels at the lug pockets.

There is very little similarity between the ground and flight spectrum shapes (Fig. 14 and 15).

The HF regime

The ground response levels are generally 100 times the flight levels. The spectrum shapes agree well except for the anomalous strong peak (rising to about $4g^2/Hz$ at 300 Hz, Fig. 16) at the forward lug pocket, which is not apparent in the flight responses. There is a peak at this same frequency, also at the forward lug pocket, in the LF test responses (Fig. 14).

4.4.3. The validity of MIL-STD-810C levels

The peak envelopes resulting from the best interpretation of this standard for the LF tests on store No. 1 are superimposed on Fig. 10 and 11 for comparison with the flight results.

The corresponding envelopes for the LF tests on store No. 2, interpreted for 3 missions (which gives the lowest levels) are superimposed on Fig. 14 and 15 for the same purpose.

The MIL-STD-810C levels are surprisingly close to the flight peaks for store No. 1; especially when it is remembered that the MIL-STD-810C envelopes are intended to apply to the peaks only.

In the case of store No. 2 the MIL-STD-810C levels are an order of magnitude higher than the flight peak levels.

The MIL-STD-810C levels for the HF test generated responses in the streamlined store (store No. 2) which were 100 times the flight responses. Does this indicate that the standard does not properly allow for the differences between aerodynamic and acoustic processes (outlined in section 4.2.) or is it that the test flights with Store No. 2 were unrepresentatively smooth in this frequency range?

4.4.4. Some general observations on the LF tests

The acceleration responses at the lug pockets are generally very high in the LF test. This applies to both stores and therefore both rigs.

It is notable that there is very little store response outside the test frequency range with the spring rig (Fig. 10 and 11) whilst there is considerable response outside the test frequency range with the X-frame rig (Fig. 14 and 15).

Furthermore the responses outside the test frequency range for store No. 2 show some similarity to the flight responses; more so than they do within the test frequency range.

The implications of these observations are not clear. The dynamic behaviour of the rigs in the frequency range encompassing the store flexural modes should be examined.

4.5. Cavity generated vibration

The acceleration responses from store No. 1 in the HF test show comparatively good agreement with flight levels except that the sharp, tall flight peaks are not raised in the ground tests. Chaplin (Ref 2) has produced evidence to show that the flight peaks are probably the result of strong narrow band forcing from aero-acoustic processes in the cavity of the store. The conspicuous peaks in the flight responses occur because the centre frequencies of the narrow band excitation from the cavity are near to store structural resonance frequencies. These centre frequencies are dependent upon airspeed to some extent. Apparent small shifts in frequency and amplitude of the flight peaks with airspeed (not presented here) are caused by the changing nearness of the excitation centre frequencies to the store structural resonance frequencies.

Cavity generated inputs may thus be responsible for the overall enhancement of flight response levels, as well as for the raising of the sharp peaks.

To summarise, the flight response levels for store No. 1 are anomalously high due to the presence of the cavity.

Broad band excitation, such as that used in the acoustically excited tests, is not as efficient at raising flexural responses as narrow band excitation such as may be generated in the cavity during flight. It follows, since there was good agreement between the acoustically excited and flight response levels, that the acoustic noise levels must have been far higher than would have been required for an enclosed store.

4.6. Interpretation of failures during test

If a failure of the specimen occurs during test its validity and importance for design purposes can only be determined when several questions relating to the failure have been answered.

- (i) Is it a genuine failure or a faulty component? Prototypes often use re-worked brackets or modified components and failures sometimes occur due to this.
- (ii) At what time in the test did the failure occur? This will show whether there were anomalies in the test at the time, and gives an indication of the severity of a genuine fatigue failure.
- (iii) Is the failure associated with a particular frequency band and if so were the test levels anomalous in that band?
- (iv) Is there a local overtesting problem?
- (v) Are the test levels too high?

In practice it is often difficult to answer these questions. Some of them, by their nature, would require a fairly extensive investigation.

These difficulties are common to all kinds of testing but are particularly relevant in the testing of these new large stores, which is so time consuming and expensive.

4.7. Availability of flight data

There is a body of opinion which believes that a new store should be brought to the flight stage as early as possible and then be flown, fully instrumented, to measure the flight vibration environment, even if the store is not fully representative of the final vehicle at this stage. However, it is suggested that with stores of the type described in this paper, which are large and complex, a version which could be flown very early in development would not be sufficiently representative.

Nevertheless it is true that in the programme associated with stores 1 and 2 flight data came too late to be of much use in modifying the tests to make them more realistic.

The difficulty of obtaining flight data is a genuine problem in this kind of work and reinforces the need for realism in testing.

5. The implications of using current test procedures for other types of store

It may be worth pointing out some of the experience gained with a rigid thick-shell store, since it has a bearing on some of the difficulties described.

At CWL the two part test procedure has not been applied strictly to any stores other than the large low density thin skinned type. However, acoustically excited vibration tests have been carried out on a thick-shell store (1000 lb class) to gain experience in the technique. In these tests, using similar noise levels and spectrum shapes to those used for store No. 2 in the same reverberant chamber, the flight response levels were generally achieved, with reasonable agreement of the spectrum shapes.

In the HF region the thick-shell shows response levels, both in ground tests and in flight, that are about 10 times the flight values obtained with store No. 2.

Thus if MIL-STD-810C was applied to stores having a comparatively rigid, thick-shell it may well be more successful than it was when applied to stores 1 and 2. The transmissibility of the thick-shell is much higher. However it is still possible that the lug pocket areas would not be representatively tested because of the rig constraints in the LF test. There would be much less likelihood of local over-testing at the vibration input point but any bands which may have to be fitted around the store at this point would modify the shell modes.

Structurally, guided weapons fall somewhere between the rigid thick-shell and the low density stores. Small high density guided weapons may be nearer to the thick-shell type.

6. Conclusions

6.1. The two part vibration test procedure applied to stores to simulate the external flight carriage environment is elaborate, time consuming and costly. It is a major item in the store development programme, but is not particularly realistic; at least in the case of the new large, low density thin-skinned stores.

6.2. There are potential advantages in being able to test complete stores realistically, but current techniques are unrepresentative to the extent that specimen failures during testing are difficult to interpret.

6.3. The lack of realism in the current two-part test technique arises mainly from the way in which the store is supported and the position of the vibration input in the low frequency test, and the differences between aerodynamic and acoustic processes in the high frequency test.

Specifically, the main problem areas are:

- (i) The dynamic criteria to be used in the design of the store support rig for the low frequency test. The MIL-STD-810C criteria do not appear to be adequate.
- (ii) Optimisation of the vibration input for the low frequency test; particularly if the store has no accessible strong points.
- (iii) Determination of the test levels in the absence of flight data; for both the low and high frequency tests.

6.4. MIL-STD-810C apparently gives a considerable overtest for large low density thin skinned stores. It appears to predict reasonable levels for fairly rigid thick-shell structures. In the one case of a large low density store with an open cavity the flight responses were enhanced by narrow band forcing arising from aerodynamic processes in the cavity. In this case the levels derived from MIL-STD-810C were much nearer to the flight values.

7. Tentative suggestions for a better approach

Although it can be argued by analogy with aircraft practice that the testing of complete stores should not be necessary, the potential advantages of being able to do this realistically are such that it seems worthwhile considering how better realism might be achieved.

The main area for concern is the low and middle frequency regime. Although there is considerable excitation up to frequencies of 2500 Hz and beyond there seems very little evidence that this high frequency input causes design problems in general. Clearly there will be specific cases where this is not true; for example when electrical relays, or structural skin panels have resonances in this frequency range. However such problems should not require tests on the complete store.

Most store acceleration response spectra in the external carriage environment show, broadly, three regimes. There is a low frequency regime extending up to about 200 Hz or so in which the responses seem to depend on the type of aircraft, the store position on the aircraft and the flight conditions. There is a middle frequency region in which the responses exhibit the flexural peaks associated with the store modes, and depend on store configuration and airspeed, and a high frequency region where the response is essentially broad band and forced, and depends mainly on airspeed.

These characteristics suggest that the low frequency responses involve store rigid body modes on a flexible aircraft, middle frequency responses involve the store flexural modes coupled with the aircraft modes if the store frequencies are comparatively low (stores 1 and 2 fall into this category), or largely decoupled from the aircraft if the store flexural frequencies are high enough.

It follows that the large flexible stores, at least, cannot be realistically tested without some representation of the aircraft influence; that is the coupling between the aircraft and store modes. This implies that even if these stores could be attached directly to a shaker by means of their suspension equipment the tests could not be realistic.

The obvious weakness of the current low frequency test is that the vibration input is applied to the store itself. It must be considerably more realistic to apply the excitation to the rig, provided the rig has suitable dynamic characteristics. If the rig could be so designed that it behaved similar to an aircraft structure in the relevant degrees of freedom over the relevant frequency range, the store should experience realistic inputs. But what kind of characteristics should the rig excitation have?

There is evidence to suggest, from flight tests with an instrumented rigid thick-shell store (Ref. 3) that the contribution to the store vibration input from the aircraft engines is very small, if not negligible. In this work the aircraft was tethered to the ground and the engines set to the thrust required for 550 Kt. Under these conditions the store response levels were about one tenth of the levels recorded in straight and level flight at the same thrust setting. (This is not entirely satisfactory because the engines would be operating under unrealistic conditions in the tethered case, and the airframe was in contact with the ground via its undercarriage, but it seems unlikely that the engine influence would increase several times in flight).

These results would suggest that the important source of excitation of the aircraft in the present context is gust type loading and low frequency atmospheric turbulence. Consequently it seems that the advocated compliant rig should be excited with something resembling a gust time history.

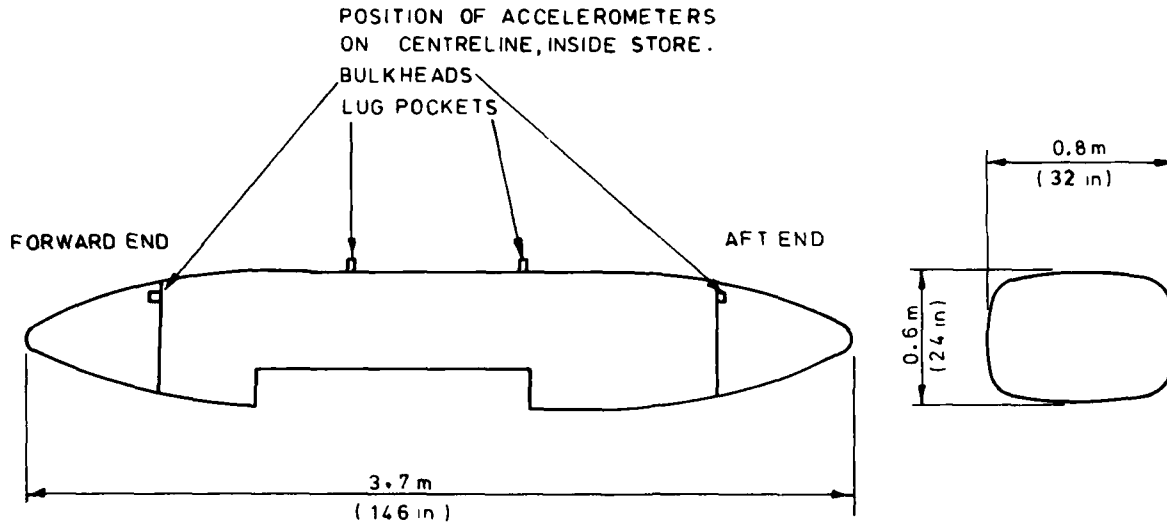
It would be a large task to design and develop such a rig; one which would have to be approached in stages. If more than 2 or 3 degrees of freedom proved to be necessary the task may be impossible. It is suggested that a feasibility study should be carried out.

References

1. Engineering Sciences Data Unit Limited
Estimation of the surface pressure fluctuations in the turbulent boundary layer of a flight vehicle 1975 Data Item 75021
2. R. Chaplin Cape Warwick Limited
A comparison of ground and flight vibration trials results on the 1Y dispenser.
1979 RDM 122
3. D. A. Williams Cranfield Institute of Technology
An assessment of results obtained from the initial vibration store flight trials.
1977 COA-DA-133

Acknowledgements

The author gratefully acknowledges the benefit gained from discussions with Mr. D. R. B. Webb of Noise Division, Aero Dept., R. A. E. and Mr. R. Chaplin, consultant to CWL. Thanks are also due to Dr. Yeh and Mr. I. Vesty of the acoustic facility at G. E. C. Whetstone, and to the trials engineers at CWL for information relating to tests in which the author took no part.



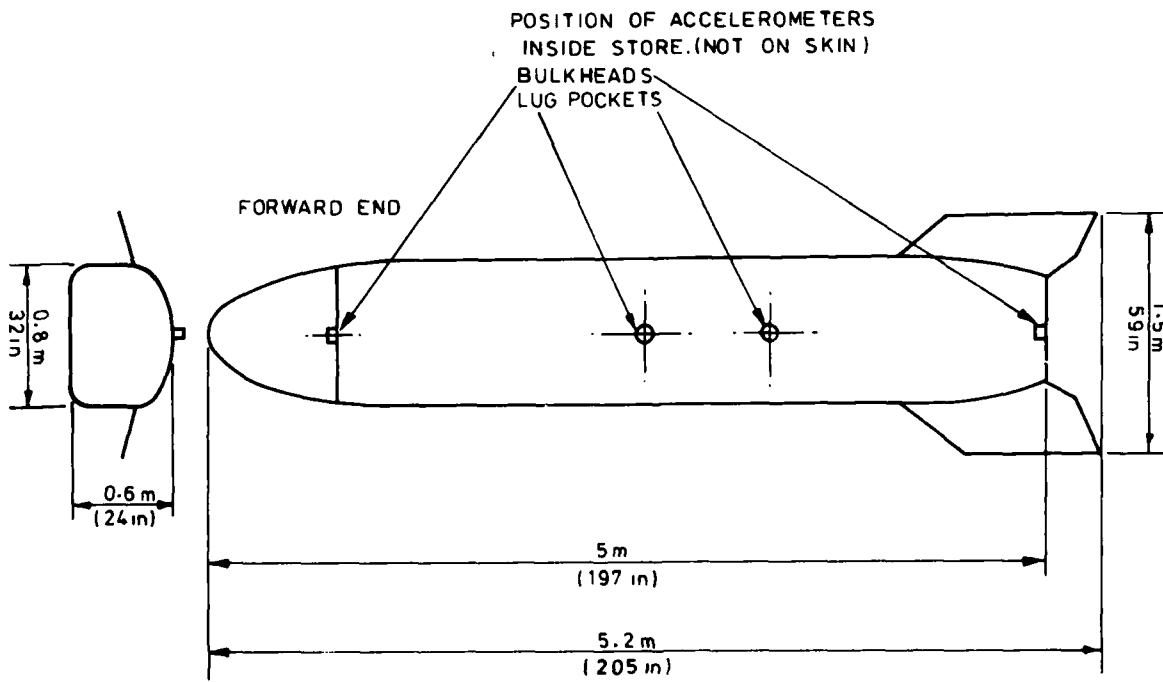
SIDE VIEW

WEIGHT 450 kg (992 lb)

NOT TO SCALE

STORE No 1

Figure 1



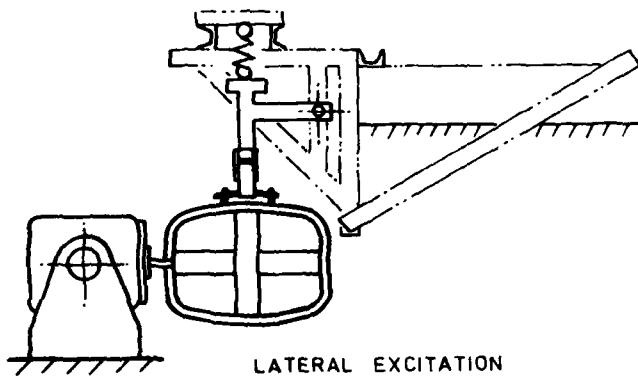
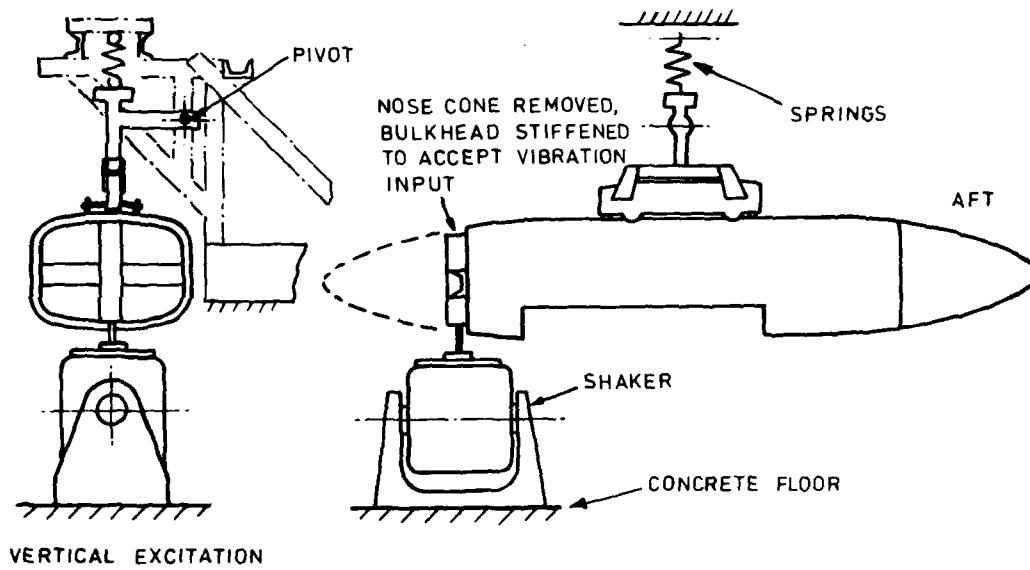
NOT TO SCALE

PLAN VIEW

WEIGHT 1300 kg (2866 lb)

STORE No 2

Figure 2



APPROXIMATE RIGID BODY MODE FREQUENCIES, Hz

VERTICAL	9.4	YAW	3.1
LATERAL	9.8	PITCH	7.5
AXIAL	4.9	ROLL	8.3

STORE No.1
LOW FREQUENCY TEST
ARRANGEMENT
(THE SPRING RIG)

Figure 3

RIG MADE FROM 250mm x 250mm x 10mm
STRUCTURAL STEEL TUBE

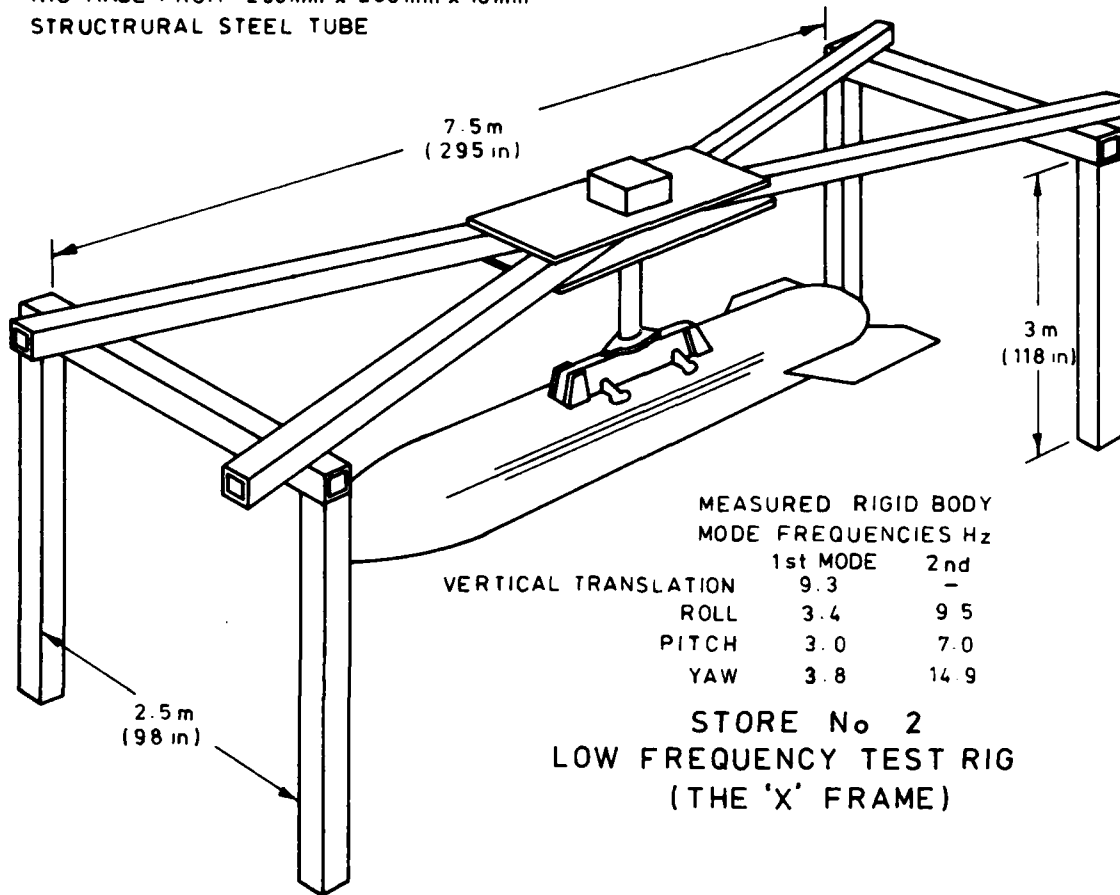
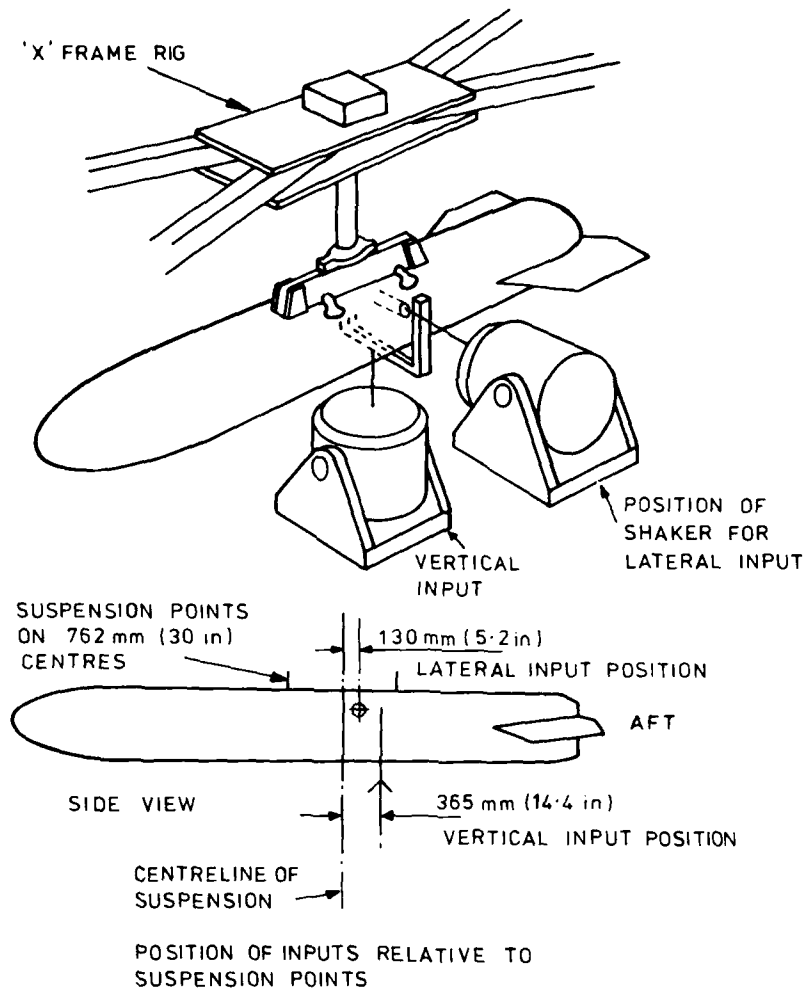
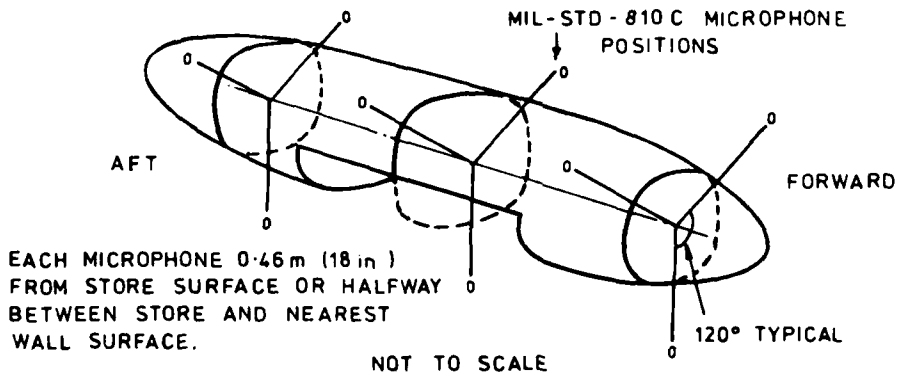
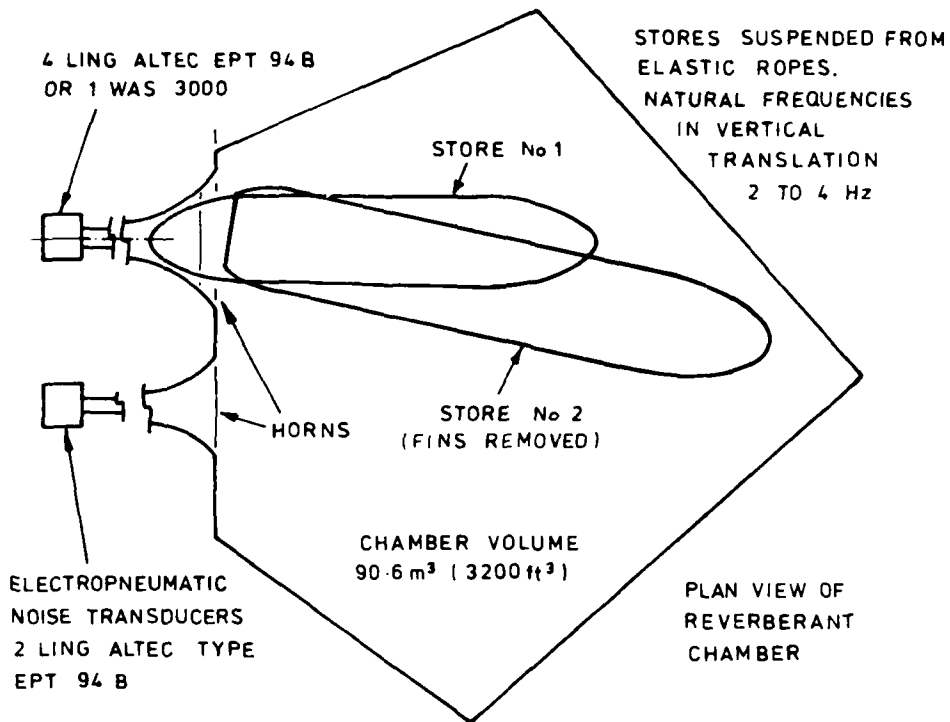


Figure 4



STORE No. 2
LOW FREQUENCY TEST
ARRANGEMENT

Figure 5

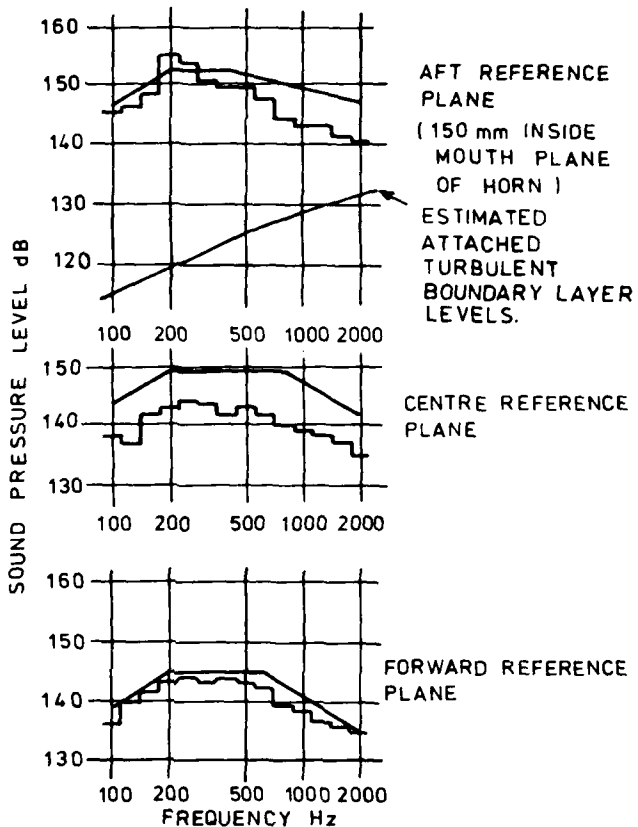


ARRANGEMENT FOR HIGH FREQUENCY
ACOUSTICALLY EXCITED TESTS , BOTH STORES

Figure 6

OVERALL SOUND PRESSURE LEVELS dB

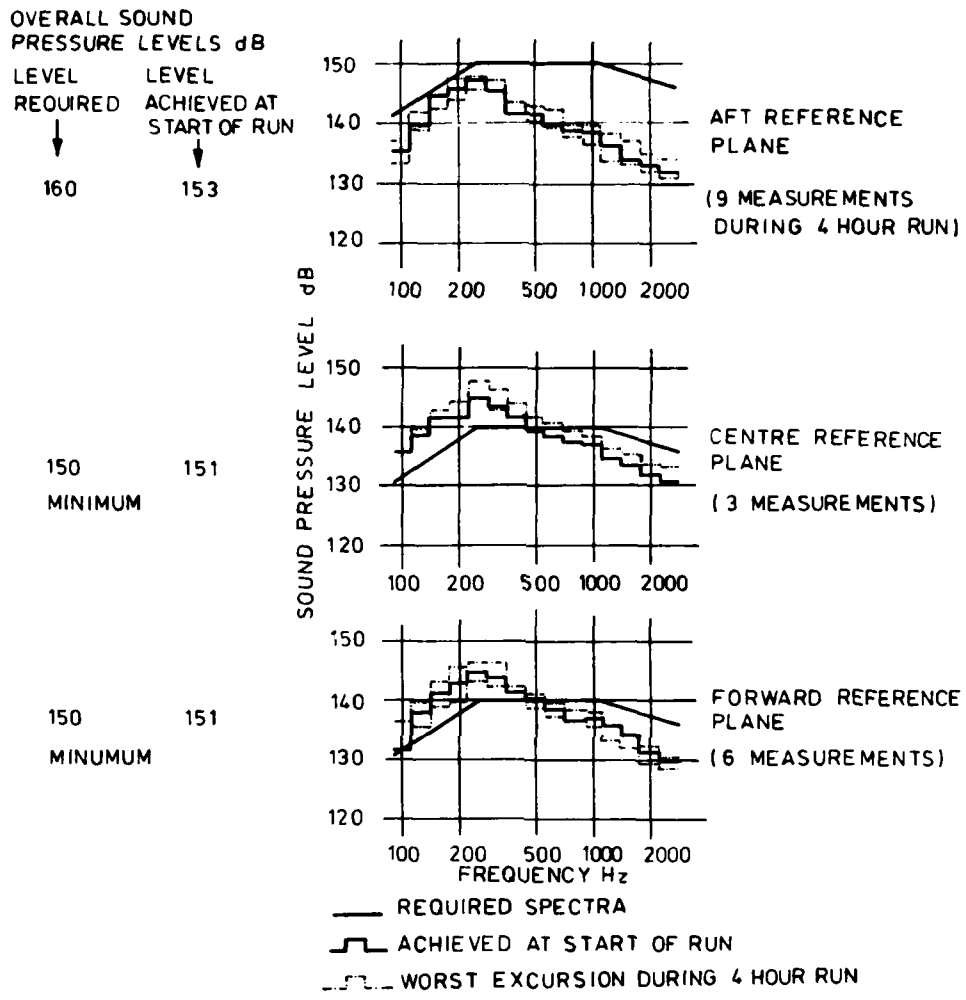
LEVEL REQUIRED	LEVEL ACHIEVED
161.8	160.5
159.6	152.6
153.9	152.5



— REQUIRED SPECTRA (ENDURANCE ENVELOPES FOR 560 Kt, SEA LEVEL)
 - - - ACHIEVED SPECTRA

STORE No 1
 HIGH FREQUENCY TEST. EXCITATION NOISE FIELD
¹/₃ RD OCTAVE BAND SPECTRA

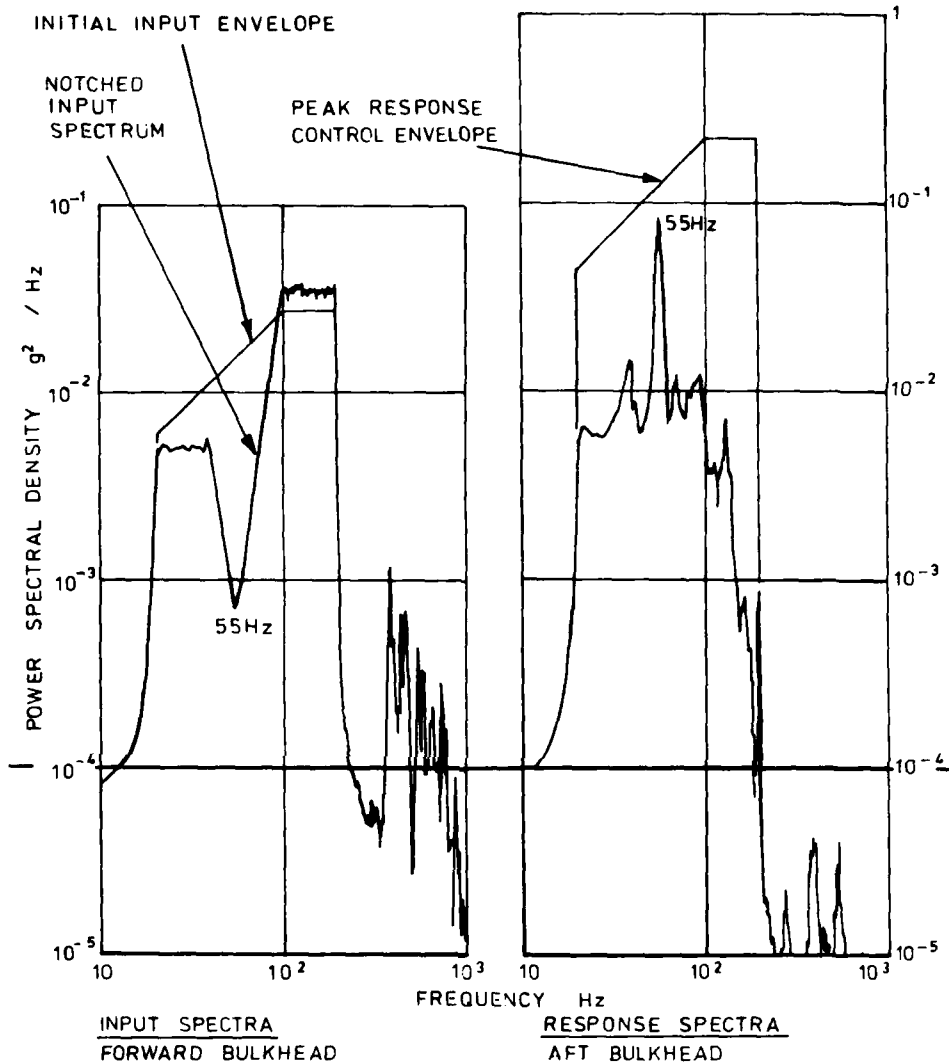
Figure 7



STORE No 2

HIGH FREQUENCY TEST. EXCITATION NOISE FIELD
 $1/3$ RD OCTAVE BAND SPECTRA

Figure 8

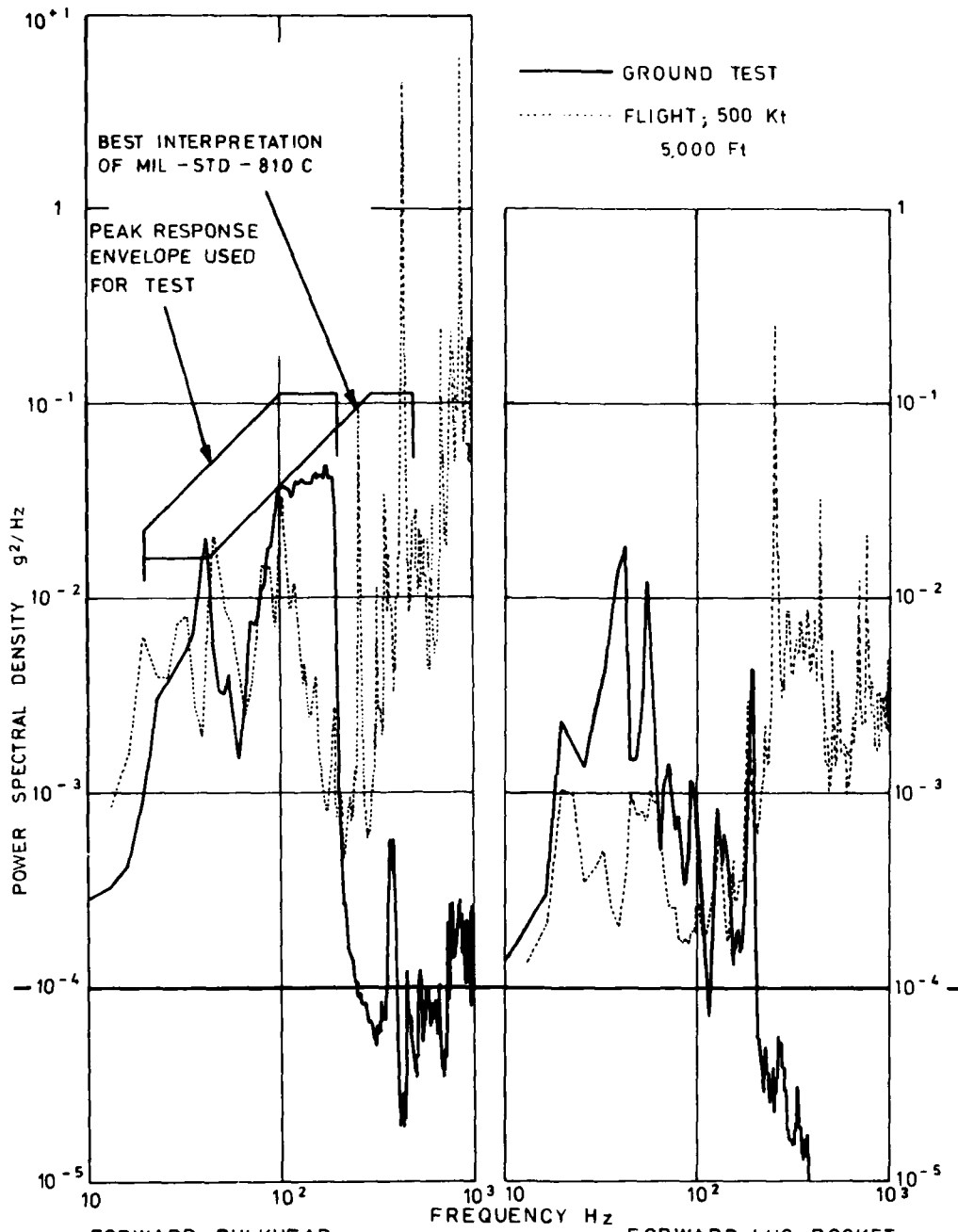


VERTICAL INPUT AND RESPONSE

ANALYSIS BANDWIDTH 1.6 Hz

STORE No 1
 LOW FREQUENCY MECHANICALLY EXCITED TEST
 INPUT AND CONTROL SPECTRA

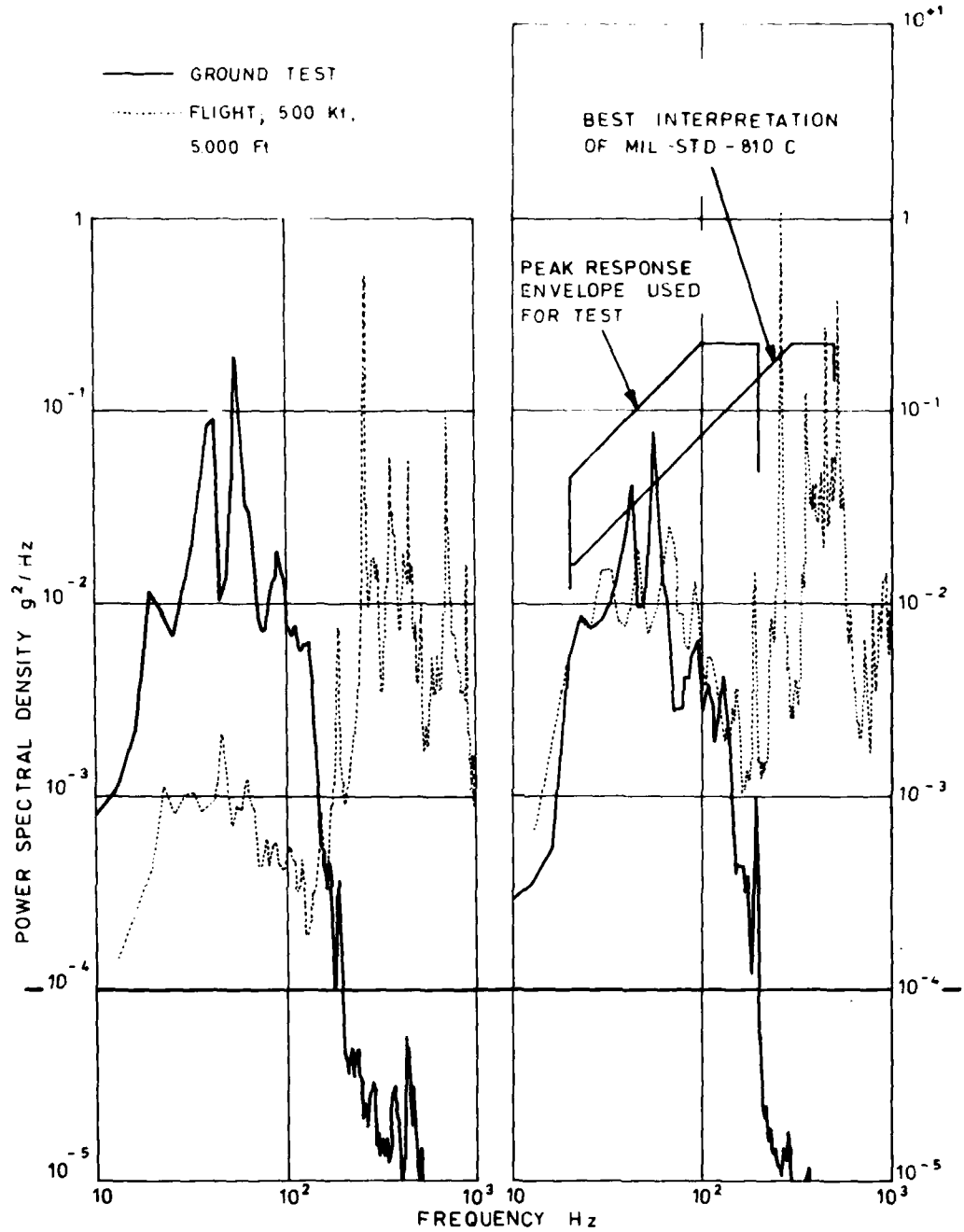
Figure 9



VERTICAL RESPONSE
ANALYSIS BANDWIDTH 3.2 Hz

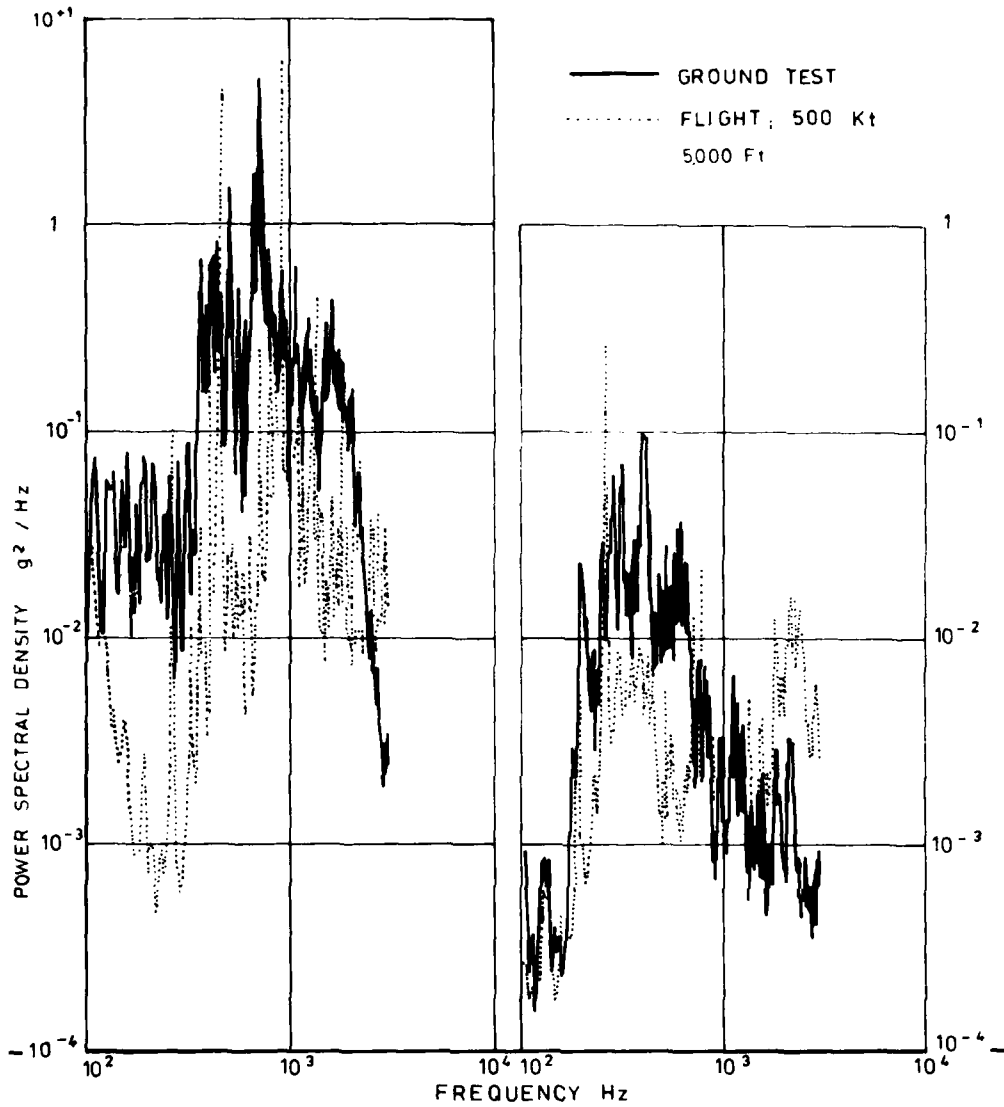
STORE No. 1
LOW FREQUENCY MECHANICALLY EXCITED TEST SPECTRA
COMPARED WITH FLIGHT SPECTRA, FORWARD END.

Figure 10



VERTICAL RESPONSE
ANALYSIS BANDWIDTH 3.2 Hz
STORE No. 1
LOW FREQUENCY MECHANICALLY EXCITED TEST SPECTRA
COMPARED WITH FLIGHT SPECTRA, AFT END

Figure 11



FORWARD BULKHEAD

FORWARD LUG POCKET

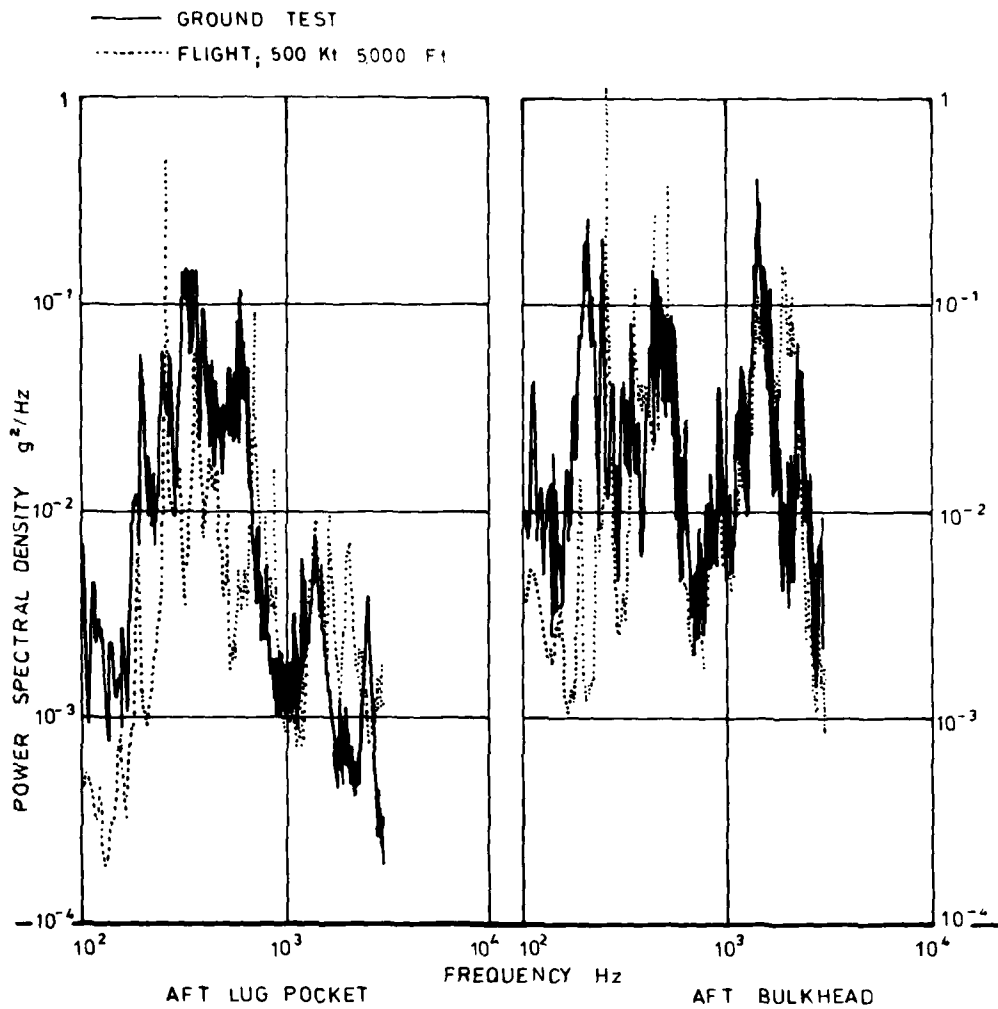
VERTICAL RESPONSE

ANALYSIS BANDWIDTH 3.2 Hz

STORE No. 1

HIGH FREQUENCY ACCOUSTICALLY EXCITED TEST SPECTRA
 COMPARED WITH FLIGHT SPECTRA, FORWARD END.

Figure 12

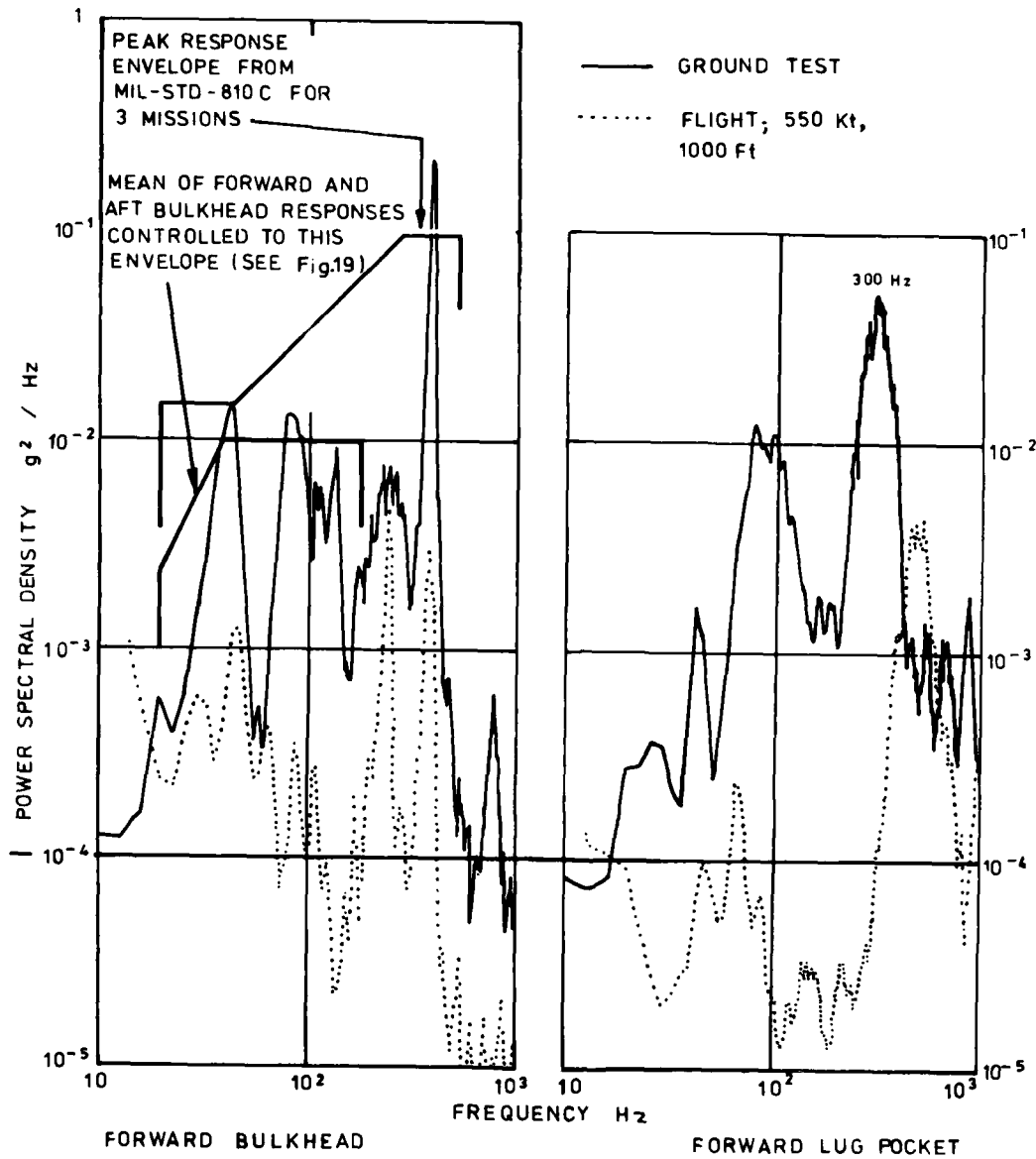


VERTICAL RESPONSE
 ANALYSIS BANDWIDTH 3.2 Hz

STORE No 1

HIGH FREQUENCY ACOUSTICALLY EXCITED TEST SPECTRA
 COMPARED WITH FLIGHT SPECTRA; AFT END

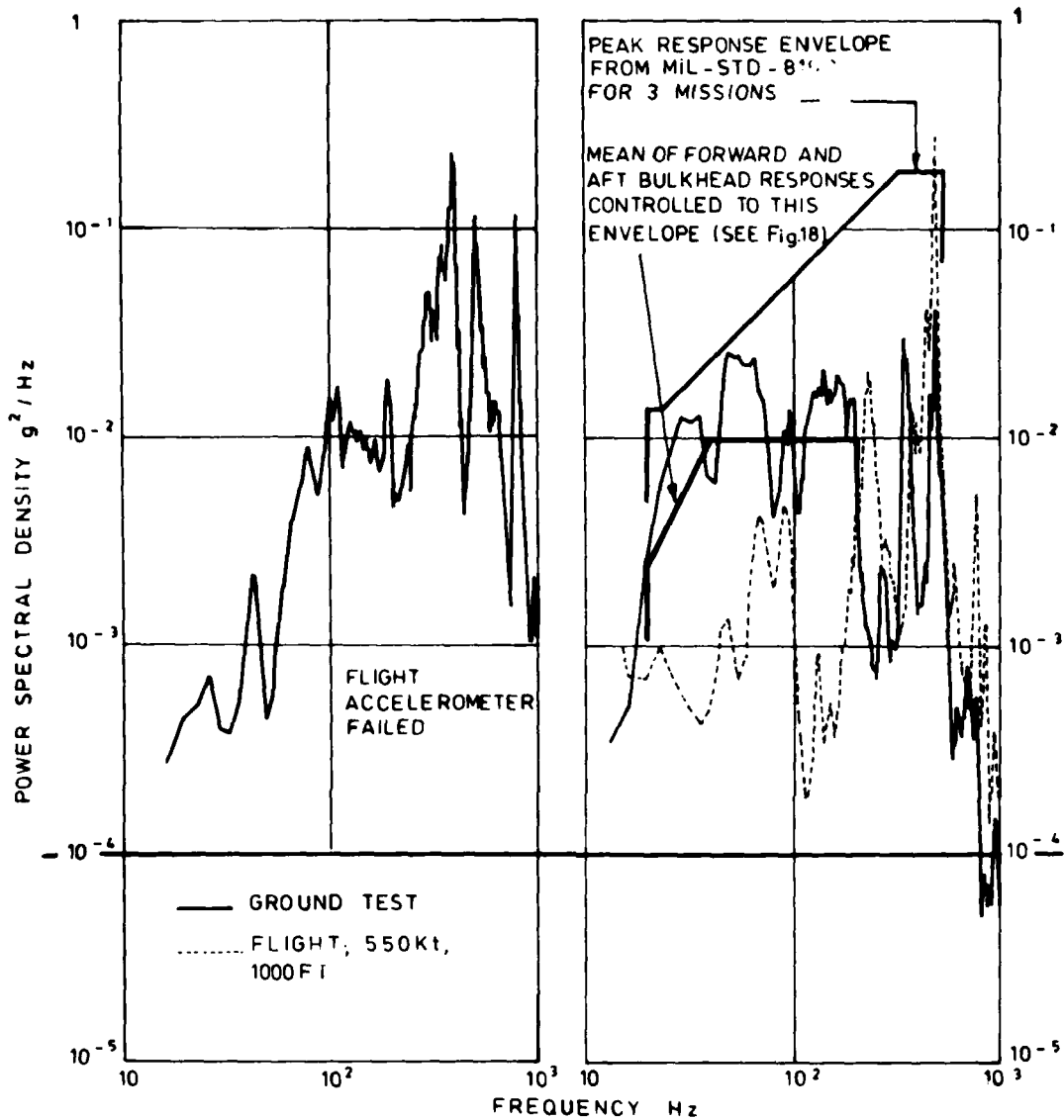
Figure 13



VERTICAL RESPONSE
 ANALYSIS BANDWIDTH 3.2 Hz
 STORE No 2

LOW FREQUENCY MECHANICALLY EXCITED TEST SPECTRA
 COMPARED WITH FLIGHT SPECTRA;
 FORWARD END

Figure 14



MIDWAY BETWEEN STORE
SUSPENSION POINTS

AFT BULKHEAD

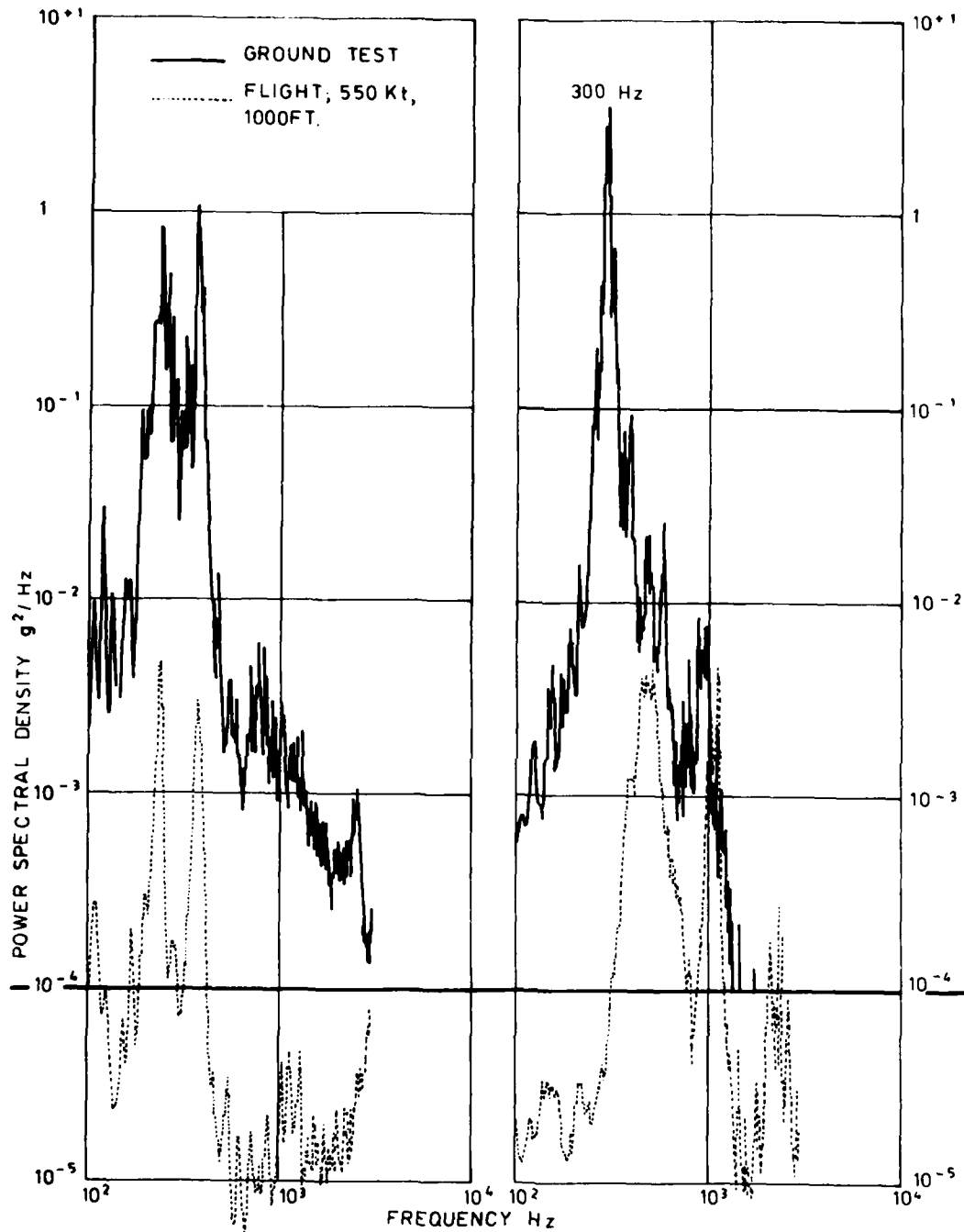
VERTICAL RESPONSE

ANALYSIS BANDWIDTH 3.2 Hz

STORE No 2

LOW FREQUENCY MECHANICALLY EXCITED TEST SPECTRA
COMPARED WITH FLIGHT SPECTRA, AFT END

Figure 15



FORWARD BULKHEAD

VERTICAL RESPONSE

FORWARD LUG POCKET

ANALYSIS BANDWIDTH 3.2 Hz

STORE No 2

HIGH FREQUENCY ACOUSTICALLY EXCITED TEST SPECTRA
 COMPARED WITH FLIGHT SPECTRA, FORWARD END

Figure 16

**PROGRES DANS L'ELABORATION
DES PROGRAMMES D'ESSAIS D'ENVIRONNEMENT MECANIQUE**

par

M.Coquelet
Centre d'Essais Aéronautique de Toulouse
23 Ave Henri Guillaumet
31056 Toulouse Cedex
France

Les équipements aéronautiques, qu'ils soient placés dans des charges extérieures ou dans toute autre partie de l'avion, sont soumis aux vibrations d'ambiance créées par le vol (engendrées par les moteurs, par l'aérodynamique ou par l'utilisation des armements).

Se pose alors à l'ingénieur concepteur de système le problème de la qualification de ces équipements vis-à-vis de ces contraintes vibratoires :

- Quelle procédure de qualification appliquer ?
- Quelle sévérité adopter pour " couvrir " l'utilisation de l'équipement ?

1°) Les normes d'essais de vibration d'équipements

La réponse aux questions posées plus haut peut se chercher dans une certaine expérience issue du passé et qui est concentrée dans certaines normes ou documents dont les principaux sont les suivants :

- MIL-STD-810 B, élaborée aux USA en 1967 et dont sont issues en grande partie les normes françaises AIR 7304 (1972) et G.A.M-T-13 (1979).
- J G 100 britannique élaborée en 1969.
- MIL-STD-810 C élaborée aux USA en 1975 et qui introduit de nouvelles méthodes d'élaboration du spectre vibratoire fondées sur une analyse des facteurs de dimensionnement, en particulier pour les charges extérieures.
- ED14A/DD160A (ref.3). Ce document a été élaboré sur une base internationale et donne des critères de sévérité pour les avions civils.

Devant l'abondance de cette documentation, on pourrait penser que tout a été dit et écrit et qu'il paraît difficile de progresser dans le domaine de l'amélioration des conditions de qualification des équipements.

Il est à porter au crédit des rédacteurs des normes qu'ils aient eu la sagesse de toujours préciser que celles-ci n'étaient qu'un guide et que " s'il était établi que l'équipement était soumis à un environnement estimé différent de celui indiqué dans la norme, il était préférable de le prendre en compte ".

On perçoit donc les limites inhérentes à ces documents : ils donnent une idée générale des niveaux de vibration auxquels on peut s'attendre mais ne peuvent prétendre couvrir avec précision toutes les configurations d'installation d'un équipement sur n'importe quel avion.

C'est ainsi qu'un équipement qualifié selon une certaine norme peut éventuellement être dimensionné de façon insuffisante, ou à l'inverse être artificiellement handicapé du point de vue poids ou coût.

La prise de conscience de cet état de fait en France a conduit les industries et les administrations compétentes à entreprendre deux catégories d'action :

- Améliorer la qualité des normes, en approfondissant les critères de choix de sévérité. Cette action veut être menée sur une base internationale.
- Se donner les moyens de mesurer, quand cela est nécessaire, l'environnement vibratoire réel à l'emplacement d'un équipement, afin d'en tirer un programme d'essai plus réaliste.

La première partie de cette conférence traitera donc des mesures vibratoires relevées en vol, la comparaison avec les normes ou documents.

La seconde partie exposera le point où en est la coopération internationale dans l'élaboration des normes.

2°) Mesures vibratoires relevées en vol

En 1976, il a été créé en France une banque de données des enregistrements vibratoires relevés sur avion. La gestion de cette banque a été confiée au Centre d'Essais Aéronautique de Toulouse, qui s'efforce de recueillir :

- les données disponibles sur les avions d'état français
- les données que peuvent lui apporter les constructeurs

L'ensemble de ces informations sont contenues dans divers documents qui couvrent les aéronaves les plus variés, tels que :

- A 300 B, Caravelle, Nord 260
- Cessna 411
- Nord 2501 et Transall
- Mirage F1, Jaguar, Alphajet, Mirage III, Mirage IV
- Mirage 2000.

Les planches n°1 à 9 présentent quelques résultats typiques contenus dans cette banque de données :

- Planche n°1 A 300 - Pylone central
- Planche n°2 C160-Transall - Plancher de soute
- Planche n°3 N2501 - Moteur droit
- Planche n°4 Caravelle - Bâti d'essai en cabine
- Planche n°5 Mirage III - Mesures sur réacteur
- Planche n°6 Mirage F1 - Soute radio arrière
- Planche n°7 Alphajet - Radio sonde
- Planche n°8 Mirage 2000 - Gonio
- Planche n°9 Mirage F1 avec charge ventrale - Attache avant

Les planches présentées montrent qu'une synthèse générale de ces informations n'est pas aisée. Cependant, les conclusions générales qui se dégagent indiquent :

- Le DD160-ED 14 présente des niveaux d'essai assez réalistes, sauf en ce qui concerne les basses fréquences.
- La norme MIL-STD-810 C ne rend pas compte de phénomènes ponctuels tels que les fréquences moteur ou le comportement localisé des charges extérieures.

3°) Etablissement des spectres d'essai à partir des données relevées en vol

La banque de données une fois constituée, il importe de pouvoir l'exploiter pour pouvoir extraire des spécifications d'essai, destinées à être insérées dans une norme ou non.

En effet, il n'est la plupart du temps pas réaliste de vouloir couvrir la vie d'un équipement en simulant les centaines voire milliers d'heures sur un excitateur, pour des raisons évidentes de coût et de délai.

On est donc amené à élaborer des méthodes de compression de temps telles que les essais ainsi effectués restent représentatifs du comportement de l'équipement sur avion.

En France, ce problème s'est posé en première urgence dans le domaine des missiles qui sont soumis à des contraintes vibratoires essentiellement dans les phases de transport logistique et d'emport tactique.

Un groupe de travail de spécialistes a été constitué au Bureau de Normalisation pour l'Aéronautique et les résultats de ses travaux font l'objet d'une série de Recommandations (voir ref.2).

- RE Aéro 612-10 - Généralités
- RE Aéro 612-11 - Guide de choix des méthodes d'établissement des spécifications d'essai
- RE Aéro 612-12 - Méthodologie
- RE Aéro 612-13 - Etablissement des spécifications d'essais par la méthode des enveloppes de densité spectrale
- RE Aéro 612-14 - Etablissement des spécifications d'essais par la méthode d'équivalence des niveaux extrêmes ou du dommage par fatigue
- RE Aéro 612-15 - Etablissement des spécifications d'essais par la méthode d'élimination des valeurs non contraignantes
- RE Aéro 612-16 - Synthèse-type des niveaux rencontrés sur véhicules terrestres (612-16)
à 18 marins (612-17) et aériens (612-18)

schématiquement ces différentes méthodes reposent sur les principes suivants :

1.1 - Méthode des enveloppes de densité spectrale (voir Ref. 11, 12)

- Augmentation générale des niveaux d'essai mais sans dépasser les valeurs maximales de l'environnement réel.
Durée d'essai : jusqu'à 20% de la durée réelle d'emploi.
- Augmentation des niveaux faibles mais sans jamais dépasser les valeurs maximales de l'environnement réel.
Durée de l'essai : 4 à 10% de la durée réelle d'emploi.
- Augmentation générale des niveaux de 10 à 20% par rapport à l'environnement réel.
Pour les vibrations aléatoires, 4 à 10% de la durée réelle d'emploi.

1.2 - Équivalence des niveaux extrêmes ou dommages par fatigue (voir Ref. 11, 12)

Cette méthode consiste à :

- Déterminer les contraintes extrêmes apportées par l'environnement réel.
- Déterminer les contraintes de fatigue
- Condenser ces deux éléments en une spécification d'essai unique

Durée d'essai : 20 à 50% de la durée réelle d'emploi.

1.3 - Élimination des valeurs non contraignantes (voir Ref. 11, 12)

Le processus est le suivant :

- Tous les niveaux de l'environnement réel inférieurs à un seuil arbitrairement choisi ne sont pas pris en considération.
- Tous les niveaux dépassant le seuil sont classés en amplitude et fréquence et groupés pour former des séquences d'essai.

Durée d'essai : 3 à 5% de la durée réelle d'emploi.

L'utilisation de ces différentes méthodes suppose la connaissance de l'environnement réel. A titre expérimental, il a été établi des synthèses-type qui donnent une idée de l'environnement réel en l'absence de mesures particulières.

Des exemples de données synthétiques sont présentés planches n°10 et 11.

A titre d'exemple, l'élaboration de spécifications-cadres pour un projet d'avion déterminé est présenté planche 12.

4°) Progrès dans la coopération internationale

Dans le domaine de l'aviation commerciale, une tradition de coopération internationale s'est progressivement développée depuis 10 ans environ au sein de la RTCA et de l'ECARF.

Le DO 160-ED 14 a été issu en 1975 sur la base d'un travail auquel ont participé des représentants des USA, de la Grande-Bretagne, de la RFA, de l'URSS et de la France.

En 1978-79 a été entreprise la première révision du document, édité en 1980 sous la référence DO 160A - ED14A qui présente des améliorations substantielles par rapport à la première version de 1975.

La philosophie de ces améliorations, fondée sur l'expérience européenne de Concorde, a été exposée au 48ème SMP à Williamsburg par MM. PAYNE & NAYLER de British Aerospace (voir Ref. 13).

La préparation du DO 160 A - ED 14 A a été menée à bien dans un esprit de coopération remarquable, à tel point que ce document a été transformé en norme ISO sous la référence ISO-7137, et a reçu l'approbation de l'unanimité moins une voix et 3 attentions des états membres.

Pour ce qui est de l'aviation militaire, la coopération n'est pas, à ce jour, aussi étroite. Il existe des normes nationales rédigées dans un esprit différent d'un pays à l'autre, rendant difficile la comparaison de qualité d'un équipement que l'on désirerait monter sur un avion construit dans un autre pays.

D'autre part, les programmes en coopération récents, en particulier la Nacelle ALLIS (Thomson CSF - Martin Marietta) impose une définition commune de spécifications.

Ceci a donc conduit l'ASTI (Association pour les Sciences et Techniques de l'Environnement) à prendre contact avec ses homologues américains, britanniques et allemands pour tenter de réfléchir ensemble à l'amélioration de la norme américaine MIL-STD-810 C.

un symposium réunissant les spécialistes concernés s'est tenu à Paris les 18 et 19 octobre 1961 (voir compte-rendu en pièce 1).

Au cours de ce symposium,

- les intellectuels européens ont fait part des difficultés d'adaptation et les adaptations à apporter à la norme MIL-STD-883.
- les intellectuels américains ont présenté les grandes lignes du projet de MIL-STD-883, devant être adopté en 1962.

En conséquence, et au vu de l'expérience faite par l'Armée, l'Etat des progrès de coopération est le principal motif aux premiers projets de MIL-STD-883 (voir réf. 1) qui ont été envoyés à l'Etat des Pays-Bas.

Il n'est pas évident, en ce sens le sentiment, en France, que la norme MIL-STD-883 présente de graves inconvénients par rapport à la MIL-STD-883, mais que les adaptations sont d'ordre secondaires, et affectent surtout les matériels, de façon à ce qu'ils soient adaptés d'un document auquel on peut être satisfait que.

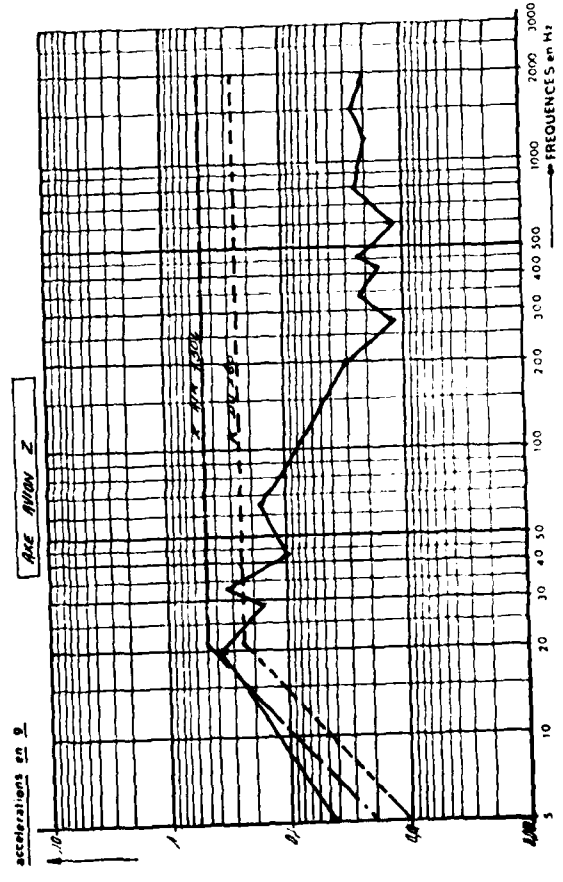
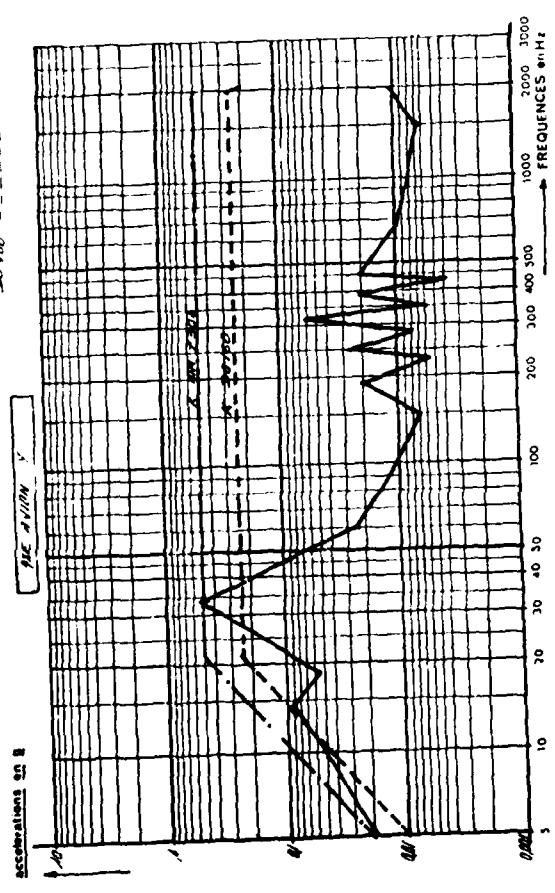
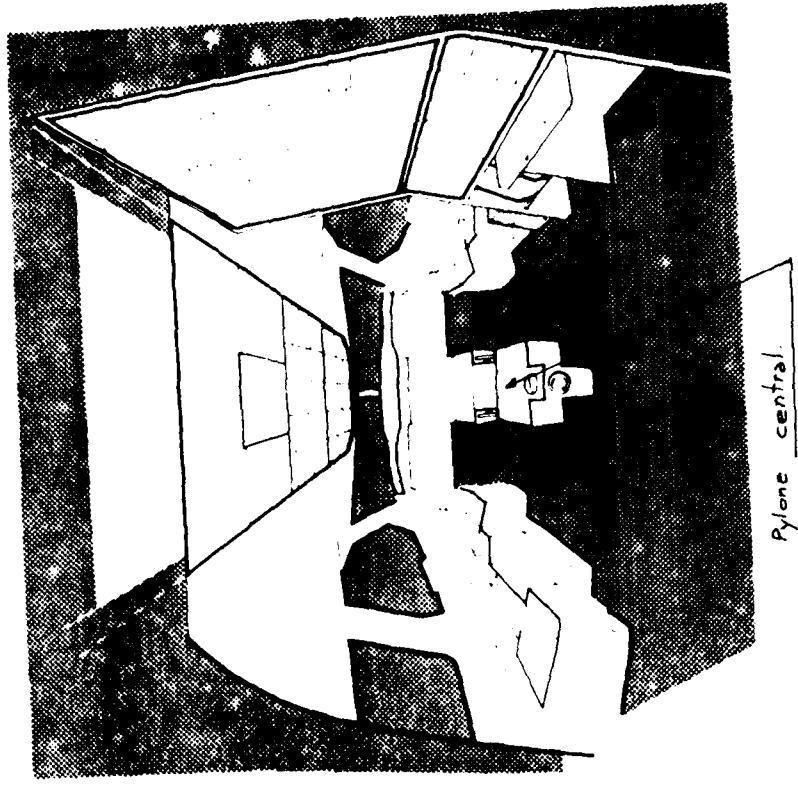
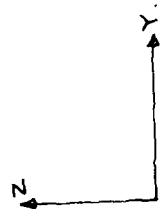
Il est à noter que l'Armée de l'Air a été particulièrement explicite et détaillé par MIL-STD-883 dans un article publié dans le journal de l'Armée de l'Air, réf. 2.

2.2. Bibliographie

- 1 - "Le matériel militaire" - aspects généraux et de détail - MIL-STD-883 (MIL-STD-883-4) - 1961, 1962
- 2 - "Le matériel militaire" - aspects généraux et de détail - MIL-STD-883 (MIL-STD-883-4) - 1961, 1962
- 3 - "Mil-STD-883 - Aspects généraux et de détail - MIL-STD-883 (MIL-STD-883-4) - 1961, 1962
- 4 - "Le matériel militaire" - aspects généraux et de détail - MIL-STD-883 (MIL-STD-883-4) - 1961, 1962
- 5 - "Le matériel militaire" - aspects généraux et de détail - MIL-STD-883 (MIL-STD-883-4) - 1961, 1962
- 6 - "Le matériel militaire" - aspects généraux et de détail - MIL-STD-883 (MIL-STD-883-4) - 1961, 1962
- 7 - "Le matériel militaire" - aspects généraux et de détail - MIL-STD-883 (MIL-STD-883-4) - 1961, 1962

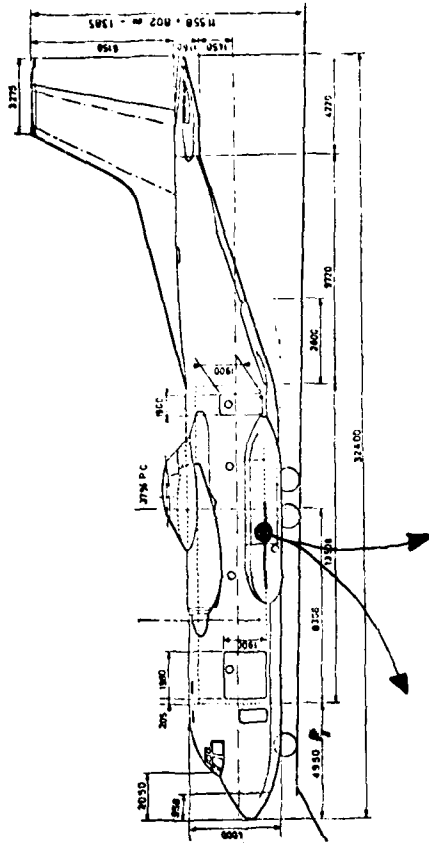
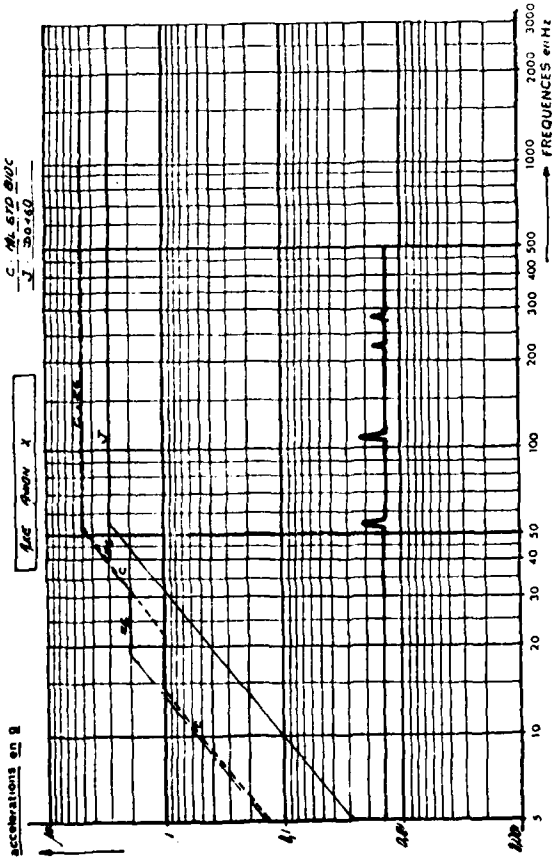
- Planche 1 -

AIRBUS A300

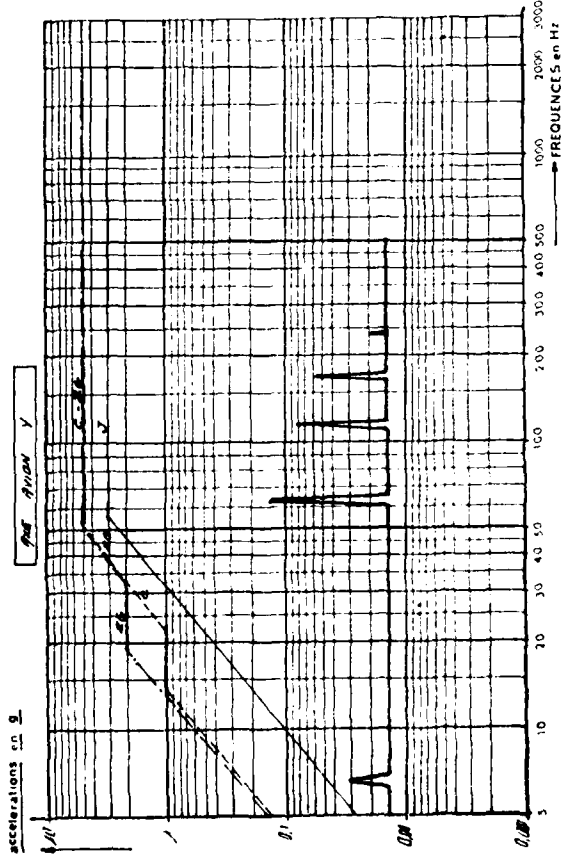
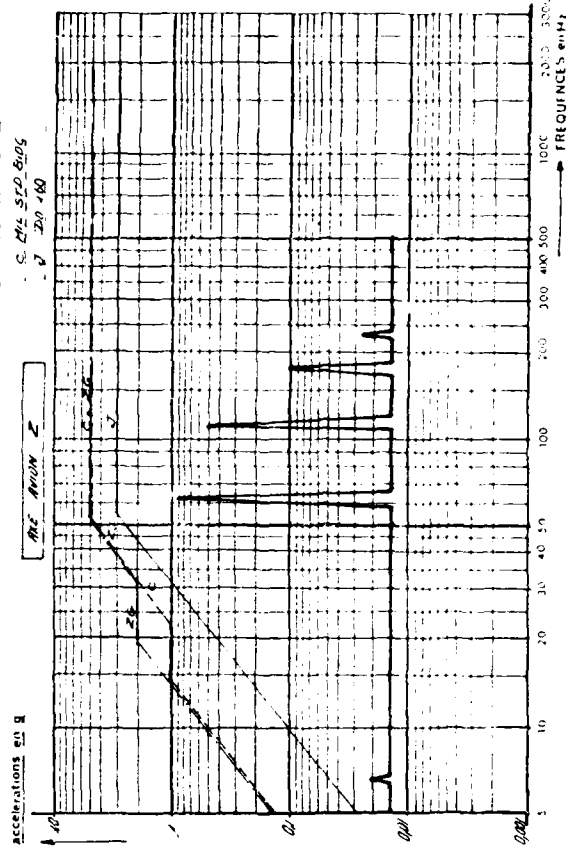


TRANSALL C 160

Z. 0. 007 7302
 C. 014 570 8105
 I. 30-10

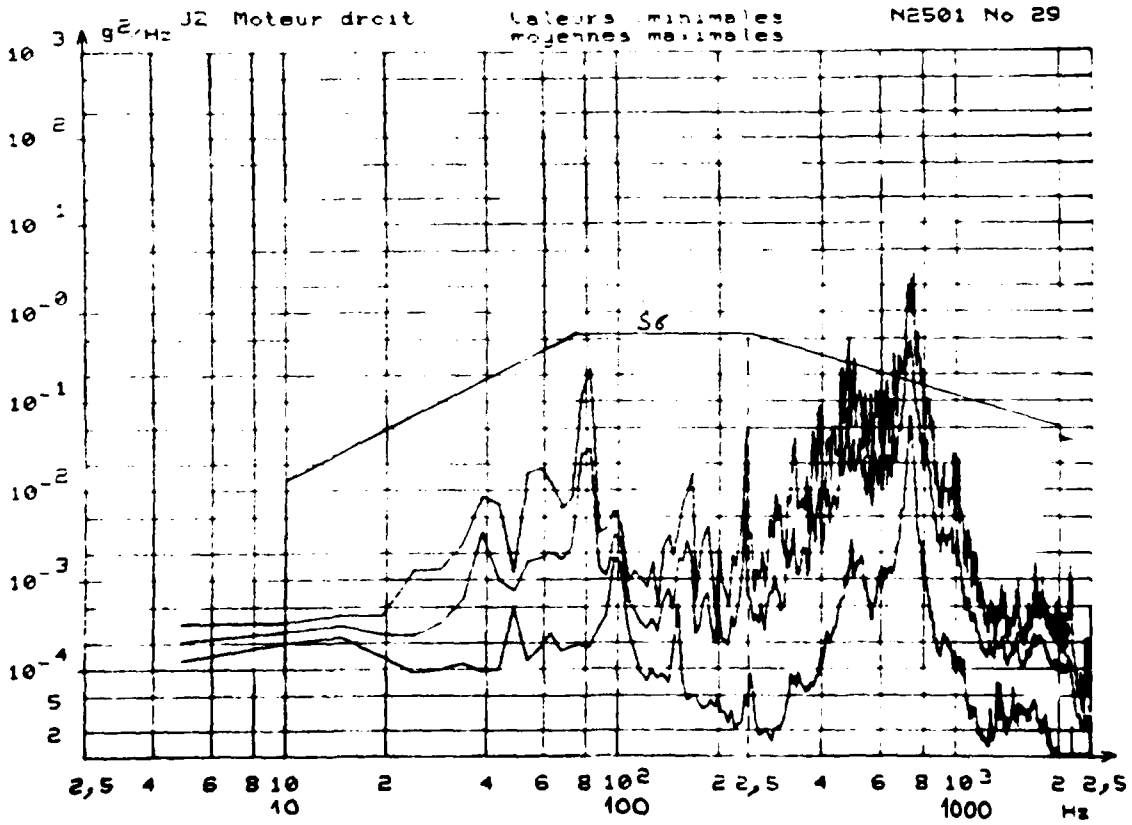
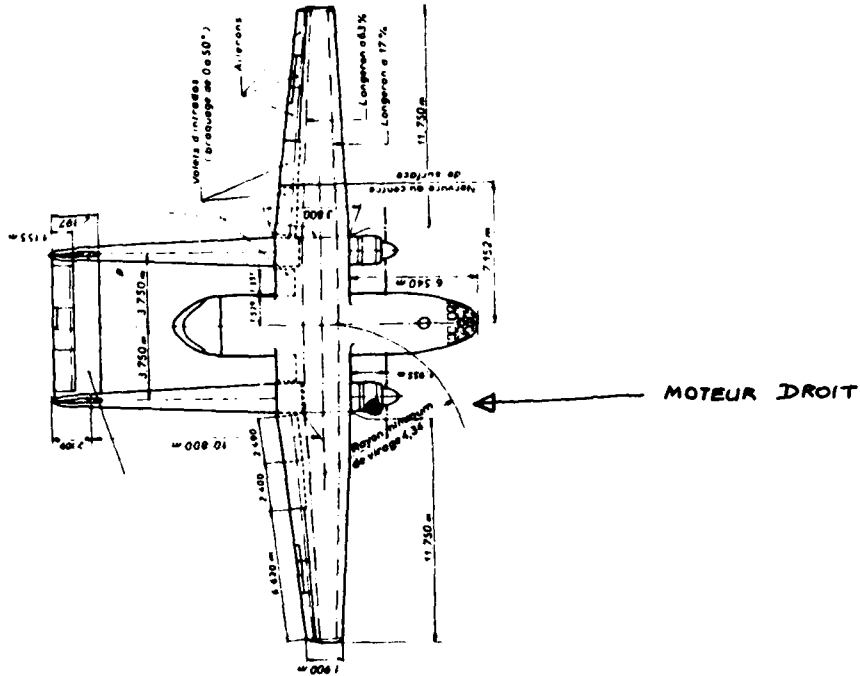


Z. 0. 007 7302
 C. 014 570 8105
 I. 30-10



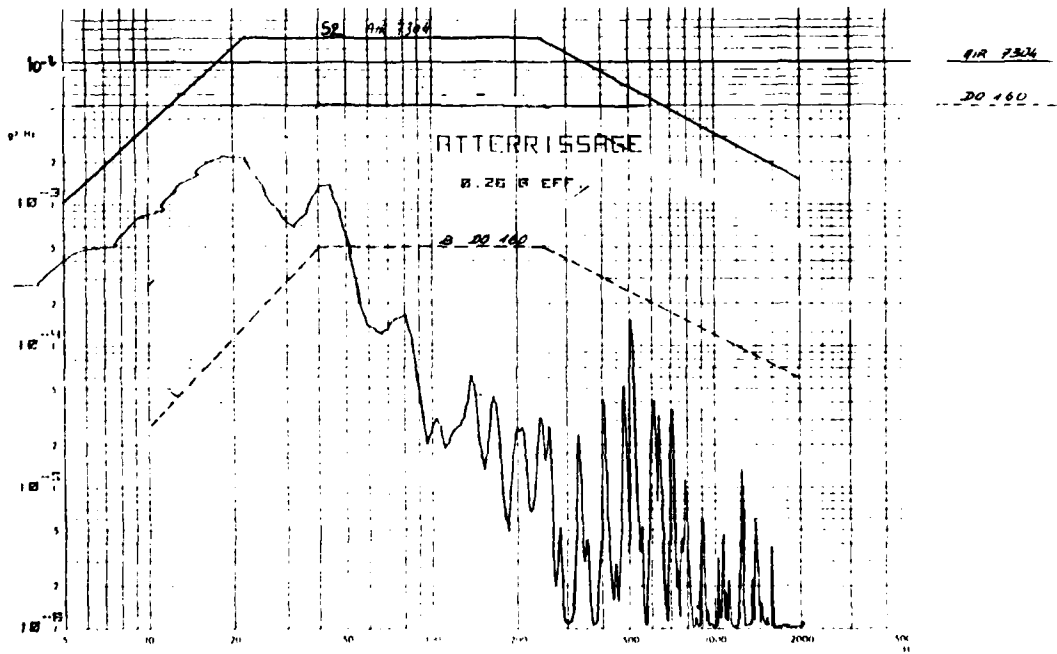
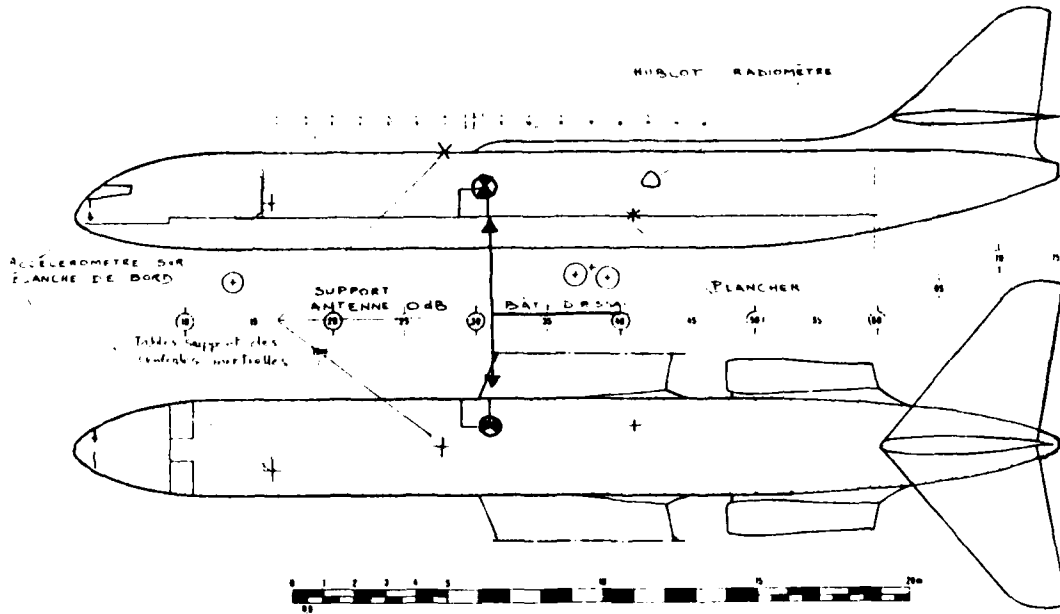
- Planche 3 -

NORD 2501



- Planche 4 -

CARAVELLE



ESSAI EN VOL NO 1 DU 13.5.76 NIVEAU IMPULSION 20

MATERIEL TEST SE 218 NO 118

ACCÉLÉROMÈTRE N° E2223D

INDICATEUR N° 7

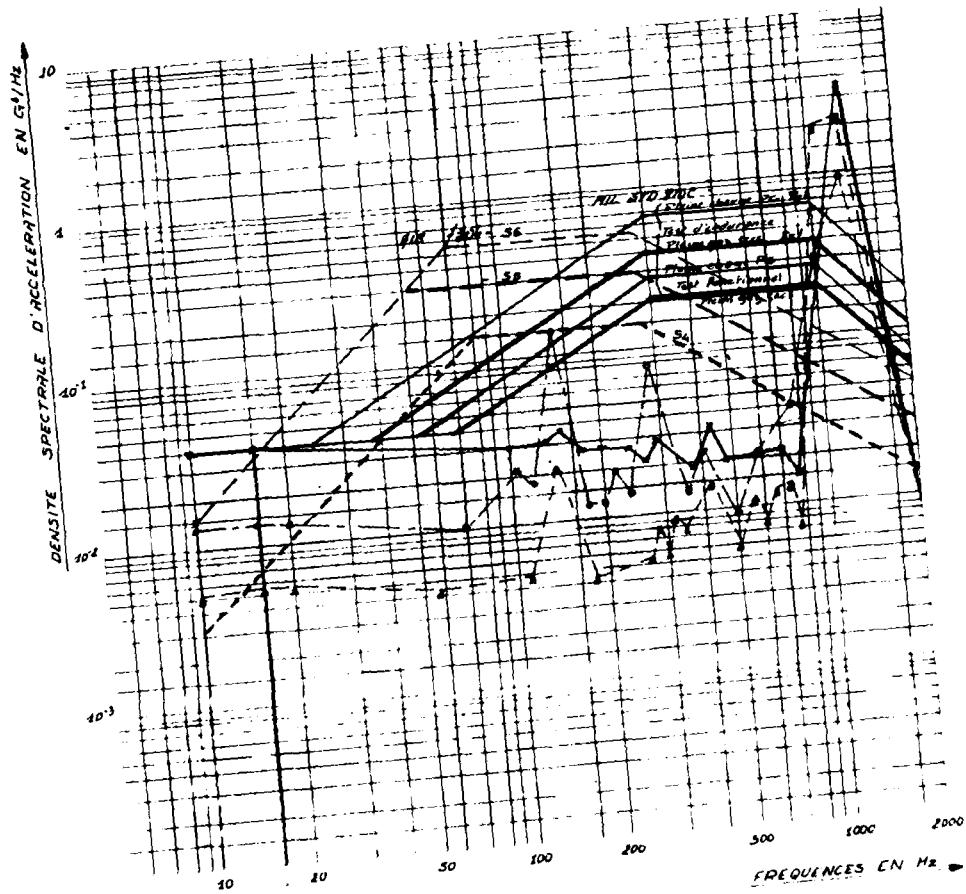
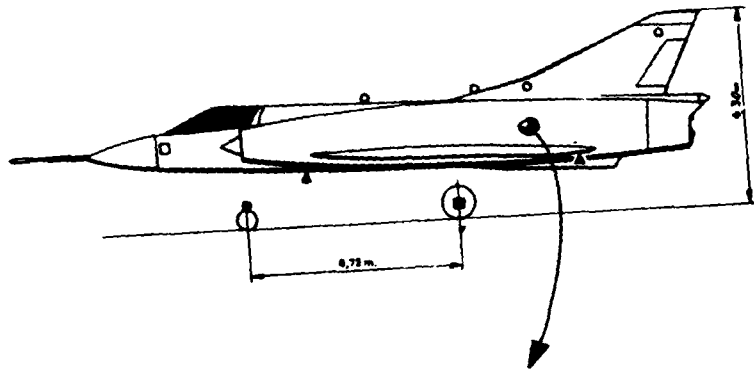
LABO D'ESSAI

DATE 15.6.1976

N° SÉRIAL N6811

ANNÉE 42

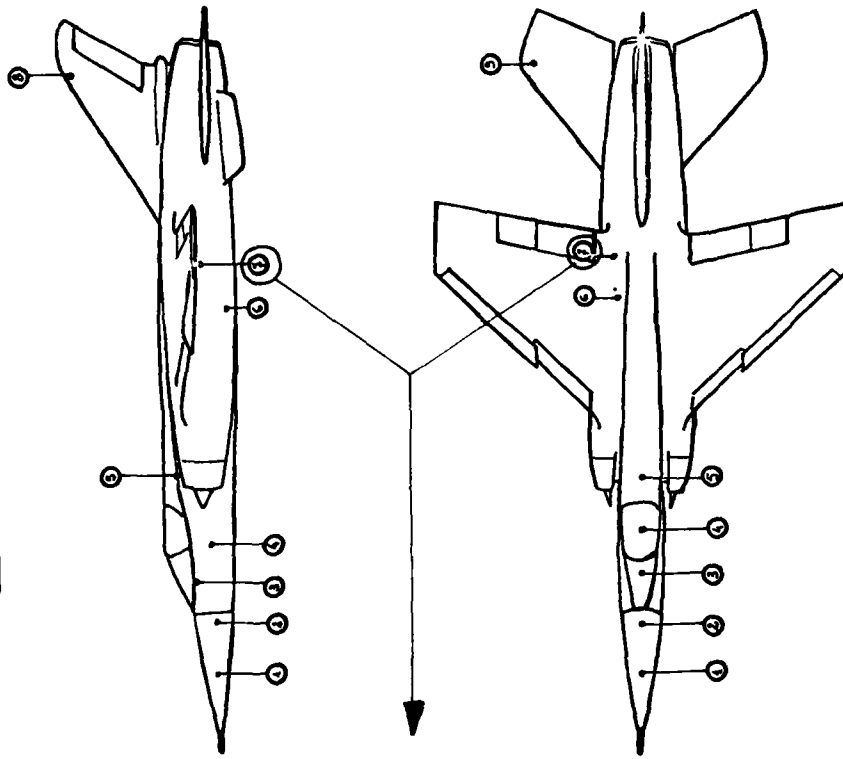
- Blanche 5 -
MIRAGE III



MIRAGE III A 07
 MESURES - REACTEUR
 SPECTRE ENVELOPPE DES VALEURS MAXIMALES
 POUR LES DOUZE PHASES DE VOL
 A12 - A11 - A10 - A9 - A8 - A7

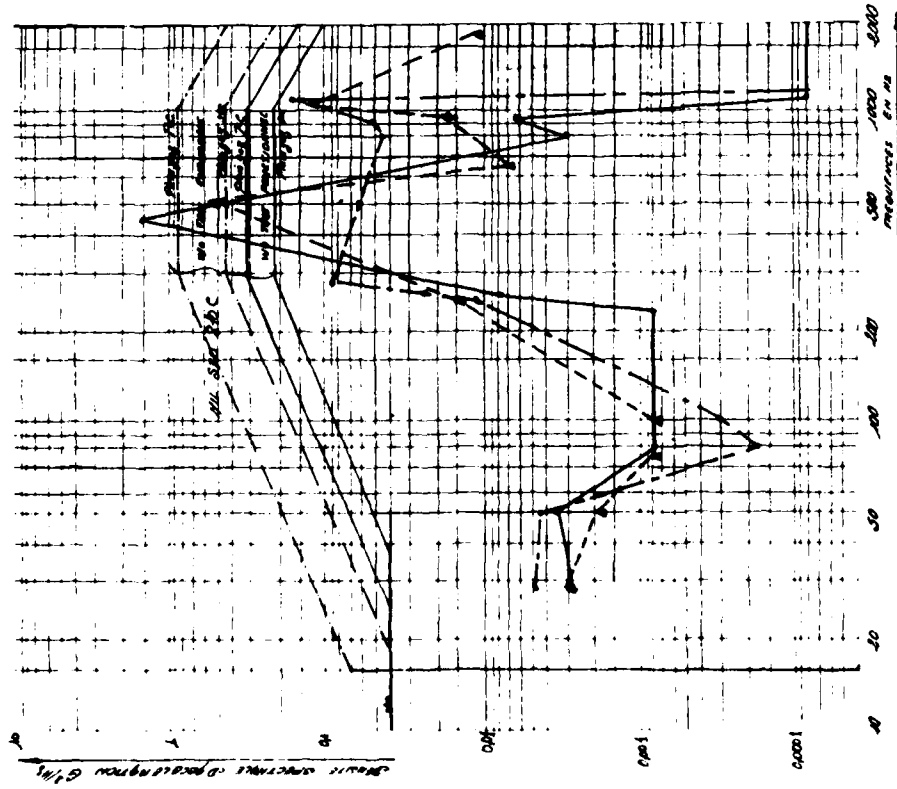
- Planche 6 -

- MIRAGE F1 -



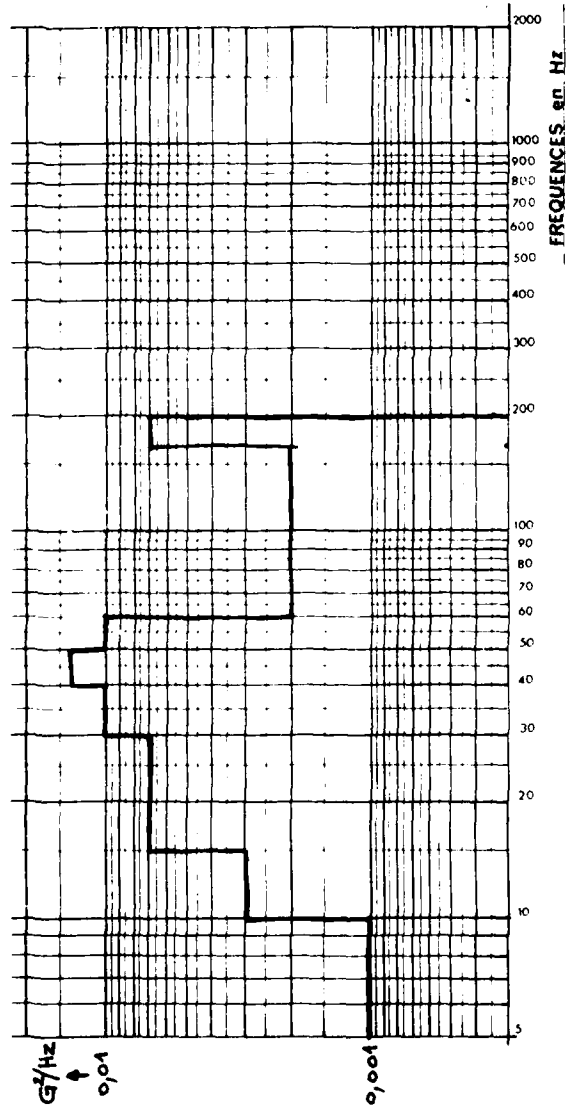
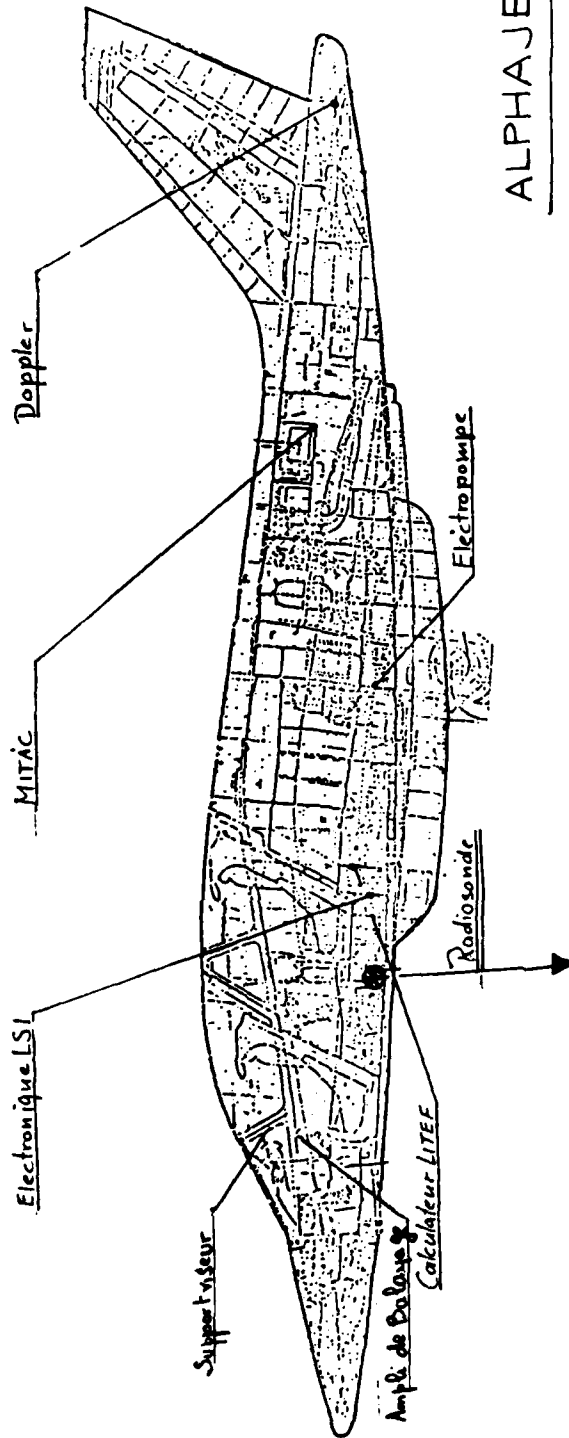
MIRAGE F1
POSITION DES PARTIES ETUDIÉES
ET DES ENREGISTREMENTS

MIRAGE F1
SUIVRE EQUILIBRE MANOEUVRE
PACS: X, Y, Z



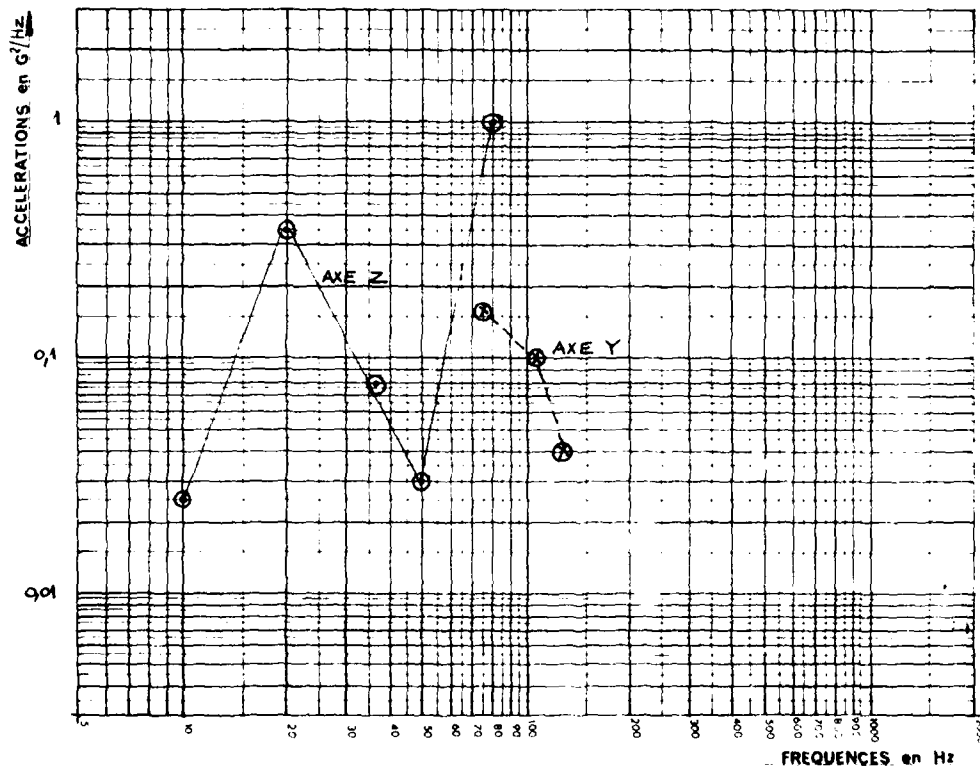
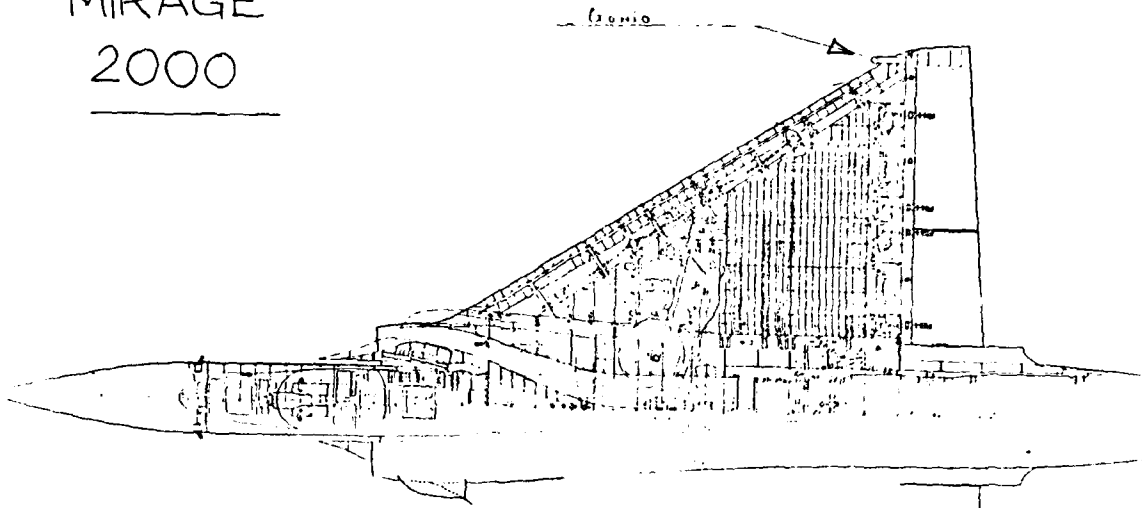
- Planche 7 -

ALPHAJET



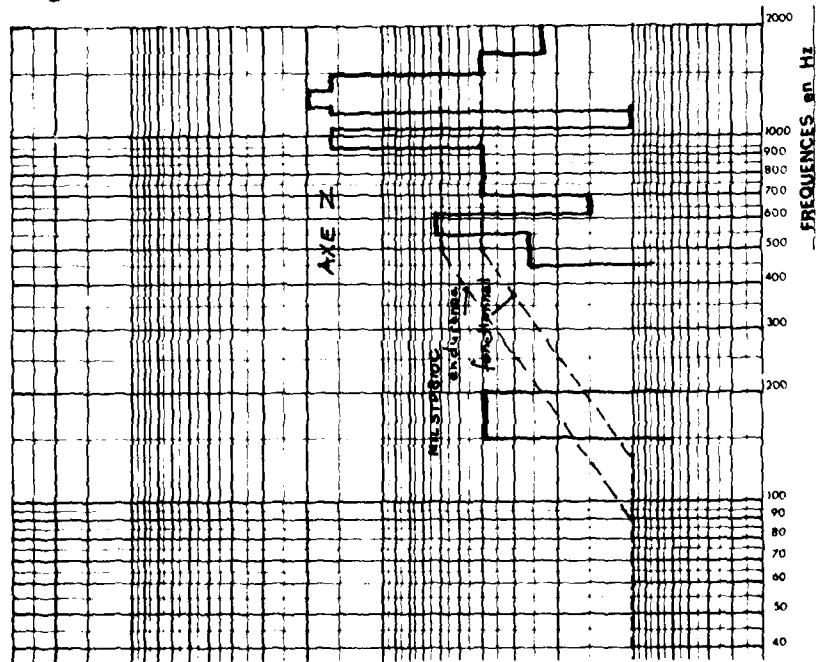
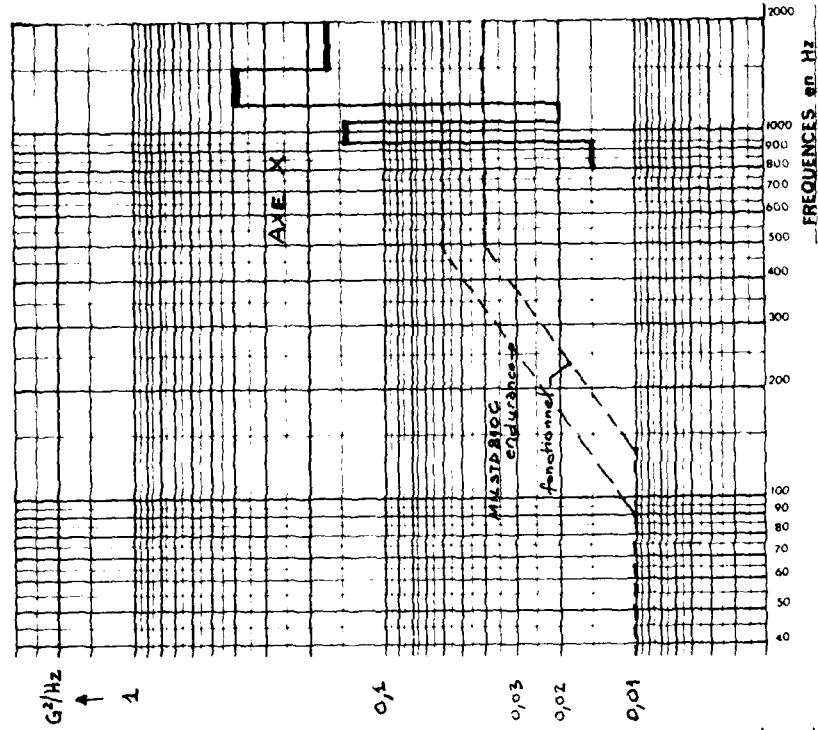
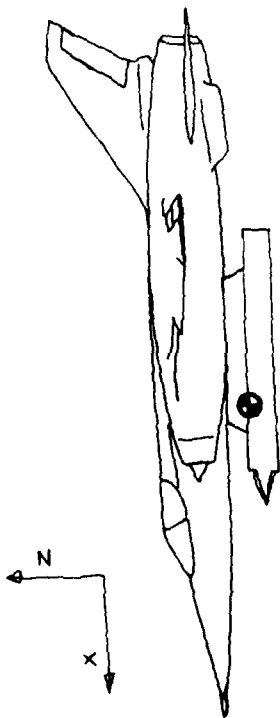
- Planche 8 -

MIRAGE
2000



- Planche 9 -

MIRAGE F1
AVEC CHARGE VENTRALE



FICHE DE SYNTHÈSE TYPE

1-NIVEAUX CRETE

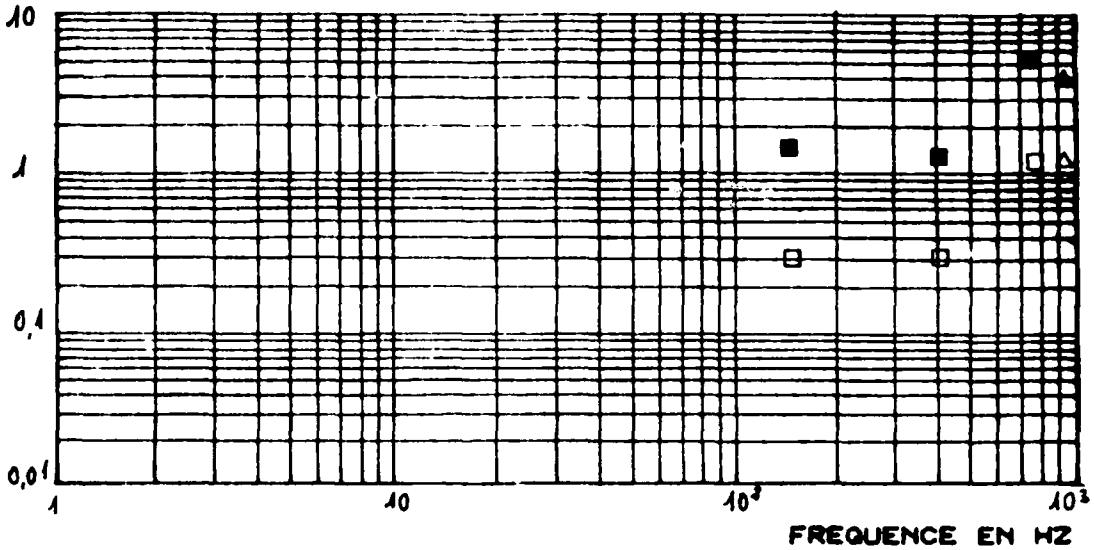
TOUS AXES

VEHICULES AERIENS

CATEGORIE C2

NIVEAUX | MAXIMA ■ ▲
LES PLUS FREQUENTS ▲ □ SITUATIONS

TOUTES CONFIGURATIONS ■ □
PALIER 600 KTS ▲ △

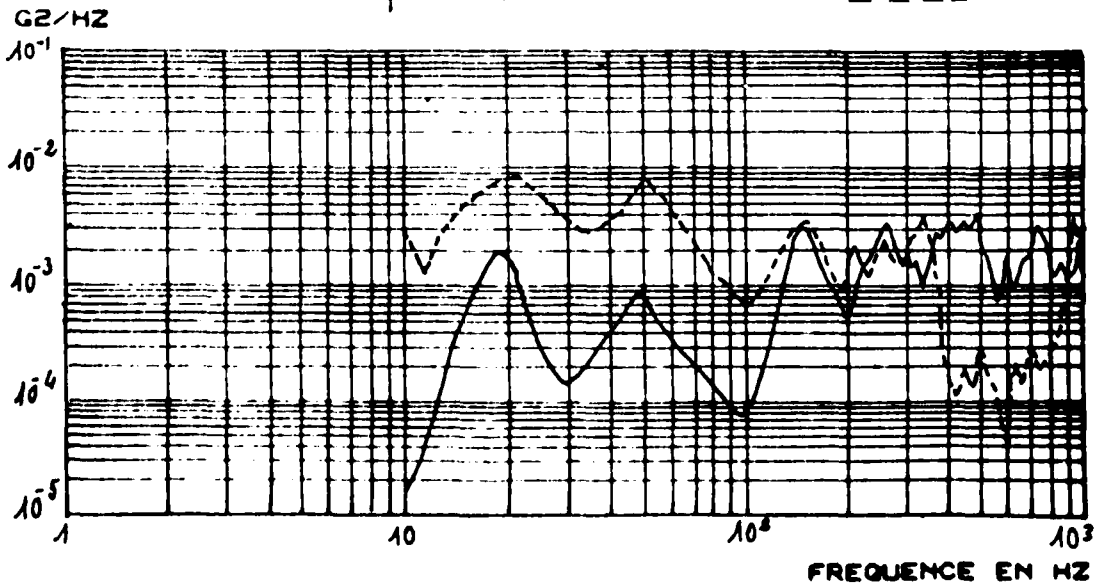


2-NIVEAUX EN G EFFICACES

SITUATIONS | TOUTES CONFIGURATIONS 0.6 G A 1 G
PALIER 600 KTS

3-ENVELOPPE DES DENSITES SPECTRALES MAXIMALES

LEGENDE | TOUTES CONFIGURATIONS ———
PALIER 600 KTS - - - - -



FICHE DE SYNTHÈSE TYPE

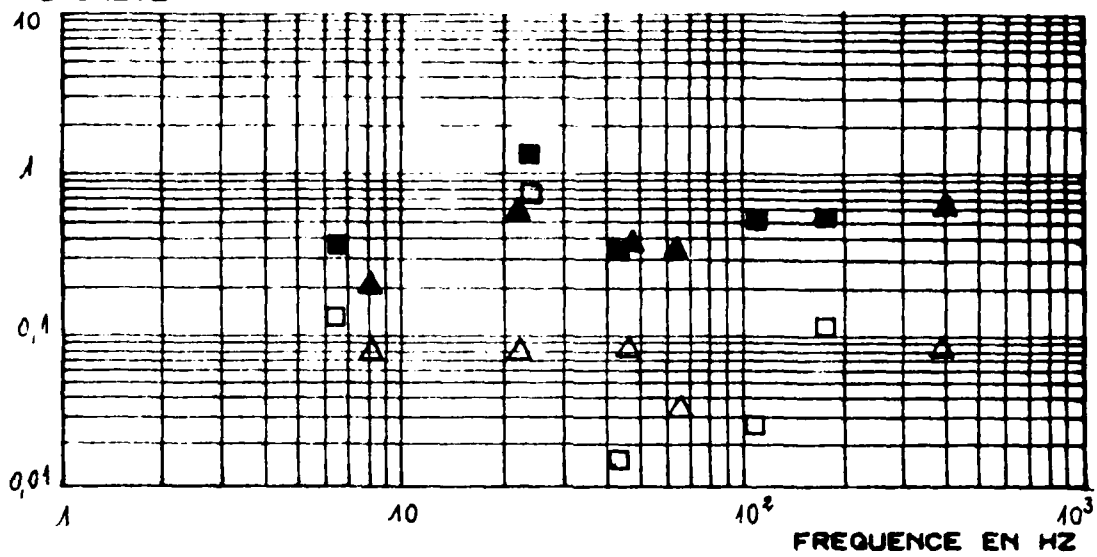
1-NIVEAUX CRETES

TOUS AXES

VEHICULES AERIENS

CATEGORIE B4

NIVEAUX	MAXIMA	■ ▲	SITUATIONS	TOUTES CONFIGURATIONS	■ □
	LES PLUS FREQUENTS	□ △		PALIER 100 KTS	▲ △

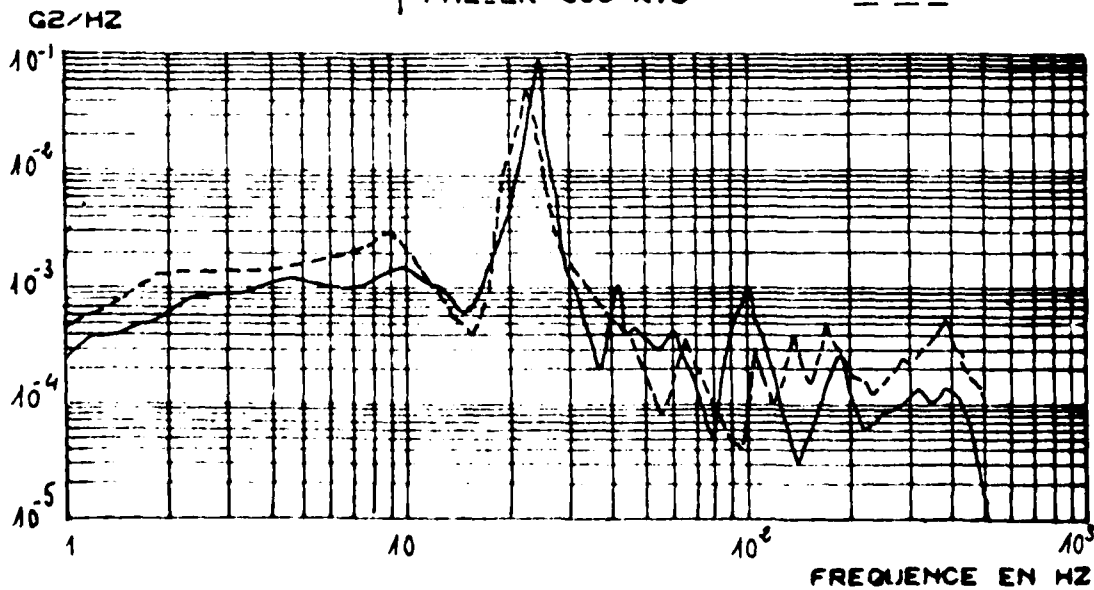


2-NIVEAUX EN G EFFICACES

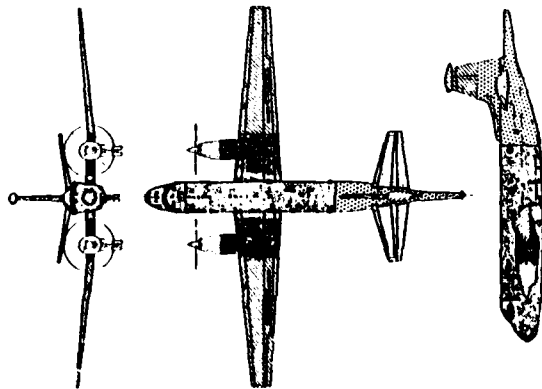
SITUATIONS	TOUTES CONFIGURATIONS	
	PALIER 100 KTS	0.28 G

3-ENVELOPPE DES DENSITES SPECTRALES MAXIMALES

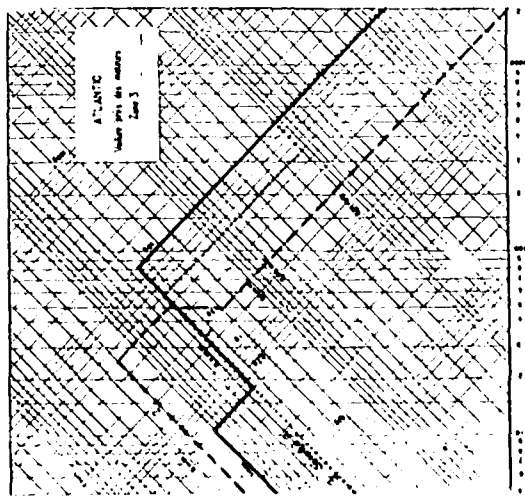
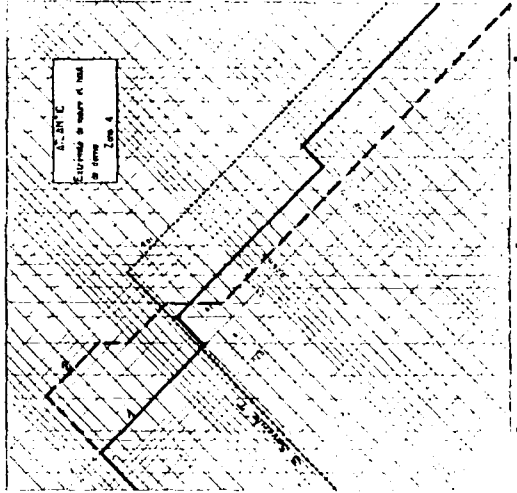
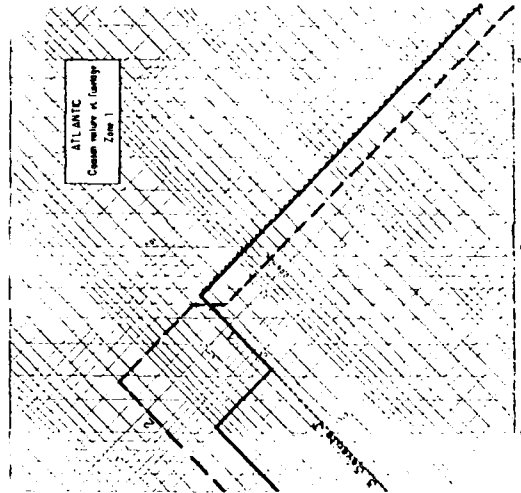
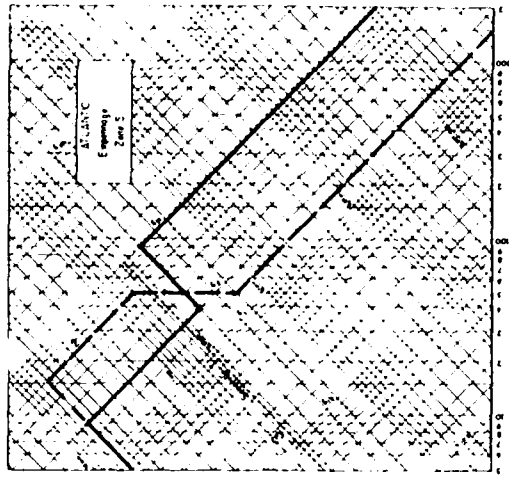
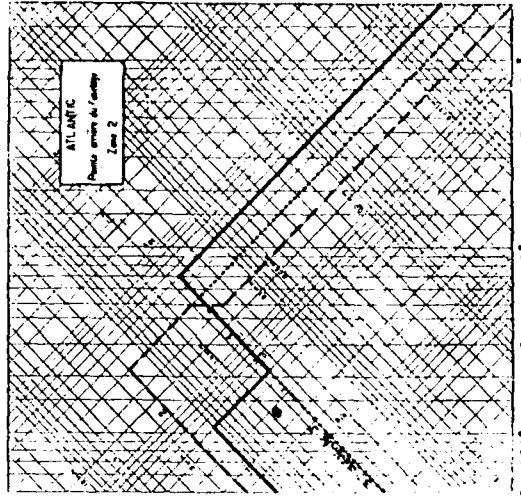
LEGENDE	TOUTES CONFIGURATIONS	—
	PALIER 100 KTS	- - -



ATLANTIC NOUVELLE GENERATION
SPECIFICATIONS EQUIPEMENTS



- 1. Equipement commercial de son and navigation propre, missile figé dans l'air.
- 2. Equipement monté sur l'appareil à l'origine de la zone 1.
- 3. Equipement monté sur l'appareil à l'origine de la zone 2.
- 4. Equipement monté sur l'appareil à l'origine de la zone 3.
- 5. Equipement monté sur l'appareil à l'origine de la zone 4.



QUALIFICATION OF EQUIPMENT FOR GUNFIRE INDUCED VIBRATION

by
A. Peacock
Group Leader Specialist Functions, Stress Office
British Aerospace Public Limited Company
Aircraft Group
Warton Division
Preston
U.K.

SUMMARY

For the Tornado Mk 1 aircraft, the method used to ensure that equipments withstand gunfire induced vibrations are described. The derivation of test spectra from rig and aircraft measurements is explained. Test failures and in service malfunctions are reviewed. A comparison with Mil specification is made. Proposals for research and for clearance of the next aircraft are given.

1. INTRODUCTION

The Tornado Mk 1 is a twin-engined, two seat, supersonic aircraft. It has a variable wing geometry to provide flexibility to meet the multi role requirements of its three sponsoring countries, West Germany, Italy and the United Kingdom. It is designed and manufactured jointly by MBB in West Germany, Aeritalia in Italy and British Aerospace, Warton Division in the United Kingdom.

British Aerospace have design responsibilities for the front fuselage in which the fixed armament, comprising 2 x 27 mm IWKA - Mauser cannon are installed. They can be fired at either High or Low rates of fire.

A large number of equipments are mounted in the vicinity of the gun and are therefore subject to the relatively brief but intense vibrations caused by gun firing.

Figures 1 - 6 illustrate the aircraft and the positions of the guns and equipment.

The methods used to ensure that the equipments withstand gunfire induced vibrations are described.

Recommendations for clearing future aircraft and for further research are made.

2. BACKGROUND

Since, at least, the early 1950's equipments have been cleared for use on aircraft by testing to levels completely defined by specifications such as Mil-Std 810 Method 514, USA, and BSG 100, UK, refs 1 and 2. The test vibrations applied were generally very severe compared with actual vibrations which occurred on aircraft, but did not cause undue hardship to the equipment designer, and resulted in an acceptable failure rate.

Until the mid 1960's no special design features or additional vibration qualification was required to cater for gunfire induced vibration. Nevertheless, equipment failures due to gunfire vibrations were infrequent.

About this time, due to introducing more powerful guns and changes in equipment design, eg. introduction of miniature amplifiers, measurements were made on several aircraft. Using data from aircraft F-4E, SUU-16 and F-5A, R.W. Sevy and J. Clark developed a gunfire vibration prediction technique, ref. 3, which was the philosophy behind the first gunfire vibration specification, ref. 4.

A major difference between this ref. 4 specification and refs. 1 and 2 specifications, was that it required random vibration testing, over the frequency range 150-2000 Hz, whereas clearance to refs. 1 and 2 could be achieved by sinusoidal testing. For more detailed comparison of spectra see paragraph 6.

3. EVALUATION

3.1 Initial Design

During the initial design phase, in the late 1960's, it was considered that:-

- . the failure rate due to gunfiring, of equipment qualified to ref. 1, would be acceptable.
- . until measurements become available, it was not possible to specify a realistic vibration level.
- . The ref. 4 gunfire vibration specification would be unrealistic.

- . For equipments close to the gun, it is not possible to meet the ref. 4 gunfire vibration requirements. Therefore, if ref. 4 is used, a large number of equipments would have to be repositioned.

Later information indicates that these assumptions are correct.

- . It was typical for designers to qualify equipments to the normal vibration requirements of ref. 1.

It was decided:-

- . To measure vibrations on a gun rig which consisted of a front fuselage.
- . Not to install anti-vibration mounts in the initial design.
- . To leave room to install anti-vibration mounts if measurements show that this is desirable.

3.2 First Measurements

3.2.1 On rig

The first vibration measurements were made on a gun rig, which represented the aircraft structural standard forward of Frame 8000, ie. the forward 8 metres of the aircraft. See figs. 5 and 6. The canopy was omitted and the cockpit area was empty apart from structure representing the ejection seats in mass. Equipment shelves and secondary structure were included. Equipments were represented by models or prototype units of the correct mass.

Vibrations were measured, in all three directions, at eighteen locations on shelves and on structure adjacent to shelf attachments. The levels were fairly high and significantly above the $.04g^2/Hz$, 'no test' level, of ref. 4.

3.2.2 On aircraft in Butts (Anti-Vibration Mounts Not Installed)

At this time the first prototype aircraft fitted with guns became available. It was installed in the butts and extensive vibration measurements were taken during gunfiring. Although different in detail the levels were similar to those measured on the rig.

3.3 Installation of Anti-Vibration Mounts

Equipment specialists advised that the levels which were measured on the equipments nearest to the gun muzzle could possibly result in redesign being required. It was desirable to reduce high frequency vibrations, about 100 Hz, say, but low frequencies, below 100 Hz, were not considered to be a problem. (It is noted that for testing to the ref. 4, Mil-Spec, the maximum level is applied over the 300-1,000 Hz range and vibrations are not applied below 150 Hz).

Therefore, for equipments mounted within 2.5 metres of the gun muzzles, other than those in the forward equipment crate (see fig. 5); anti-vibration mounts (which attenuate high frequencies but amplify low frequencies) were installed between structure and equipment shelves, or for equipment attached directly to structure, between the structure and equipment.

Since the resulting increase in deflection at the lower frequencies could reduce the accuracy of one of the pilots' instruments, the forward equipment mounting was not changed. The design of the main crate mounts included rubber bushes, which are a form of anti-vibration mount.

Anti-vibration mounts were not installed in the cockpits or at equipment or shelves more than 2.5 metres from the gun muzzles, since the measured levels were not as severe.

3.3.1 Gun Rig Measurements

This modification was made on the gun rig and vibrations again measured. As expected, the levels at higher frequencies were significantly attenuated, but at relatively low frequencies were amplified. However the 'no test' level $0.04g^2/Hz$ was exceeded on most equipments.

3.3.2 On aircraft in Butts (Anti-Vibration Mounts Installed)

Following installations of the anti-vibration mounts, the prototype aircraft was returned to the butts and extensive vibration measurements were again performed. In some cases, at some frequencies, the levels were higher than measured on the gun rig.

3.4 Clearance for Prototype Airfiring. Table Testing

Prior to airfiring, it was necessary to demonstrate that 'safety critical', ie. failure of which could result in loss of aircraft or crew, equipments would not fail or malfunction due to gunfire induced vibrations.

Each of the, approx. 30, safety critical equipments was installed on a vibration table and vibrated, to levels, measured on the aircraft during butt firing or on the rig, for five minutes in each axis.

In order to minimise delay between completion of butt firing and air firing, the first equipments were table tested to levels measured on the rig.

Where aircraft butt levels exceeded rig levels repeat testing to the butt levels was carried out.

If failures occurred, equipment was modified and the test repeated.

3.5 Prototype Aircraft Air Firing Trials Table Testing

3.5.1 Initial Trials

During the initial airfiring trials, the vibrations measured in each flight, were compared with the levels to which safety critical equipments had been tested, before clearing the aircraft for the next flight.

The airfiring levels were generally lower than the butt levels. However, for nine equipments, in one or more axes, air firing levels exceeded butt levels over part of the frequency range. For these equipments and axes, repeat table testing was carried out at the air firing levels.

Since, the increase in levels did not coincide with equipment resonant frequencies, the overall grms was less during air firing, and the rate of equipment malfunction had not increased as a result of gunfiring; it was not considered necessary to delay the next flight until table testing had been completed.

3.5.2 Full Prototype Clearance

During the aircraft life, the total duration of gunfiring will be more than 5 minutes. It was therefore decided to increase the table test time for each equipment and axes to a total of 15 minutes. In the additional testing, levels measured during air firing have been used.

3.6 Pre-Series Aircraft Measurements

A pre-series aircraft, with equipments and structure more representative of the production standard has been instrumented to measure gunfire induced vibrations.

Levels at the radar, which was not installed on the prototype aircraft, have been measured during butt firing and will be measured during air firing.

Measurements at a few of the same locations as for the prototype aircraft, generally showed similar levels. Therefore it was not necessary to repeat the table testing on any equipment.

3.7 Production Equipment Clearance

Production equipments which are either 'safety critical' i.e. failure of which could result in loss of aircraft or crew, or 'mission critical' i.e. failure of which could result in the mission being aborted, have been table tested to gunfire induced vibrations.

About 70 equipments were tested compared with 30 prototype equipments. The increase is due to a large number of safety critical equipments as well as the inclusion of mission critical equipments. (The number of safety critical prototype equipments is relatively small due to the aircraft being monitored by telemetry).

At several times in the whole programme a review was undertaken to see whether a pragmatic solution and demonstration by careful testing on the ground and in the air could suffice. However, in view of the importance of the programme, a rigorous approach was specified.

4. COMPARISON OF VIBRATION LEVELS. DERIVATION OF TABLE TEST SPECTRA

4.1 Measurements

During rig firing, vibrations were measured on wooden mass correct dummy equipments and also on aircraft structure, and equipment shelves.

On the aircraft during butt firing, measurements were made on safety critical equipments, and at a few locations on aircraft structure and equipment shelves. This involved the use of both ground and aircraft instrumentation.

During air firing, only 9 vibrations could be recorded during each shoot. But a switch allowed 3 different sets of 9 vibrations to be measured in each flight. In total measurements were made in all three directions on or adjacent to, about twenty equipments, and in one or two directions on or adjacent to a further ten equipments. The majority of the accelerometers were mounted on the equipments, with only a few mounted on the shelves adjacent to the equipments.

In every shoot a minimum of ten rounds were fired from the gun, single gun firing; or each gun, both guns firing.

4.2 Comparison of Levels

Levels during firing at the low rate of fire were generally lower than during firing at the high rate of fire but produced peaks at different frequencies, the gunfire rate and its harmonics.

The levels during flight are generally less than the levels during butt firing. But for some equipments the in-flight levels were higher over part of the frequency range, see fig. 7.

No change in vibration level with 'g' or speed has been observed see fig. 8. There is scatter between levels measured at nominally identical flight conditions see fig. 9.

On both rig and aircraft, vibrations were measured for two gun and single gun firing, and for both rates of fire.

4.3 Table Test Spectra

The method of obtaining table test spectra is shown in figure 10.

For initial clearance, prototype equipment was tested to the envelope of measured levels at the high rate of fire. The sinusoidal vibrations which occur at the gunfire frequency and its harmonics were not applied.

For clearance of production equipment and final clearance of prototype equipment, the test levels were the envelope of levels measured on aircraft or rig, increased by 3 dB over the full frequency range. This is a factor of 2 ($= \text{antilog } 10 \frac{3}{10}$) on (acceleration)² and a factor of 1.414 ($= \sqrt{2}$) on acceleration. The factor is similar to that used for aircraft metallic structures which are designed and tested to 1.5 times the maximum accelerations which are expected to occur. Sinusoidal vibrations which occur at the gunfire frequency and its harmonics were applied. The production equipment was tested to high and low rate of fire, and to butt levels. Since the test levels included a safety factor, it was not necessary to factor the test times, which are therefore based on predicted gun usage.

For initial prototype clearance, where the vibrations were measured on wooden dummy equipments on the rig, the dummy equipment was installed on the vibration table to obtain input test spectra. The test equipment was then installed on the table and the same input levels applied.

During table testing of prototype equipment to vibrations measured on aircraft, the control accelerometer on the test equipment was mounted at the identical position to the accelerometer on the aircraft, and it was no longer necessary to obtain input levels.

For many production equipments, vibrations measured on another equipment mounted on the same shelf were used. That equipment had to be installed on the vibration table in order to determine input spectra.

The test spectra for a typical equipment is shown in graphical and tabular form in figures 11 and 12 respectively.

5 EQUIPMENT FAILURES. TABLE TEST EXPERIENCE/SERVICE EXPERIENCE

5.1 Table Test Experience

During table testing, some circuit breakers tripped and contactors bounced. Design modification consisted of changing the local stiffness of the equipment structure upon which the breakers or contactors were mounted. One solution was to mount circuit breakers on a proprietary damping panel, the outer layers being metal and the inner layer a proprietary damping material.

Other failures consisted of nuts backing off, soldered joints failing and amplifiers coming loose from cards. These were easily solved by small changes in the locking method, position of hold down wires, or bonding to cards. Many of these failures were due to the quality control during build of the test box being lower than for aircraft equipment. Use of the correct quantity of 'Araldite', a proprietary glue, solved several of the problems.

5.2 In Service Experience

For the aircraft which has carried out the most gunfire, an analysis of the defect rate over a fifteen month period prior to airborne gunfire, and a fifteen month period during airborne gunfire trials, showed that gunfire vibration has little effect on defect rate either collectively or on individual items, see fig. 13. 16 equipment defects were attributed to gun firing vibration. These equipments all had faults that were highlighted during the firing of the guns. The faults, stripped threads, loose wires; earth wires disconnected, incorrect crimps and incorrectly fitted printed circuit boards would very likely have eventually been exposed during normal flying and were largely a function of quality control.

6. COMPARISON OF TEST SPECTRA WITH MIL-SPECS

For equipment installed in the forward equipment crate, a comparison of test spectra obtained from MIL SPECS, refs. 4 and 5, with the spectra we derived from measurements on aircraft is shown in figures 14 and 15. The levels measured during one air firing shoot are shown for comparison.

Major differences between the specifications are:-

6.1 Mil-Std 810B Method 519.1 Vibration Gunfire

Random vibration testing is required over the frequency range 150-2000 Hz, with constant maximum level between 300 and 1,000 Hz. No vibration below 150 Hz and no sinusoidal inputs are required.

Except for a reduction for equipments whose mass is greater than 80 lbs, the levels are completely defined by the distance of the equipment from the centroid of the gun muzzles and the kinetic energy of the rounds when leaving the muzzle. Levels decay with distance from the centroid of the gun muzzle.

Testing is for 15 minutes in each of the three axes.

If the maximum level is less than $.04g^2/Hz$ testing is not required.

6.2 Mil-Std 810C Method 5192 Vibration Gunfire

Random vibration applied over the range from 0.8 times the gunfire frequency to 2,000 Hz and swept sinusoidal vibrations at the gunfire frequency and its first three harmonics. (Sweep range is $0.8f_1$ to $1.2f_1$, $1.6f_1$ to $2.4f_1$, $2.4f_1$ to $3.6f_1$ and $3.2f_1$ to $4.8f_1$ where f_1 is the gunfire frequency).

Unlike 810B Method 519.1, the random level varies over the frequency range. In addition to energy of the round when leaving the gun muzzle, and distance from the centroid of the gun muzzles, the levels are dependent upon whether the equipment is mounted on primary or secondary structure, and other parameters such as distance from aircraft surface, whether the gun protrudes clear of the aircraft etc.

It is noted that, in this specification the energy of the rounds is 'explosive energy minus kinetic energy' whereas the 810B Method 519.1 it is 'kinetic energy' alone.

Testing is for 15 minutes in each of the three axes.

Unlike 810B Method 519.1, a minimum level below which testing can be deleted is not specified.

For equipments mounted on secondary structure, the random levels are up to 23 dB lower and the sinusoidal levels up to 17 dB higher than if they were similarly mounted but on a primary structure. See figs. 14 and 15.

6.3 BAe's Test Spectra

Random vibration is applied over the frequency range 10-2,000 Hz, and, if measured on aircraft, sinusoidal vibrations at the gunfire frequency and its first three harmonics.

Sinusoidal vibrations do not always occur and are rarely required at more than the gunfire and one other harmonic.

Total test time is 21 minutes in each of the three axes. (10 minutes to low rate of fire, airfiring, 5 minutes to high rate of fire, airfiring 1 minute high rate of fire butt firing).

6.4 Comparison

If the forward equipment crate is primary structure, which we consider to be the case, figures 14 and 15 show that the later Mil-Spec, Mil-Std 810C Method 519.2, test requirements are more severe than those we have determined from measurements on aircraft.

If the Mil-Spec levels for equipment on secondary structure were used, the sinusoidal levels would have been excessive but the random levels too low.

Within the scope of this paper it is not possible to detail the pragmatic relation between the sinusoidal testing to ref. 1 and gunfire induced random vibrations.

7. RESEARCH PROPOSALS

Research is required to obtain a better understanding of gunfire induced vibrations.

7.1 The current specifications mainly take account of the gun blast energy and the distance from the muzzle to the equipment. It is recommended that a mathematical model should be developed to take account of structural stiffness and damping. The large bank of data which exists within the industry can be used in the development of the model.

7.2 In theory, it should be possible to reduce vibrations by changes to the blast deflector, and to the aircraft structure in the immediate vicinity of the muzzle.

Several 'ad hoc' modifications to the deflector and fuselage structure were tested on the gun rig, but made only small changes to equipment vibrations. Further theoretical and test work to determine optimum blast deflector design is recommended.

8 PROPOSAL FOR CLEARANCE OF EQUIPMENT ON FUTURE AIRCRAFT

In the initial design phase, the 'normal' random vibration test spectra of ref. 6, which is dependent on engine conditions and aircraft flight envelope; the gunfire test spectra of ref. 5; and gunfire test spectra used for the current aircraft, factored by gun blast energy, will be compared.

For the region where the gunfire spectra are significantly above the 'normal' vibration levels, all equipments, or the shelves on which the equipments are mounted, will be anti-vibration mounted.

Only one vibration test, to cover 'normal' and 'gunfire induced' vibrations, will be carried out on each equipment.

For 'safety critical' equipments the level at every frequency will be the greater of the 'normal' or 'gunfire induced' vibrations. Any sinusoidal input, which may be required at gunfire frequency, will be obtained from measurements on our aircraft, since the ref. 2 levels are excessive (see para. 6).

For equipments which are not safety critical, the test spectra will be not less than the 'normal' spectra of ref. 6, but can be less than the gunfire test spectra, which are inevitably very severe compared with vibrations which occur on aircraft. It is expected that this will be sufficient to achieve an acceptable in service defect rate, see para. 5.2.

Butt and airfiring measurements will be required on prototype aircraft to confirm that the test levels applied to safety critical equipments have not been exceeded.

REFERENCES

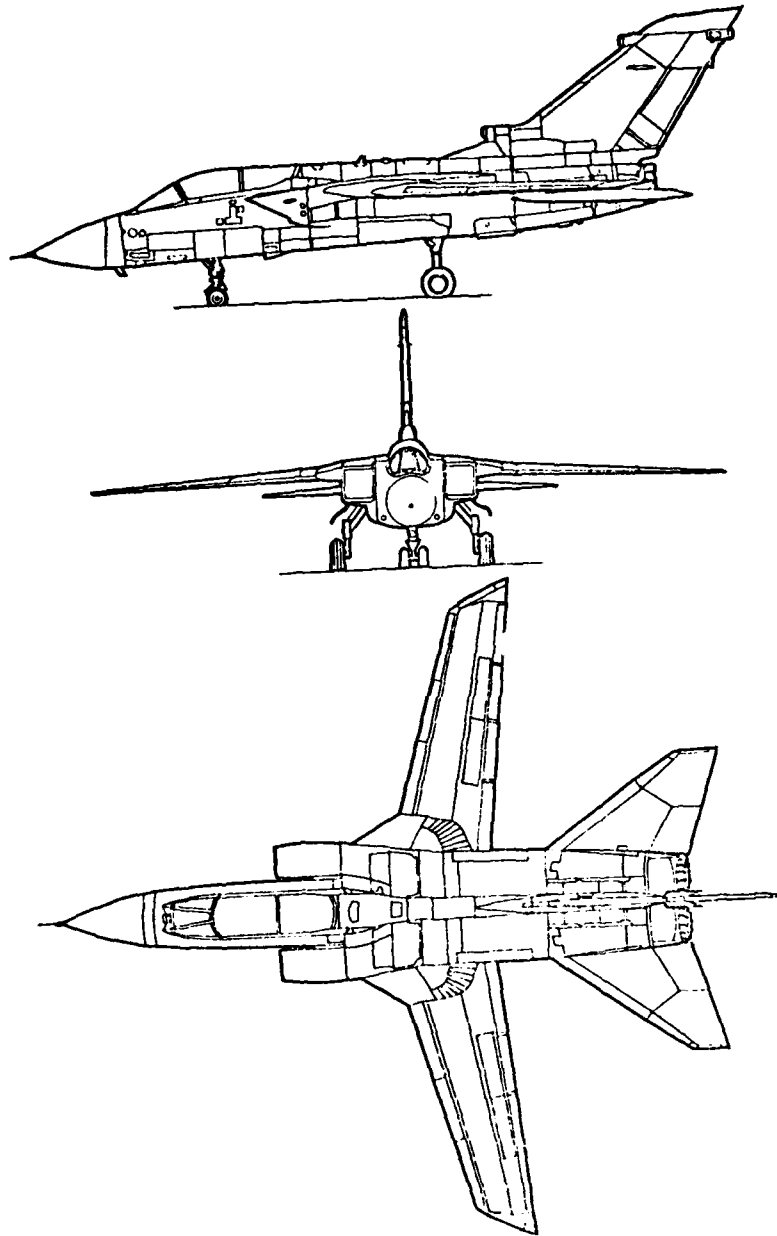
- 1 Mil-Std-810 B Method 514.1 Vibration 1969
- 2 British Standard, 2G.100 Part 2. Environmental and Operating Conditions 1962
- 3 Robert W Sevy, James Clark. AFFDL-TR-70-131. The Development of Prediction Methods and the Synthesis of Equipment Vibration Techniques, 1970
- 4 Mil-Std 810 B Method 519.1 Gunfire Vibration, Aircraft, 1975
- 5 Mil-Std 810 C Method 519.2 Gunfire Vibration, Aircraft, 1975
- 6 Mil-Std 810 C Method 514.2 Vibration, 1975

LIST OF FIGURES

- Fig. 1 Tornado Mk 1
- 2 Tornado Mk 1 Outline of Structure
- 3 General Assembly of Front Fuselage
- 4 Installation of Gun in Front Fuselage
- 5 Installation of Equipment in Front Fuselage
- 6 Right Hand Side Bay Equipment and Gun
- 7 Comparison of Air and Butt Firing Levels
- 8 Overall 'g' RMS plotted against Airspeed and Normal 'g'
- 9 Scatter in Measured Levels. Single Gun Firing at 1 'g'
- 10 (2 sheets) Equipment Clearance. Test Spectra
- 11 Typical Test Spectrum Graphical Form
- 12 Typical Test Spectrum. Tabular Form
- 13 Defect Rate
- 14 Comparison of Test Spectra with Mil Specifications
- 15 Comparison of Test Spectra with Mil Specifications Sinusoidal Vibrations at Gunfire Frequency.

TORNADO Mk.1

FIG 1



TORNADO Mk.1 OUTLINE OF STRUCTURE

FIG 2

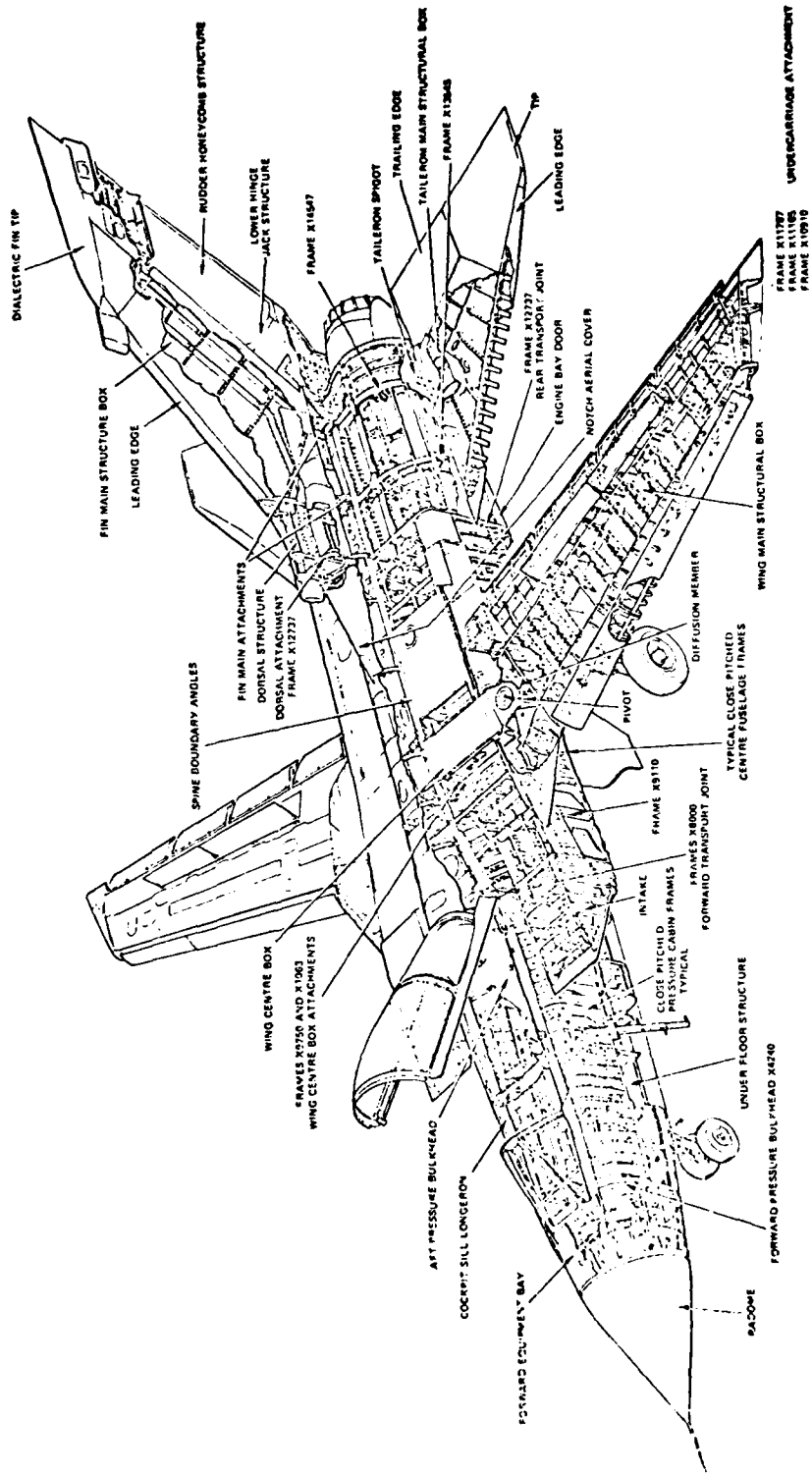
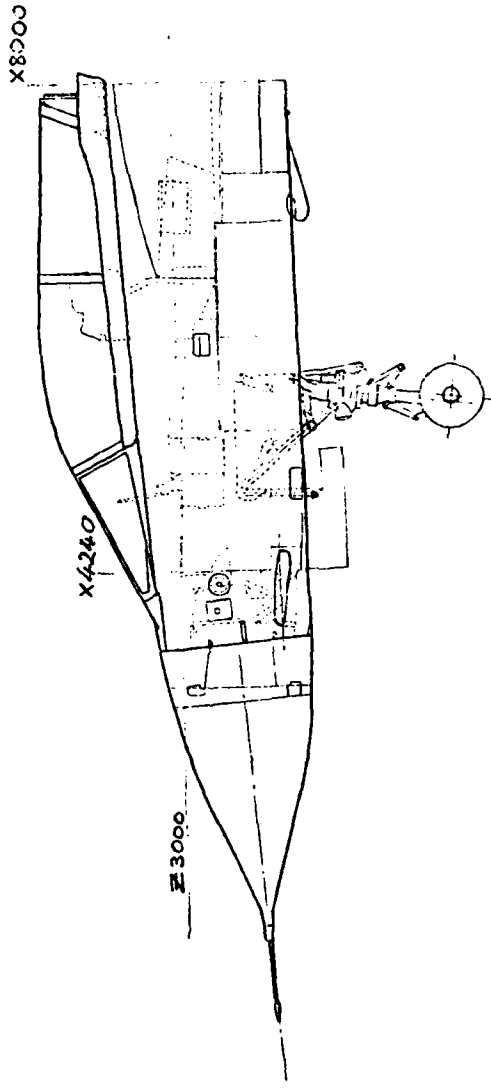


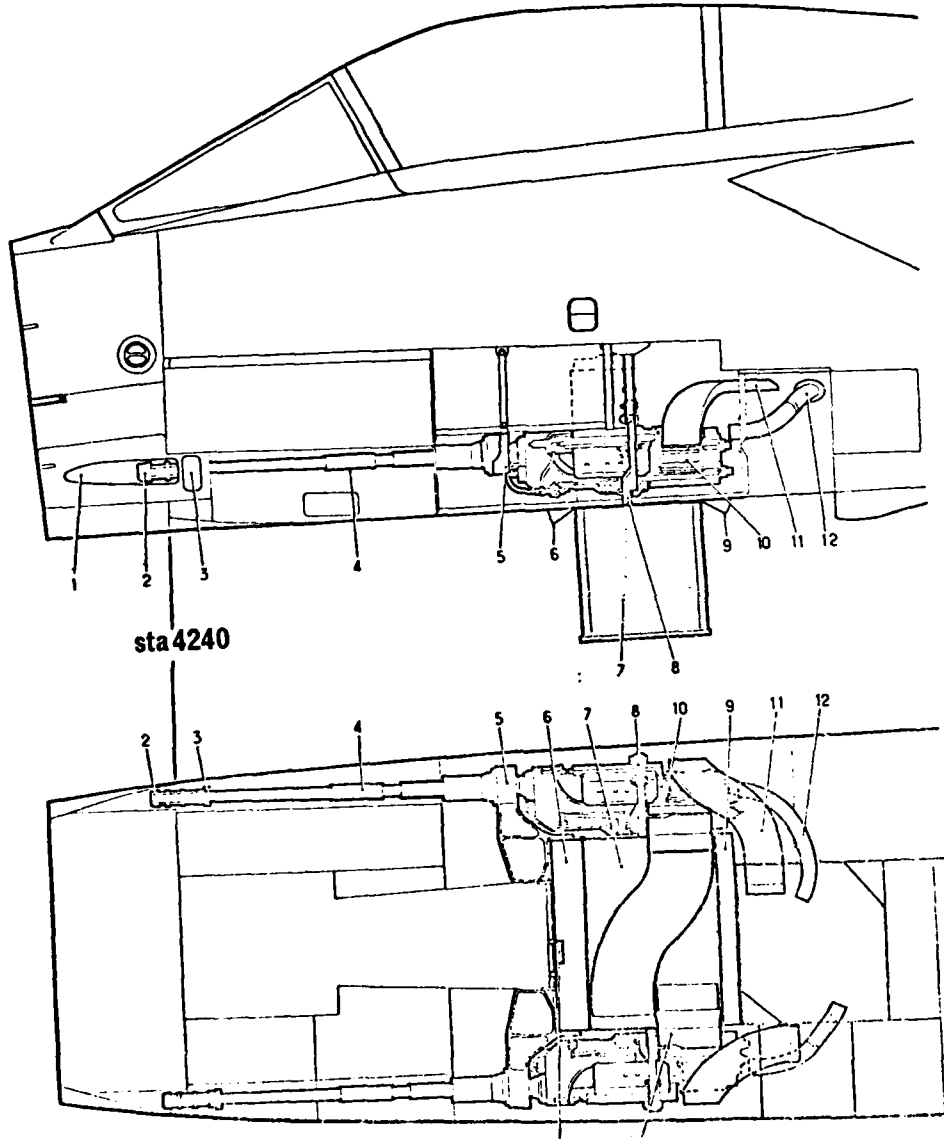
FIG 3

VIEW OF FRONT FUSELAGE



INSTALLATION OF GUNS IN THE FRONT FUSELAGE

FIG 4



INSTALLATION OF EQUIPMENT IN THE FRONT FUSELAGE

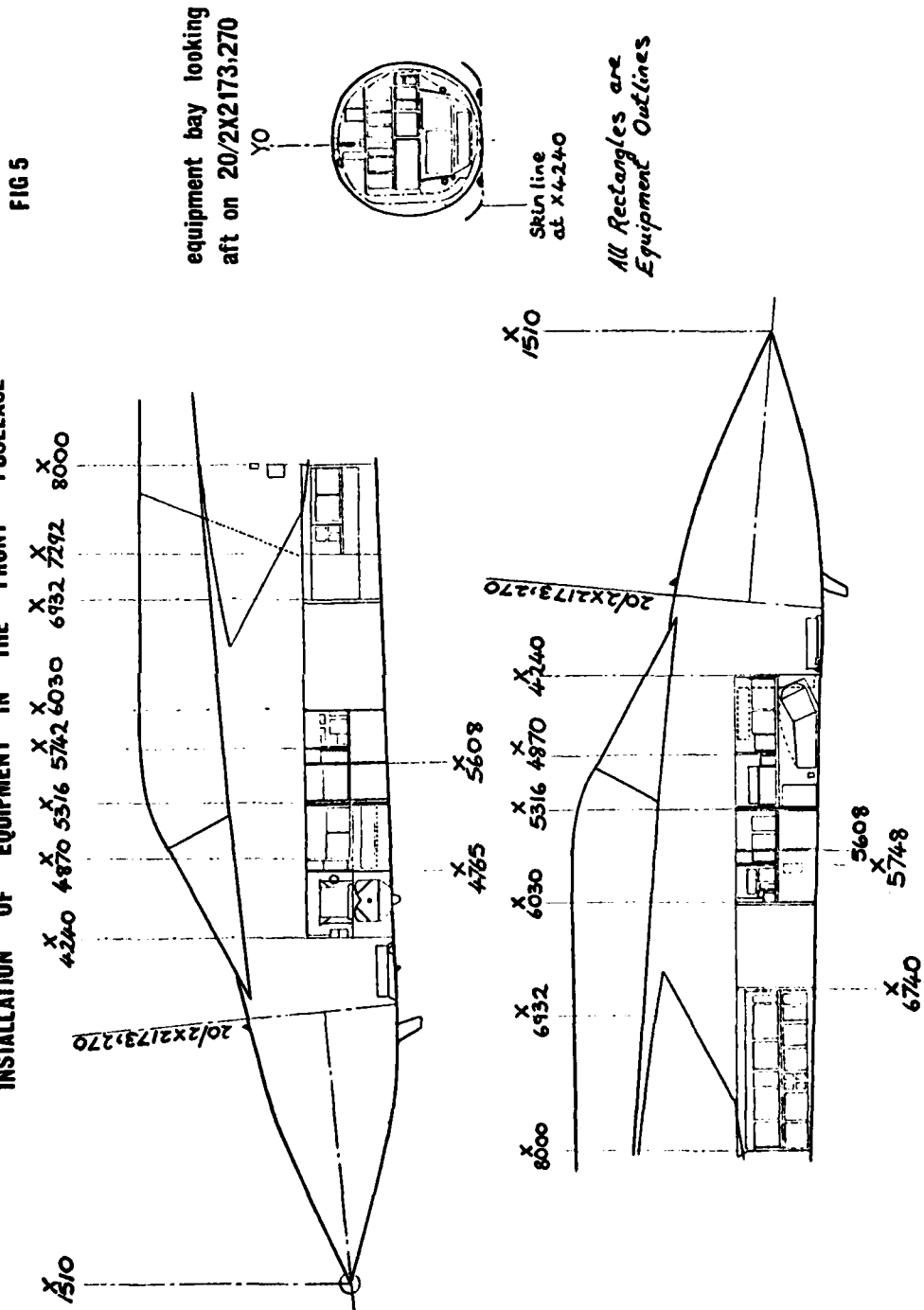
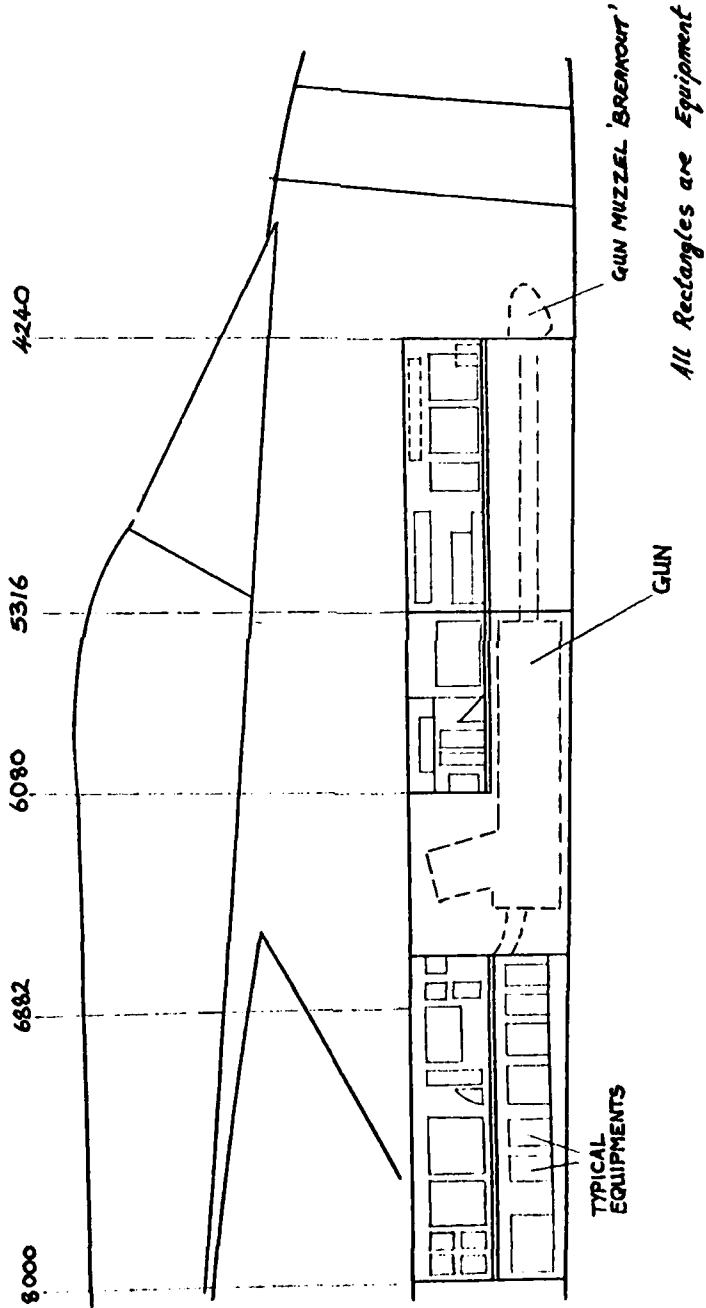


FIG 6

RIGHT HAND SIDE BAY EQUIPMENT AND GUN



TYPICAL
EQUIPMENTS

GUN

GUN MUZZEL 'BREAKOUT'

All Rectangles are Equipment Outlines

FIG 7

COMPARISON OF AIR AND BUTT FIRING LEVELS

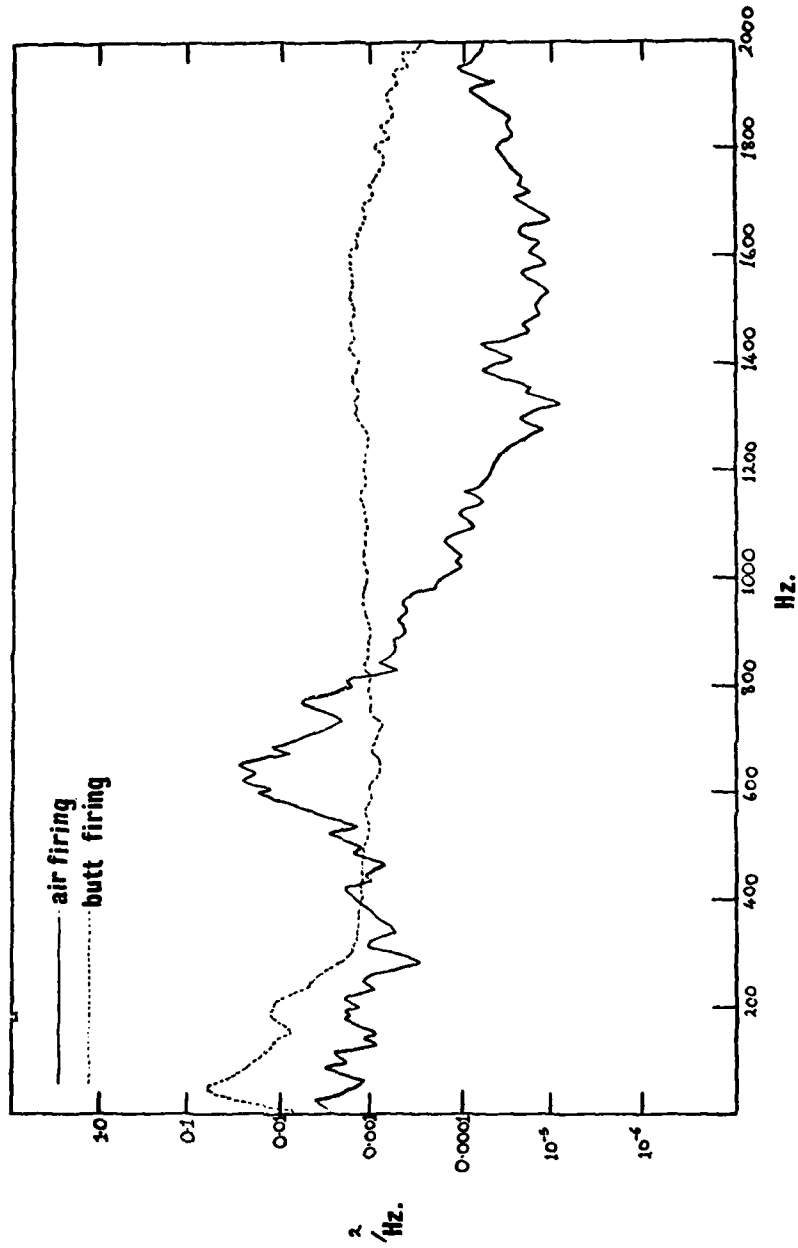
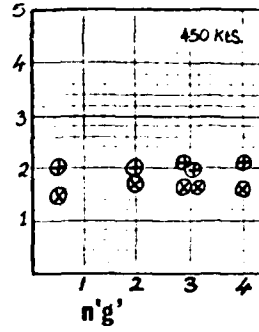
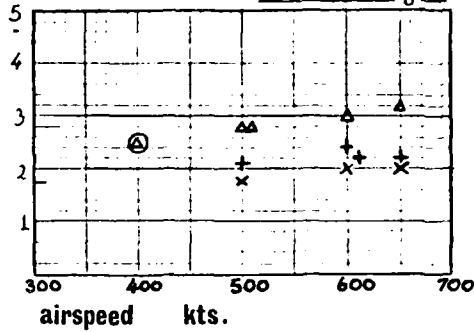


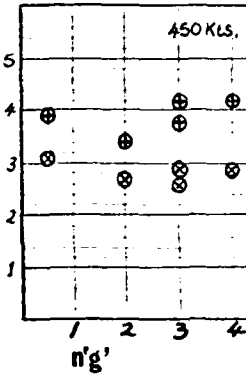
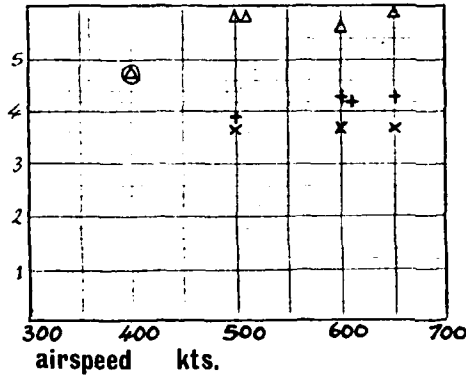
FIG 8

OVERALL 'g' RMS PLOTTED AGAINST AIRSPEED AND NORMAL 'g'

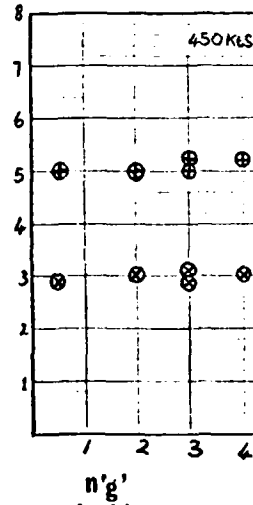
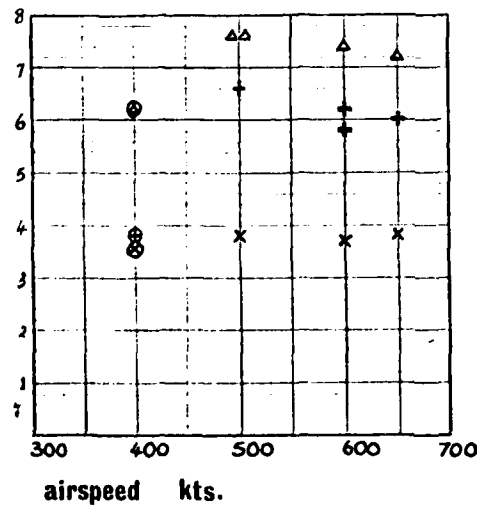
overall 'g' rms
0-2 kHz
LONGITUDINAL



overall 'g' rms
0-2 kHz
LATERAL



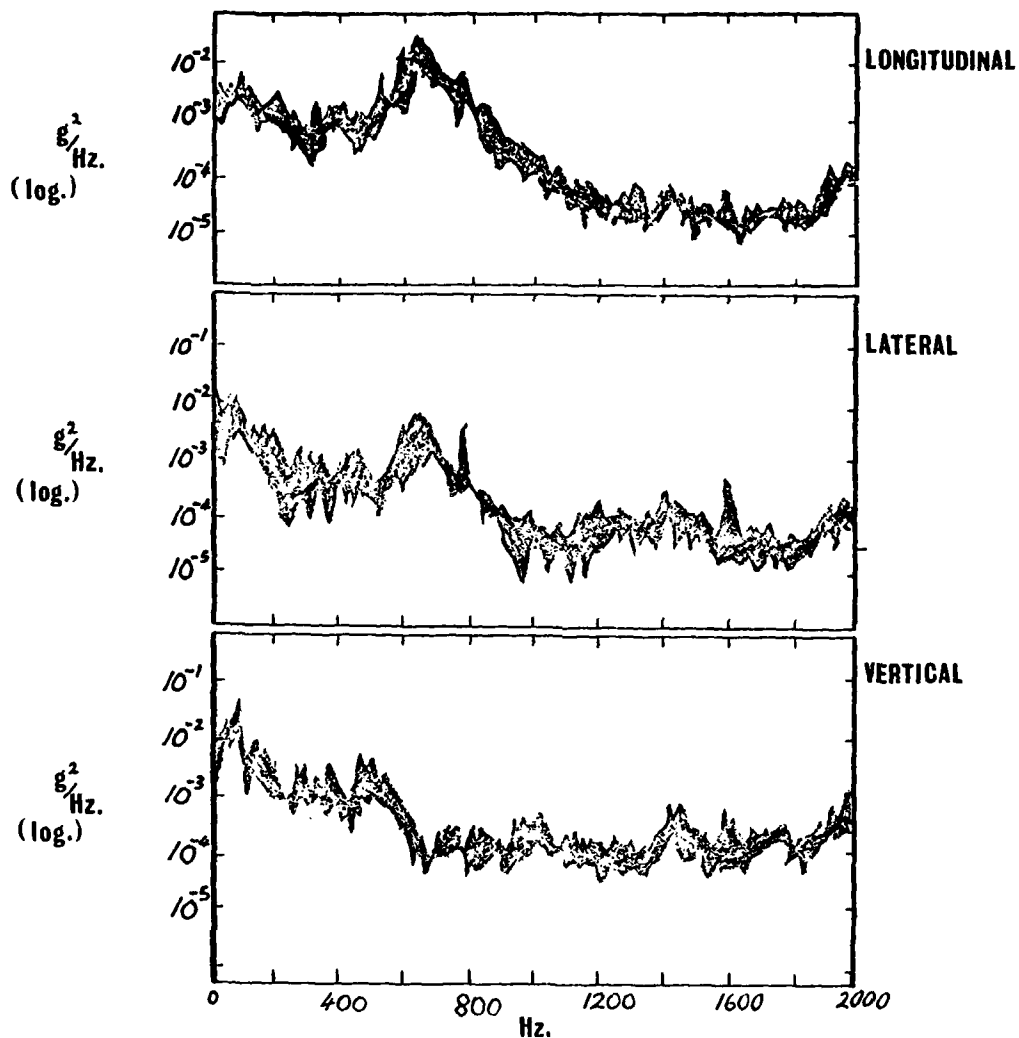
overall 'g' rms
0-2 kHz
VERTICAL



KEY	ft.	left gun	right gun	double gun
	15000	x	+	Δ
	20000	⊗	⊕	⊙

FIG 9

SINGLE GUN FIRING AT 1'g'



<u>flight</u>	<u>shoot</u>	<u>rounds</u>	<u>IAS(kts)</u>	<u>alt.(ft)</u>
x	1	12	400	15000
x	4	20	400	15000
x	10	29	300	15000
y	1	11	400	15000
y	8	22	400	15000

FIG 10
1 of 2

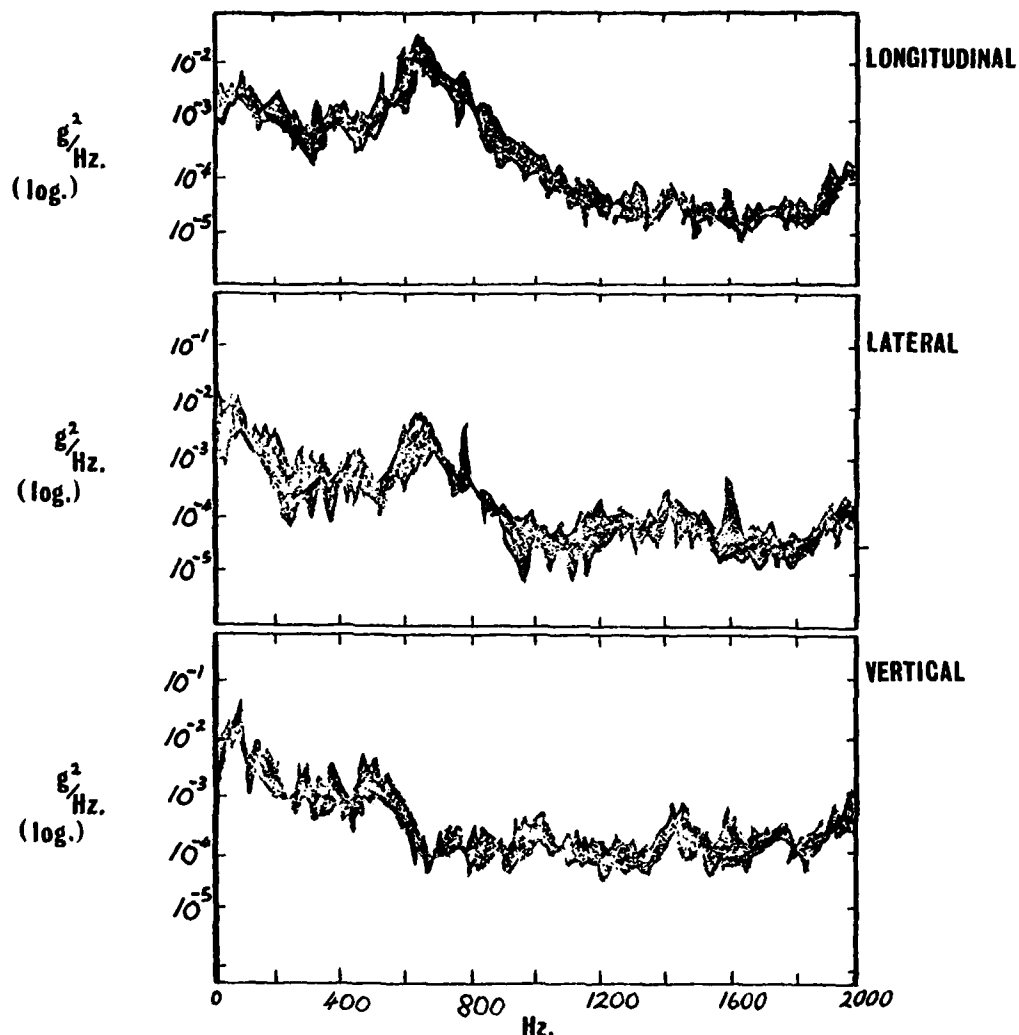
Equipment Clearance. Test Spectra

h.r.o.f. high rate of fire, l.r.o.f low rate of fire

Clearance	Test Spectra	Duration	Data Source	Derivation of Spectra
A. Prototype equipment for air firing	2 guns hrof. No sinusoidal inputs. No safety factor.	5 minutes in each direction	A1. Measured on dummy equipment on rig. A2. Measured on aircraft equipment during butt firing. A3. Measured adjacent to equipment on aircraft or on rig.	Envelope measured vibrations. Mount dummy equipment on table. Control to envelope measurements and measure input to equipments. Mount actual equipment on table and control to input levels. Mount actual equipment on table and control at the identical location, to the envelope of measured levels. Mount actual equipment on table and control input to the envelope of measured levels.
B. Repeat test where required as a result of initial air firing measurements.				
			As for A. but using levels measured during air firing	
C. Full Prototype clearance	2 guns hrof. No sinusoidal inputs. 3 db increase in level to provide safety factor.	5 minutes in each direction	C2. Measured on aircraft equipment during air firing. C3. Measured adjacent to equipment during air firing.	Mount actual equipment on table and control, at the identical location, to 3 db above the envelope of measured levels. Mount actual equipment on table and control input to the envelope of measured levels.

FIG 9

SINGLE GUN FIRING AT 1'g'



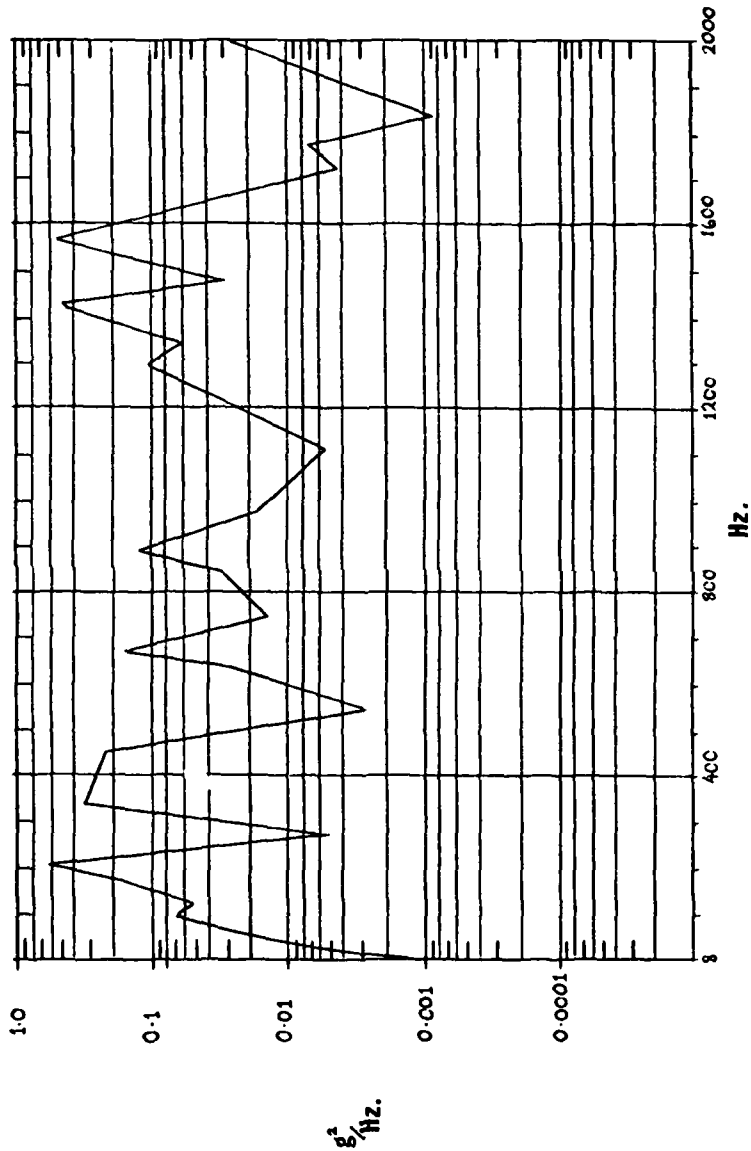
<u>flight</u>	<u>shoot</u>	<u>rounds</u>	<u>IAS(kts)</u>	<u>alt.(ft)</u>
x	1	12	400	15000
x	4	20	400	15000
x	10	29	300	15000
y	1	11	400	15000
y	8	22	400	15000

FIG 10
2 of 2

Clearance	Test Spectra	Duration	Data Source	Derivation of Spectra
D. Clearance of Production Equipment	1 gun hrof air firing	10 minutes in each direction	D1. Measured on an equipment on the same shelf.	Install the equipment on which vibrations have been measured on the table and control, at the identical location, to 3 dB above the envelope of measured levels. Measure the required input spectra. Install the equipment to be cleared on the table and apply the measured input spectra.
	2 guns hrof air firing	5 minutes in each direction		
	1 gun hrof butt firing	1 minute in each direction	D2. Measured on the shelf on which the equipment is installed.	Install the equipment on the table and control the input to 3 dB above the envelope of the measured spectra.
	Sinusoidal input at gun firing frequency and harmonics included. 3 dB increase in level to provide safety factor.			

TYPICAL TEST SPECTRUM

FIG 11



BUTTS HIROF x 2GUNS · LAT. STANDARD SPECTRUM · TOTAL 'g' R.M.S. 12.45

FIG 12

24 1780.0 0.00780
 25 1230.0 0.00077
 26 2000.0 0.02602

TOTAL GRMS IS 12.45
 LINE NO. 711

TEST NO. 2
 11 TEST IDENTIFICATION
 TEST IDENTIFICATION -

GRAPH LABEL - BUTTS HIROFX2GUNS
 LAT

LINE NO. ?

SINES TO ADD ARE:-

1.5GPK AT X HZ

2.0GPK AT 2X HZ

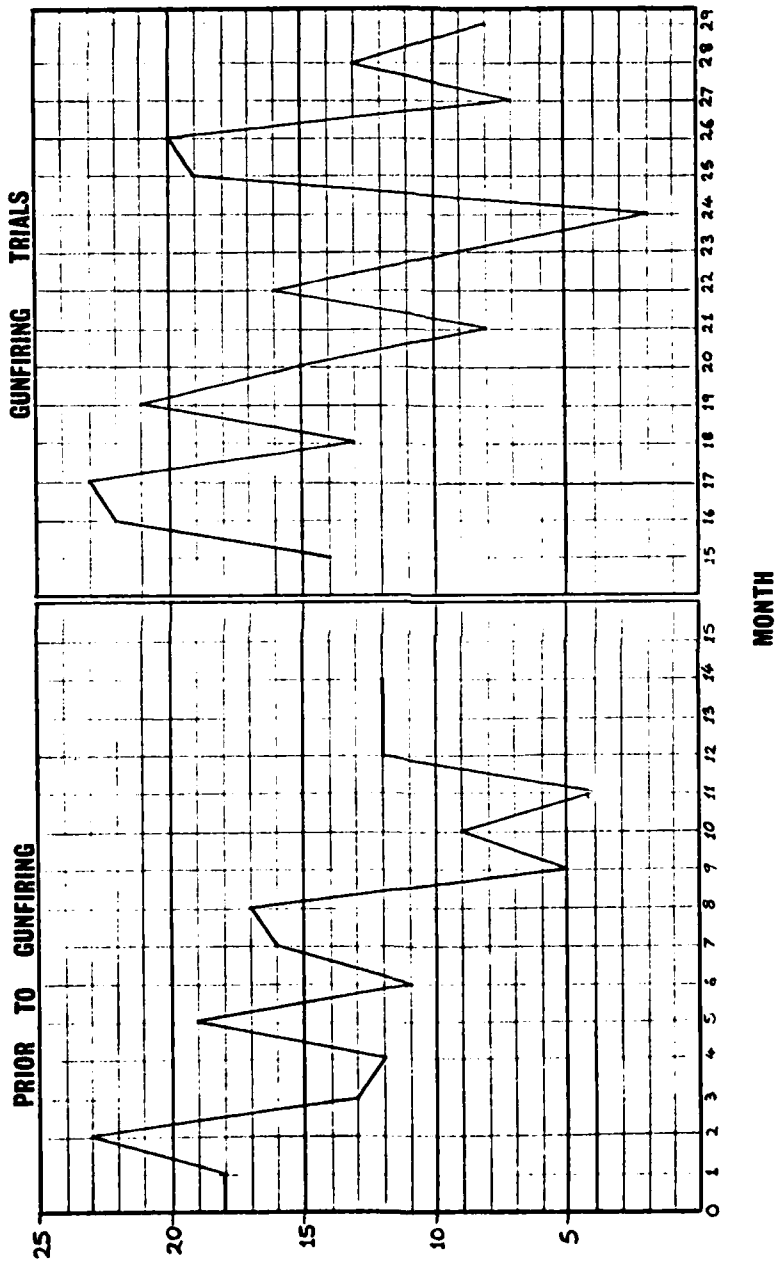
2.0GPK AT 3X HZ

where X is gunfire rate.

TEST NO.	2	15			
'g' SPECTRUM		2000			
STARTING FREQUENCY		8.00			
ENDING FREQUENCY		0.00			
INITIAL SLOPE					
FINAL SLOPE					
BREAKPOINT NO		FREQUENCY HZ.		AMPLITUDE G**2/HZ	
1		40.0		0.01200	
2		112.0		0.06506	
3		140.0		0.04606	
4		190.0		0.20014	
5		220.0		0.72000	
6		240.0		0.09002	
7		280.0		0.00431	
8		350.0		0.32013	
9		460.0		0.23514	
10		550.0		0.00250	
11		650.0		0.02502	
12		680.0		0.16008	
13		750.0		0.01301	
14		850.0		0.03107	
15		900.0		0.13012	
16		980.0		0.01653	
17		1120.0		0.00520	
18		1300.0		0.11024	
19		1350.0		0.05706	
20		1430.0		0.50042	
21		1480.0		0.02801	
22		1570.0		0.53007	
23		1730.0		0.00400	

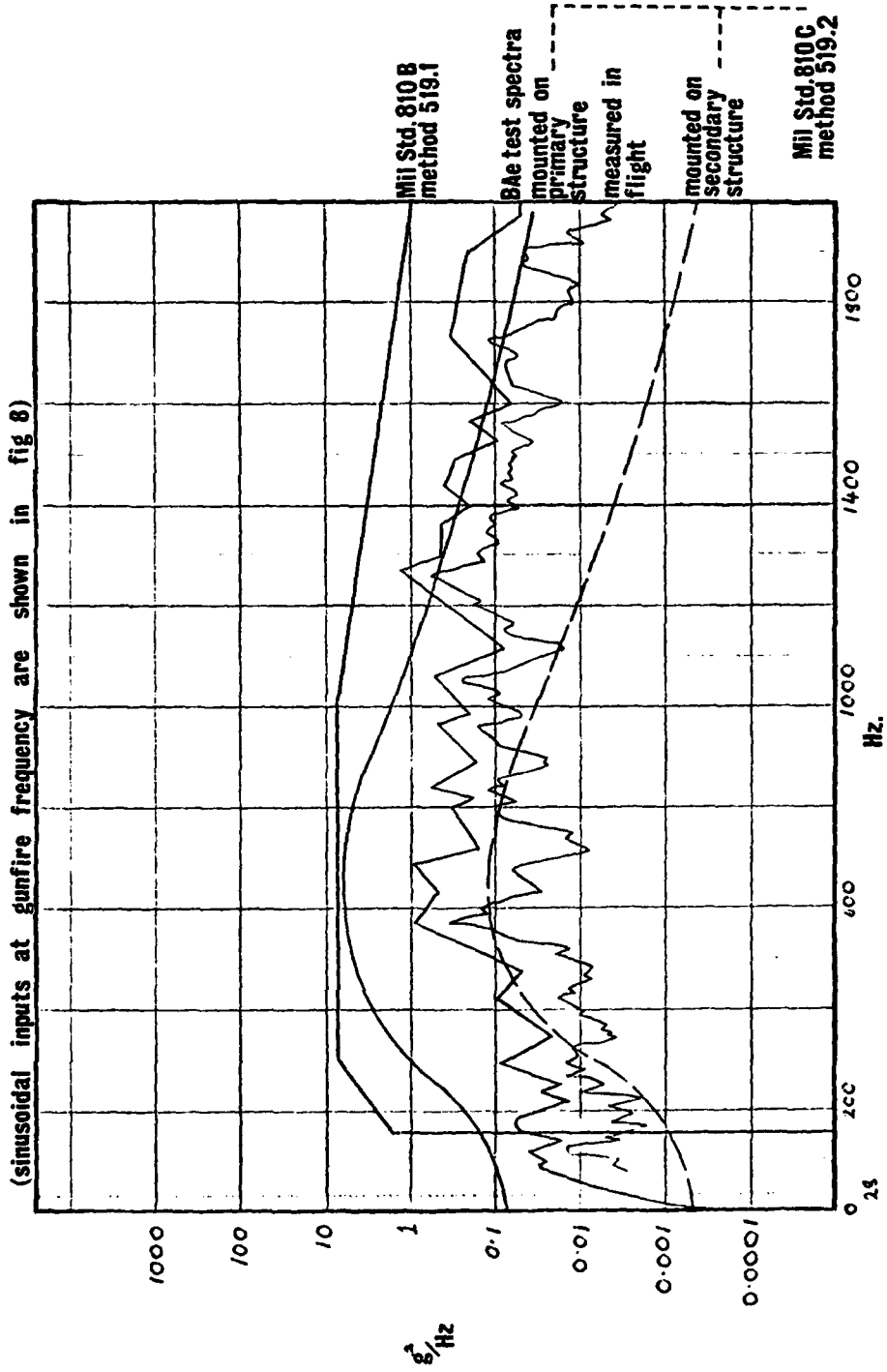
DEFECT RATE

FIG 13



COMPARISON OF TEST SPECTRA WITH MIL-SPECIFICATIONS, TYPICAL EQUIPMENT, VERTICAL DIRECTION

FIG 14



Comparison of test spectra with Mil-Specification
sinusoidal Inputs at Gunfire Frequency

A. Mil Std. 810 B method 519.1 No sinusoidal inputs required.

B. Mil Std. 810 C method 519.2

B.1 Equipment mounted on primary structure

Sinusoidal sweep from 0.8 X to 1.2 X.

$f_1 = X$ Hz G peak 5.0

$f_1 = 2X$ Hz G peak 5.0

$f_1 = 3X$ Hz G peak 5.4

$f_1 = 4X$ Hz G peak 5.7

B.2 Equipment mounted on secondary structure

Sinusoidal sweep from 0.8 X to 1.2 X

$f_1 = X$ Hz G peak 41.9

$f_1 = 2X$ Hz G peak 42.3

$f_1 = 3X$ Hz G peak 16.1

$f_1 = 4X$ Hz G peak 7.1

C. B Ae test spectra

2.0 g peak at X Hz.

DYNAMIC QUALIFICATION TESTING OF F-16 EQUIPMENT

by
H. E. Nevius
Engineering Specialist
and
W. J. Brignac
Engineering Specialist Senior
GENERAL DYNAMICS
P. O. Box 748
Fort Worth, Texas 76101

SUMMARY

Vibration prediction methods and qualification test procedures are presented for F-16 equipment. Measured vibration levels are also compared to the predictions.

The most severe vibratory environment is produced by the muzzle blast pressure during gunfiring. Gunfiring vibration was measured during the YF-16 prototype program which indicated a correlation between vibration levels and distance from the gun port. Vibration data is presented verifying this relationship. Vibration qualification testing for the gunfiring environment uses a sweeping sinusoidal test level to simulate the gunfiring harmonics combined with a random background level which represents the vibration caused by the muzzle blast noise.

Nongunfiring random vibration test levels are shown for F-16 airframe zones. The prediction procedures were based on a relationship between vibration and dynamic pressure using measured data from other aircraft.

Vibration levels have been measured on fuselage mounted stores. Predicted levels using Military Standards appear to be overly conservative when compared to the measured levels.

Other measured dynamic environments are presented which include; (1) wing tip missile response to store ejection from wing pylons and to jet wake encounter, (2) buffet response at high-angles-of-attack. It is shown that high-angle-of-attack operation does not induce significant vibratory levels on the F-16.

INTRODUCTION

The development of vibration qualification criteria for new aircraft systems generally uses Military Standards as guides. The requirements of the Military Standards are updated using applicable measured data from other aircraft. F-16 vibration qualification criteria was derived in a similar manner using measured data from the YF-16 prototype program and the F-111 in conjunction with the procedures of MIL-STD-810.

A principal concern was the effect of gunfiring on equipment located in the vicinity of the gun muzzle. The relative location of the gun and equipment bays is shown in Figure 1.

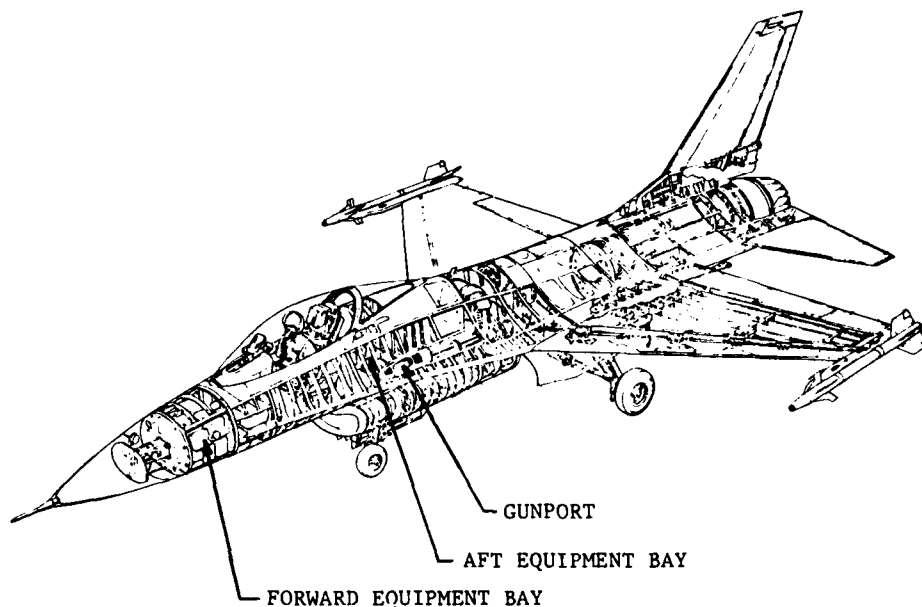


FIGURE 1 F-16 GENERAL STRUCTURAL CONFIGURATION

Basic armament for the F-16 includes a six barrel 20mm gun and air-to-air missiles on each wing tip. The gunport is located adjacent to the aft equipment bay (aft of the crew compartment). The gun mechanism and cartridge drum are mounted in the center fuselage section, just forward of the wing. Equipment components located in the aft bay are subjected to the highest vibration on the airplane due to the muzzle blast pressure at the gunfiring rate of 100 rounds-per-second. The forward equipment bay, in front of the cockpit, receives a relatively small amount of gunfiring vibration.

Other features of the F-16 include capabilities as a multirole high performance (speed and load factor) tactical fighter with air-to-air and air-to-ground weapon delivery. It is powered by a single afterburning turbofan engine (Pratt and Whitney F100-PW-100) with a maximum thrust in the 25,000 pound class. Stores of various types can be carried on underwing pylons, on the fuselage centerline, and on each side of the inlet.

A nongunfiring vibration criteria was derived in addition to the gunfiring vibration levels for equipment located throughout the airplane. External stores were not covered in the initial F-16 vibration criteria. All stores used at the beginning of the program were existing stores, already qualified for other high performance airplanes.

A measurement program was conducted to verify that the equipment qualification levels were adequate. Included in the measurement survey was an investigation of low frequency vibratory response due to store ejection, buffet, and jet wake encounter. Measurements were also recorded on two fuselage mounted external stores.

GUNFIRING VIBRATION

During the development of the prototype YF-16, there was some concern for equipment located in the aft equipment bay and the cockpit area near the gunport. There was also a concern for the pilot when subjected to the muzzle blast noise. At the beginning of the program, military specifications did not cover the gunfiring environment. Consequently, a ground gunfiring test was conducted on the YF-16 to investigate cockpit noise, stress levels on structure around the gunport, and performance of the 20mm gun and to measure vibration levels.

Results from this ground gunfiring investigation provided a verification of the adequacy of the structural design to withstand the muzzle blast pressure loads. A redesign of the instrument panel was required with vibration isolators installed to protect the instruments which were only qualified to 2g's.

A lead/vinyl sheet material was added to the cockpit sidewalls to reduce the noise entering the cockpit. Pilots comment that the gunfiring noise is "noticeably loud but does not cause discomfort." Microphone measurements indicate no problems when the pilot is wearing a standard helmet.

The vibration measurements were used to derive a correlation between vibration and distance from the gunport. A least-square statistical analysis was performed on the measured data and the 95% confidence line represents the vibration-versus-distance relationship plotted on log-log paper as shown in Figure 2. The roll-off at the higher levels was obtained from F-111 gunfiring data. The equation for the straight line portion of the curve (from 45 to 300 cm) is:

$$\pm g's = 890/D(\text{cm}) \quad (1)$$

where: D = Distance from gunport

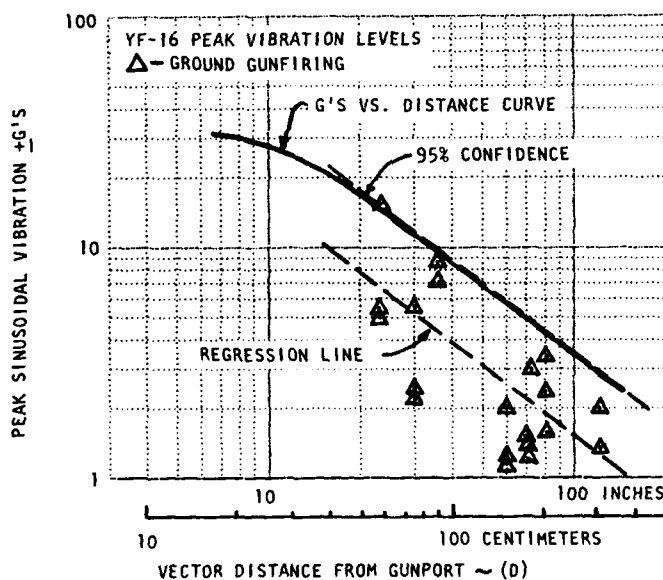


FIGURE 2 YF-16 MEASURED GUNFIRING VIBRATION

Gunfiring also produces random vibration due to muzzle blast noise. This random vibration is most noticeable in the 300 Hz to 1000 Hz frequency range. The gunfiring measurements were analyzed in terms of Power Spectral Density (g^2/Hz) to determine the random background vibration levels.

A curve was derived for the random background vibration in the same manner used to develop the sinusoidal level. Gunfiring random vibration relative to distance from the gunport may be obtained from the following:

$$g^2/\text{Hz} = 3.8/D(\text{cm}) \tag{2}$$

Figure 3 shows the sinusoidal and random vibration levels as a function of the distance from the gunport. The sinusoidal curve is the same as shown in Figure 2.

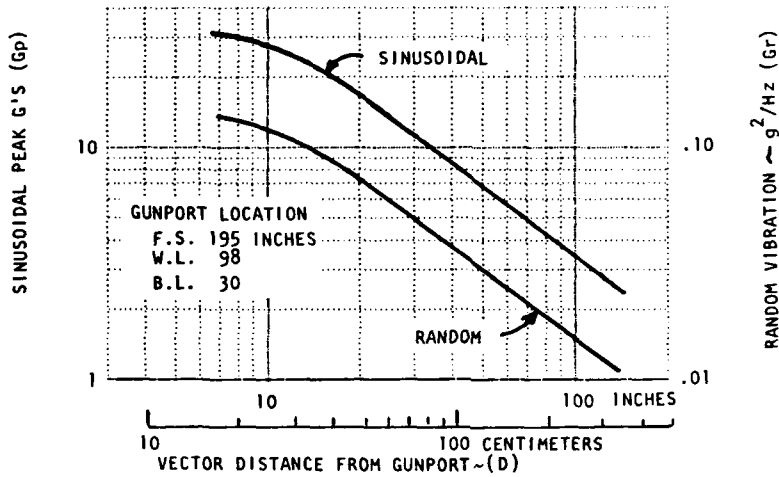


FIGURE 3 GUNFIRING VIBRATION VERSUS DISTANCE FROM GUNPORT

The above curves are used to define the vibration levels required in qualification test procedures.

GUNFIRING QUALIFICATION TEST

The vibration qualification test for gunfiring consists of a sweeping sinusoid combined with a random background level. The frequency spectrum for the test is presented in Figure 4.

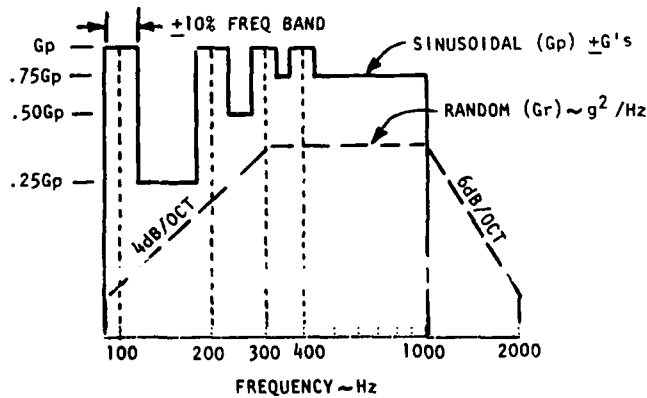


FIGURE 4 FREQUENCY SPECTRUM FOR COMBINED RANDOM AND SINUSOIDAL GUNFIRING VIBRATION

The solid line is the sinusoid which is swept from 90 Hz to 1000 Hz following the peaks and valleys shown. The peaks represent the first four harmonics of the gunfiring rate with a $\pm 10\%$ frequency band on each side of the harmonic. The dashed line is the random vibration background level. The maximum level occurs between 300 Hz to 1000 Hz and reduces at 4dB/octave to 100 Hz and 6dB/octave to 2000 Hz. Values for maximum sinusoidal level (G_p) and random level (G_r) are obtained from equations (1) and (2) or from the curves on Figure 3.

Test duration required for the F-16 is one hour of sinusoidal sweeping per axis plus six resonance dwells in the harmonics for 5 minutes each. Five minutes at dwell plus sweep time is equivalent to 50,000 rounds which is the specification requirements.

GUNFIRING VIBRATION MEASUREMENTS

A typical spectral analysis of a gunfiring burst is shown in Figure 5. The plot shows the response at the harmonics of the 100 rounds per second firing rate.

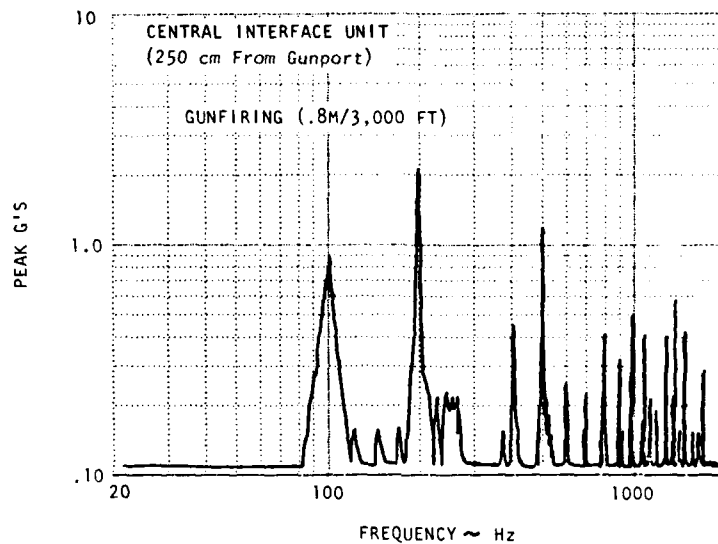


FIGURE 5 SPECTRUM PLOT FOR GUNFIRING VIBRATION

The significant peak levels from this type of analysis are the data points plotted in Figure 6. Gunfiring vibration from 24 accelerometers located at a distance of 100 cm to 320 cm from the gunport is included on Figure 6.

Inflight gunfiring vibration measured on the F-16A (single seat) and F-16B (two seats) are compared to the curve derived from the YF-16 ground gunfiring test. This comparison provides a verification of the adequacy of the prediction procedure for inflight F-16 gunfiring.

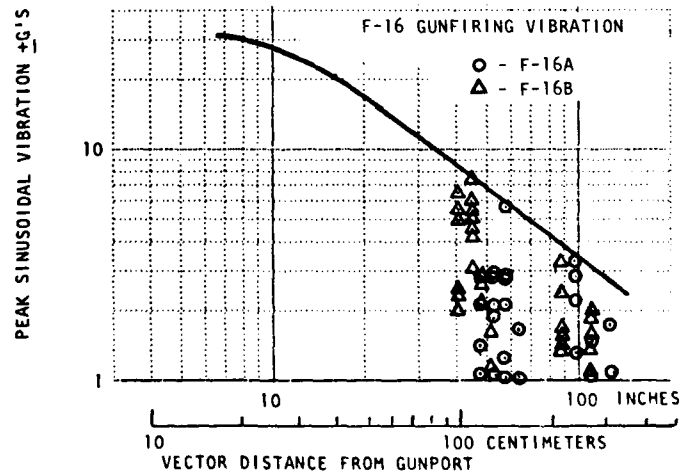


FIGURE 6 F-16 MEASURED GUNFIRING VIBRATION

NON-GUNFIRING VIBRATION

Other significant vibratory environments are associated with jet engine exhaust noise and inflight aerodynamic flow. The extreme aft engine location on the F-16 eliminated jet exhaust noise as a vibratory problem.

The increase in flow turbulence in the aft fuselage causes higher vibration than seen in the forward fuselage with smooth surfaces and no discontinuities. The F-16 is divided into four fuselage zones of vibration plus the wing and tail zones. Figure 7 shows the zones along with the maximum g^2/Hz required for performance qualification testing.

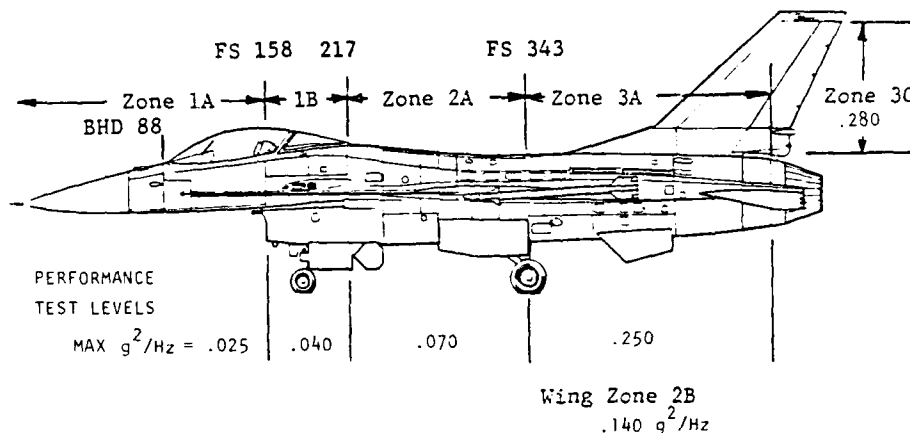


FIGURE 7 F-16 ZONES OF VIBRATION

The maximum predicted random vibration level for each zone was derived using YF-16 and F-111 measured data. It was established that the random vibration levels varied as the square of dynamic pressure according to the following equation.

$$W_0 = Kq^2 \quad (3)$$

where: W_0 = random vibration level at a given flight condition (g^2/Hz)

K = a constant depending on airframe location

q = dynamic pressure (N/cm^2 or lbs/ft^2)

Thus, it is seen that the maximum vibration levels will occur at the maximum operational dynamic pressure. The value of the constant (K) is provided in the procedures of MIL-STD-810C (Method 514.2) or can be established from measured data. Constants (K) were established for each F-16 zone and the maximum operational dynamic pressure used to compute the performance level (W_0) for each zone presented in Figure 8.

AIRCRAFT ZONES	TEST LEVELS MAX PSD g^2/Hz		
	ENDURANCE	PERFORMANCE	A
1A - Fwd Fuselage	.033	.025	.02
1B - Aft Equip. Bay	.053	.040	.02
2A - Center Fuselage	.093	.070	.04
2B - Wing Except Tip	.186	.140	.04
2C - Wing Tip + Launcher	.186	.140	.04
3A - Aft Fuselage	.330	.250	.04
3B - Engine Mounted Equip.	-	-	-
3C - Hor. Tail & Vert. Tail Except Tip	.370	.280	.04
3D - Vertical Tail Tip	.370	.280	.04
SUPPLEMENTARY SINUSOIDAL TEST	Peak σ	Peak g	
2C - Wing Tip + Launcher (4-10 Hz)	7.5	5.0	
3D - Vertical Tail Tip (15-20 Hz)	10.0	7.5	

FIGURE 8 VIBRATION QUALIFICATION TEST LEVELS

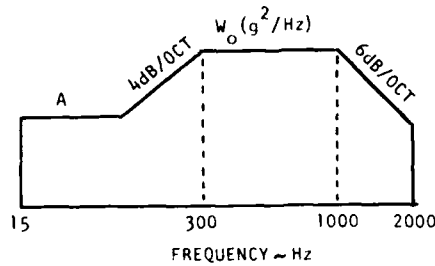


FIGURE 9 FREQUENCY SPECTRUM FOR RANDOM VIBRATION TEST

The frequency spectrum of Figure 9 was obtained from MIL-STD-810C. The "A" level is the value for low frequency random vibration given in Figure 8.

VIBRATION QUALIFICATION TEST (NONGUNFIRING)

The F-16 random vibration qualification testing is patterned after the procedures outlined in MIL-STD-810C. Two tests are required.

- (1) Performance Tests - The equipment component must meet specified performance while being vibrated at the performance test levels. These test levels are the levels which occur at the maximum flight condition that the F-16 can fly. One hour of testing in each of the three orthogonal axes is required using the Figure 8 performance levels and Figure 9 frequency spectrum.
- (2) Endurance Tests - This test is an accelerated level so that a relatively short test will be equivalent to the equipment service life. Equipment functioning is not required during the test but must meet specified performance after the test. The endurance test level is determined from the following equation.

$$W_o = (q/q_{max})^2 (W) (N/T)^{1/2} \quad (4)$$

where: q_{max} = maximum dynamic pressure
 q = limit dynamic pressure $5.8N/cm^2$ (1200 lbs/ft^2)
 W = performance vibration level
 N = number of high performance flight hours
 T = test duration (hours)

The number of missions flown in the high dynamic pressure range are obtained from an aircraft usage document. For the F-16, approximately 300 flight hours are accumulated over the service life of the airplane at dynamic pressures greater than 1200 pounds per square foot. The dynamic pressure limit is the value prescribed in MIL-STD-810C. A higher limit could be used but then the number of flight hours would be less which should give about the same results.

The endurance test levels shown in Figure 8 are about one-third higher than the performance levels.

A supplementary sinusoidal test is required for equipment mounted on the wing tips and tail tips. These low frequency sinusoidal levels represent the structural response of the basic modes of vibration.

VIBRATION MEASUREMENT SURVEY

Seventy accelerometers were located near equipment components to investigate a wide range of flight conditions. The general locations of these transducers are shown below in Figure 10.

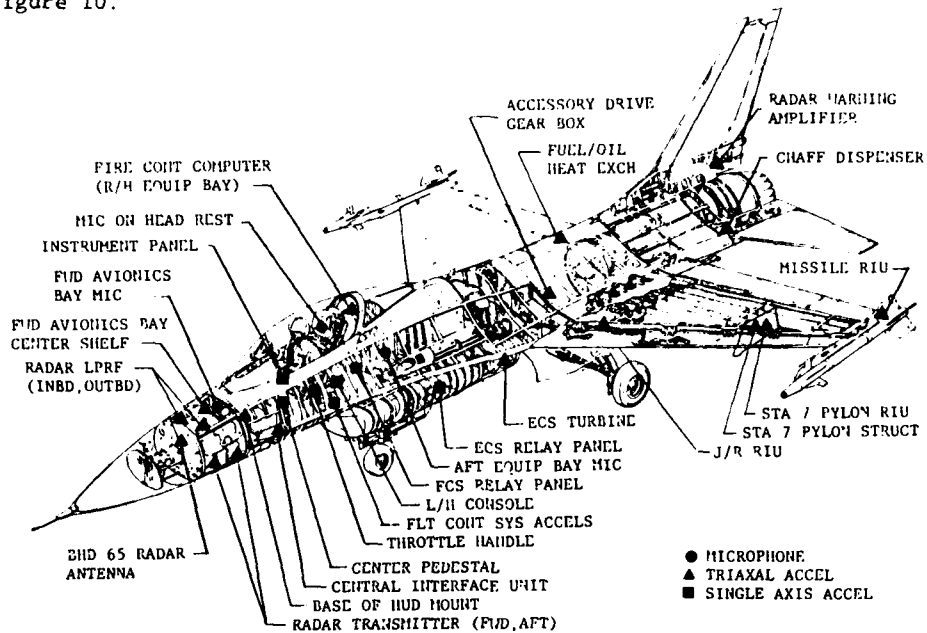


FIGURE 10 TRANSDUCER LOCATIONS FOR VIBRATION SURVEY

The purpose of the vibration survey is to verify the adequacy of the predicted vibration qualification test levels presented in Figure 8. Most of the transducers are located in the equipment bays and in the cockpit to measure the gunfiring environment.

DATA ANALYSIS AND PRESENTATION

Data analysis of the recorded vibration levels is accomplished in a manner which provides a direct comparison between the predicted levels and the measured environment. For gunfiring, a narrow band frequency analysis is performed to obtain peak g's versus frequency. The significant levels in the gunfiring harmonics are plotted versus distance from the gunport. The results are similar to the earlier test on the YF-16 prototype airplane (Figure 2). The regression line has the same slope and the equation for vibration versus distance remains the same.

Acceleration spectral density analysis (g^2/Hz) is used to analyze nongunfiring random vibration. Maximum response levels and the corresponding frequency are plotted on g^2/Hz -versus-frequency plots to show a comparison between measured data and the required vibration test envelope.

FORWARD EQUIPMENT BAY VIBRATION

The following figures show the required vibration test level for several aircraft zones along with measured data. Figures 11 and 12 present data for the forward fuselage (Zone 1A). In Figure 11, it can be seen that the required test level is adequate for the radar equipment area and is conservative in the low frequency range.

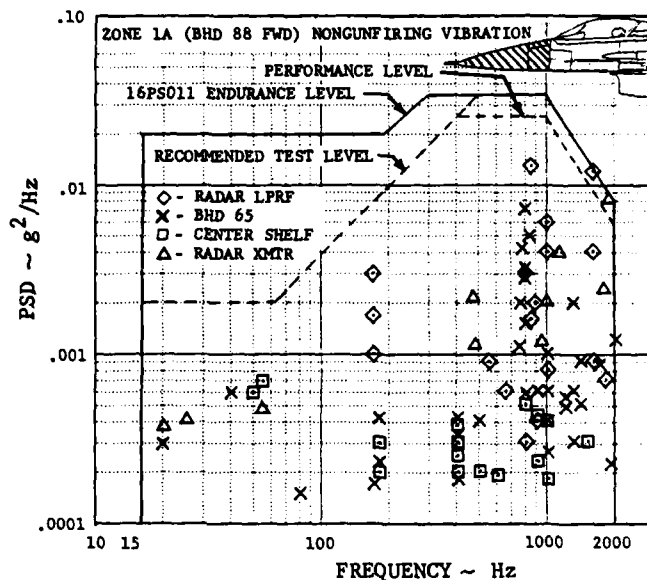


FIGURE 11 VIBRATION MEASUREMENTS IN THE FORWARD EQUIPMENT BAY

Consequently, the radar specified test levels were reduced to the dashed line shown. The maximum g^2/Hz (above 500 Hz) remained the same as specified in the F-16 Environmental Criteria Document (16PS011B). The points shown on these plots represent several flight conditions, including take-off, transonic flight, and high performance flight.

COCKPIT VIBRATION

Figure 12 shows the data measured in the cockpit. The cockpit is part of Zone 1A and is shown separately only to see if the vibration levels are different from the equipment bay.

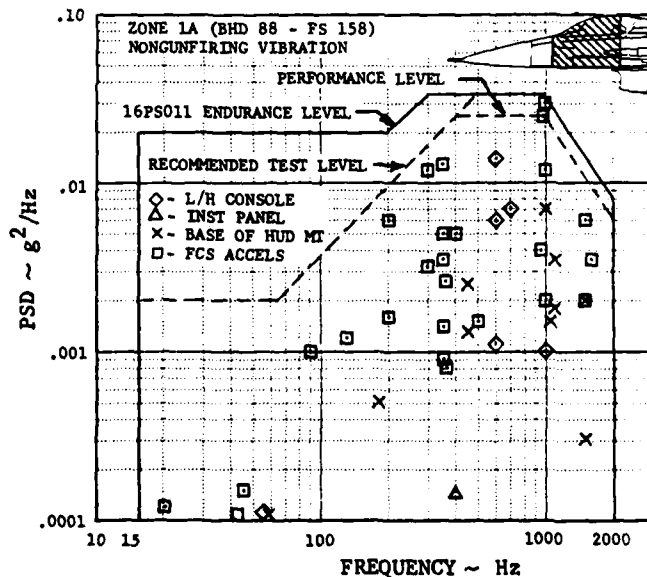


FIGURE 12 VIBRATION MEASUREMENTS IN THE COCKPIT

The cockpit measurements indicate the same amount of conservatism in the requirements for the low frequency range as noted for the forward equipment bay. The instrument panel vibration levels are insignificant. This proves the effectiveness of the rubber grommets supporting the instrument panel for the nongunfiring environment as well as gunfiring.

AFT EQUIPMENT BAY VIBRATION

The highest nongunfiring level measured in the aft equipment bay (Zone 1B) was recorded at the base of the Fire Control Computer (FCC). Four flight conditions are shown in Figure 13. This type of presentation is an envelope of the maximum response levels recorded for a particular flight condition. An inspection of the data shows that high dynamic pressure flight produces the highest vibration level. The low frequency response is caused by atmospheric turbulence associated with flight over the desert at Edwards Air Force Base, California.

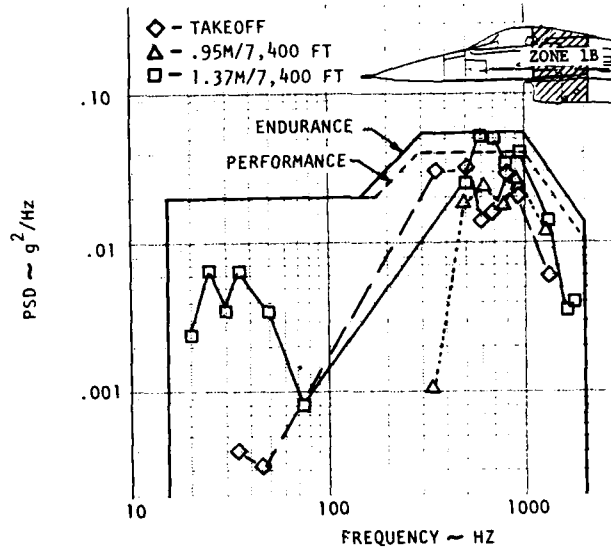


FIGURE 13 VIBRATION MEASUREMENTS IN THE AFT EQUIPMENT BAY

The endurance and performance test levels for Zone 1B are included on the data plot. No change in specified test levels was recommended for the aft equipment bay (Zone 1B) or for any of the remaining aircraft zones.

AFT FUSELAGE VIBRATION

Measured vibration levels in the aft fuselage were well within the required test level except in the dragchute compartment. The dragchute compartment is an extension of the rudder island structure directly above the engine exhaust nozzle. Either the dragchute or an ECM Package is installed in this compartment on the Norwegian and Belgium airplanes. Figure 14 shows a sketch of the aft fuselage with the location of the triaxial accelerometer on the ECM Package aft rail.

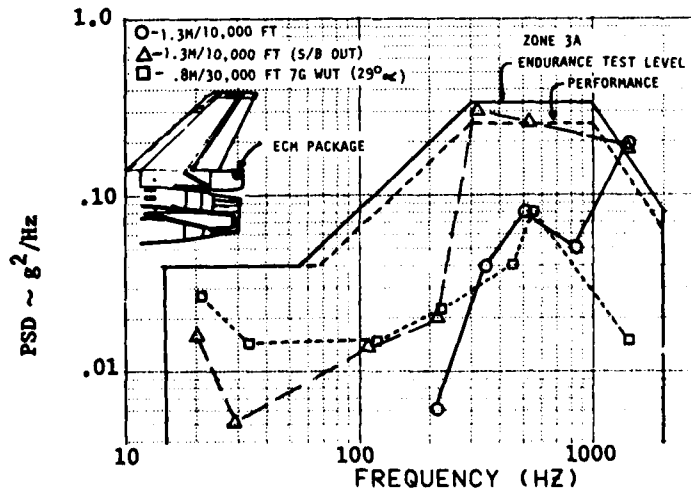


FIGURE 14 AFT FUSELAGE VIBRATION IN THE DRAG CHUTE COMPARTMENT

Three flight conditions are presented in Figure 14. High vibration levels occur when the speed brakes are extended which provides overall vibration levels about twice as high as level flight. As expected, the high "G" wind-up-turn produced low frequency response of the structure. Maneuvers are investigated further in the section on "Other Dynamic Environment."

Measurements recorded during a maximum power takeoff were surprisingly low, considering the closeness of the dragchute structure to the engine exhaust nozzle. The overall vibration level during takeoff was about half as high as the level flight measurements.

WING VIBRATION

An envelope of vibration data from two triaxial accelerometers located on the wing tip and wing front spar are presented in Figure 15. Transonic flight and subsonic maneuvers produce higher vibration than recorded during the high performance flight. The predicted vibration test requirements are considered adequate for this zone of the airplane.

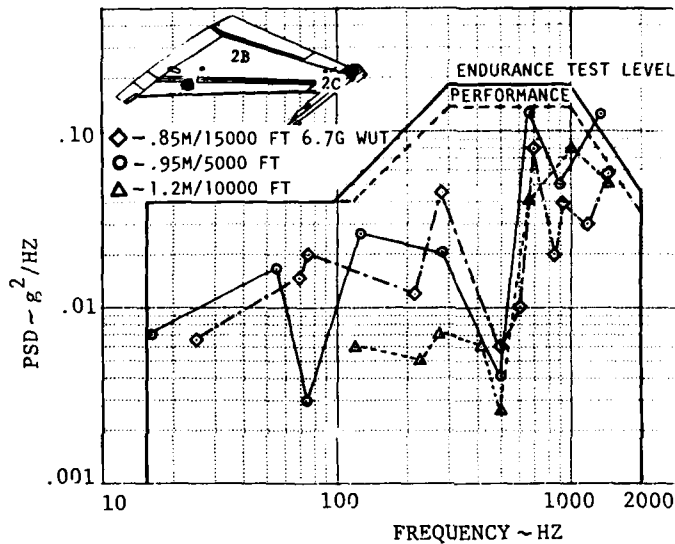


FIGURE 15 VIBRATION MEASUREMENTS IN THE WING

OTHER DYNAMIC ENVIRONMENTS

Equipment located on the wing tip and in the tip of the vertical tail must operate in transient environments produced by some relatively severe flight conditions, such as:

1. Wing tip response due to store ejection from wing pylons.
2. Jet wake encountered while chasing a maneuvering aircraft.
3. Maneuvers which produce high angle-of-attack.

STORE EJECTION SHOCK LOADS

Figure 16 shows the amplitude and duration of the wing tip response when a 2000 pound store is ejected from pylon Stations 3 and 7, (BL 120) while pulling a 4G maneuver. A shock test of 30 G's with a 40 millisecond duration is required for wing tip equipment.

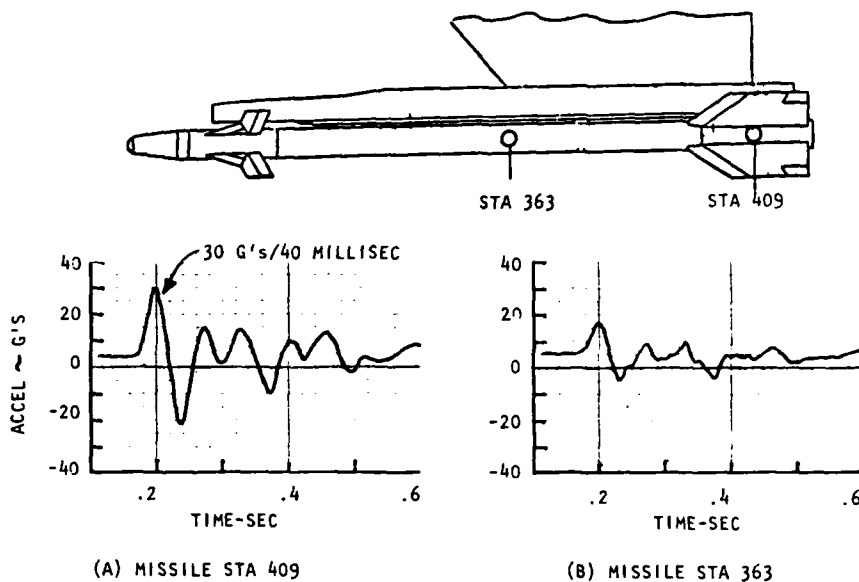


FIGURE 16 WING TIP RESPONSE DUE TO STORE EJECTION

AIRCRAFT WAKE ENCOUNTER

Aircraft wake encounter can represent a severe environment during air combat maneuvering. During air-to-air gunnery training, fighter aircraft frequently pass within a few hundred feet of one another. Although experienced pilots attempt to avoid directly penetrating the wake of another aircraft, this is not always possible. During flight testing, the F-16 deliberately flew through the wake of a maneuvering aircraft to investigate wing loads. The result was a large rolling moment applied to the aircraft plus wing tip missile oscillations. The wing tip dynamic response was similar in amplitude to the response measurements for store ejection. Consequently, the wing tip shock test requirement representing store ejection, is also adequate for the dynamic environment of jet wake encounter.

MANEUVER BUFFET

Maneuver buffet was investigated with accelerometers on the wing tip launcher and on the vertical tail tip. The results of the buffet investigation indicated that more response was due to low altitude atmospheric turbulence than was caused by maneuvers. Vibration data was recorded during sustained turns to provide a constant angle-of-attack (α). The flights were flown at 30,000 feet to eliminate the effects of atmospheric turbulence. High angles-of-attack usually produce severe buffeting on the tail surfaces. However, the F-16 flew to an angle-of-attack of 24° without recording high levels on the tail. Figure 17 shows the vertical tail frequency spectrum for a 5.8G wind-up-turn and low altitude flying with atmospheric turbulence.

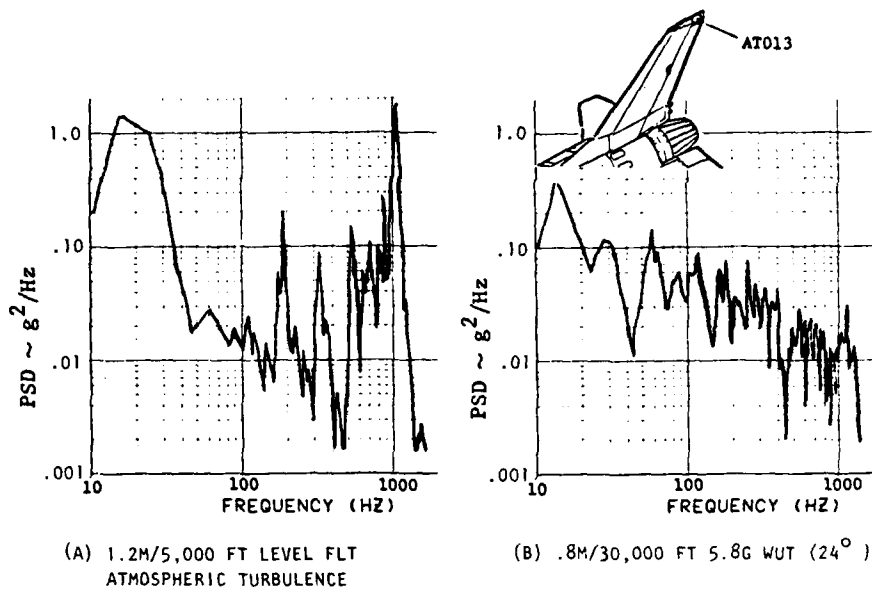


FIGURE 17 VERTICAL TAIL LATERAL RESPONSE

A real time oscillograph record is shown in Figure 18 to evaluate the low frequency response. Peak g's is more easily understood and can be compared to the supplementary sinusoidal requirement for fin tip equipment.

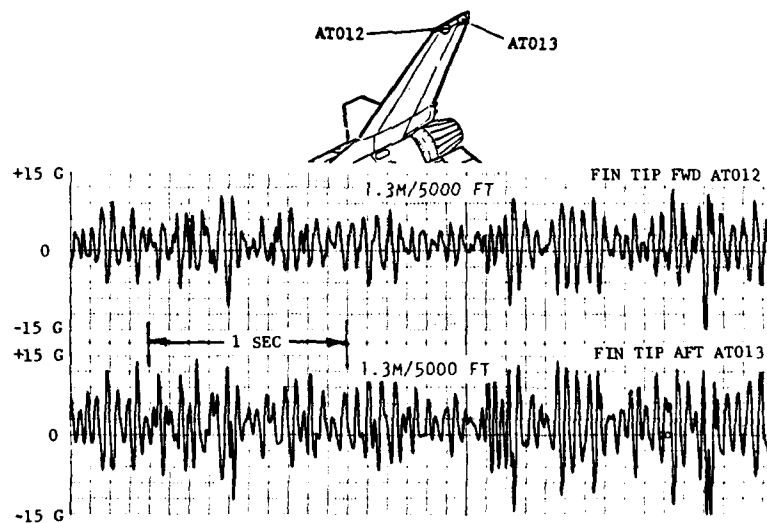


FIGURE 18 VERTICAL TAIL OSCILLOGRAPH RECORDS

These records show a randomly fluctuating amplitude with a maximum peak of +12 G's. The supplementary sinusoidal test level of +10 G's (presented in Figure 8) appears to be a good requirement for the vertical tail.

Wing tip records were similar to the vertical tail. Low altitude flight with atmospheric turbulence produced higher levels than sustained wind-up-turns at high altitude. The tip response was randomly fluctuating with maximum peaks of +10 G's.

EXTERNAL STORES

The vibratory environment associated with externally carried stores is a function of the shape and size of the store and the amount of turbulent airflow around the store. Aircraft vibration is not generally transmitted to the store but aircraft performance capabilities may influence the store environment.

A vibration estimation can be performed for several types of stores using the procedures of MIL-STD-810. However, electronic pods are not covered in the prediction procedures; therefore, a vibration survey was conducted on two electronic pods on the F-16 to investigate the vibration environment for this type of store. Figure 19 shows the results from eight accelerometers on a lightweight pod (70 pounds) attached to the inlet pylon on the R/H side.

Inlet spillage when the throttle is retarded was expected to be the worst flight condition for a lightweight pod on the inlet. However, the results indicated that high speed/low altitude flight and high angle-of-attack all produce about the same level of vibration.

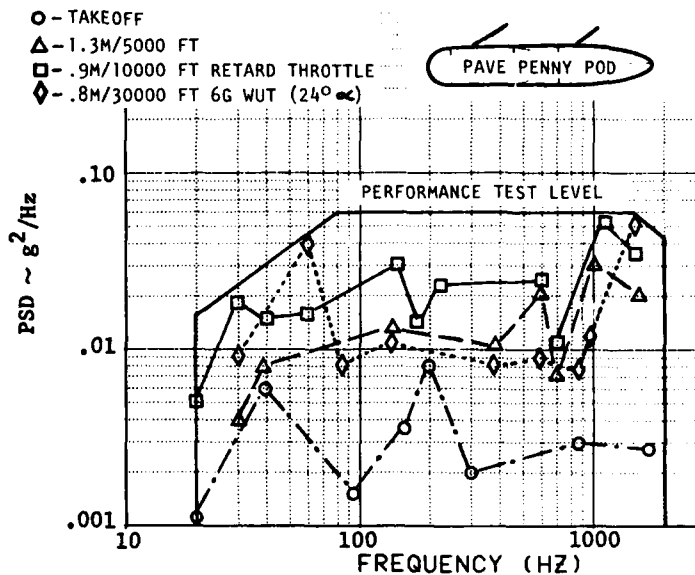


FIGURE 19 PAVE PENNY POD VIBRATION MEASUREMENTS

The other pod surveyed was a relatively heavy (320 pounds) laser designator pod which was also attached to an inlet pylon. The flight test program investigated the transonic flight region along with maneuvers. In Figure 20, it can be seen that the only significant vibration occurs in the high frequency range. When comparing the lightweight pod to the heavy pod, there is much less low frequency response recorded for the heavy pod.

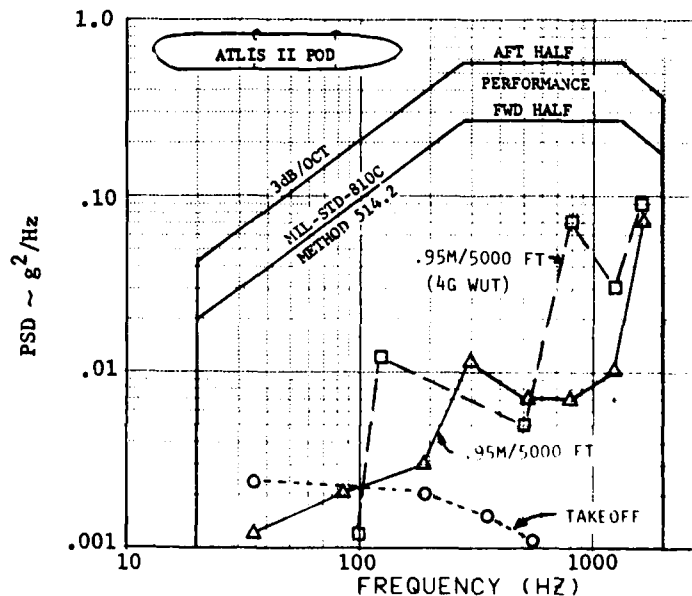


FIGURE 20 ATLAS II POD VIBRATION MEASUREMENTS

Included in Figure 20, is the calculated test level using MIL-STD-810 prediction procedures. The required levels appear to be too conservative. This conservatism is caused by a factor of four increase in the estimated levels because there is no prediction category for electronic pods. Eliminating the factor of four would produce more reasonable test levels.

Another store survey was conducted on a B-61 weapon (700 pounds) mounted to the fuselage centerline pylon. Sixteen accelerometers were recorded at 1.2M at 500 feet above ground level. Figure 21 shows the levels which envelop the maximum data at four locations on the store.

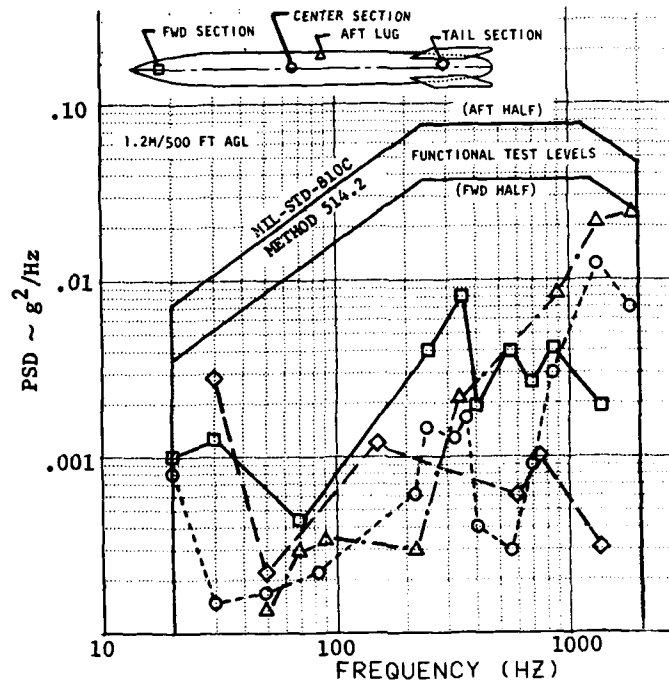


FIGURE 21 B-61 VIBRATION MEASUREMENTS

Considerable atmospheric turbulence is associated with flight at 1.2M at 500 feet above ground level and this is indicated by the nose and tail response at low frequencies.

Included on Figure 21 are the predicted test levels using the calculation procedures of MIL-STD-810. Here again, the predicted levels are conservative when compared with measured data. However, the predicted levels are not unreasonable and the low measurements may be due to the compact, aerodynamically clean configuration of the B-61 weapon.

In conclusion, the vibration prediction procedure for equipment installed in stores is adequate for missiles and bombs. However, the military specification should be updated to include additional stores categories, especially electronic pods.

DEVELOPMENT OF VIBRATION QUALIFICATION
TEST SPECTRA FOR THE F-15 AIRCRAFT

by

G. R. Waymon
Section Chief, Structural Dynamics

McDonnell Aircraft Company
McDonnell Douglas Corporation
P.O. Box 516
St. Louis, Missouri
63166
U.S.A.

Summary

The vibration test spectra used for an F-15 Eagle were based on analytical predictions combined with measured data from similar aircraft. The low frequency vibration below approximately 50 Hertz results primarily from aircraft response to gusts, buffet, landing, and taxi excitation. Vibration at higher frequencies is primarily associated with acoustical excitation and gunfire. The airplane was divided into regions of comparable vibration levels. The test levels were derived using the predicted spectra and applying factors to define a performance and an endurance test. F-15 flight measured data were used to update these predictions for the present test spectra.

Introduction

This paper is intended to define the vibration criteria used for the F-15 aircraft initially and the effects of measured data on updating the original criteria. As might be expected the original criteria were based on analytical predictions that were modified by experimental data accumulated on similar aircraft. Since the F-15 is a high performance air superiority type aircraft similar to the series of F-4 Phantoms, it was felt the environments of these aircraft would be similar and therefore experimental data obtained on an F-4 were used in shaping the environment for the F-15. The philosophy of testing for the F-15 was an extension of an apparent successful philosophy used on the Phantom. The test procedures derived were consistent with those of MIL-STD-810.

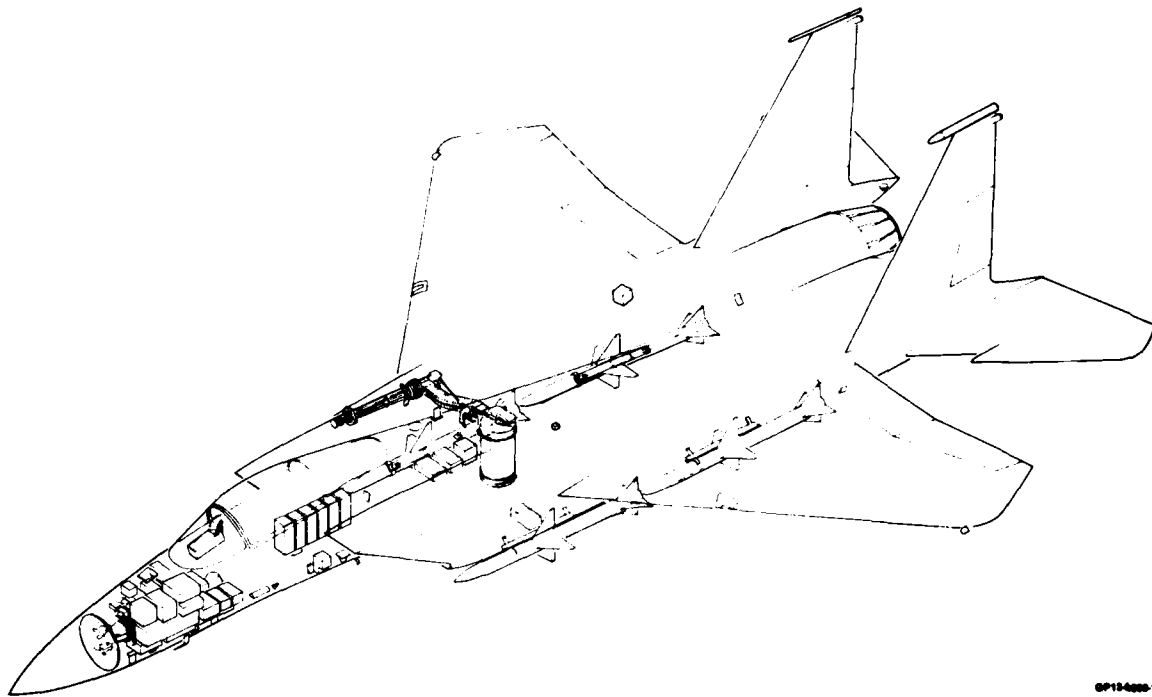
The basic philosophy here is to define the minimum test levels required to demonstrate confidence that whatever equipment is being tested will survive the environment that it will be exposed to and for the period of time for which the total aircraft is being designed. It is recognized that whatever prediction methods are used will not accurately define the actual environment the equipment will see for any location in the aircraft and for all flight profiles that will be flown. The intent is to predict parts of the aircraft that will have different levels of vibration severity and take advantage of these different levels in locating equipment and determine the susceptibility of the equipment to these levels. Testing to these levels should emphasize the detection of weaknesses in the equipment design rather than the ability to pass a somewhat arbitrary test level.

An interior arrangement of the F-15 is shown in Figure 1 showing most of the equipment installed in the forward one-third of the aircraft. The avionic equipment is located primarily in the forward fuselage in three equipment bays. These equipment bays are located forward of the cockpit, below the cockpit, and on both sides of the nose-wheel-well compartment. In addition to the basic aerodynamic and engine effects on the vibration environment, other significant impacts on the F-15 vibration environment are the internal gun, the environmental control system, and the accessory drive system. The internal gun is mounted in the right hand wing root with a muzzle blast deflector and recoil adapters that minimize the impact on the avionic equipment. Mechanically transmitted gunfire-induced vibrations are minimized because of the mass of the gun supporting structure and the long transmission path. The environmental control system which provides cooling for all equipment and the cockpit is located in the center fuselage just aft of the cockpit. The accessory-drive system which is the link between the engine and rotating equipment such as the hydraulic pump, generator, and jet fuel starter is located in the aft part of the fuselage and produces a significant environment on its own. The F-15 design flight profile along with the air superiority mission have been incorporated into the environmental vibration levels to be discussed herein.

Original Criteria

The design of the F-15 was a continuation of fighter aircraft design by McDonnell Aircraft Company (MCAIR) and therefore, a continuation of the vibration philosophies used on similar aircraft such as the F-4, F-3H, and F-101. The test levels specified for the F-15 implement the requirements of MIL-STD-810 modified by available analytical and empirical data. The original definition of vibration for the F-15 divided the aircraft into 10 regions as shown in Figure 2. These regions define test requirements for any

equipment located within that region. Regions 1 through 5 define the vibration environment of the basic aircraft for normal operating conditions. Regions 6 and 7 define vibration environment for external stores; while regions 8, 9, and 10 define vibration areas that are affected by gunfire and will need a supplemental gunfire requirement. Each zone consists of two separate requirements, a totally sinusoidal requirement for non-electronic equipment and a sine-plus-random requirement for electronic equipment.



GP15-000-1

Figure 1. F-15 Internal Arrangement

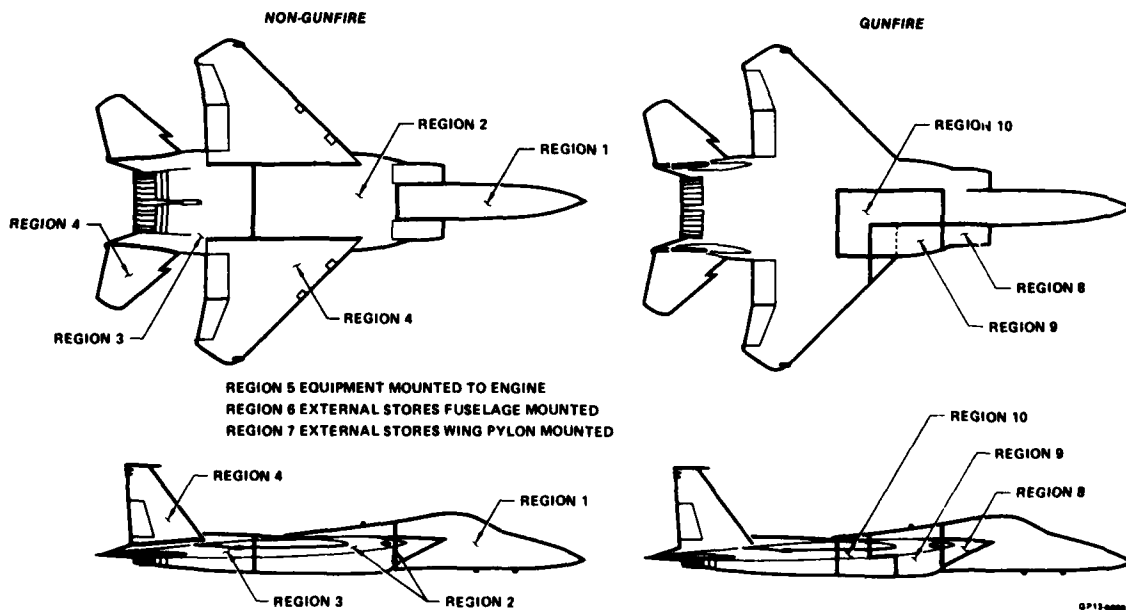


Figure 2. Vibration Regions

Conditions considered in predicting the F-15 vibration levels included engine ground runs, taxi, afterburner takeoff and climb out, maximum dynamic pressure conditions, gusts, high-load-factor windup turns, transonic flight, deceleration, landing, and gunfire. From these analyses it was determined that the F-15 low frequency vibration, below approximately 50 Hertz, results primarily from the aircraft response to gusts, landings, and taxi excitation. Vibration at frequencies above the aircraft's basic structural frequencies is primarily associated with acoustical excitations and gunfire.

Figure 3 presents a representative spectrum for the original test levels and presents both sinusoidal and random vibration levels for non-gunfire flight conditions. Figure 4 presents the gunfire requirements for a wing-root-mounted 20mm gun. Techniques used in deriving these curves are covered in the following paragraphs. The test curves reflect both a performance level test and an endurance level test for the non-gunfire and performance only for the gunfire.

The performance level test is a short duration test (5 minutes) designed to show the equipment can operate satisfactorily while being vibrated to the worst environment experienced on any given flight. The long endurance level test (30 minutes) conducted at a higher level is intended to demonstrate the equipment will not be damaged or degraded by exposure to the performance level vibration for a long duration (4000 hours). Satisfactory operation is demonstrated only before and after this test. There is also a supplemental real-time gunfire test of both sinusoidal and random testing for equipment located in regions affected by the gun mounted in the wing root.

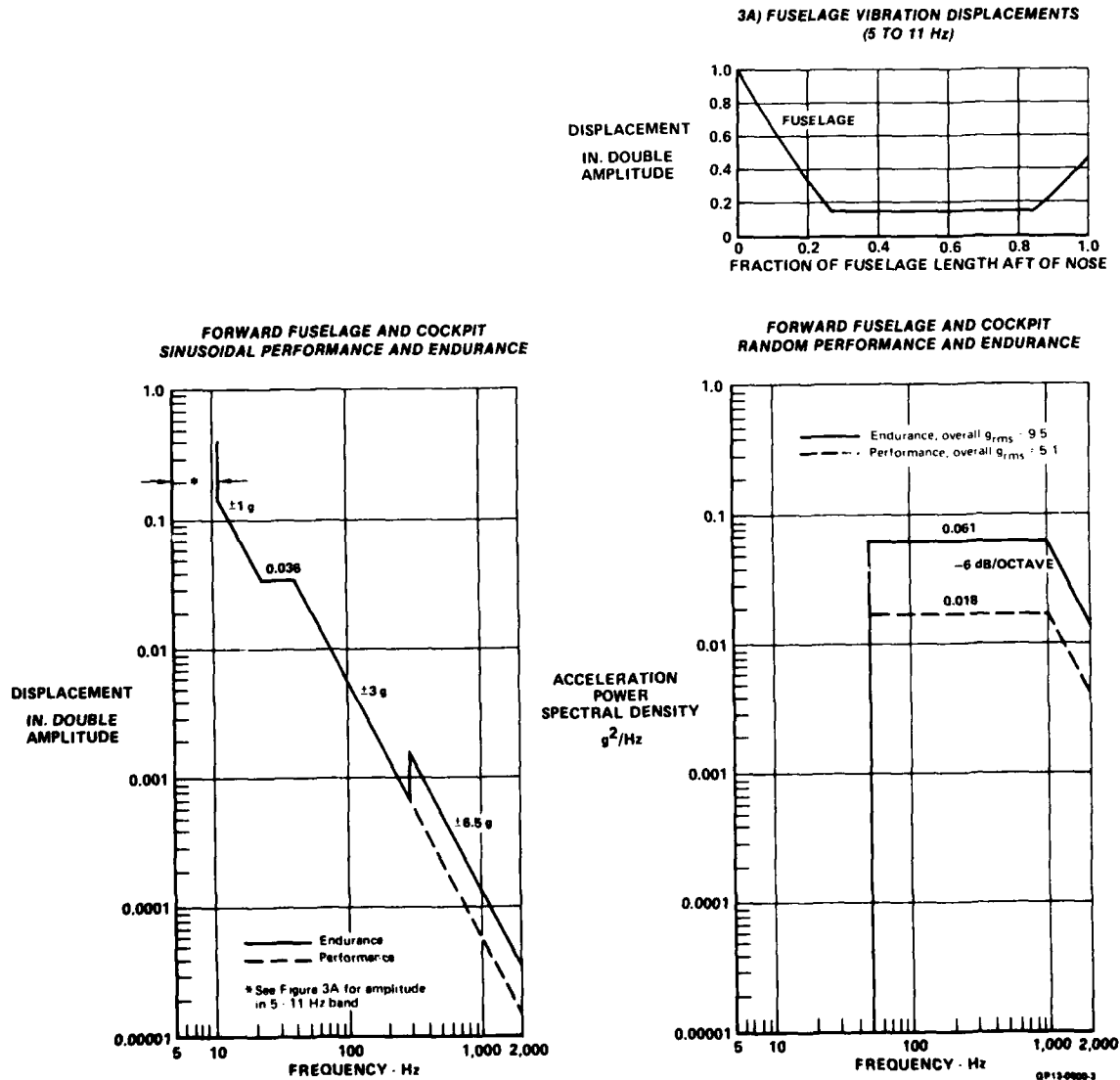


Figure 3. Region 1 Vibration Test Levels

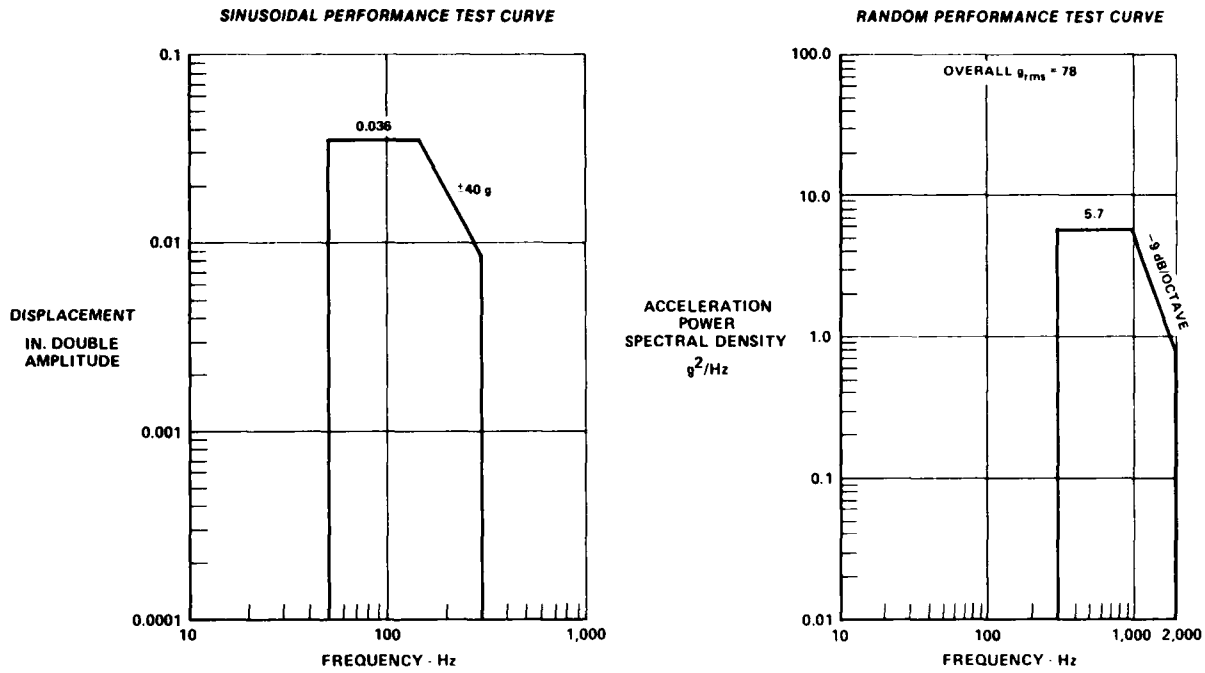


Figure 4. Region 8 Gunfire Vibration Test Levels

Acoustically Induced Vibration

Vibrations associated with higher octaves are caused primarily by engine and boundary layer noise. Estimates of these acoustically induced vibration levels for Regions 1, 2, and 3 of the F-15 were made, utilizing a technique correlating the internal vibration level with the external sound pressure level. This correlation technique was developed by P. T. Mahaffey and K. W. Smith in "A Method for Predicting Environmental Vibration Levels in Jet-Powered Vehicles," (Reference 1). The vibration prediction procedure may be broken down into the following steps:

1. Determine overall external sound pressure levels
2. Determine the frequency spectrum of the noise field at selected locations on the airframe
3. Using the frequency spectrum and overall sound pressure levels from above, determine the octave band sound pressure levels
4. Using sound pressure level versus acceleration correlation curves, determine the vibration level in each octave.

In order to develop confidence in this technique, a comparison was made between the results obtained in Reference 1 and available measured data utilizing an RF-4C aircraft (Reference 2). In each case, the correlation technique does a reasonably good job of predicting the vibration levels. It is believed this prediction technique provided realistic estimates of the acoustically induced vibration environments for the F-15 since the check case, the RF-4C, has aft engine locations and structural parameters similar to the F-15.

The vibration prediction procedure may be used to determine the internal vibration levels corresponding to any flight condition; however, typical fighter-type aircraft encounter their most severe acoustically induced vibration levels during afterburner runup, low-altitude transonic, or high-altitude maximum velocity flight.

The first step towards defining the acoustic environment was the identification of the external noise sources. Boundary layer noise, in both smooth flow and areas of separated flow, engine noise, and auxiliary power unit noise are the primary external noise sources on the aircraft. In the following sections, methods of predicting these noise sources are established and substantiated for use in the design and test criteria.

The F-15 external boundary layer noise has been predicted utilizing an empirical approach with verification provided by data measured on F-4 aircraft. Figure 5 presents the overall external boundary layer noise levels for the F-15 throughout the primary mission.

"Methods of Flight Vehicle Noise Prediction" (Reference 3), presents a method for predicting the overall boundary layer noise level (SPL) which is equation (1).

$$SPL, db = 20 \text{ Log}_{10} (\text{Dynamic Pressure, PSF}) + 86 \quad (1)$$

MISSION PHASE	PHASE TIME (HR)	ALTITUDE (FT)	AVERAGE MACH NUMBER	OVERALL SOUND PRESSURE LEVEL, dB RE 0.0002 MICROBAR		
				130	140	150
GROUND OPERATION	0	SL	-			
ACCELERATION	0.03	SL	0.75	[Hatched bar]		
OPTIMUM RANGE CLIMB AND CRUISE	0.396	42,700	0.88	[Hatched bar]		
DESCENT	0.043	10,000	0.88	[Hatched bar]		
CRUISE TO AND FROM COMBAT	0.144	10,000	0.55	[Hatched bar]		
COMBAT	0.034	10,000	0.90	[Hatched bar]		
OPTIMUM RANGE CLIMB AND CRUISE	0.395	42,700	0.88	[Hatched bar]		
DESCENT	0.054	SL	0.88	[Hatched bar]		
20 MIN LOITER AND LANDING	0.333	SL	0.31	[Hatched bar]		

GP13-0800 5

Figure 5. F-15 Overall External Boundary Layer Noise Levels for the Primary Mission

Measured data from "Vibration and Acoustic Measurements on the RF-4C", (Reference 2), are presented in Figure 6. From this figure it can be seen that equation (1) provides an adequate and generally conservative prediction of the overall boundary layer noise levels at both subsonic and supersonic flight conditions.

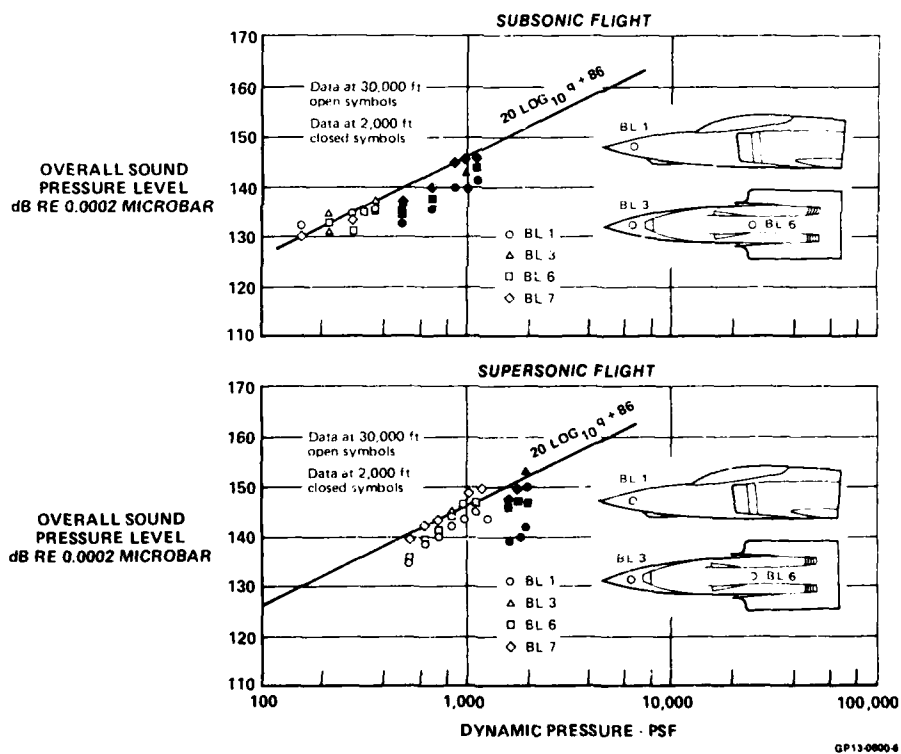


Figure 6. Measured Overall Sound Pressure Level

An empirically modified approach to the determination of the boundary layer noise frequency spectrum is presented in "Structural Vibrations in Space Vehicles" (Reference 4). This approach provides an octave band distribution that has good correlation with F-4 supersonic data. For the subsonic case, it was necessary to modify the spectrum to increase the power in the lower octave bands. Figure 7 presents sample comparisons of measured octave band frequency spectrums from RF-4C versus data predicted by methods of Reference 4.

AD-A112 533

ADVISORY GROUP FOR AEROSPACE RESEARCH AND DEVELOPMENT--ETC F/6 1/3
DYNAMIC ENVIRONMENTAL QUALIFICATION TECHNIQUES.(U)

DEC 81

AGARD-CP-318

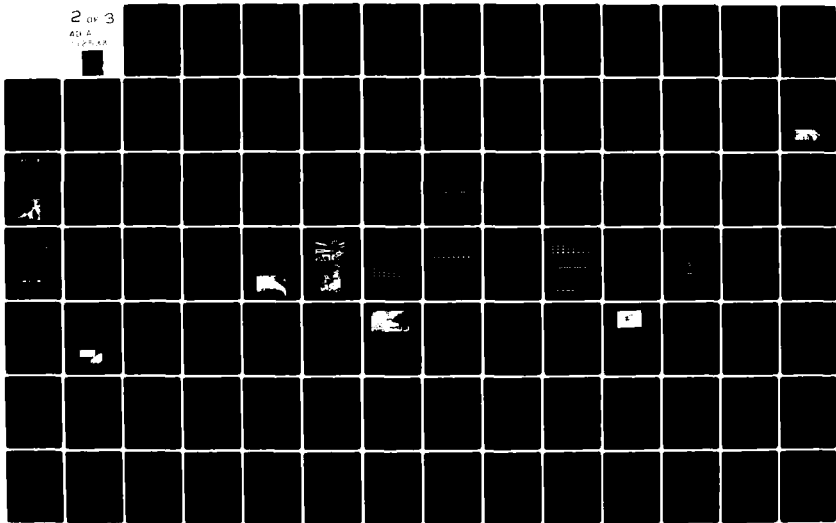
UNCLASSIFIED

NL

2 of 3

AD A

CP-318





2.8 2.5



Resolution Test Chart
1963

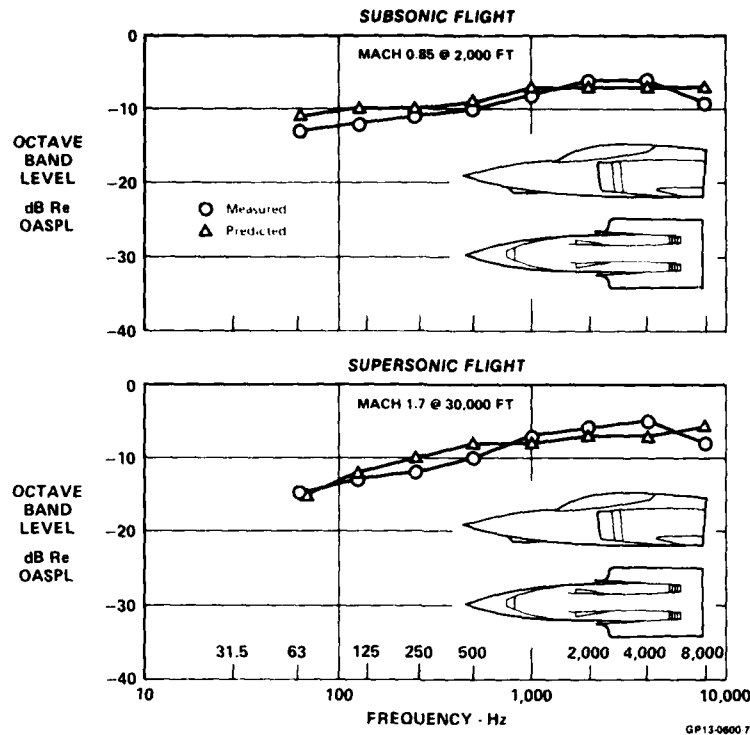


Figure 7. Octave Band Distribution Measured vs Predicted

Jet Engine Noise

The F-15 Pratt & Whitney F100 engines are turbofan engines. The jet engine noise is generated at the jet exhaust and the inlet noise is generated by the fan and compressor. The inlet noise is normally 10 to 20 db lower at the source than the jet exhaust noise at its source. Since the F-15 installation has an inlet duct approximately 18-feet long, the inlet noise effects on the forward aircraft area will be of less importance. "On Prediction of Acoustic Environments from Rockets" (Reference 5) presents a method of predicting jet engine noise. MCAIR has modified this basic prediction technique based on data from "Noise Produced by Aircraft During Ground Runup Operations" (Reference 6) and correlation with data from "Methods of Flight Vehicle Noise Prediction" (Reference 3). This prediction technique gives the sound power level as a function of the expanded jet exit velocity and nozzle exit diameter.

To determine the sound pressure level (SPL) at any point other than the source, the reduction of SPL due to the sound radiating from a source must be accounted for. The loss can be from spherical expansion of sound (no reflecting plane) or hemispherical expansion (with a reflecting plane). For spherical expansion, the loss is determined by equation 2.

$$\text{SPL, db} = -10 \log_{10} 4 \pi (\text{Distance, Ft})^2 \quad (2)$$

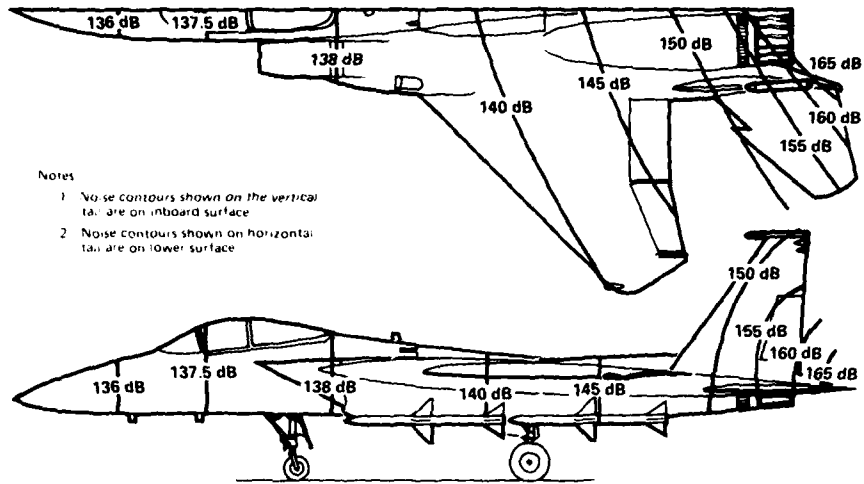
For hemispherical expansion, the loss is determined by equation 3.

$$\text{SPL, db} = -10 \log_{10} 2 \pi (\text{Distance, Ft})^2 \quad (3)$$

In addition, a distance from the nozzle correction was required to obtain good correlation with data from "Methods of Flight Vehicle Noise Prediction" (Reference 3).

The predicted jet engine overall noise levels on the F-15 for ground runup at maximum afterburner power are presented in Figure 8. For ground runup at military power, the overall noise levels will be nine db lower. In flight, the engine noise field is diminished and translated downstream. Figure 9 presents the jet engine noise frequency spectrum.

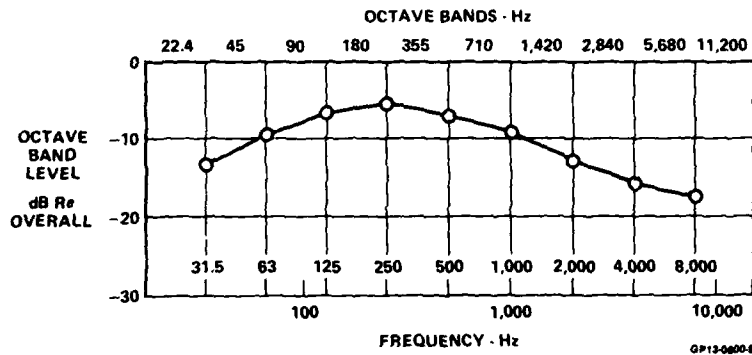
Steps 1, 2, and 3 of the prediction procedure were performed to determine the octave band sound pressure levels for each of the flight conditions. Figure 10 presents these data for Region 1. This figure indicates that for Region 1 the maximum sound pressure level occurs during low altitude transonic flight. This same procedure was used to predict the sound pressure levels for Regions 2 and 3. These conditions then established the maximum predicted vibration levels in each region. Figure 11 was utilized to establish the vibration levels and Figure 12 presents the predicted sinusoidal and random vibration levels so established for Region 1.



- Notes
1. Noise contours shown on the vertical tail are on inboard surface
 2. Noise contours shown on horizontal tail are on lower surface

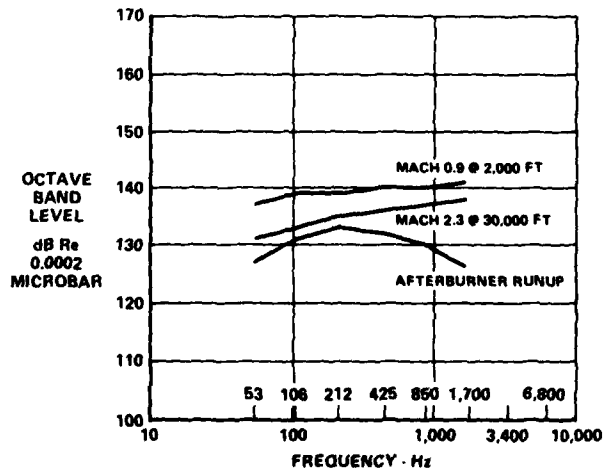
GP13-0600-8

Figure 8. Overall Sound Pressure Level Contours for Ground Runup at Maximum Afterburner Power



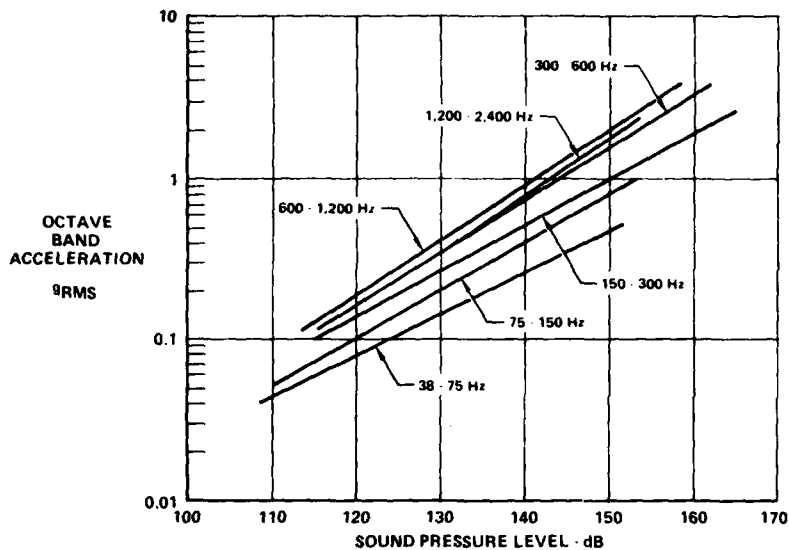
GP13-0600-9

Figure 9. Jet Engine Noise Frequency Spectrum



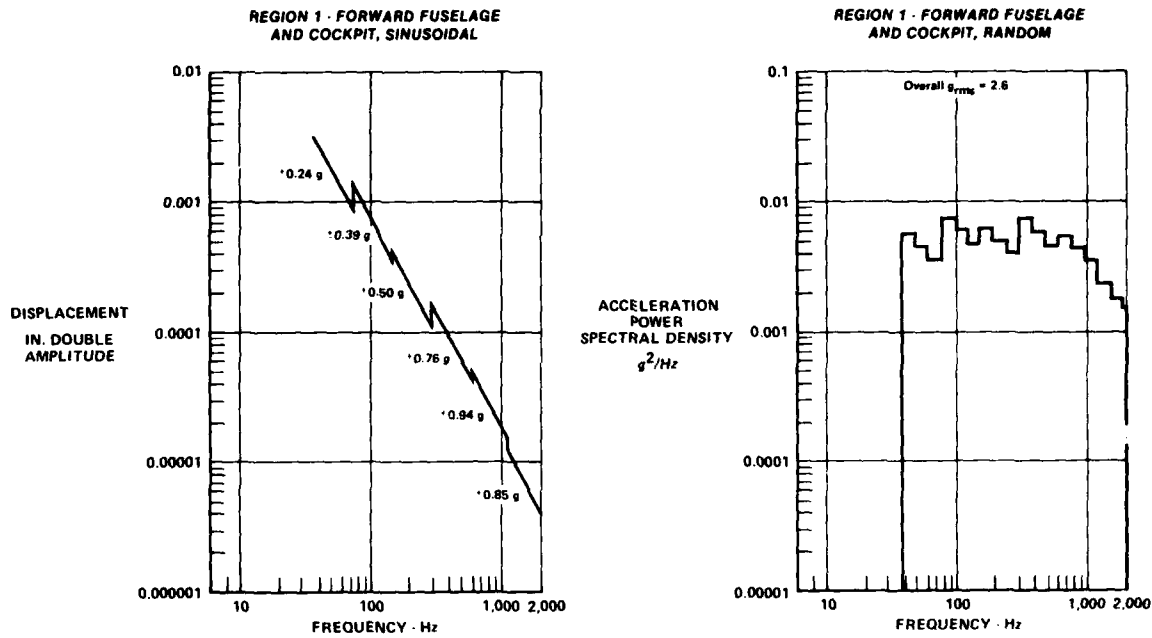
GP13-0600-10

Figure 10. External Sound Pressure Levels for Region 1



GP13-0600 11

Figure 11. Acceleration vs Sound Pressure Level
Correlation Curves



GP13-0600 12

Figure 12. Vibrations

The first phase of the analysis was conducted using the digital program "LAND", to compute main gear reactions during landing. This reaction was obtained on a rigid aircraft, and included the flexibility and damping of the main gear and tire. To obtain the flexible aircraft response due to landing, a direct analog computer was used to model the flexibility of the fuselage and wing, using a beam-rod analog. The main gear reactions from the "LAND" program were used as the forcing function on the analog computer, and time histories of the accelerations at various points on the aircraft were obtained.

Gust

The evaluation of aircraft response to turbulence for the F-15 is based on the treatment of the vertical wind gust input as a random continuous time function. The vibratory accelerations of the aircraft are calculated by power spectral density methods for a representative cruise condition in the air superiority mission. The condition is for a gross weight of 32,700 pounds and a Mach number of 0.88 at an altitude of 42,700 feet. Six aircraft degrees-of-freedom were included in the analysis. They consisted of rigid body pitch and vertical translation, the first two normal vibrations modes for the wing, and the first two free-free fuselage vertical bending modes. The power spectral

density of the acceleration along the aircraft fuselage and along the wing elastic axis were calculated for a root-mean-square gust velocity input of three feet-per-second. This level of gust intensity is defined in AFFDL-TR-66-5B (Reference 7), as being a composite average for all gusts encountered during flight. The peaks in the acceleration response occur at frequencies of .4, 5.7, 12.4, and 24.4 Hz. These frequencies correspond to the aircraft short period (rigid body pitch), first fuselage bending, and first and second wing modes, respectively. The responses in the short period mode and first wing modes predominate, with the remaining modes contributing a lesser amount. These results are used to define the low frequency fuselage environment. Representative sinusoidal vibration levels for each resonant vibration frequency can be approximated from the area under each response peak in the power spectral-density response plots. The results of this evaluation are compared to the landing and taxi requirements in Figure 13.

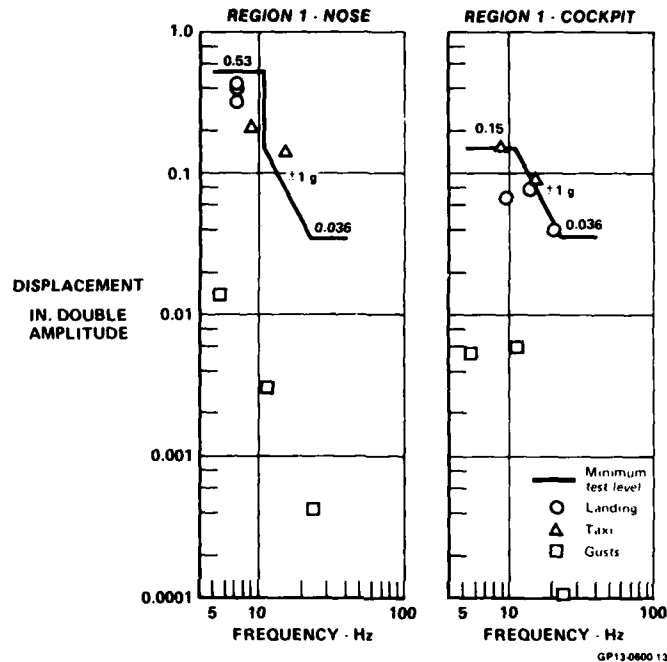


Figure 13. Low Frequency Vibration Displacement, Fuselage

Taxi

Taxi analyses were conducted on a dynamic idealization of the F-15 to determine equipment vibration environments. This analysis was conducted on the CEAC direct analog computer, utilizing photo formers to generate the landing gear input to the wing. This input was computed, with a digital program, on a rigid airplane idealization, which included the nonlinear effects of tire and strut. A maximum of two consecutive 1-cosine shaped bumps were considered for the runway shape, with two-inch amplitudes and 30-inch lengths. The results of this analysis are compared with the F-15 equipment vibration qualification test levels in this report. These test levels, which are based on landing analyses and surveys of similar aircraft, are shown in Figure 13 and are adequate for the average acceleration experienced during taxi.

Gunfire

Due to the wing root location of the internal gun system, the inlet duct and blast diffuser protect the avionics equipment bays from any significant blast pressures. Acoustically induced vibration from gunfire, therefore, does not represent the most severe vibration environment in equipment bays forward of the muzzle. Gunfire will, however, induce structure-borne vibration of significant levels in areas adjacent to the gun system, due to oscillatory recoil forces. These recoil forces will induce substantial vibratory response in the frequency range from the fundamental frequency of the lowest firing rate (4000 shots per minute) to several harmonics about the highest firing rate (6000 shots per minute).

Predictions of the vibration environment in areas surrounding the gun system were based on experience gained on the MCAIR F-4E program. Figure 14 presents the maximum acceleration levels measured during the F-4E program versus distance from the gun breach. These levels are applicable to a 20mm gun system. These levels are then used to determine the gunfire qualification test levels presented in Figure 4.

A review of the gunfire data obtained during the development of the F-4E gun system indicates a sinusoidal test will most closely simulate the gunfire fundamental firing frequency environment. These spectra are supplemented by the random curves of Figure 4. The gunfire test procedures used represent a "real time" test.

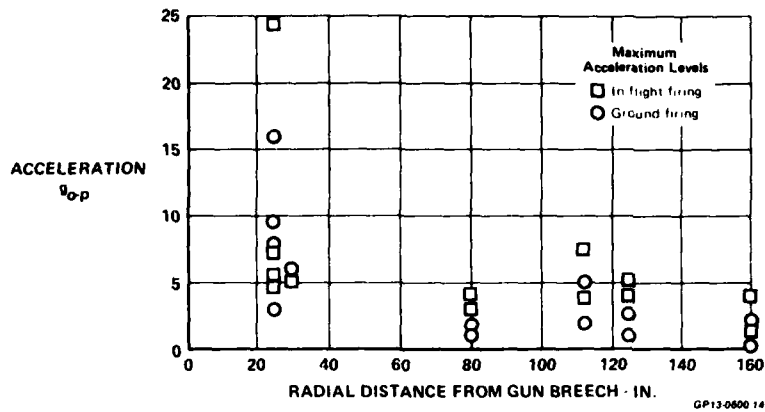


Figure 14. Vibration Levels Measured During 20 mm Gunfire

Test Curves From Predictions

Test levels for vibration are established to insure satisfactory operation of the equipment in the environment in which it will be placed (performance) and to demonstrate an operational life requirement (endurance). Vibration testing to insure compliance with each of these requirements, performance and endurance, may be accomplished using either sinusoidal or random testing. Estimates of the required minimum test levels, using either testing technique, are presented herein.

The predicted high frequency vibration levels derived earlier and presented in Figure 12 represent "average" vibration levels expected in Region 1. Therefore, they must be adjusted by a series of factors, shown in Figure 15, to arrive at information which may be considered generally applicable for qualification testing. The low frequency vibration levels of gusts, landings, and taxi are computed short duration maxima and, therefore, require no additional factoring to derive test levels.

TYPE OF VIBRATION TESTING	FACTORS TO CONVERT FROM PREDICTED LEVELS TO TEST LEVELS				PERFORMANCE TEST LEVEL	ENDURANCE TEST LEVEL
	(a)	(b)	(c)	(d)		
SINUSOIDAL	1.5	1.7	1.3	1.7 TO 2.5	(a) (b) (c) = 3.3	(a) (b) (c) (d) = 5.6 TO 8.3
RANDOM	1.5	-	1.3	1.75 TO 1.85	(a) (c) = 2.0	(a) (c) (d) = 3.4 TO 3.6

- (a) - Factor to account for not measuring or predicting most severe environment.
 (b) - Conversion of sinusoidal data from root mean-square (rms) to zero-to-peak for 1/3 octave bands.
 (c) - Factor to account for testing separately for each axis whereas vibration occurs along all axes simultaneously in service environment.
 (d) - Accelerated life factor applied to performance test levels to obtain endurance test levels (varies with octave band and region of the aircraft).

GP13-0000-15

Figure 15. Summary of Factors Employed in Converting Predicted Levels to Test Levels

For sinusoidal performance testing, utilizing test procedures called out in Reference 8, the predicted levels shown in Figure 12 are multiplied by the factors described above. The performance levels, thus calculated are shown as the dashed lines and are compared to the levels specified as the minimum performance test levels in Figure 16 for Region 1. In no case are performance test levels less than 3 g's called out for frequencies of 40 Hertz or greater since this is considered to be the minimum level for a meaningful test. Test levels at frequencies below 50 Hertz are based on the results of the aircraft response to gusts, landings, and taxiing, as well as comparison with published data on fighter aircraft.

For random performance testing, utilizing test procedures called out in Reference 8, the spectrum shape shown in Figure 16 covering the 50 to 2000 Hz bandwidth was derived from the predicted 1/3 octave band vibration spectra for Region 1. This same spectrum shape is used for all random testing between 50 and 2000 Hz. For frequencies below 50 Hz, equipment is tested sinusoidally to the performance levels previously developed.

To weight the vibration level in each region as a function of flight condition, it is necessary to have information on the projected operational usage of the aircraft. A tabulation, derived from a mission analysis for the F-15 showing the breakdown of utilization at different flight conditions is presented as Figure 17. The flight time and predicted vibration level for each flight condition are used in equation (2) to derive the vibration level for a 30-minute accelerated life endurance test for sinusoidal vibration and a two-hour test for random vibration. This accelerated life vibration test will impose upon the equipment fatigue damage equivalent to the operational life of the aircraft.

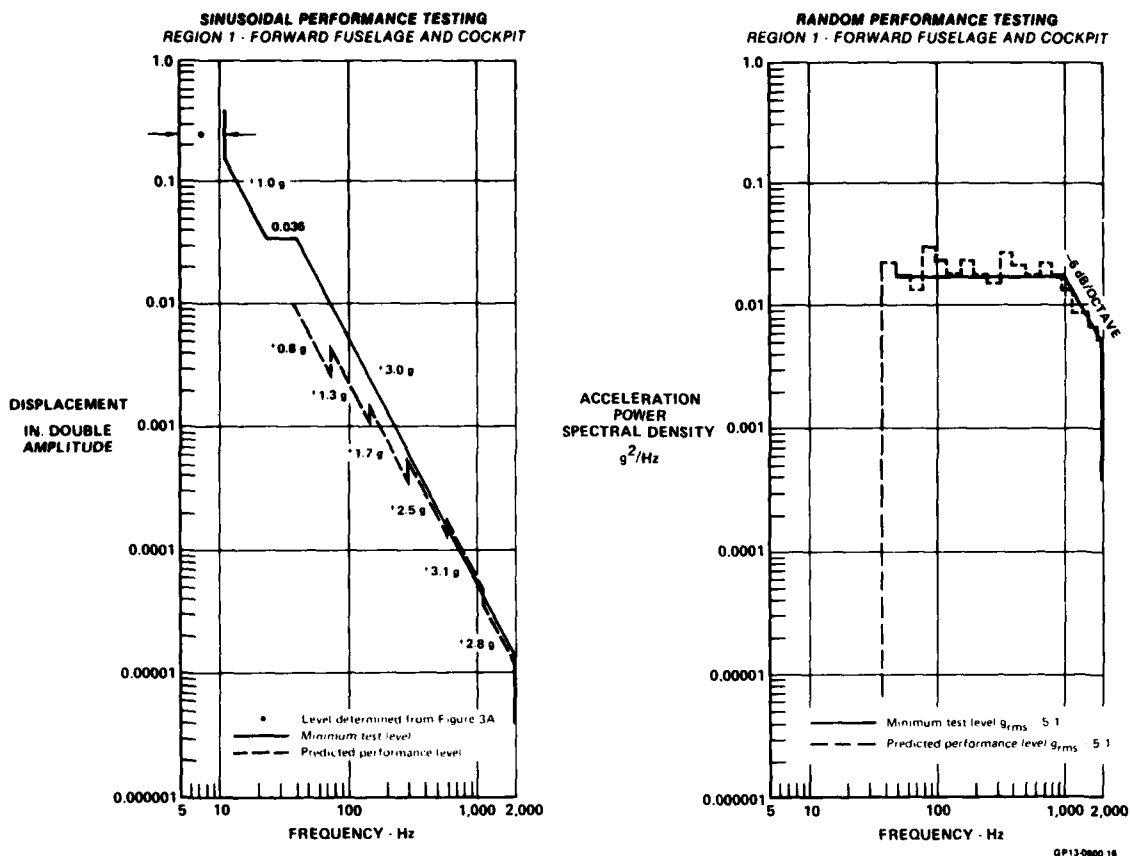


Figure 16. Vibration Test Levels

FLIGHT CONDITION	PERCENT FLIGHT TIME	HOURS
GROUND RUNUP AND TAKEOFF	—	53
AT CRUISE SPEED AT LOW ALTITUDE	20	800
ABOVE CRUISE SPEED AT LOW ALTITUDE	10	400
AT CRUISE SPEED AT HIGH ALTITUDE	55	2,200
IN SUPERSONIC FLIGHT	1	40
IN CLIMBS AND DESCENTS	14	560
TOTAL	100	4,053

Figure 17. Times at Various Flight Conditions
Based on F-15 Mission Analysis

For sinusoidal endurance testing, utilizing test procedures called out in Reference 8, an accelerated life factor was derived by the technique developed in Reference 9. Endurance test levels are established within the limitations that they should at least equal performance test levels. The structure of the equipment being tested behave fairly linearly at these levels relative to the performance test levels and they should result in realistic test times. This may be accomplished by use of stress versus number of cycles to failure curves (S-N diagrams). Since an item of equipment is usually made up of a number of different materials, the test level is patterned for the material with the most critical S-N curve. For typical equipment, this most critical S-N curve results in a time compression factor of

$$\left(\frac{\text{Flight Time}}{\text{Equivalent Time}} \right) = \left(\frac{\text{Reference Acceleration}}{\text{Actual Acceleration}} \right)^{8.7} \quad (4)$$

Utilizing this procedure, the required sinusoidal endurance levels were calculated for Region 1. These calculated endurance levels, shown as the dashed lines, are compared to the levels specified as the minimum endurance test levels in Figure 18. In no case are endurance test levels less than 3 g's called out for frequencies of 50 Hertz or greater.

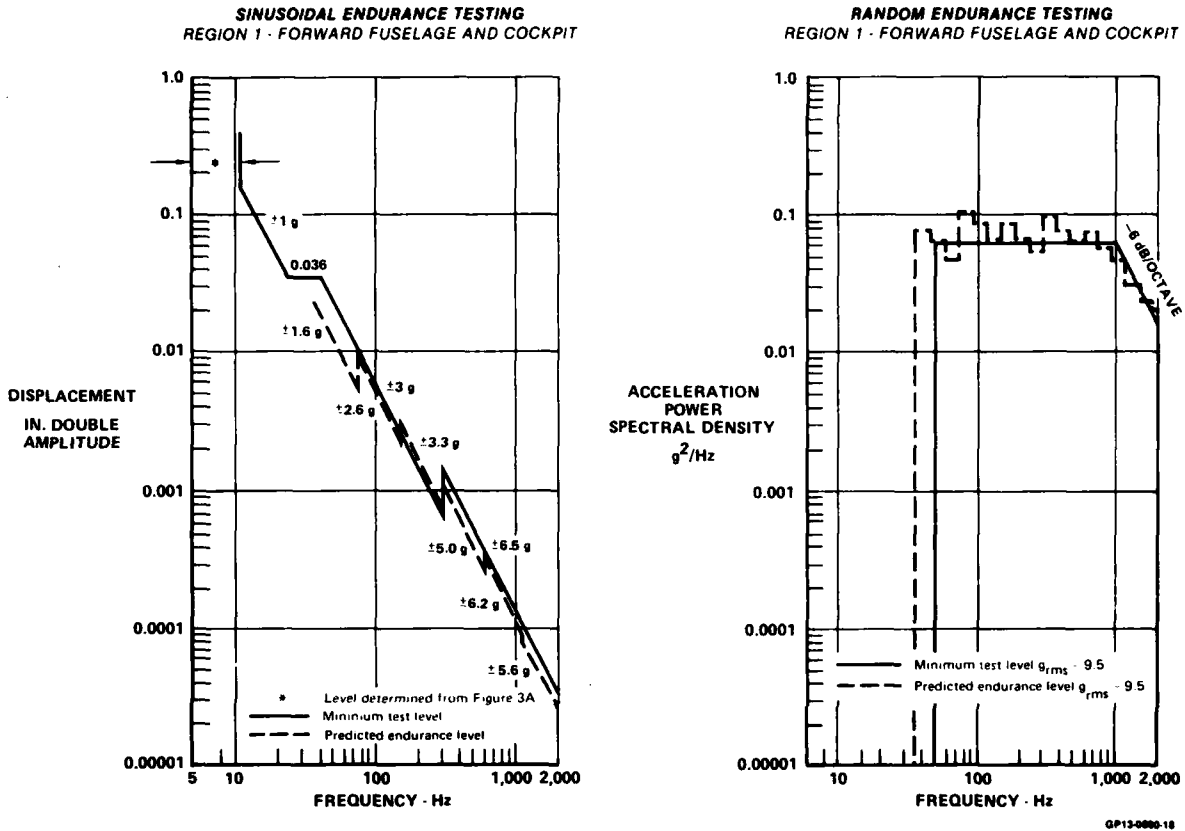


Figure 18. Vibration Test Levels

For random endurance testing, utilizing test procedures called out in Reference 8, a technique equivalent to that developed for establishing the sinusoidal endurance test was used to determine the accelerated life factor. Using the same critical S-N curve selected for sinusoidal endurance testing, the relationship developed in Reference 9 between acceleration power spectral density (PSD) and time for a random input is

$$\left(\frac{\text{Flight Time}}{\text{Equivalent Time}} \right) = \left(\frac{\text{Reference PSD}}{\text{Actual Acceleration}} \right)^{4.35} \quad (5)$$

The same procedure, used in calculating the sinusoidal endurance levels, is employed whereby the required test PSD level necessary to yield fatigue damage equivalent to the operational life of the aircraft is determined for a two-hour accelerated life test. Figure 18 presents the required random vibration test levels for a two hour endurance test for Region 1. For frequencies below 50 Hertz, sinusoidal testing to the levels previously determined is utilized, that is, no life factor is used for frequencies below 50 Hertz.

Flight Measurement Program

The flight test program consisted of selecting representative locations throughout the airplane and installing tri-axial accelerometers at these locations. Figure 19 gives an indication of relative emphasis on the more significant parts of the airplane where most of the equipment is installed. The flight conditions where significant vibration levels were anticipated were called out as shown in Figure 20. These flight test conditions were intended to cover the complete aircraft envelope. Although specific test points were specified for the flight test program it is significant to note that these points may not be attained nor duplicated exactly for each set of measurands. These deviations will be accounted for in the adjustment factors applied to the data.

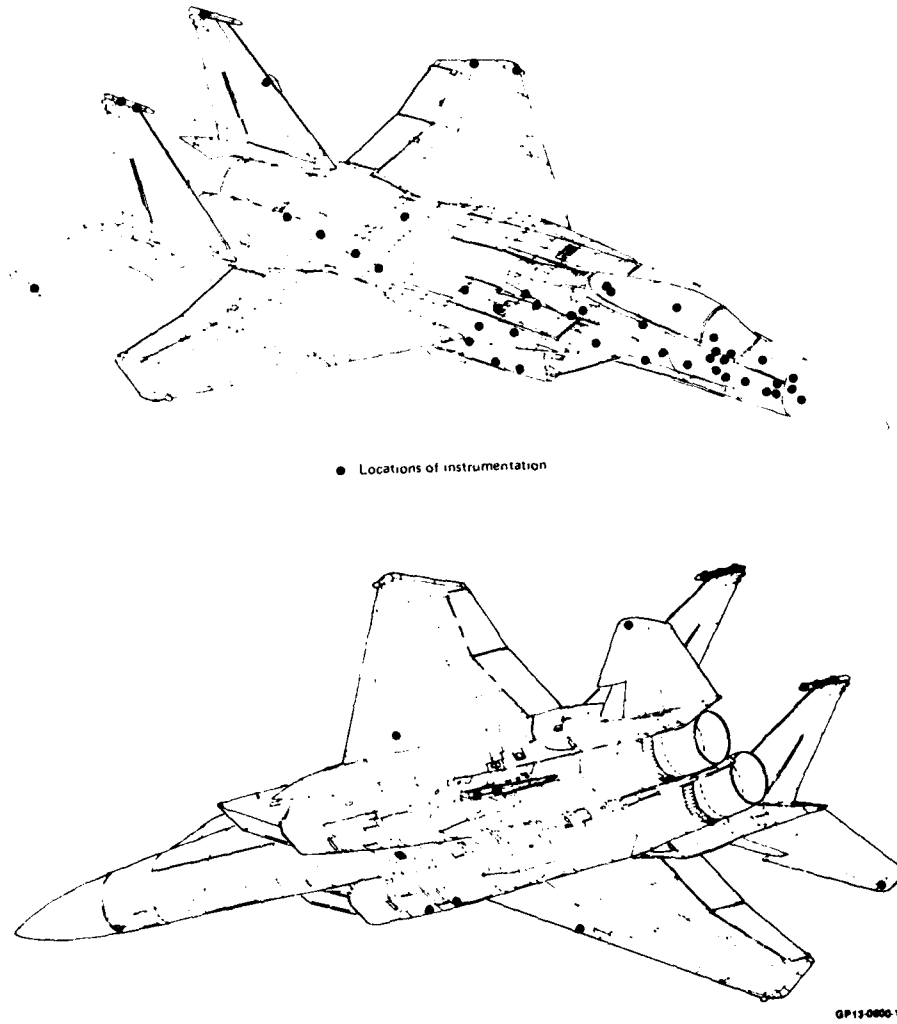


Figure 19. Vibration Instrumentation Locations - F-15

NON-GUNFIRE MANEUVER		GUNFIRE MANEUVER	
TAXI		GROUND GUNFIRE	
MIL POWER TAKEOFF		FLIGHT GUNFIRE	
A/B TAKEOFF			
CLIMB			
10,000 FT	1 g, MACH 0.8 1 g, MACH 0.9 1 g, MACH 0.95 1 g, MACH 1.12 WIND-UP TURN ROLLING PULL-OUT SYM PULL-UP A/B ACCELERATION S/B DECELERATION	10,000 FT	1 g, 180 KEAS 1 g, MACH 0.85 1 g, MACH 0.9 1 g, MACH 0.95
25,000 FT	1 g, MACH 0.8 1 g, MACH 0.9 1 g, MACH 0.95 1 g, MACH 1.12 1 g, MACH 1.47 WIND-UP TURN ROLLING PULL-OUT SYM PULL-UP A/B ACCELERATION S/B DECELERATION	25,000 FT	1 g, MACH 0.9 1 g, MACH 0.95 1 g, MACH 1.47
40,000 FT	1 g, MACH 0.8 1 g, MACH 0.9 1 g, MACH 0.95 1 g, MACH 1.12 1 g, MACH 1.5 1 g, MACH 2.0 WIND-UP TURN ROLLING PULL-OUT SYM PULL-UP A/B ACCELERATION S/B DECELERATION	40,000 FT	1 g, 180 KEAS 1 g, MACH 0.95 1 g, MACH 1.6 1 g, MACH 2.0
S/B DESCENT			
DESCENT			
LANDING APPROACH			
TOUCH DOWN			
ROLLOUT			
ENGINE GRD RUN			
AIR-TO-AIR MISSILE SEP			
AIR-TO-GRD STORE SEP			
TANK JETTISON-I/B PYLON			

GP13-0600 20

Figure 20. Flight Conditions for Vibration Data

Once data are obtained for all test points, the acceleration-versus-time strip-charts are reviewed for specific points where further data reduction is to be performed. For these points, one-third octave and power spectral density analyses are performed.

For each set of measurands the data are collected for all flight conditions flown and data are overlaid on the same plot to accumulate a composite curve for that location. Two types of composite curves were made: (1) One-third octave plots showing inches double amplitude versus frequency for the sinusoidal data and (2) g^2/Hz versus frequency for the random data. One-third octave data are accumulated on the same plot to obtain the relative frequency contributions of all flight conditions. These plots are used to define the measured data for the sinusoidal test criteria. Examples of measured composites are shown in Figure 21 for both sinusoidal and random data.

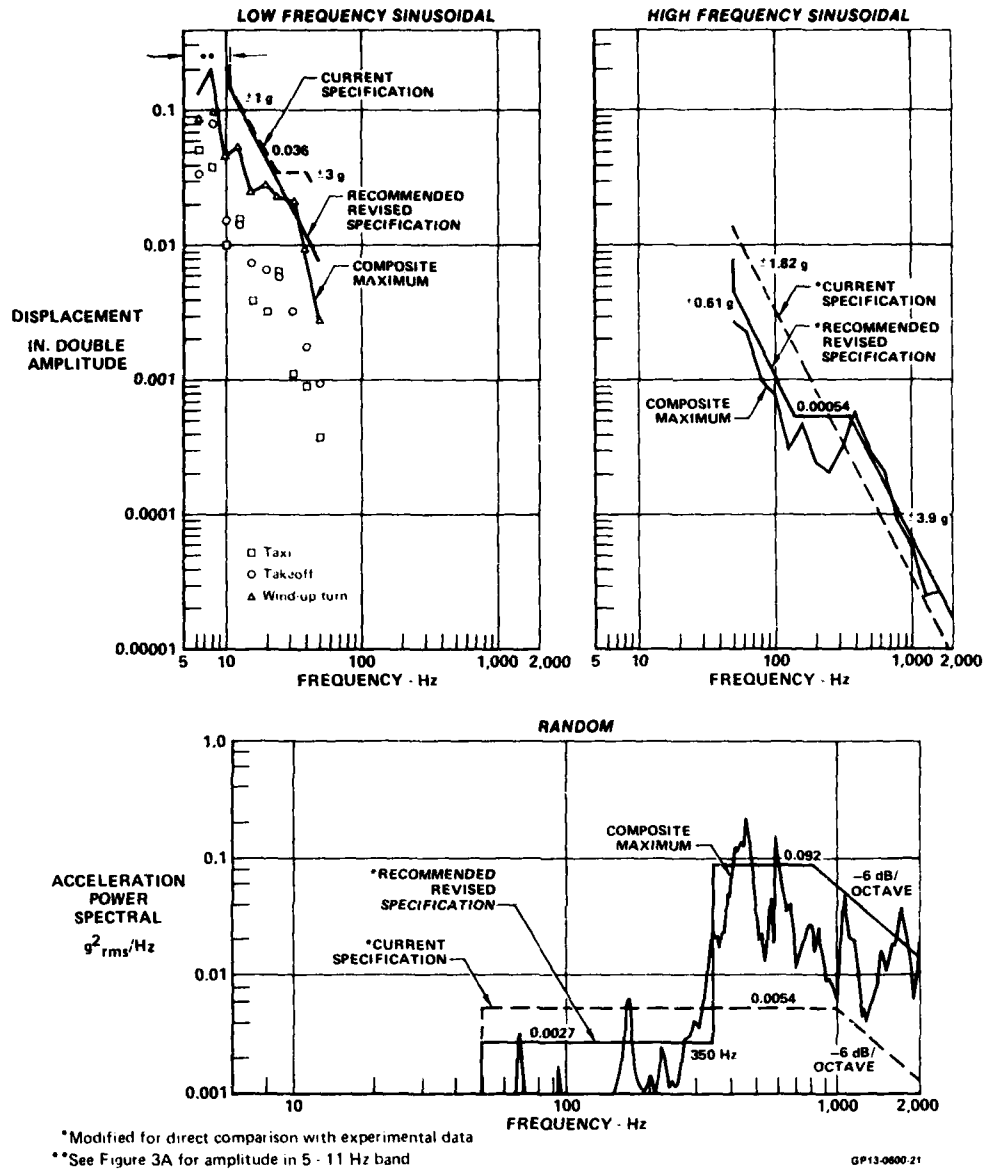


Figure 21. Region 1 Vibration Levels - Non-Gunfire Forward Fuselage

For random data, the composite of all the measured data in the axis or axes of interest is accumulated on the same PSD plot similar to the sinusoidal one-third octaves. Then, envelope the composite peaks and compute the overall RMS level ($G_O(RMS)$). Then lower the entire envelope uniformly such that its overall RMS level matches the maximum overall RMS level of the measured data.

$$G^2/Hz (Ref) = (G^2_O/Hz) \left(\frac{G_m}{G_O} \right)^2 \quad (6)$$

This spectrum is then treated similar to predicted data. A similar composite was made of the low frequency data in the frequency range of 5-11 Hz, which corresponds to the fuselage fundamental modes. Data are presented as a function of fuselage location and compared to the existing specification which reflects the fundamental bending mode shape. This comparison is shown in Figure 22.

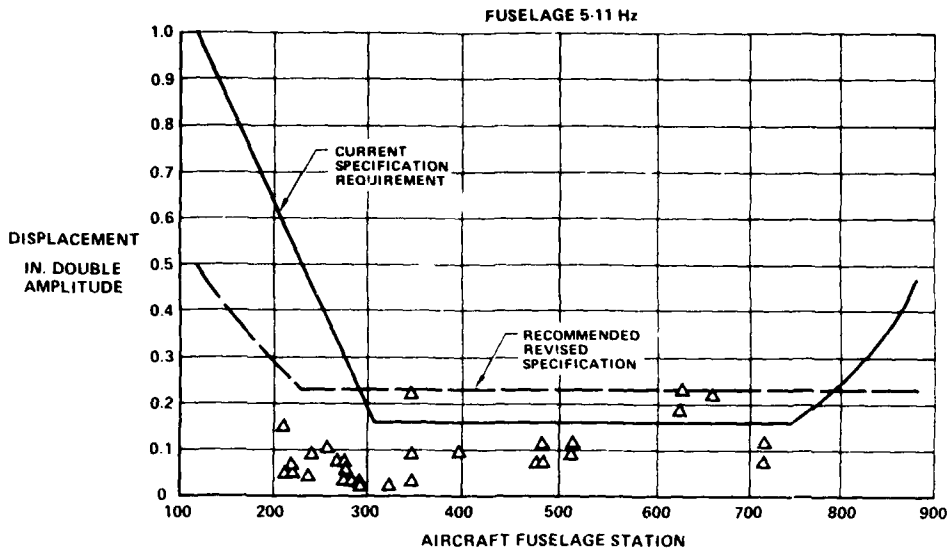


Figure 22. Low Frequency Vibration Levels and Specification Requirements
Region 1

Zoning

After review of the composite data for each location, all locations that show similar levels are then collected to form a region similar to the regions used for the predicted data. These new regions are defined in Figures 23 and 24 for both non-gunfire and gunfire.

Test Curves From Measured Data

Once the data were accumulated as composite curves and grouped into representative regions it was then necessary to establish test curves for performance and endurance testing. The method used to establish test curves was similar to that used for establishing test curves from predicted data.

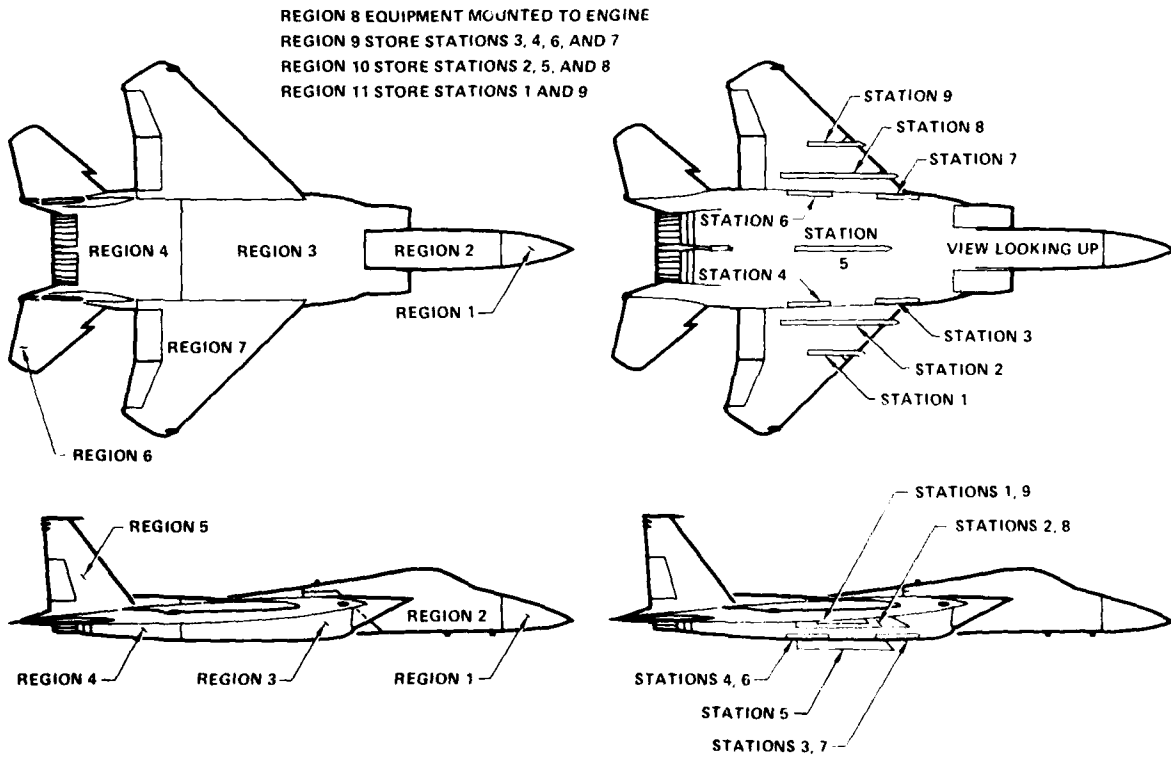


Figure 23. Vibration Regions
Non-Gunfire

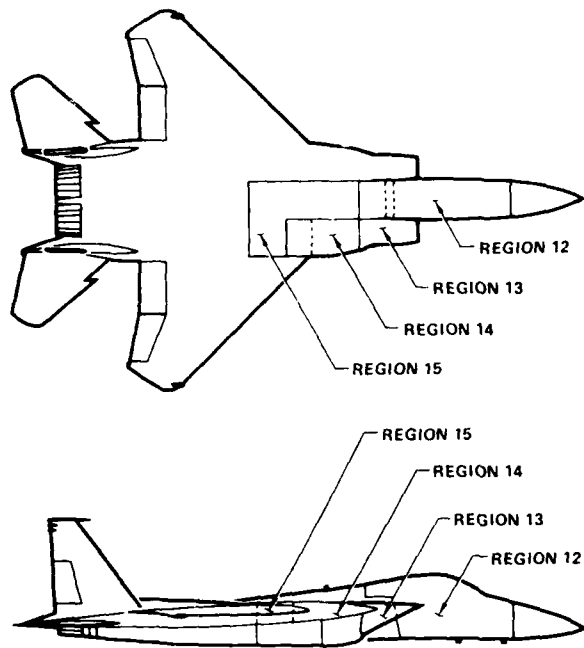


Figure 24. Vibration Regions
Gunfire

GP13-0800 24

To obtain the performance spectrum, multiply the composite spectrum by the factors a and c from Figure 15. Factor "a" (=1.5) accounts for not measuring the most severe environment and factor "c" (=1.3) accounts for measuring separately along each axis when vibration occurs in all three axes simultaneously. This process was used for both sinusoidal and random spectra. The factors for the random spectrum are applied to the power spectral density as follows:

$$G^2/\text{HZ (Ref)} (ac)^2 = G^2/\text{HZ (Perf.)}$$

To obtain the endurance spectra multiply the performance spectra by the accelerated life factor for the service life desired.

For a service life of 4000 hours the accelerated life factor is;

Sinusoidal

$$\frac{G_{o-p} \text{ (End.)}}{G_{o-p} \text{ (Perf.)}} = \left(\frac{T_o}{.5} \right)^{1/n} \quad (7)$$

Where T_o is the number of hours the equipment will be exposed to this environment in a 4000 hour lifetime.

Similarly for the random spectra this equation becomes;

Random

$$\frac{G^2/\text{HZ (End.)}}{G^2/\text{HZ (Perf.)}} = \left(\frac{T_o}{2} \right)^{2/n} \quad (8)$$

These resulting test curves are shown in Figures 25 and 26.

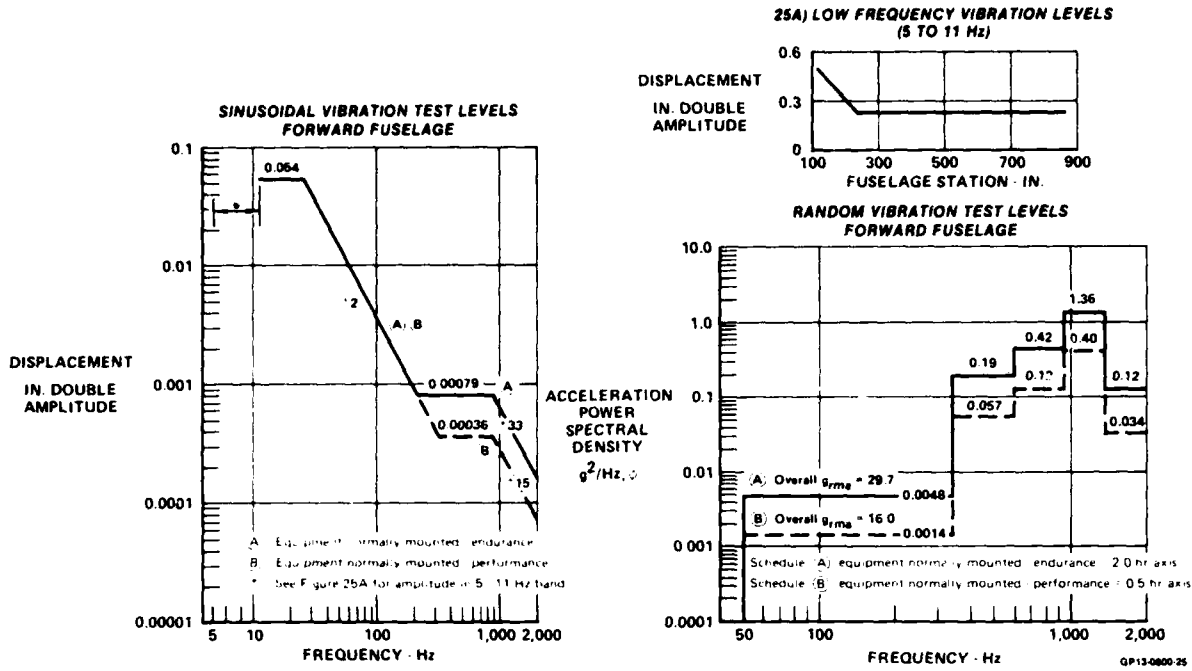


Figure 25. Region 1 Non-Gunfire Vibration Test Levels

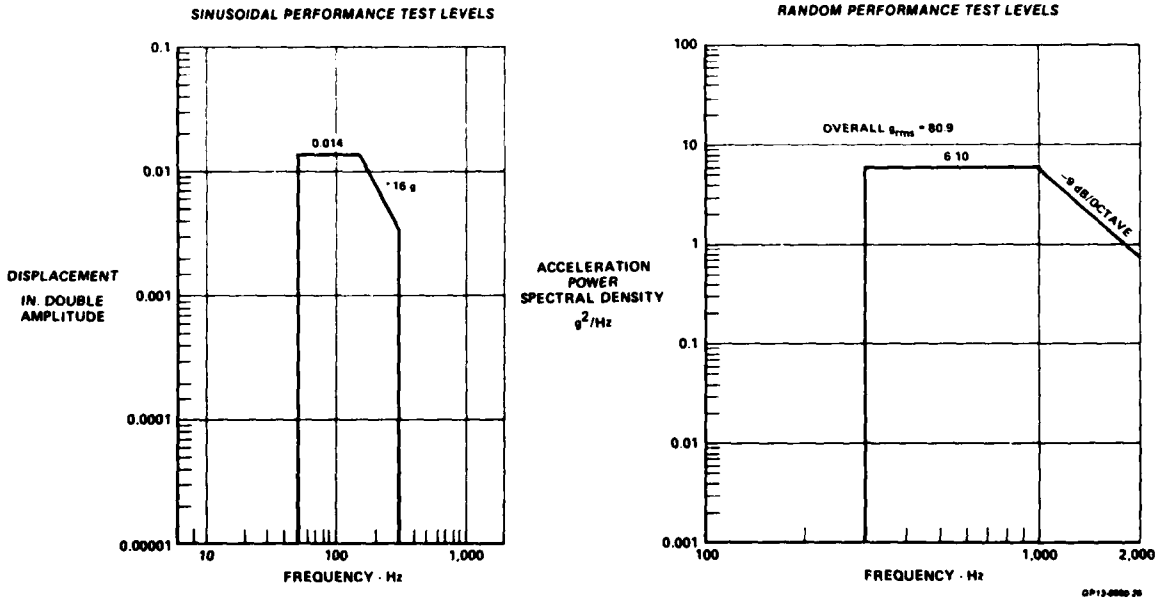


Figure 26. Region 13 Gunfire Vibration Test Levels

Conclusions

This program shows there is a definite need to adjust the vibration requirement for jet aircraft to take advantage of the differences in severity of vibration in locating and testing of equipment that might be susceptible to vibration. It is intended to emphasize the importance of using the vibration test level as an investigative tool as opposed to arriving at some absolute test level to be used as a demonstration of meeting a specification. The philosophy used for the F-15 was one of trying to determine basic weaknesses in an equipment design and to initiate redesigns based on time to failure as well as levels used.

Measured vibration data used for comparison with the original predictions were obtained well into the design and production phase of the F-15. They indicated the vibration test levels should be generally higher in the frequency range above 200 Hz and below 50 Hz and lower in the frequency range from 50 - 200 Hz. Based on this comparison with predictions, the original qualifications were considered adequate since most of the equipment critical frequencies fall in the 50 - 200 Hz range.

REFERENCES

1. Mahaffey, P. T., and Smith, K. W., "A Method for Predicting Environmental Vibration Levels in Jet-Powered Vehicles", August 1960, Shock, Vibration and Associated Environments Bulletin No. 28,
2. Hinegardner, W. D., Dreher, J. F., Hermes, P. A., "Vibration and Acoustic Measurements on the RF-4C Aircraft", November 1967, USAF TM SEF 67-4,
3. Franken, P.A., et al., "Methods of Flight Vehicle Noise Prediction", November 1958, USAL WADC TR-58-343,
4. Eldred, K., et al., "Structural Vibrations in Space Vehicles", December 1961, USAF WADD-TR-61-62,
5. Chobotov, V., Powell, A. Ramo Wooldridge Corp. "On the Prediction of Acoustic Environments from Rockets", June 1957, Report GM TR-19
6. Clark, W. E., et al., "Noise Produced by Aircraft During Ground Run-Up Operations", June 1957, WADC TN 56-60,
7. Houbolt, J., "Preliminary Development of Gust Design Procedures Based on Power Spectral Analysis Techniques", July 1966, USAF AFFDL-TR-66-58,
8. Tucker, P. B., McDonnell Douglas Corp., "F-15 Vibration, Shock, and Acoustic Design Requirements and Test Procedures for Aircraft Equipment", Dec 1969, MCAIR Report H100 Volume I, Section II, CDRL Item A090
9. Katz, H., Waymon, G. R., MDC "Utilizing In-Flight Vibration Data to Specify Design and Test Criteria for Equipment Mounted in Jet Aircraft", February 1965, The Shock and Vibration Bulletin No. 34,
10. Bendat, J. S., "Probability Functions for Random Responses: Prediction of Peaks, Fatigue Damage, and Catastrophic Failures", April 1964, NASA CR-33.

EQUIPMENT VIBRATION QUALIFICATION
FOR HARRIER AND HAWK AIRCRAFT

by

D.C. Thorby
British Aerospace Public Ltd. Co.
Aircraft Group
Kingston-Brough Division
Richmond Road
Kingston-upon-Thames
Surrey KT2 5QS, UK

SUMMARY

Equipment for later versions of the Harrier and all versions of the Hawk aircraft has been cleared for flight vibration using test procedures based on the current British Standard, 3G100. The rationale used in applying this Specification, and the flight vibration test procedures are briefly outlined from a practical viewpoint.

1.0. INTRODUCTION

The VTOL Harrier aircraft was developed from the Kestrel prototype, and entered service with the RAF as the Harrier GR.Mk.1. It is known as the AV8A in the United States. The two latest variants are the Sea Harrier FRS Mk.1 for the Royal Navy and the McDonnell-Douglas AV8B.

The Hawk is an advanced jet trainer, with strike capability, and is currently in service with the RAF and a number of other air forces. It is powered by a single Rolls-Royce Adour engine.

All equipment vibration specifications for these aircraft have been based on BS3G100 since 1969 when it replaced BS2G100, so what follows is essentially a practical account of using BS3G100 for about twelve years.

2.0. OUTLINE OF BS3G100 AND SOME COMMENTS.

The essential provisions are:

- (i) Initial and final resonance searches.
- (ii) Vibration endurance test with wide-band random the preferred method; frequency ranges 10-60Hz and 60-1000Hz.
- (iii) Choice of standard test levels, .0005 g^2/Hz to .05 g^2/Hz (Fig.1).
- (iv) Alternative test methods for vibration endurance test = sinusoidal sweep (Fig.2), narrow-band random or resonance dwell.
- (v) Vibration endurance test time determined by equipment usage, but maximum 50 hours (divided into 20 hours vertical, 20 hours lateral, 10 hours longitudinal).

Some general comments on applying it are:

- (a) The use of standard test levels in constant g^2/Hz , but with a possible change at 60Hz is both simple and adequate for most purposes.
- (b) Suppliers are required to discuss any proposals for the use of two of the permitted test methods - resonance dwell and narrow-band random sweep. Resonance dwell is really only suitable for structurally simple equipment where the resonances are well-defined and obvious. Modern miniaturised equipment, which may contain undetectable resonances obviously cannot be tested by this method. There is no objection, in principle, to narrow-band random testing, and it has some theoretical advantages over swept sinusoidal testing, for example the amplitude distribution of the excitation may represent random flight vibration more closely. The difficulty is that there is a temptation to make the power spectral density level within the narrow band equal to that specified for wide-band testing. Due to the sweep, each equipment resonance is excited for only a small proportion of the time, so the total test time has to be considerably increased. This can be compensated by an increase in spectral density, but the factor will depend on the particular test equipment, so agreement between the parties concerned is essential.
- (c) The determination of the duration of the vibration endurance test from the proposed utilisation of the equipment, as suggested in BS3G100, is very difficult in practice, and tends to spoil the essential simplicity of the specification. For Harrier and Hawk equipment this calculation, in any case, tends to require the maximum 50 hours, so this has always been specified. This test time is far longer than is required by any other national specification, and there may be a case for reducing it, at least for simpler equipment.

3.0. GENERAL PROCEDURES.

At the design stage of an aircraft, a great deal of equipment must be ordered well before a prototype exists. Some vibration test requirements must be issued, and these can only be based on standard specifications or measurements on similar aircraft. It is as well to err on the high side at this stage, both to ensure safety, and also because it is far easier, contractually, to reduce the requirements than to increase them. Cases where suppliers are having difficulty can be treated individually, on merit.

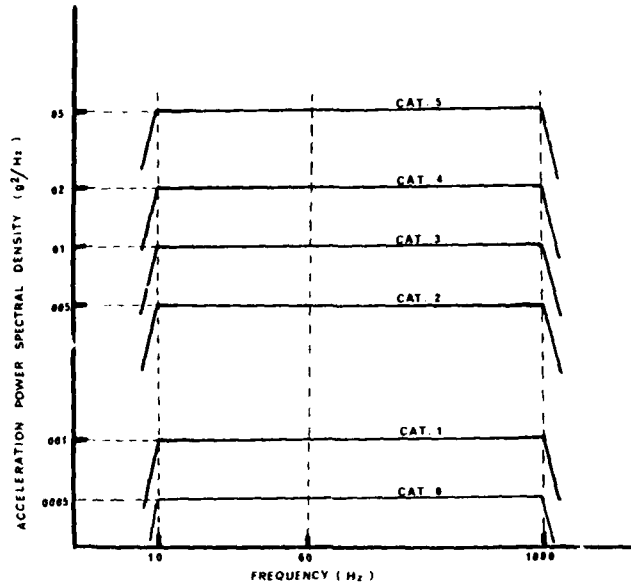


FIG. 1 STANDARD BS3G100 VIBRATION CATEGORIES — RANDOM

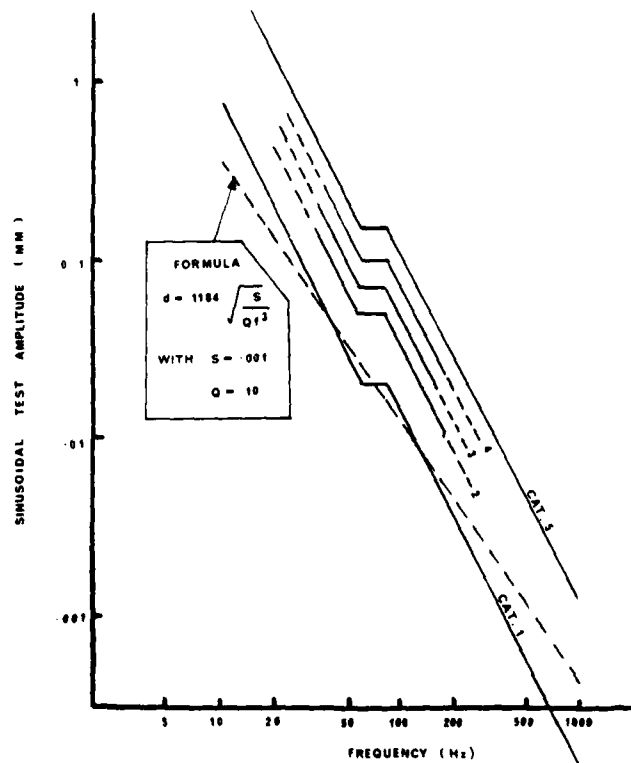


FIG. 2 STANDARD BS3G100 VIBRATION CATEGORIES — SINUSOIDAL

As soon as possible in the flight development programme vibration measurements are made, and a much more realistic specification can be issued. In the case of aircraft with a long development life such as the Harrier it is found that much more equipment tends to be purchased against the test-based specification than the original arbitrary specification. It is desirable to carry out the vibration flight tests immediately after flight flutter tests. This is the earliest time that the whole flight envelope can be covered, and instrumentation requirements are similar, although the positioning of the accelerometers for flight vibration recordings, and the recording bandwidth, will be different from the flutter requirements. We believe that it is worth retaining the flutter accelerometers as an extra set of vibration pick ups to obtain useful data on the vibration of aircraft extremities.

At B.Ae. Kingston, environmental specifications are administered by the Airworthiness and Avionics Departments, but a Structural Dynamics Specialist checks Suppliers test proposals and, after the tests have been carried out, the final report.

Twelve years ago some Suppliers in the UK were puzzled by references to power spectral density, but fortunately the position has now changed, and most are familiar with wide-band random test requirements and can carry them out.

4.0. HARRIER.

Original equipment for Harrier development batch aircraft was purchased against the current British Standard at that time, BS2G100 (Grade A). Fairly comprehensive flight vibration measurements were made in 1966. In those days spectral analysis was carried out with tape loops and analogue filters: 1/3 - octave analysis was normal. As a result of the measurements the vibration test levels were changed, but the method remained sinusoidal. With the introduction of BS3G100 in 1969, this was adopted as a framework for a revised test specification and wide-band random tests were specified for the first time on this aircraft. Fig.3 shows the vibration regions adopted. A rationale, based on BS3G100, and described below in 7.0. for converting other test specifications for comparison with the requirements was laid down.

Vibration levels on the Harrier tend to be high, well above the highest category proposed by BS3G100 ($.05 \text{ g}^2/\text{Hz}$) in aft regions, largely due to excitation of the tail by jet noise. In these regions the highest vibration is encountered on the ground. Vertical take off and landing do not produce excessive vibration, since the jets are then deflected downwards, well away from the aircraft structure. As with most highly manoeuvrable aircraft, the worst vibration in flight is associated with high angle of attack in turns.

5.0. HAWK.

BS3G100 was used to set the equipment test levels (at $.02 \text{ g}^2/\text{Hz}$) initially. Subsequent measurements (Fig.4 shows typical accelerometer locations) have shown this to have been a reasonable choice. It is exceeded at the extremities of the aircraft, generally not in those regions occupied by sensitive equipment. As would be expected, it is those manoeuvres involving separated wing flow, high - g turns, and since this is a trainer, spins, which produce the worst vibration.

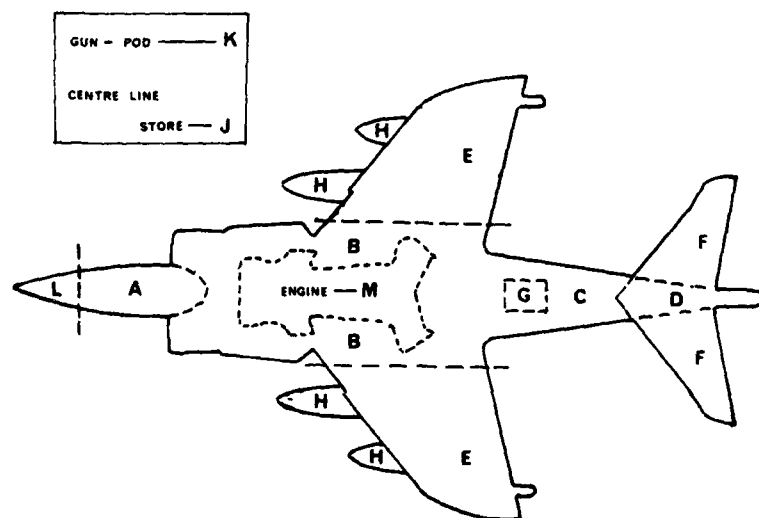


FIG. 3 HARRIER VIBRATION ZONES

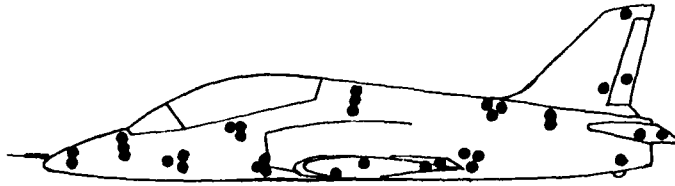


FIG. 4 TYPICAL HAWK ACCELEROMETER POSITIONS

6.0. FLIGHT VIBRATION TESTS.

In principle, power spectra, like Fig.5, normally in g^2/Hz , are required at each accelerometer location in each manoeuvre for several aircraft configurations. In practice, this could lead to a formidable number of spectra, most of which would show negligible vibration level. One way to avoid this is to produce a continuous record of mean square or root mean square vibration level in various frequency bands. Fig.6, for example, shows the RMS output from two pickups for the whole of a Harrier test flight. The pilot's voice track and identification pulses enable each manoeuvre to be identified, and power spectra can be produced covering significant manoeuvres only. It is desirable to divide the total frequency band into four or five contiguous narrow bands to give a rough idea of spectrum shape; if the choice of which spectra are to be produced is based on the total RMS (Fig.6), high spectral densities in particular narrow frequency bands may be missed. The averaging time of such a device is important. Simple lag smoothing, with a time constant in the order of 0.2 - 0.5 second has been found suitable.

6.1. Non-stationarity.

The main analysis problem, particularly with small, manoeuvrable aircraft, is non-stationarity of the signals. This is illustrated by the record (Fig.7) from a $4g$ turn in a Harrier test flight. The record of total RMS vibration shows that in this extreme case the most severe vibration exists for less than one second. Care is necessary to ensure that this worst vibration is captured by the analyser, and that an excessive period of lower level does not 'dilute' the power density measurement. Also, a power spectrum based on (say) only a half-second of data will be statistically unreliable. There appears to be no entirely satisfactory answer to this problem, but the following could be considered:

- (a) Use of the "shockspectrum" rather than the conventional averaged power spectrum. The shock spectrum records the maximum response of a variable-frequency single-degree-of-freedom filter to the signal.
- (b) Ensemble averaging of a number of similar manoeuvres.
- (c) Flight procedures can be modified to contrive a longer data sample in some cases - for example a turn may be prolonged.
- (d) Factors may be applied to the power density measurement to allow for the non-stationarity. These can perhaps be based on the ratio of peak to mean of the wide-band response. This has occasionally been justified by showing that the spectrum shape does not change appreciably for considerable changes in total response at one aircraft location.

7.0. VIBRATION TEST RATIONALE.

If power spectra are measured in flight, and subsequently equipment is subjected to the same spectral density on a test table, for a period of time representing the life of the equipment, then no factors, with one possible exception, need to be applied, in theory. (This exception, less

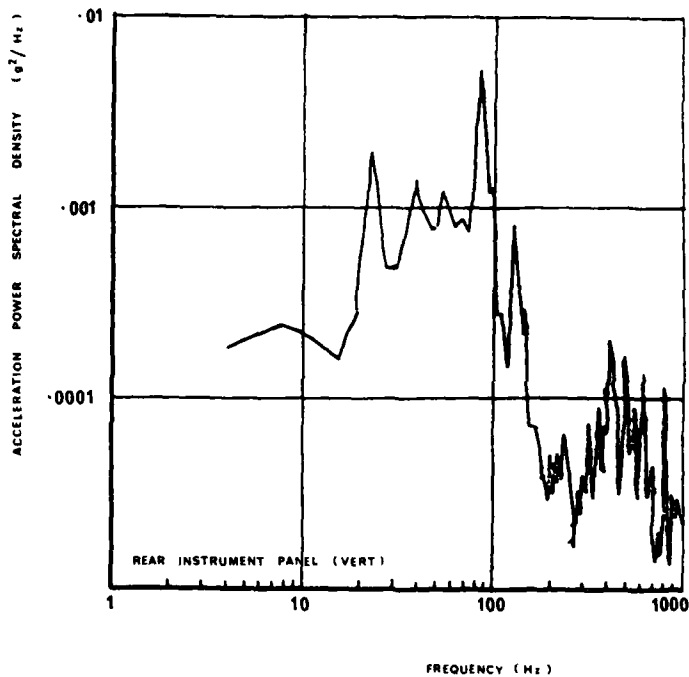


FIG. 5 TYPICAL HAWK FLIGHT VIBRATION SPECTRUM

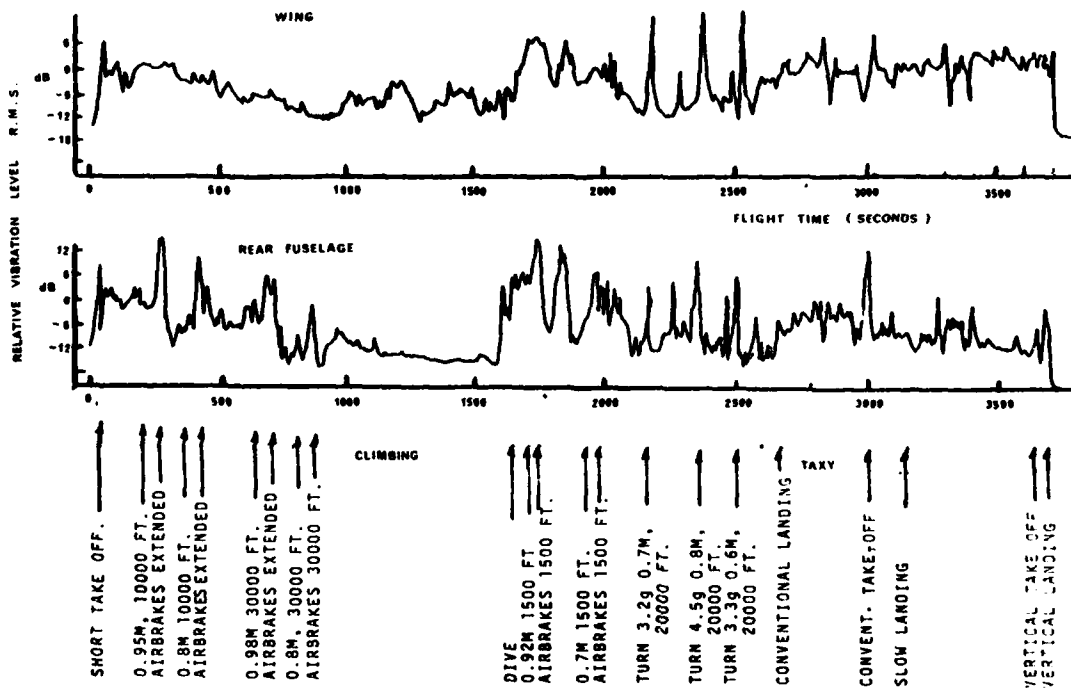


FIG. 6 ROOT MEAN SQUARE VIBRATION LEVELS FOR AN ENTIRE HARRIER TEST FLIGHT

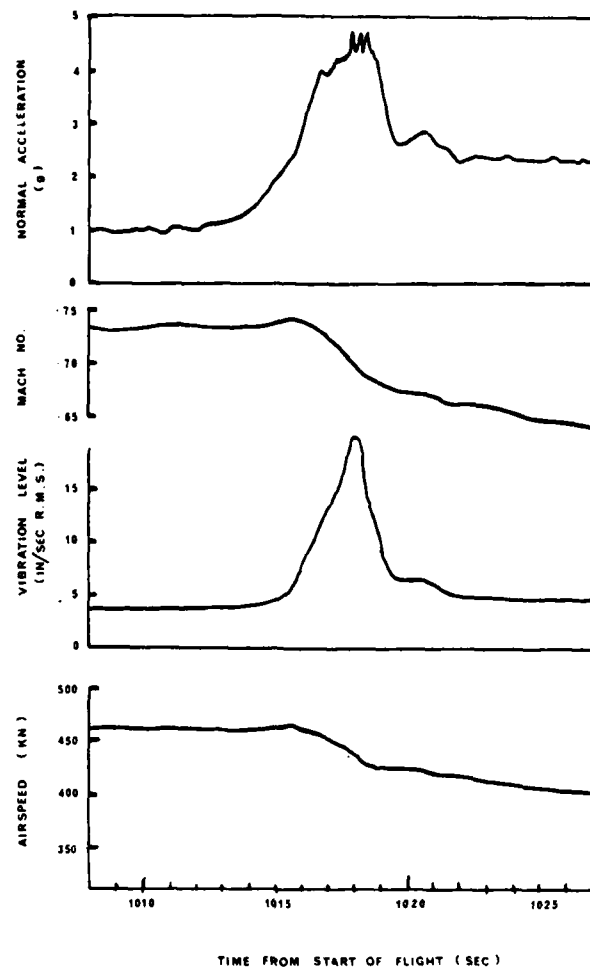


FIG.7 EXTREME EXAMPLE OF NON - STATIONARY VIBRATION (HARRIER)

important now than formerly, when relatively coarse analysis bands were used, is a correction for the fact that aircraft structural resonances could have much narrower band-width than the analyser, so significant peaks in the spectrum could be smoothed out).

The ideal situation mentioned above, of course, is never attained : the testing may be sinusoidal rather than random; it is perhaps carried out for 3 hours instead of 6000 hours, and is of constant amplitude (at any frequency) rather than variable. Some set of rules for converting a random signal to an "equivalent" sine wave, or increasing amplitudes to allow reduction in test time, are required. It is relatively easy to define a set of rules : the problem is that they do not usually bear close inspection. They mostly involve Miner's law, and fatigue damage proportional to some power of test amplitude. Nevertheless, it is essential to have some rules for conversion, and all we can do is to ensure that they are conservative, as far as possible, and are not used out of context, that is to say they are valid only for equipment survival, not functioning. For the sake of consistency, our rules are based on BS3G100, as follows:

- (1) Vibration amplitude scaling may only be such as to increase test levels, due to the possible existence of a fatigue limit (i.e. that level of stress below which failure would never occur).
- (2) Damage proportional to the fifth power of amplitude is assumed, so, for example if the test amplitude is doubled, the time may be reduced by a factor of 32.

- (3) Random power spectral density may be converted to a sine wave by the relationship

$$d = 1184 \sqrt{\frac{S}{Qf^3}}$$

where d = sinusoidal amplitude (mm)
 S = power spectral density (g²/Hz)
 Q = magnification at resonance
 f = frequency (Hz)

This expression can be reproduced if the implicit factors are known:

- (a) The RMS of the sine wave must be 1.27 times that of the random wave based on Miner's law and fifth power damage.
- (b) Amplitude scaling by 2.09 to reduce test time by a factor of 40, because of the short time actually spent at resonance in a swept sinusoidal test. (The sinusoidal test time can then be equal to the random in test time).

The formula is used to convert the standard random levels (Fig.1) to equivalent sinusoidal levels (Fig.2) by fixing Q at the average value of 10. In Fig.2 the resulting line is shown for one spectral density, together with the approximation used in the specification.

By means of these relationships (however dubious their derivation) it is possible to translate one specification into another, and this often has to be done, in order to see whether equipment tested to say MIL-STD-810B (USA) or AIR 7304 (France) meets the requirements for Harrier or Hawk.

The above applies, of course, only to relatively compact equipment which can reasonably be considered to be attached to aircraft structure at a point. Structures, and this must include external stores and equipment racks will generally require a more realistic and complete treatment.

7.1. Survival or Operation Tests.

Comment should be made on the important difference between survival and correct operation of the equipment being tested. As far as survival is concerned, an overtest is usually permissible, and there is much to be said for the old, very severe, sinusoidal tests. Such a test will find the insufficiently-supported pipe, wire, capacitor, circuit board, etc, and the cure is usually obvious. There is a class of very difficult problems, however, not involving structural failure, but incorrect operation, often due to "microphony". Radar and other high-frequency devices are prone to this problem: the small dimensional changes caused by vibration, although not damaging, cause the device to operate incorrectly. Cockpit instruments can also mis-read seriously due to vibration.

In cases like this the onus is upon the aircraft manufacturer to define the vibration environment very precisely, far more precisely than for survival purposes. Usually special test flights with carefully placed accelerometers are required, and the actual random spectra must be reproduced faithfully during the ground test.

8.0. CONCLUDING REMARKS.

The aims of this account of equipment vibration qualification at British Aerospace, Kingston, have been, first, to introduce our national specification BS3G100, and secondly to present our current test philosophy for comparison with other firms, as a preamble to future international standardisation. No originality is claimed for the procedures described, and in general they should not necessarily be taken as representing those in use at other sites within British Aerospace.

ACOUSTIC NOISE TEST AS PART OF THE DYNAMIC
QUALIFICATION PROGRAM IN AEROSPACE

by

G. Bayerdörfer
Industrieanlagen-Betriebsgesellschaft mbH
Einsteinstrasse 20
D-8012 Ottobrunn

Summary

The paper describes the mechanisms of noise generation for the purpose of acoustic qualification tests. Special emphasis is given to the modal density of acoustic noise fields in enclosures, such as reverberation chambers. A test program shows, that for small components a sufficient modal density can be achieved in relative small test chambers.

Where applicable small chambers are favourable because of the lower test costs. The author finds that this advantage can not be used because of the global nature of the test spectrum, defined in MIL-STD-810 C. He therefore suggests to specify two test spectra: one for tests with small components and one for tests with bigger assemblies.

1. Introduction

The dynamic qualification of aerospace equipment is usually achieved by the following two tests:

- the vibration test, which incorporates electro dynamic or electro pneumatic shakers and a mechanical fixture to couple the exciters with the test item
- the acoustic noise test, in which the test item is placed inside an enclosure and excited by fluctuating pressure fields.

The acoustic noise test is not a substitute for the vibration test but rather a complement, because of the two reasons:

- the acoustic excitation covers a wider range, especially in the high frequencies
- the acoustic pressures are acting on the whole surface of the test item which again gives a better coupling in the high frequencies.

The essential part of the specifications for acoustic noise tests are the frequency-spectra such as shown in Fig. 1. The spectra are usually defined either in Oct.- or 1/3 Oct.-values. The specification further asks for a suitable reverberation chamber to produce a diffuse sound field and a uniform sound energy density throughout the enclosure.

The acoustic spectrum can either be based on measured or estimated values as in the case of the SHUTTLE-spectrum, or it is given in a standardized form such as in the MIL-STD-810 C.

The comparison of the two spectra in Fig. 1 shows that the SHUTTLE-spectrum is more individual in so far, as it approximates the real conditions as close as possible (shape of spectrum, low frequency end, width of tolerance band).

The acoustic test spectrum specified by MIL-STD-810 C is of more global nature. It can be considered as an envelope of many individual spectra of different applications. The idealized shape and the width of the tolerance band have been chosen such as to cover most of the practical cases.

The obvious advantage of MIL-STD-810 C is, that a simple test method is provided to the user. Less advantageous is the fact, that due to the global nature, the real loading of the test specimen can vary considerably and that in some cases unnecessary test effort is created.

In order to illustrate this situation a small test program has been conducted, which will be discussed under chapter 3. For a better understanding it is however necessary to explain the mechanism of noise generation in more detail

2. Noise Generation System

In Fig. 2 the general arrangement of a noise generation system is presented. The individual components contribute through their acoustical characteristics to the noise spectrum, achievable in the test chamber.

- Noise Generator, its relevant data are the acoustic power, frequency range of modulation, magnitude of overtones, noise content of the turbulent gas flow.
- Exponential Horn, the shape determines the efficiency of acoustic coupling and the cut-off frequency at the low end.
- Reverberation Chamber, the size and shape determine the density of acoustic chamber modes, the treatment of the surface governs the absorption factor.
- Medium, the molecular absorption depends on the transmitting medium in use. For instance N_2 has lower molecular damping than air at high frequencies and therefore gives rise to higher sound pressure levels.
- Test Item, depending on the size of the test item the acoustic chamber modes and the absorption are affected.

For the commonly used electro pneumatic noise generation the system works such, that pressurized gas (Air, N_2) is modulated by opening and closing slots, through which the gas has to pass. Each opening creates a pressure shock, which is expanded through the exponential horn and transmitted to the test chamber. The modulation is achieved according to wide band signals so that a broad frequency range of pressure fluctuations is obtained.

These driving pressures excite resonances in the test chamber which give rise to the sound pressure level at the corresponding frequencies. The resonances can be considered as three dimensional standing waves, their patterns are usually described as the chamber modes. The wave length of the chamber modes is inversely proportional to their frequencies. In other words: low frequency modes need large dimensions of the test chamber, otherwise they can not be excited.

For example, if a chamber mode at the frequency 100 Hz is required, then it is necessary that at least one dimension of the chamber is in the order of 3 m length.

Of course a single mode is not sufficient, to provide a uniform sound energy density as asked by the specification. A general recommendation is to have at least 20 modes in the lowest octave band of interest.

From this it can be derived, that in order to have a good modal density at 100 Hz the chamber must have dimensions of 4 to 5 meters or a volume of about 100 m³.

These relationships are not explained in MIL-STD-810 C, nor in the new draft of ISO/DIS 2671.2. The reason probably is to keep these standardized specifications as simple as possible for the user.

On the other hand it is worthwhile to know the lowest Oct. band that has to have sufficient modal density for a specific test item. With this knowledge a better matching in regard to the necessary chamber size is possible.

In order to illustrate this on a real component the following test work was performed.

3. Acoustic Test Program

An electronic box, as shown in Fig. 3, was instrumented with two accelerometers, one on the outside casing, one on an inside plate. This box was tested in three different acoustic chambers:

- Small Chamber, $V = 5 \text{ m}^3$, (Fig. 4)
- Medium Chamber, $V = 206 \text{ m}^3$, (Fig. 5)
- Large Chamber, $V = 800 \text{ m}^3$, (Fig. 6)

In each chamber an acoustic spectrum was generated with a spectral distribution according to the MIL-STD-810 C specification, and with an Overall Sound Pressure Level (OASPL) of 150 db.

The response of the electronic box and the fluctuating pressures of the exciting noise field were analysed in terms of power spectral densities (psd) by means of a digital computer with a virtual filter bandwidth of 2,4 Hz.

The results of these measurements are contained in Fig. 7 and 8. From Fig. 7 the PSD-plots of the fluctuating pressures inside the three test chambers can be seen.

The large chamber ($V = 800 \text{ m}^3$) shows a sharp increase in acoustic energy at about 40 - 50 Hz, which can be attributed to the cut-off frequency of the exponential horn (37 Hz). From there the distribution towards the higher frequencies is relatively smooth with no pronounced peaks and troughs.

The plot for the medium chamber ($V = 206 \text{ m}^3$) exhibits at the low frequency end a similar rise at about 100 Hz. Between 100 Hz and 150 Hz there is a remarkable gap, but onwards from 150 Hz the energy distribution is continuous.

The small chamber ($V = 5 \text{ m}^3$) finally contains very pronounced peaks and troughs up to approximately 500 Hz. From there the energy distribution becomes more uniform.

These troughs at the low frequencies result from lacking chamber modes. This becomes clear by the indication of the lowest 20 modes octave band.

In Fig. 8 the vibration response of the electronic box is presented. As can be easily seen from the plots, the same vibration response is measured, regardless in which of the three chambers the box was tested.

This result is not surprising, as the dominant vibration response occurs in a frequency range (500 - 750 Hz) in which all three test chambers have uniform and nearly equal energy distribution (Fig. 7).

The identity of vibration response would have been completely diminished, if a test item were investigated whose dominant resonances lie at about 100 Hz or even lower.

At such low frequencies the small chamber would not give any meaningful results. The same would apply to the medium chamber for frequencies between 30 - 80 Hz.

4. Conclusions

What conclusions can be drawn from this experiment?

- In order to perform a good qualification test it is necessary to have a sufficient modal density of the acoustic excitation in the frequency range, in which the test item exhibits its dominant vibration response.
- Small test items, such as electronic boxes etc. do not need the lower end of the frequency spectrum (63 Hz) as defined in MIL-STD-810 C.
- Big test items, such as a Spacelab Pallet may need an extension towards the lower frequencies which goes beyond the 63 Hz band. In this case a sufficient modal density must be maintained even in the 31 Hz Oct. band.
- As a conclusion from these different requirements it is suggested to specify not only one standardized spectrum, according to which all kinds of acoustic noise tests have to be performed, as presently prescribed by MIL-STD-810 C. Instead of this it would be more meaningful to have two spectra. One which contains the low frequencies which are necessary in testing bigger parts, such as assemblies etc. The other spectrum should begin at about 125 Hz with a horizontal part between 250 Hz and 2 kHz.

The second spectrum should be identical with ISO/DIS 2671.2 in its final version, because both are intended for the same test items, namely electronic components (Fig. 9).

5. List of Figures

- Fig. 1. Test Spectra
- Fig. 2. Noise Generation System
- Fig. 3. Test Item
- Fig. 4. Test Chamber ($V = 5 \text{ m}^3$)
- Fig. 5. Test Chamber ($V = 206 \text{ m}^3$)
- Fig. 6. Test Chamber ($V = 800 \text{ m}^3$)
- Fig. 7. Power Spectral Density of Noise Fields
- Fig. 8. Power Spectral Density of Vibration Response
- Fig. 9. Comparison of Standardized Test Spectra

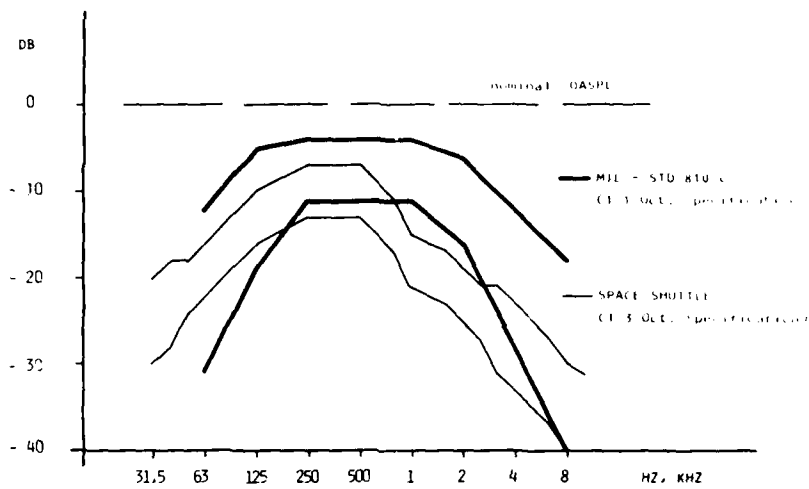


Fig. 1.
Test Spectra

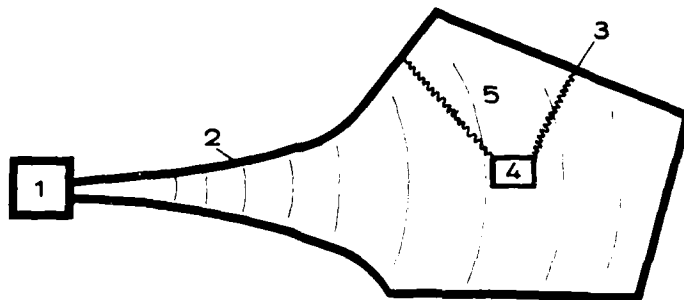


Fig. 2.
Noise Generation
System

- 1 NOISE GENERATOR
- 2 EXPONENTIAL HORN
- 3 REVERBERATION CHAMBER
- 4 TEST ITEM
- 5 MEDIUM (AIR, N₂)

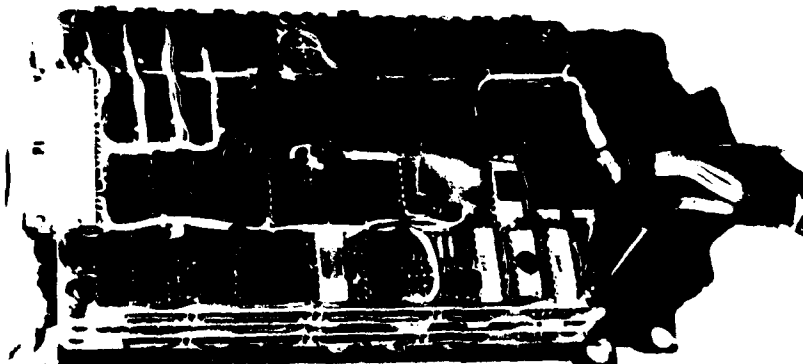


Fig. 3.
Test Item

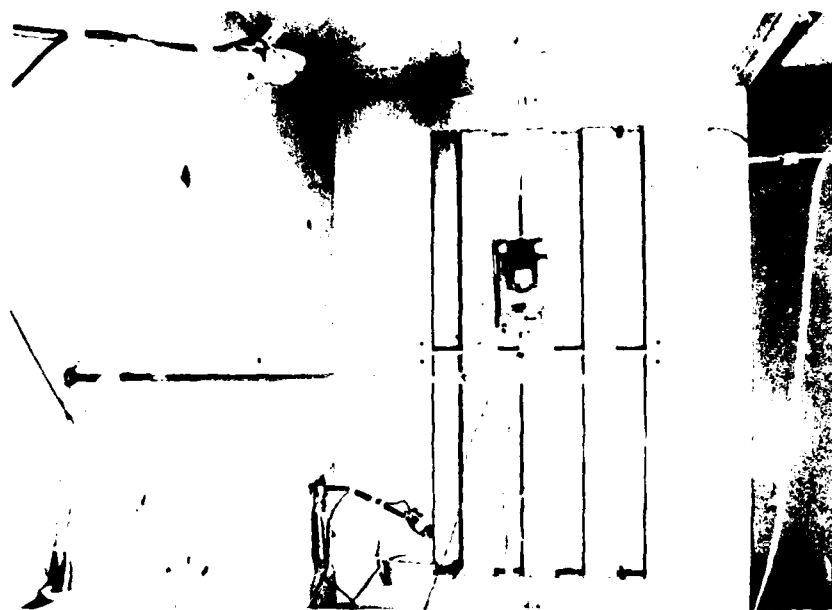


Fig. 4.
Test Chamber
(V = 5 m³)



Fig. 5.
Test Chamber
(V = 206 m³)



Fig. 6.
Test Chamber
(V = 800 m³)

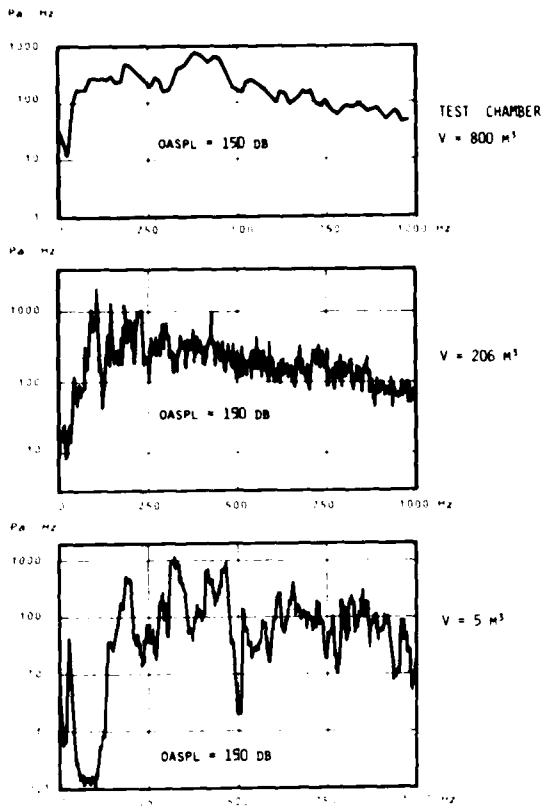


Fig. 7. Power Spectral Density of Noise Fields

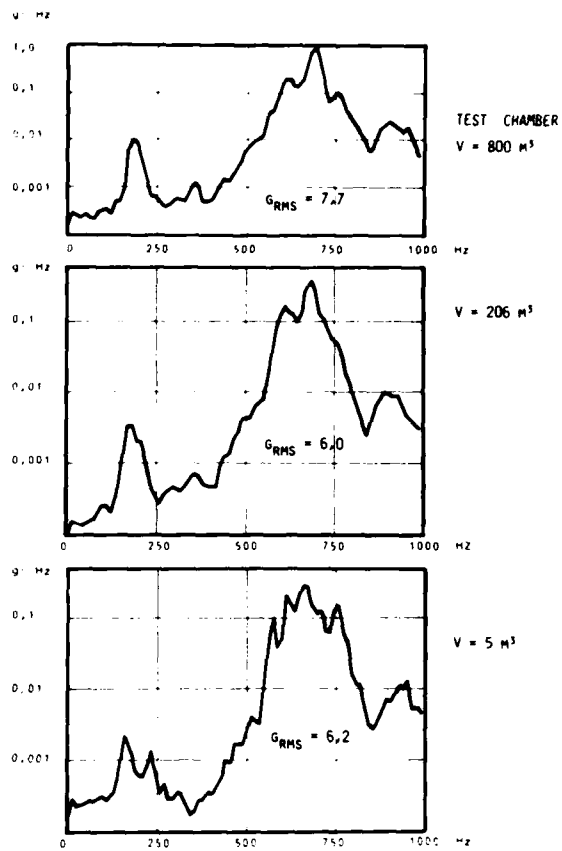


Fig. 8. Power Spectral Density of Vibration Response

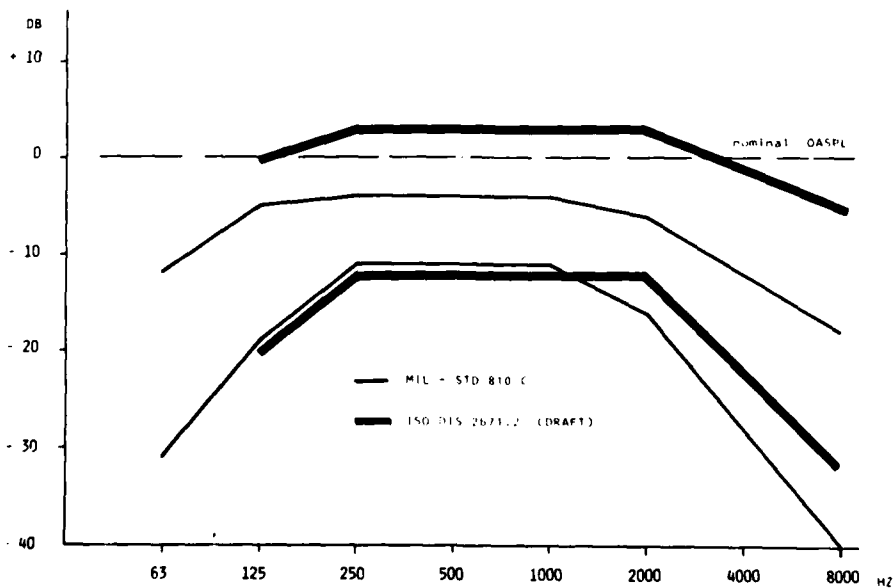


Fig. 9. Comparison of Standardized Test Spectra

VIBRATION QUALIFICATION OF EXTERNAL A/C STORES AND EQUIPMENT

by

M. STEININGER and G. HAIDL
 MESSERSCHMITT-BÖLKOW-BLOHM GmbH.
 Aircraft Division
 P.O. Box 80 11 60, 8 Munich 80
 W.-Germany

ABSTRACT

Prediction Methods for a first assessment of vibration levels and spectra are described and application results are compared with measured vibration environment in relevant flight conditions. Some remarks, concerning signal nature and analysis technique are given in the first part of this paper.

A second part deals with the technique of simulating a representative dynamic environment in the laboratory especially for external store configurations. Different mounting and excitation methods as well as selection of shaker control reference signals are compared and discussed. Requirements for test facilities, for instance mounting rigs and shaker capabilities are also presented.

1. INTRODUCTION

The purpose of the environmental qualification of an equipment is to prove its resistance against environmental influences. Equipment design and development is based upon contractual defined environmental conditions (declaration of design and performance). These requirements have strong influence upon the development costs of an equipment. Normally, no flight measurements are available at this time to evaluate the real environmental conditions - in our case the vibrations. At best, measurements on similar equipment under similar installation conditions can be taken into account for defining the qualification spectra. Therefore, predicted levels and test procedure as given in standards are used for the development phase. During the prototype phase, measurements have to be taken to confirm or finalize the formal qualification test levels for production equipment. At this time, the equipment design is normally fixed and further modifications are expensive. Therefore, the prediction method should meet the real environmental conditions as close as possible to avoid overtesting or undertesting the equipment. A step forward to a more realistic simulation of vibration environment was reached, when sinusoidal testing was replaced by random testing which is incorporated in MIL-STD. 810 C (US-Standard), BS 3G.100 (British Standard) and AIR 7304 (French Standard).

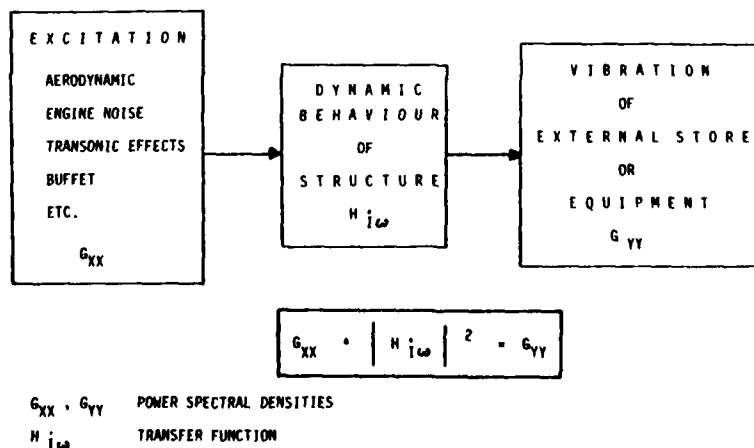


FIG. 1 COHERENCE BETWEEN EXCITATION AND VIBRATION

Systematic considerations of the sources of excitation, e. g. aerodynamic and engine noise, are able to improve the prediction methods. Not only the nature and severity of excitation source, however, is responsible for the vibration of an individual equipment, also the transmissibility characteristic of the structure is of importance. Local resonances or low damped modes may lead to severe conditions not covered in predicted spectra (following the standard). This applies especially for external store configurations with relatively low attachment frequencies.

To get a representative simulation under laboratory conditions the dynamic behaviour of the structure as well as the environmental conditions and exposure time must be taken into account. The test procedures and levels have to be defined in accordance with the capabilities of the test laboratory, and the test time has to be limited with respect to the costs by equivalent test time compression.

2. COMMON METHODS OF LEVEL PREDICTION

The MIL-STD. 810 C, Method 514.2 (US-Standard), for instance, defines the test procedure and level prediction for vibration qualification. For equipment and assembled stores the qualification test with wideband random excitation consists of three parts: Initially, the first half of the "functional test" is performed which covers the maximum vibrations during captive flight phase. Next step is the "endurance test" which serves as a "fatigue test" with equivalent increased levels related to the short laboratory test time. Last, the second part of the "functional test" is carried out. The functional test normally lasts 1 hour per axis, during which the equipment must function. The duration of the endurance test is about 1 - 2 hours, at which the test specimen is not operating. In order to allow a flexible adaptation of qualification levels in severity and frequency limits, a series of basic parameters is used in the prediction of vibration levels: the number of anticipated service missions, the max. aerodynamic pressure, the averaged store weight density and the store geometry. The kind of store mounting configuration is regarded by additional factors. In this way, for every individual store an individual test spectrum is provided.

	MIL-STD 810 C	BS3G.100	AIR 7304
TEST SEQUENCE	FUNCTIONAL TEST ENDURANCE TEST FUNCTIONAL TEST	RESONANCE SEARCH ENDURANCE TEST RESONANCE SEARCH	RESONANCE SEARCH ENDURANCE TEST RESONANCE SEARCH
EXCITATION TYPE	RANDOM: (15) 20- MAX. 2000 HZ	SINE SWEEP: 10-1000 HZ RANDOM: 10-60 HZ, 60-1000 HZ	SINE SWEEP: 5-2000 HZ RANDOM: 10-2000 HZ
TEST TIME	1/2 + 1 + 1/2 HOURS/AXIS	≤ 50 HOURS FOR 10-60 HZ ≤ 50 HOURS FOR 60-1000 HZ	2 1/2 HOURS/AXIS
LEVEL DEPENDENT ON	EQUIPMENT LOCATION MAX. AIRSPEED ENGINE NOISE EQUIPMENT WEIGHT NO. OF MISSIONS ETC.	EQUIPMENT LOCATION VIBRATION CATEGORY DEFINED BY FLIGHT CONDITIONS	EQUIPMENT LOCATION EQUIPMENT WEIGHT

NOTE: NORMAL QUALIFICATION TEST FOR EQUIPMENT INSTALLED IN MILITARY AIRCRAFTS. IF DIFFERENT TEST METHODS ARE PROPOSED, THE RANDOM TEST WAS SELECTED.

FIG. 2 STANDARD COMPARISON

In the British Standard BS 3G.100 no specific test procedure for assembled external stores is supplied. Generally, a vibration qualification test consists of an initial and final resonance search to investigate the structural behaviour of the test specimen on the basis of a sine sweep excitation, and an "endurance test" which covers the accumulated service time, related to higher vibration levels to get test times ≤ 50 hours with narrow band and ≤ 50 hours wide band random excitation. For test level definition the duration times and vibration categories of all ground and flight conditions are

estimated and accumulated at the most severe vibration category, using an equivalent damage concept. During this test, the specimen shall operate without malfunction. Five vibration categories are supplied which were selected in accordance with the equipment location and flight condition. The frequency range of the narrow and wideband random test is 10 - 60 Hz and 60 - 1000 Hz respectively.

The test sequence of the French Standard AIR 7304 is similar to the British Standard: After an initial resonance search with a sine sweep excitation, an endurance test is conducted, followed by a final resonance search. The endurance test for military aircrafts lasts 2 1/2 hours per axis, the excitation is a wide band random from 10 to 2000 Hz with a level dependent on the location of equipment. Vibration levels for qualification of external stores are not supplied. Under certain circumstances the vibration level may be reduced up to 50 % with equivalent test time increase.

The levels predicted with the above described methods are frequently adapted and finalized on the basis of measurements of the prototype phase. For definition of qualification levels, the aircraft may be subdivided in several zones of different severity of vibration. As an example, qualification zones of aircraft and stores are shown in Fig. 3.

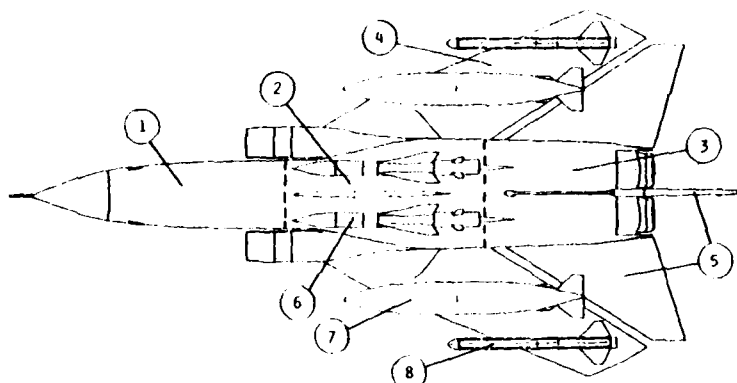


FIG. 3 SUBDIVISION IN SEVERAL VIBRATION ZONES

3. VIBRATION MEASUREMENTS AND ANALYSIS FOR EXTERNAL STORE CONFIGURATIONS

For an assessment of realistic test requirements measurements taken on aircraft carried stores will be considered in the following. The analysis technique will be discussed and some measured levels will be compared to MIL-STD predictions. Furthermore, some special flight conditions will be shown which are not covered by level prediction in accordance with standards.

3.1 Pickup Installation and Analysis Technique

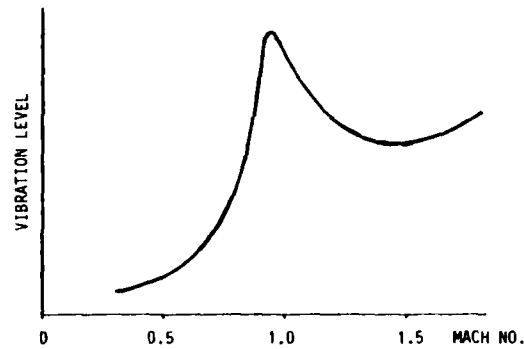
For direct comparison of measured vibrations with qualification data, or definition of qualification spectra, it is recommended to instrument an external store with accelerometers at stiff points of the nose and tail section (primary structure). If desired, the vibrations can also be measured at the attachment point of any individual internal equipment to define the dynamic environment of this device.

To get a flight vibration survey over the full mission profile (e.g. take off, straight and level flight, manoeuvres with high g-load, buffeting and transonic conditions, landing), time slices of representative vibrations have to be selected from the performed flights for analysis. A time slice which is assigned for analysis should have stationary or nearly stationary flight condition and a length which allows an average minimum of 20 to 30 computer time blocks to minimize accidental effects with short duration.

Useful information for flight vibration survey includes tabled overall RMS values and peak values related to different flight conditions as well as frequency spectra (power spectral density = PSD) and representative time histories.

For comparison with qualification level, vibration measurements of the full mission profile are needed, especially of the transonic range (Ma 0.90 - 0.95) and manoeuvres with high g-load. If such a flight condition is not available in performed flights, an extrapolation over the Mach number can be helpful. A typical curve for the overall vibration level against airspeed is given in Fig. 4.

FIG. 4 TYPICAL VIBRATION LEVEL
VS MACH NUMBER



Safety factors have to be applied because of differing frequency spectral distributions which leads to transgression of the smooth predicted vibration spectra within single frequency ranges. Further safety factors may be added because of higher peak to RMS-ratio in flight than in qualification testing, where a ratio of about 3 is usual in accordance with the Gaussian distribution.

3.2 Measured Vibration Environment and Comparison to Qualification Level

3.2.1 Air to Air Missile

The measured dynamic environment of an air to air missile carried on the wing pylon is shown in Fig. 5.

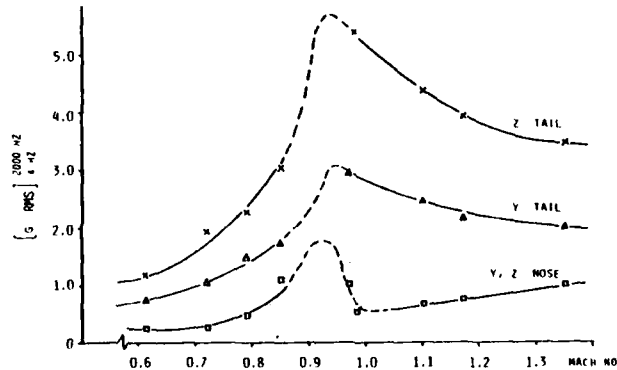


FIG. 5 MISSILE ENVIRONMENT UNDER STABILIZED FLIGHT CONDITION

The diagram contains the overall RMS vibration level versus Mach number of the pickups attached to a stiff point in the nose and tail section of the store. The vibration on the nose is about equal in y- and z-axis and, therefore, plotted as one line. The range between Ma 0.85 and 1.0 is drawn as a dashed line because of uncertainties due to transonic effects. This diagram shows only the vibration level of the straight and level flight. To demonstrate the influence of manoeuvres with various g-loads, Fig. 6 shows measurements taken at a store nose section. The vibration level of a manoeuvre condition for this store increases strongly with the g-load. In the tail section, only minor differences were found between straight and level flight and manoeuvres.

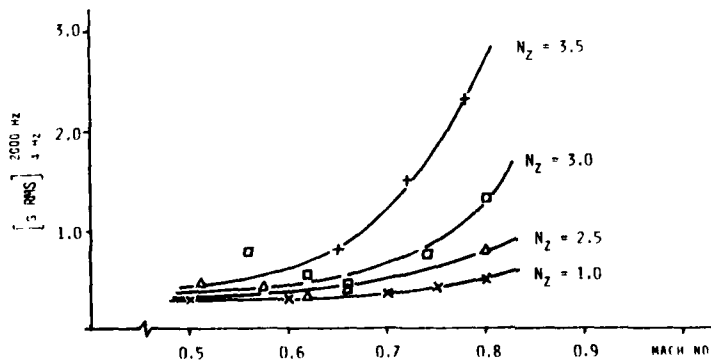


FIG. 6 MISSILE ENVIRONMENT VS MANOEUVRE LOAD N_z

The maximum analyzed overall RMS value in Fig. 5 is about 5.8 g. For all flight operation conditions and related exposure times, an equivalent endurance vibration level related to 1 hour was calculated as described in 4.3. From this procedure, an endurance overall RMS value of 11.3 g for the z-axis of the tail section is resulting including a factor of + 3 db to cover differing spectral distributions and narrowband peaks. The endurance test level predicted according to MIL Std. 810C-514, Procedure IIA has a RMS value of 9.1 g established with the minimum level of 0,04 g²/Hz. The predicted value, therefore, does not fully satisfy the real requirement.

3.2.2 Instrument Pod

In the following, measurements of a middle sized underwing instrument pod are presented to show particular effects of vibrations during manoeuvres and to illustrate the distribution of vibrations over the length of the store. The store is shown in Fig. 7. All accelerometers are attached to stiff points of the store structure to pick up a representative vibration of the section.

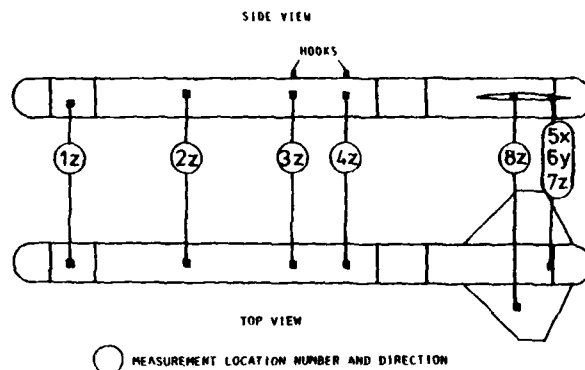


FIG. 7 PICKUP INSTALLATION IN INSTRUMENT POD

Vibration data up to about Ma 0.9 were measured and analyzed. They give a good indication of problems which can occur and have to be taken into account during the definition phase of final qualification of equipment and assembled stores.

In Fig. 8, a survey of vibration overall RMS levels up to 2000 Hz at constant altitude in subsonic range taken from straight and level flights and manoeuvres up to a maximum of 2 g as well as take off and thrust reverse phase are presented.

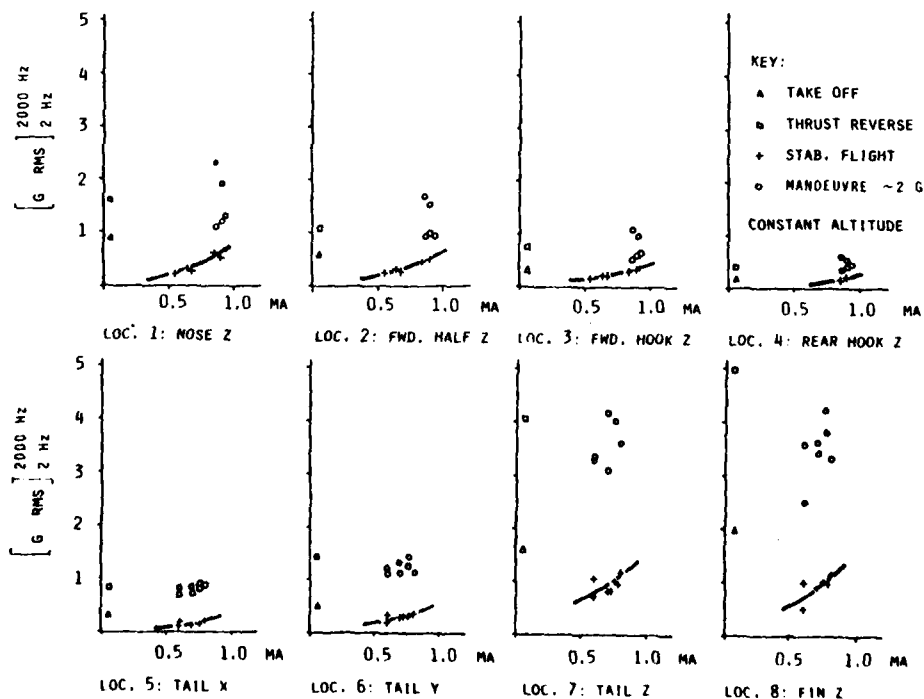


FIG. 8 VIBRATION ENVIRONMENT OF INSTRUMENT POD

For comparison with these data the predicted vibration RMS levels according to MIL-Std. 810 C, Method 514, procedure II A, valid for installed equipment are tabled:

	forward half of pod	rear half of pod
functional test	6.1 g RMS	12.3 g RMS
endurance test	8.0 g RMS	14.4 g RMS

The measurements indicate the following trends:

- The vibration levels in the forward half of the store are lower than the levels of the rear half (factor of about 4). This is in correlation to the prediction in MIL-Std. 810 C. Of particular interest are the vibration levels in the attachment area of the store: They are lower than the vibration levels of the nose section during stabilized flight as well as during manoeuvres.
- As shown in Fig. 8, the vibrations during manoeuvres are always higher than the vibrations during straight and level flight. Also ground operations (take off, thrust reverse) produce a noticeable vibration level.

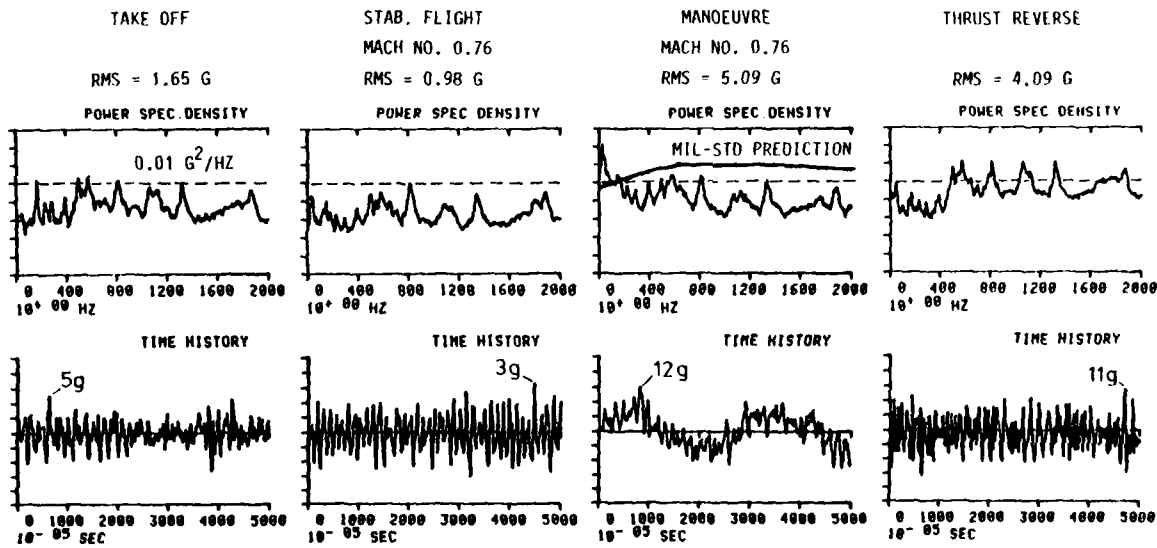


FIG. 9 SPECTRA AND TIME HISTORIES OF DIFFERENT FLIGHT CONDITIONS

- The spectral distribution above 200 Hz is about the same for all flight conditions, as shown in Fig. 9. In the low frequency range (< 200 Hz) significantly higher values are noted in the manoeuvre case, especially in the frequency of the low damped wing torsion-store pitch mode. This leads to high vibration levels not covered in any level prediction method.

The predicted qualification spectrum for the full flight envelope, according to MIL-Std. 810 C, procedure IIA, is compared in Fig. 9 with a Mach 0.76 manoeuvre case.

3.2.3 Missile Launcher

The following measurements presented are taken from flights with a launcher for a large heavy missile carried on fuselage station or i/b wing station. In Fig. 10, the available results are given in terms of overall RMS values. Large differences were found in frequency spectra and overall vibration level between the two stations: The vibration levels of the launcher carried at fuselage station are up to 4 times higher than those of the launcher carried at i/b wing station. This may be caused by the more disturbed airflow in the vicinity of a/c fuselage. It is also of interest that, in some cases, the vibrations of the forward section of launcher are higher than those of the aft section.

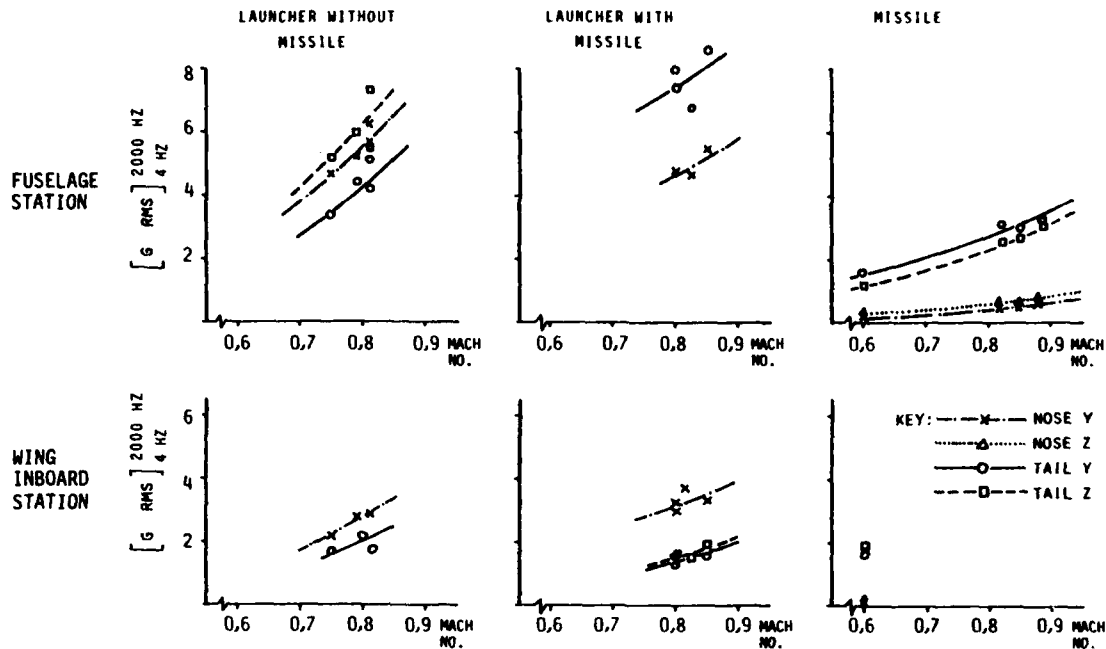


FIG. 10 VIBRATION ENVIRONMENT OF A LAUNCHER AND MISSILE

Considering relevant methods of level prediction for equipment installed in a launcher, either one of the two procedures in MIL-Std. 810C may be used: procedure IA, if the launcher is classified as a pylon, or procedure II, if the launcher is classified as an external store. The resulting overall RMS values are tabled in the following.

	functional test		endurance test	
Procedure IA	17.1 g		26.5 g	
	fwd. half	rear half	fwd. half	rear half
Procedure IIA	6.9 g	9.8 g	8.1 g	10.2 g

The shown flight vibration measurements of launcher indicates, that the use of the levels predicted from procedure IA is closer to real environmental conditions than that from procedure II.

4. VIBRATION QUALIFICATION TESTS IN LABORATORIES

The vibration qualification should be performed under conditions which avoid over-testing as well as insufficient qualification. Therefore the mounting of the equipment or store in conjunction with the location of the control reference has to be carried out in such a way that representative vibrations are resulting. Also, the test spectra should have realistic levels and distributions. A vibration survey for all planned missions may be helpful. The final selection of qualification levels and test setup requires a long time experience and practice to perform a successful work.

4.1 Test Setup

4.1.1 Equipment

Common practice in testing individual equipment is to mount the test specimen by its normal mounting devices to the shaker table directly or by means of a rigid fixture. For vibration control, the attachment plane is taken as equipment input reference.

Predicted data or data obtained from measurements normally provide representative vibration values for the primary structure. In specific cases of equipment mounted on shelves or trays the transmissibility characteristic has to be taken into account. Examples are given in Fig. 11.

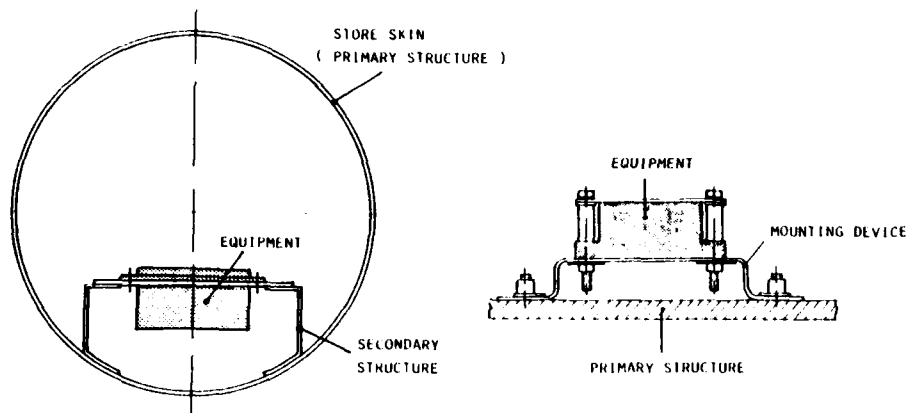


FIG. 11 EQUIPMENT INSTALLED IN STORE

If the transfer function between primary structure and equipment input can be assessed or measured, the test specimen can be attached rigidly to the shaker table, and the defined qualification spectrum of primary structure can be translated to equipment input by $G_{yy} = |H_{i\omega}|^2 \cdot G_{xx}$

G_{xx} PSD of primary structure
 G_{yy} PSD of secondary structure
 $H_{i\omega}$ Transfer function

An example of such a transfer function is given in Fig. 12. For comparison, the predicted transfer function according to MIL-Std. 810C, Method 519 is plotted as a dashed line where the fundamental resonance frequency is set to 100 Hz.

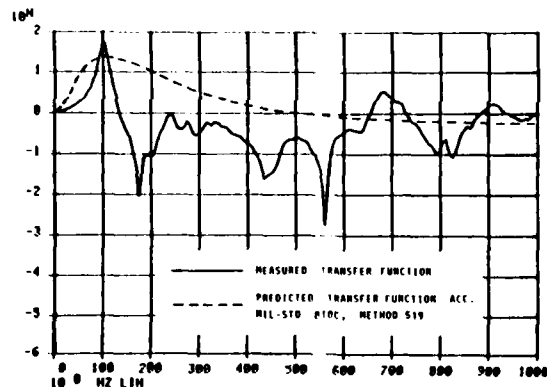


FIG. 12 TRANSFER FUNCTION PRIMARY TO SECONDARY STRUCTURE

For shock mounted equipment, experience shows that sometimes the required vibration at the equipment input can not be produced by excitation via shock mounts because of low pass characteristic of mounting devices. In such a case, a combined test with acoustic excitation can be helpful, where the high frequency content of equipment vibration mainly is produced by acoustic noise.

4.1.2 Assembled Stores

The vibration qualification of the assembled store has the purpose to check all internal equipment in their real position and installation and can also be used to get confidence about other subsystem components, e.g. suspension devices.

The test levels predicted according to MIL-Std. 810C (Method 514, Procedure IIB, assembled stores) are response levels with reference to the vibration of suitable hard points at forward and rear end of the store. Only at defined resonances the full vibration level is applied. At frequencies outside of resonances the vibration level is decreased by 6 dB from the level specified for the forward end of store. Therefore, to get realistic dynamic behaviour the mounting has to be simulated as close as possible.

In MIL-Std., two mounting methods are proposed. Sketches are given in Fig. 13.

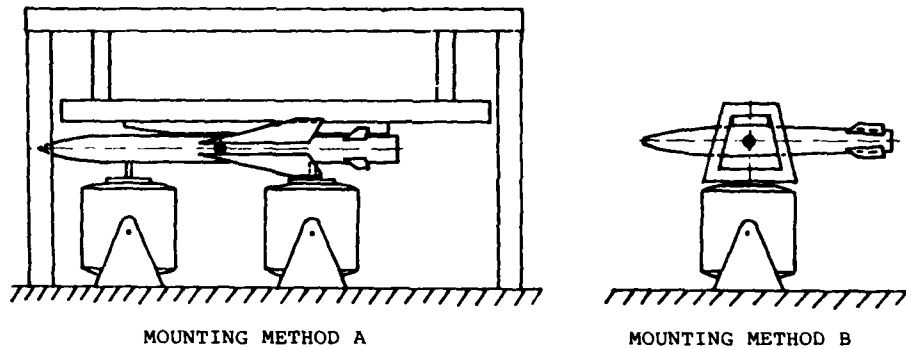


FIG. 13 TEST SETUP

In mounting method A, the store is suspended by its normal mounting arrangement from a rig. The shaker is connected to a stiff structural point of the store by means of a rod. In alternate mounting method B, the store is attached to the shaker with a stiff rig using its normal mounting lugs.

The mounting method A allows to establish different vibration levels at the forward and rear reference point of store by varying the shaker attachment point. Also, it permits excitation of the fundamental modes roll, pitch and yaw.

Considering the excitation by the boundary layer noise where the forces are acting directly on the store skin, the attachment of the exciter to the store allows a more representative excitation than introducing excitation from the suspension points as used in method B. If the excitation of the store is transmitted from the wing or fuselage, which appears to be the case for manoeuvre buffet, mounting method B permits a force input closer to the real environment.

4.2 Remarks to Qualification Procedure

4.2.1 Level Prediction according to MIL-Std. 810C

In British and French standards no level prediction of external stores is provided. According to MIL-Std. 810C, the qualification level is given by the following formula: The power spectral density for the lower frequency range (see Fig. 14) is given by

$$W_1 = 5 \cdot 10^{-3} \cdot A_1 \cdot B_1 \cdot C_1 \cdot D_1 \cdot E_1 \quad [G^2 / \text{HZ}]$$

The factors A_1, \dots, E_1 permit the adaption to the characteristics of store and store configuration. For the upper frequency range, the level is predicted by

$$W_2 = 5 \cdot 10^{-5} \left(\frac{q}{\rho} \right)^2 \cdot A_2 \cdot B_2 \cdot C_2 \cdot D_2 \cdot E_2 \quad [G^2 / \text{HZ}]$$

ρ is the averaged store weight density and q the max. flight dynamic pressure with certain limitation. The factors A_2, \dots, E_2 have the same function as above mentioned for factors A_1, \dots, E_1 . For endurance test, these values are multiplied by the "time compression fatigue factor" whereby T is the test time per axis and N the number of anticipated service mission.

$$W_{\text{END}} = W_{\text{FCT}} \cdot \left(\frac{N}{3 \cdot T} \right)^{1/4}$$

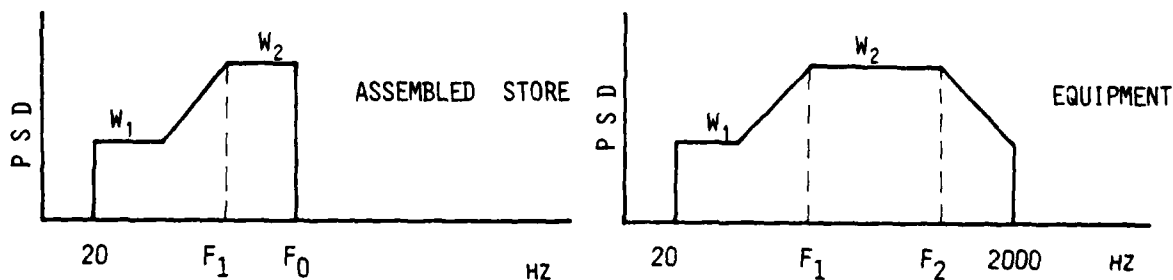


FIG. 14 QUALIFICATION SPECTRA ACC. TO MIL-STD 810C, METHOD 514, PROCEDURE II

The spectrum shape is shown in Fig. 14. For equipment installed in stores, a frequency range from 20 to 2000 Hz is required. For assembled stores, the frequency range is extended from 20 Hz to a flexible frequency limit f_0 which depends on the store skin thickness t and the one-half diameter of store R in the following way:

$$F_1 = 10^5 \cdot \left(\frac{t}{R^2} \right) \quad [\text{HZ}]$$

$$F_2 = F_1 + 1000 \quad [\text{HZ}]$$

$$F_0 = F_1 + 100 \quad [\text{HZ}]$$

Further regulations are given for exceptional cases which are not presented here.

4.2.2 Level Specification

As already shown in some comparisons (see 3.2) vibration level prediction often has limited correlation to the real environment. This is due to the high number of parameters influencing the store vibrations. Therefore, the most confident way for definition of qualification spectra and levels is the use of real measurements. For this purpose especially flight conditions and configurations with high vibration levels are of interest. For definition of test levels an accumulation procedure (see 4.3) can be applied. Safety factors may be introduced to account for the possibility of not measuring the most severe environment and to ensure enveloping narrow-band peaks.

But in many cases, adequate measurements are not available in time. Therefore, the qualification level may be specified according to MIL-Std. 810C, Method 514. For equipment installed in stores, the level depends on the location inside the store. If the equipment is in the rear half, the power spectral density is 2 or 4 times higher than at installation in the forward half. With reference to measurements presented in 3.2.2, the vibrations in the middle of the store near the attachment points are even lower than those of the nose section. Therefore, a store could be divided into a forward, a center and an aft vibration zone, whereby the qualification level of the forward and center zone may be the same. Further measurements can provide a broader basis for zoning.

4.2.3 Level Adjustment

The qualification spectra are related to equipment input in case of test of an individual equipment and to store response reference points at the nose and tail section in case of test of assembled stores, whereby the full vibration level has to be applied only at "significant resonance response peaks", the rest of the spectrum is 6 dB down from the calculated values for the forward half of store. For determination of "significant resonance response peaks" a random vibration shall be applied using an input spectrum defined for the store mounted forward accelerometer, but 6 dB down from the calculated level.

In case of excitation of store via suspension points (mounting method B, see Fig. 15), the input spectrum may be related to the suspension rack. Resonance peaks are identified by an output level at store forward and rear reference points 6 dB or higher than the input level.

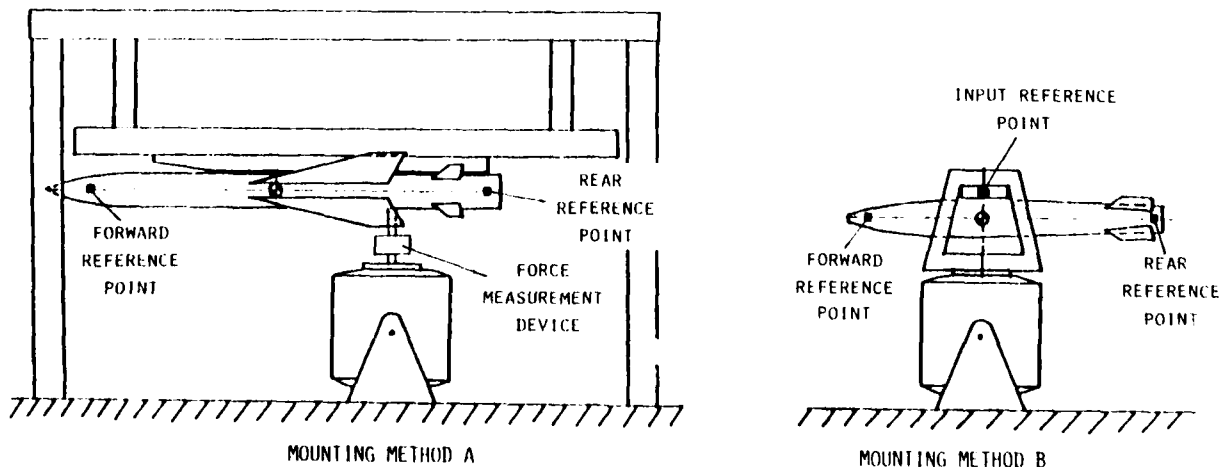


FIG. 15 REFERENCE POINTS ON TEST SETUP

In case of mounting method A, the excitation is introduced by shaker, linked to the store skin. The definition of resonance peaks based on 6 dB amplification between store response and input acceleration is not practicable. A reasonable way for identifying resonances is the computation of transfer function between store response acceleration and shaker force at reduced excitation level. During the qualification test run, the power spectral densities for the resonance frequencies shall be equal or higher than those defined for qualification. The rest of the spectrum shall have a level of 6 dB down from the specified level.

4.2.4 Functional and Endurance Test

In MIL-Std. 810C it is foreseen first to perform half an hour of the functional vibration test, followed by the endurance test and the second half of a hour of the functional test. The reason of this test sequence is to show the correct function of test specimen before and after "fatigue" (endurance) test. Only during functional test, the test specimen shall be operating as in normal service.

The factor between functional and endurance test level is the "fatigue" factor

$$\left(\frac{K \cdot N}{T} \right)^{1/\alpha}$$

which relates longer actual service time to the short laboratory test time with higher levels. N is the number of anticipated service missions, whereby every mission is assessed to one hour, and T is the test time. The value K represents the portion of mission time spent in high dynamic vibration environment and is estimated to 1/3 in MIL-Std. 810 C. For the value α in the exponent, the number 4 is established. It is derived from material data. The French standard AIR 7304 also provides an α of 4. In British standard BS 3G.100, a value α of 2.5 is used. This leads to levels in BS which are even higher. Practical experience indicates that the fatigue factor is assessed too pessimistic. With respect to the mission profile of a fighter aircraft, about 5 percent of the mission time are spent in high vibration environment (Ma 0.9 - 0.95, manoeuvres, take off, landing etc.). Therefore, a value $k = 1/20$ seems to be a realistic number for introduction into the fatigue factor formula.

If a failure occurs during the endurance test, the following functional test will show the resulting malfunctions. An examination of the unit will reveal the failure mode. It should be taken in mind, however, that the endurance test level is an increased level due to time compression and the fact that this concept has some restrictions. Especially in case of nonlinear system behaviour of mechanical or electronic components, it has to be checked whether realistic dynamic qualification requires longer endurance test time with reduced level or whether equipment modification is necessary.

4.2.5 Testing at low Frequencies

As mentioned in 4.1.2, in conjunction with an adequate simulation of store suspension and an excitation of the store at a point outside the center of gravity, also the fundamental modes pitch, roll and yaw can be excited to get a realistic store vibration behaviour in this frequency range. For this purpose, the frequency band has to be extended to the lowest frequency of interest (down to 4 Hz for heavy stores).

During high buffet manoeuvres the vibration level of the low frequency range (< 200 Hz) exceeds the specified levels by far (see 3.2.2). These vibrations can be covered adequately by an additional qualification test with a sine sweep, belonging from the lowest frequency of interest up to about 100 or 200 Hz, because the time history of a buffet manoeuvre is often more harmonic in nature (see Fig. 9).

The definition of such an additional test requirement should be based on suitable flight vibration measurements.

4.3 Accumulation of Vibration Levels for Endurance Test

The intention of the level accumulation is to get test spectra for the endurance test. To avoid impracticable long test times especially in conjunction with high costs, the vibration levels related to real time have to be translated to short time by equivalent level increase.

Following the MIL-Std. 810C the endurance ("fatigue") test level is given by an increase of the functional level by the "fatigue factor" (see 4.2.4), dependent upon

number of service missions and test time. In British standard BS 3G.100, a general accumulation method is used to define the endurance qualification level.

To develop laboratory test levels from flight vibration measurements or to get data for comparison of real measurements to qualification endurance level, an accumulation procedure can be applied. The basis for this procedure is the collection of all operation conditions and exposure times of the store and the related vibration levels.

For example, the British Standard BS 3G.100 distinguishes 10 different vibration severity categories (see Fig. 16).

- | |
|--|
| 1. ATMOSPHERIC TURBULENCE (SEVERE) |
| 2. ATMOSPHERIC TURBULENCE (NORMAL) |
| 3. UNPREPARED RUNWAY OPERATION |
| 4. NORMAL RUNWAY OPERATION |
| 5. HIGH EXTERNAL NOISE LEVELS > 140 DB |
| 6. HIGH EXTERNAL NOISE LEVELS > 150 DB |
| 7. HIGH EXTERNAL NOISE LEVELS > 160 DB |
| 8. AERODYNAMIC BUFFETING OR TRANSONIC FLIGHT |
| 9. LOW - LEVEL HIGH SPEED FLIGHT |
| 10. CRUISE (SUPERSONIC) |

(Table 1 of BS 3G.100 Part 2, Section 3, Subsection 3.1)

FIG. 16 DIVISION IN VIBRATION SEVERITY CATEGORIES

Also different store configurations have to be taken into account.

For the time compression with equivalent vibration level increase a relation between vibration level and test time is needed. The MIL-Std. 810C gives the following formula:

$$\left(\frac{W_1}{W_2} \right)^\alpha = \frac{T_2}{T_1}$$

where W_1 , W_2 are Power Spectral Densities (g^2 / Hz), T_1 , T_2 represent the test time, and the exponent α is assessed to 4 for electronic equipment. Concerning the overall RMS value, the formula alters to

$$\left(\frac{RMS_1}{RMS_2} \right)^{2\alpha} = \frac{T_2}{T_1}$$

where RMS = overall RMS value.

After selection of a reference vibration level which has to be higher or equal to the highest measured or assessed level, all flight conditions with their vibration levels and exposure times as expected during the full aircraft life can be translated to the reference vibration level by equivalent time reduction. The sum of the "normalized" exposure times together with the reference vibration level is the basis for definition or endurance test.

To cover differences in the real spectrum compared to the smooth qualification spectrum and to ensure enveloping narrow band peaks, a safety factor can be introduced, which may have a value of about 3 dB.

A diminution of validity of time reduction with equivalent level increase is the assumption of a linear system behaviour, which is not fully given at most aircraft stores.

5. SPECIAL DYNAMIC ENVIRONMENT

The dynamic environment during flight can be significantly increased by vibroacoustic phenomena or transient excitation, caused by launching a missile, firing pyrotechnic devices from dispenser pods etc.. Examples are given to show the need of implementation in qualification tests.

5.1 Vibroacoustic Phenomena in Cavities

Gaps between multiple store carriers and fuselage or open windows on pods can lead to significant aerodynamic cavity flow interactions producing large fluctuating pressures about stores and related components. Flight vibration analysis of relevant cases show clear harmonic signal content at dominant frequencies. Measured responses at primary structure revealed up to 15 g peak in discrete frequencies (see Fig. 17).

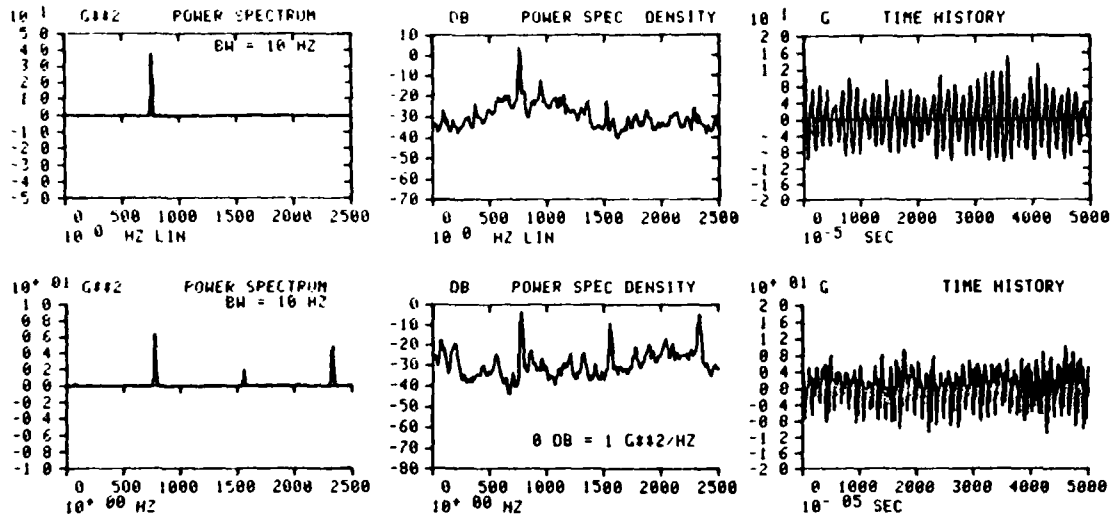


FIG. 17 ANALYSIS OF VIBRATIONS CAUSED BY CAVITIES

Such phenomena are not predictable, however, they have to be taken into account in dynamic qualification procedures.

5.2 Blast and Impulsive Loading

During launching phase of a missile or during sequential firing of pyrotechnic devices from dispenser pods high vibrations can be produced which are superimposed to aerodynamic and engine noise excited environment. As shown in Fig. 18, short impulse duration produces high frequency vibration of considerable accelerations. To cover sequential firing in laboratory qualification tests, shock pulse sequences of short pulse duration, high density random or a combination of both with accumulated real time can be applied.

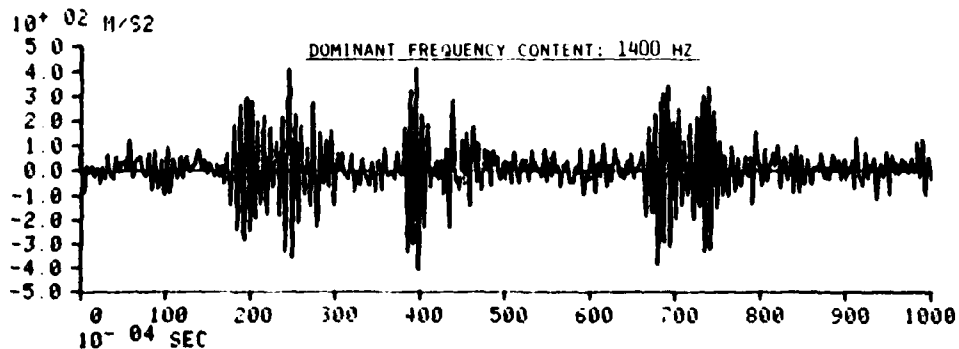


FIG. 18 TIME HISTORY OF FIRING FROM A DISPENSER POD

6. SUMMARY AND CONCLUSIONS

Considering present standard procedures considerable progress in realistic dynamic environmental testing has been reached compared to earlier stages. Random test procedures e.g. in MIL-Std. 810C as well as systematic aerodynamic pressure and engine noise related prediction methods for test tailoring marked substantial evolution in this field. Vibration measurements on modern fighter aircrafts however, indicates that even more knowledge about dynamic system behaviour and about excitation sources is necessary to improve prediction and environmental test technique. Trends in aircraft structural design as well as operational requirements result sometimes in increasing vibration problems. Of major interest in this field is the implementation of buffet-, buzz- and transonic effects which may lead to additional testing of the low frequency band for store configurations.

Broad dissemination of flight vibration measurements is helpful for prediction of qualification level.

The use of commonly applied test procedures and agreement about test setup and test time e.g. in assembled store testing is an important task to get a better basis in comparing qualification test results.

Statistic monitoring of laboratory test produced failures, and comparison and evaluation of in-service occurred malfunctions and other problems provide a useful information in assessing the realism of dynamic environmental testing.

REFERENCES

- | | | |
|-----|---|---|
| /1/ | MILITARY STANDARD | Environmental Test Methods
MIL-Std. 810C, March 10, 1975 |
| /2/ | BRITISH STANDARDS
INSTITUTION | General Requirements for Equipment in Aircraft
BS 3G.100: Part 2, December 1969 and Amendments |
| /3/ | FRENCH STANDARD NORME
AIR 7304 | Conditions d'Essais d'Environnement pour Equipments
aéronautiques, 20 Décembre 1972 |
| /4/ | EARLS, David L. | Technical Progress On new Vibration and Acoustic
Tests for proposed MIL-Std. 810C, "Environmental
Test Methods"
The Journal of Environmental Sciences,
July/August 1973 |
| /5/ | DREHER, J.F.
LAKIN, E.D.
TOLLE, E.A. | Vibracoustic Environment and Test Criteria for
Aircraft Stores during Captive Flight
Shock and Vibration Bulletin No. 39, Supplement
April 1969 |
| /6/ | FROST, W.G.
TUCKER, P.B.
WAYMON, G.R. | Captive Carriage Vibration of Air-to-Air Missiles
on Fighter Aircraft
The Journal of Environmental Sciences, September/
October 1978 |
| /7/ | WAFFORD, J.H. | Application of MIL-Std. 810C Dynamic Requirements
to USAF Avionics Procurements
AGARD R-682 |
| /8/ | HAIDL, G.
LODGE, C.
ZIMMERMANN, H. | Dynamic Environments and Test Simulation for Qualifi-
cation of Aircraft Equipment and external Stores
AGARD R-682 |
| /9/ | EGBERT, H. | MIL-Std. 810D - a Progress Report
The Journal of Environmental Sciences,
March/April 1981 |

AIRCRAFT FUEL TANK SLOSH AND VIBRATION TEST

by

Dipl. Phys. Helmut Zimmermann, VFW,
Abt. Dynamik/Aeroelastik
2800 Bremen, Germany

Summary

A dynamic qualification test for a subsonic and a supersonic external drop tank for a European fighter is presented. The requirements for this qualification test are derived from Mil-T-7378A of the USAF. The test rig and the specimens are described and the measuring results are discussed. For the supersonic tank as well as for the subsonic tank the measuring results show, that for a certain slosh angle an eigenfrequency of the rig increases the amplitudes at the excitation position and the accelerations on the tank.

For the subsonic tank it seems that a tank eigenfrequency will be excited for the nose down position of the tank. The qualification requirements are critically examined and proposals for improvements are given.

It is proposed that instead of using an arbitrary vibration amplitude and frequency for excitation, frequency ranges and amplitudes which are averaged out of flight measurements at the tank attachment points on the aircraft be used and that the demand for a certain input amplitude at the top of the attachment bulkheads and an output amplitude at the bottom of the attachment bulkheads be deleted.

I. Introduction

The tank slosh and vibration tests should provide confidence in the structural integrity of external fuel tanks and in the reliability and performance of their equipment under conditions which they will encounter during their service life.

External fuel tanks and their equipment are exposed to a wide variety of dynamic environments during ground and flight operations. The dynamic environment is due to:

- a) manoeuvre movements of the aircraft and its rigid body movements,
- b) frequency responses due to dynamic loading of the aircraft by gusts, landing impacts etc. and aircraft internally generated vibrations such as hydraulic pumps, engine vibrations etc., which are transmitted via the attachment points of the tanks in form of accelerations.

For the qualification of an external tank and its equipment useful methods for predicting the dynamic environments are needed. The qualification tests for a tank should be independent of the special aircraft type for which the tank is used. Therefore it is necessary to generalize and accumulate the different dynamic environmental conditions an external fuel tank is exposed to.

The structural loads of the tanks caused by manoeuvres are influenced by their fuel content and for intermediate fuel states the loads are amplified by the sloshing of the fuel.

Due to the different dynamic loadings mentioned above a unique combination of slosh and vibration loadings in a qualification test appears basically sound in concept, since it provides some confidence in the structural integrity of the fuel tanks. In the Mil-T-7378A a slosh and vibration qualification test procedure is given. For the dynamic qualification of different external drop tanks, developed in several countries of the western world this test procedure was used in its main points.

II. Test Requirements for Subsonic and Supersonic Drop Tanks for a European fighter

For the subsonic and supersonic drop tanks of an European fighter the slosh and vibration tests are outlined in requirements which are in agreement with the Mil-T-7378A. The requirements used in their main parts, say the following:

1. Tank and Test Rig

Each drop tank will be mounted in a test rig using a dummy pylon. This will incorporate the M.A.C.E. attachment units and fuel, air and electrical connectors as per the aircraft installation.

acknowledgment: The slosh and vibration test for the drop tanks were performed at IABG. The author thanks Mr. Dipl.-Ing. Raasch of IABG for putting the test material at his disposal, and for significant contributions to the discussion.

The test rig will be capable of a pitch movement of $\pm 15^\circ$ of the tank horizontal fuselage datum, and simultaneously vibrating the tank at a frequency of 2000 cycles per minute or to the most damaging frequency normally experienced on the aircraft. The tank centre line when mounted on this assembly shall be at least 20 ins. from the slosh axis. Each tank will be assembled in the test rig and filled two thirds full of water at ambient temperature, i.e. centre compartment full the remaining quantity proportioned between forward and aft compartments in the ratio of their respective volumes.

2. Slosh-, Vibration frequencies and amplitudes

If practical, the slosh cycling will be commenced first at a frequency of 16 to 20 cycles per minute (preferably 17 c.p.m.). Vibration will then be applied at a frequency of 1940 to 2000 cycles per minute (preferably 1970 c.p.m.) with a minimum peak to peak amplitude of 0.020 inches measured at the tank attachment points and a minimum average peak to peak amplitude between the top and bottom of the tank at the bulkheads below the attachments of 0.032 inches. These amplitudes are to be recorded over a period of at least 30 seconds to obtain mean peak signal values.

3. Tank Calibration and strain gauges monitoring

Each tank will be strain gauged adjacent to the forward and aft joints. The strain will be calibrated against bending moment at the joint by applying loads at the nose and tail. By monitoring the strain gauges, the bending moments at the forward and aft joints will be checked and these must not exceed 10% of the ultimate design bending moments.

4. Test time

The two thirds full pressurised tank is to be simultaneously slosh and vibration tested for 25 hours. No leakage or structural failure is permissible during this test.

5. Vibration

Following the slosh and vibration test, the tank will be completely filled with water and pressurised. It will be vibrated only for a period of 10 minutes at a frequency of 1940 to 2000 cycles per minute and mean peak to peak amplitudes at the bulkheads below the attachments specified in point 2.

6. Inspection

No dampness or leakage at any point other than filler caps is permitted during either of above tests. Following the tests, the tank is to be drained and a leakage check acceptable to the procuring agency conducted. The tank shall be opened and inspected for evidence of failure such as sagged panels, buckled plates, loose bulkheads, rivets or severe metal wear. Any leakage during or after slosh, vibration or structural damage shall be cause for rejection.

III. Test Specimens

In this report the slosh and vibration tests carried out on subsonic (1500 l) and supersonic (1000 l) external drop tanks are described. Fig. 1 shows in principle an external drop tank. Each tank is composed of three compartments.

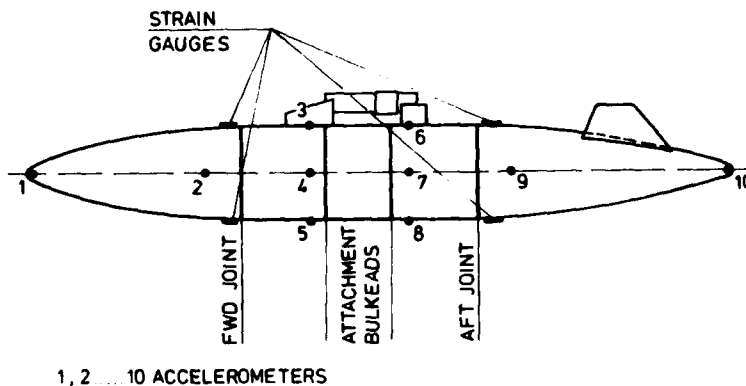


FIG. 1 SKETCH OF THE DROP TANK

For example for the subsonic tank with a total capacity of 1500 l for the combined slosh and vibration tests the centre section was completely full with 569 l while the forward and aft sections were filled in the ratio of the front and rear compartment capacities, until the total tank was filled to 2/3 of its capacity. This means that the forward compartment was filled with 271 l and the aft compartment with 181 l. Adjacent to the joints on the top and the bottom you see the strain gauges for monitoring the bending moments.

The figure shows the location of the ten accelerometers, two each on the forward and aft compartment and three at each bulkhead below the attachment points positioned at the top in the middle and at the bottom of the bulkhead. The acceleration outputs of the accelerometers 3, 5, 6 and 8 at the top and the bottom of the bulkheads below the attachment points were integrated to obtain the average displacement according to the requirement. The requirement demands that the peak to peak displacement averaged between the top and the bottom at each bulkhead be at least 0,032 inches as a mean value over a period of 30 seconds.

A displacement pick-up at the tank attachment was used to control the stroke of the cylinder for the vibration movement and to monitor that the applied vibration at the attachment had a peak to peak amplitude of at least 0,02 inches.

IV. Description of the combined slosh and vibration test rig and measuring equipment

The slosh and vibration test for the subsonic and supersonic tank were carried out by the IABG (Industrie-Anlagen-Betriebsgesellschaft) of Germany in Ottobrunn. Fig. 2 shows a sketch of the slosh and vibration test rig with the tank assembled.

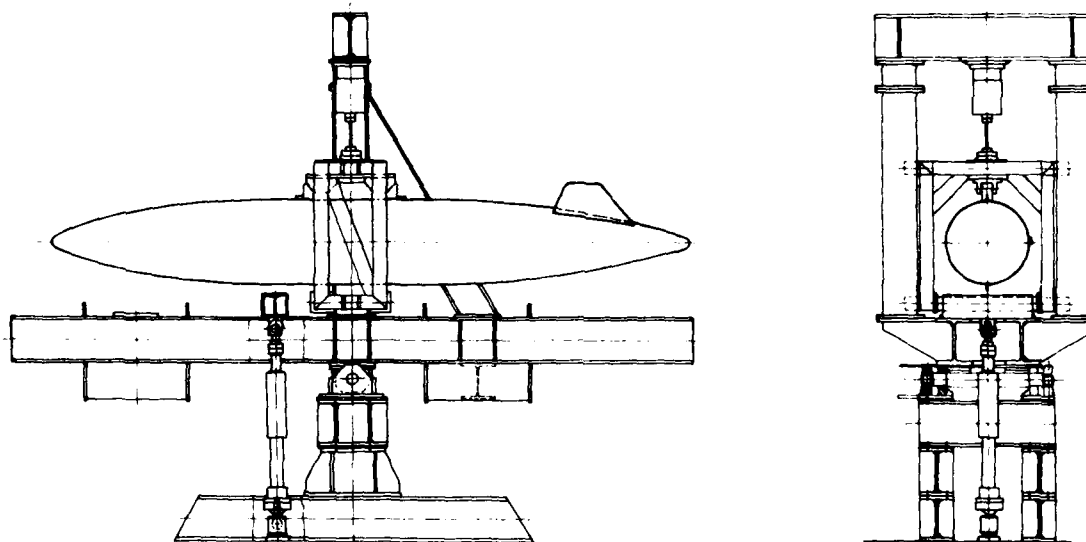


FIG. 2 TEST RIG

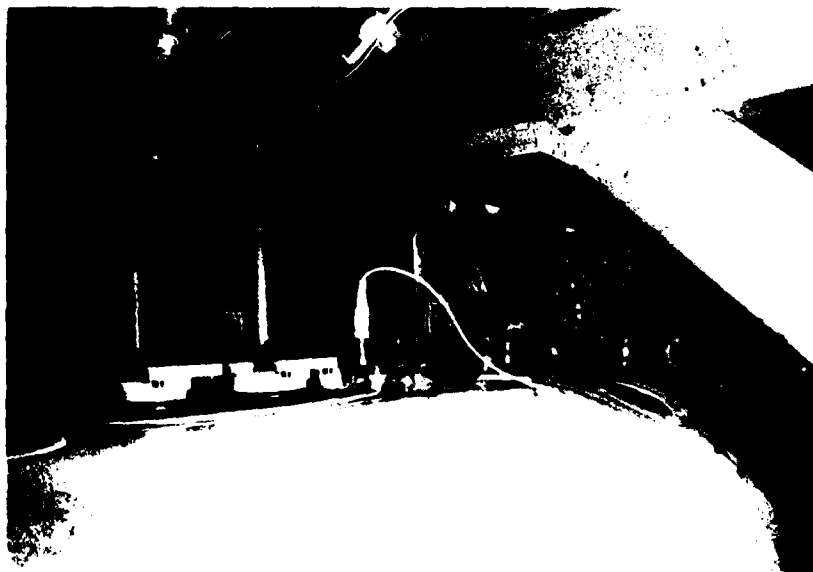


FIG. 3 EJECTION RAM UNIT

The tank was fixed with the original ejection ram unit, shown in Fig. 3, to a frame which was laterally supported by rubber bearings. The rubber bearings had a very small rigidity in the vertical plane and a very large rigidity in the horizontal plane. The vibration were induced into the frame by a 6000 daN hydraulic cylinder. The centre line of the tank was 1200 mm above the slosh axis. The slosh movements were generated by a 160 kN hydraulic cylinder. From this figure 2 you can recognize that the whole rig is turned round a pivot to introduce the sloshing movement. The frame which holds the tank, the vibration exciter (hydraulic cylinder) and the different accelerometers on the tank, as well as the measuring equipment is shown in Fig. 4 and 5.



FIG. 4 TEST RIG WITH TANK

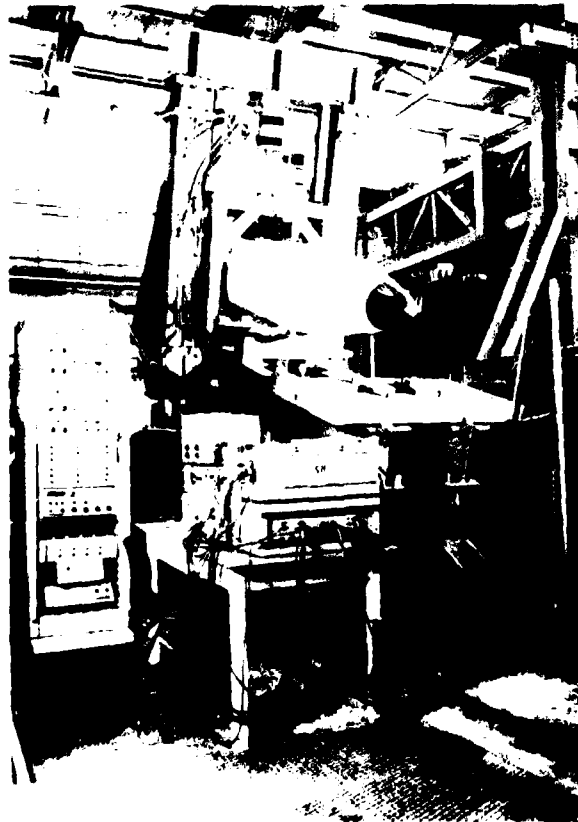


FIG. 5 TEST RIG IN INCLINED POSITION

Fig. 5 shows the rig in an inclined position. Fig. 4 shows also the pivot and the cylinder for the slosh movement.

V. Combined Slosh and Vibration Test and Results

As well the subsonic as the supersonic external drop tank were submitted to a 25 hours combined slosh and vibration test. For this test the air pressure in each of the tanks amounted to 103 KPa, the mean vibration frequency was 32,8 Hz, and the amplitude $\pm 0,25$ mm. The mean slosh frequency was 0,3 Hz and the slosh angle $- 15^\circ$. During these tests some interruptions occurred because of cracks occurring adjacent to the attachment saddles of the tank but these things will not be considered in this report. During the tests following measuring results were recorded.

- stroke of the cylinder for the vibration movement
- stroke of the cylinder for the slosh movement
- ten acceleration pick-ups
- two strain gauge bridges attached near the aft and forward joints.

For the supersonic tank the vibration amplitude was not kept constant, because of a resonance of the test systems when the nose of the tank was up. However, the requirements for the mean value of the amplitudes at the top and the bottom of the attachment bulkheads were fulfilled. They are higher than 0,032 inches for the two bulkheads for the supersonic as well as for the subsonic tank.

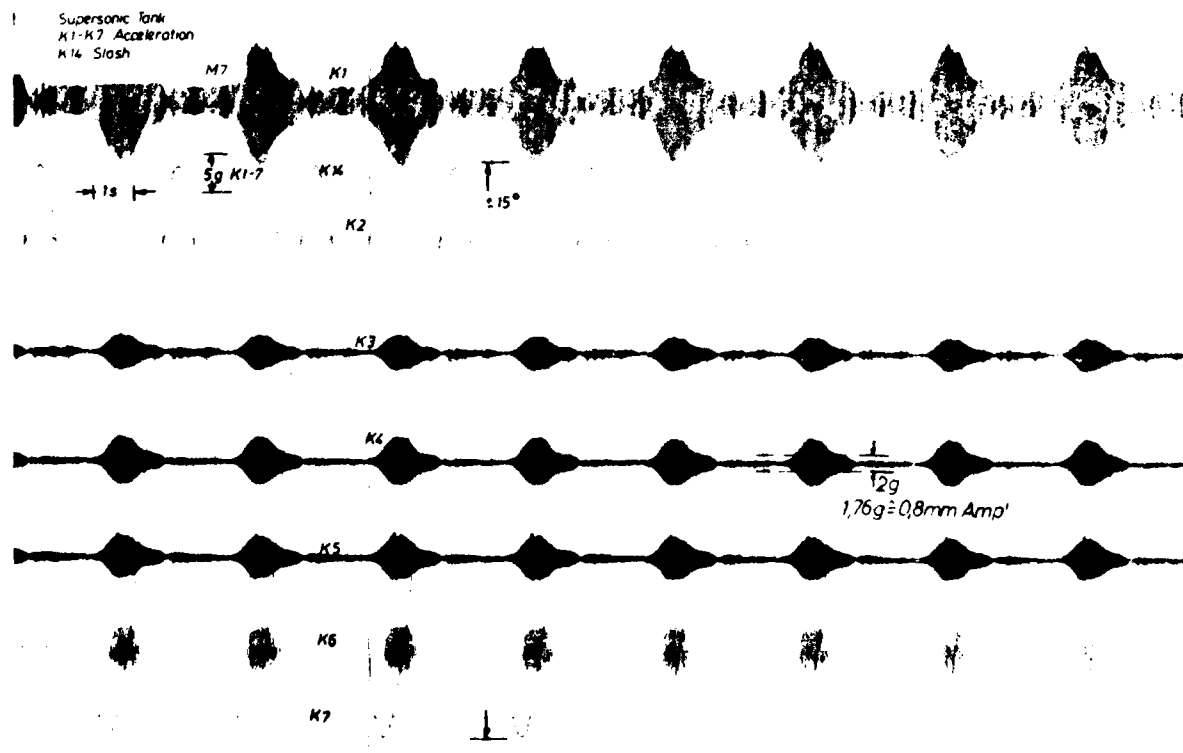


FIG. 6 RECORDED MEASURING RESULTS FOR THE SUPERSONIC TANK

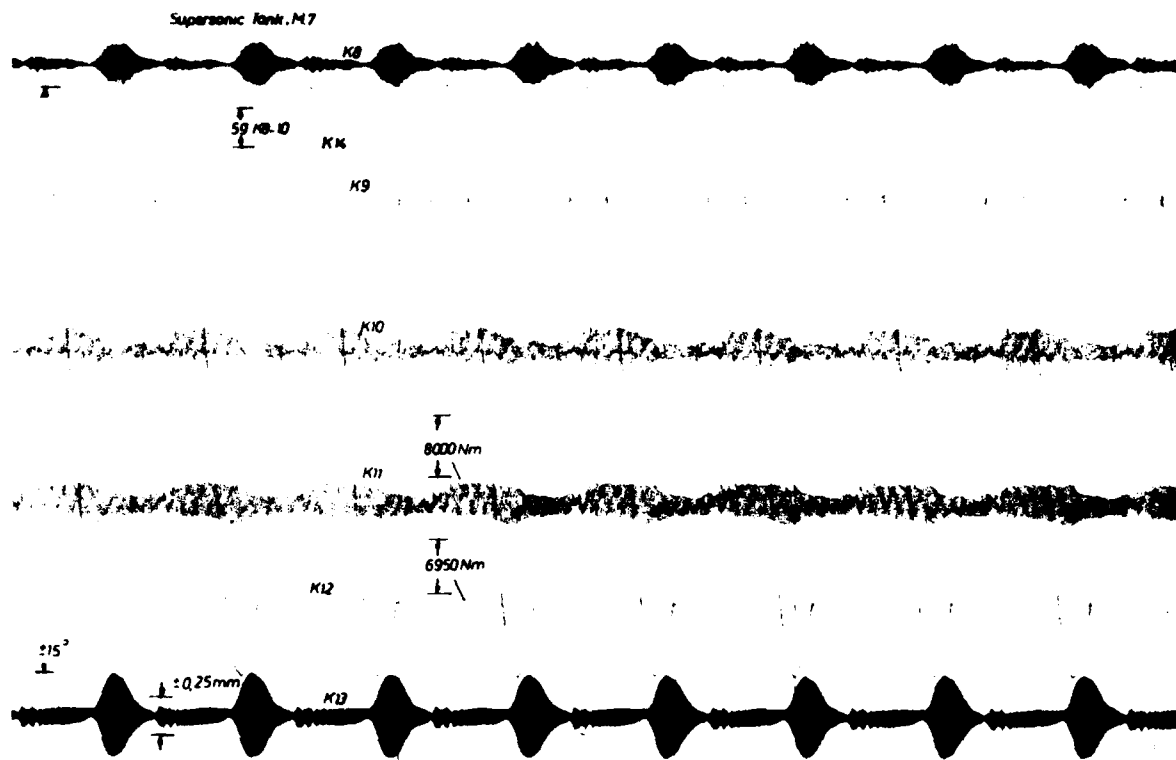


FIG. 7 RECORDED MEASURING RESULTS FOR THE SUPERSONIC TANK

Let us start with discussing the results for the supersonic tank. Fig. 6 and 7 show the measuring results for a time period for the ten accelerometers, from K1 to K10, the two bending moments track K11 and K12, the vibration amplitude K13 and the slosh amplitude K14. The sign definition for the slosh movement record of the tank is as follows: the maximum means nose down, the minimum means nose up.

The figures show big peaks in the vibration amplitudes after the minimum of the slosh amplitude (nose up). With the exception of the signal of the accelerometer located at the rear position of the tank the signals of all the accelerometers show at the same time magnified amplitudes. These magnifications occur with the same period as the slosh frequency. The strain gauge bridges show bigger signals during the sloshing movement of the tank from nose down to nose up than for the sloshing movement from nose up to nose down. The signal of the accelerometer at the rear position of the tank shows the same amplitude magnification as the signals from the strain gauge bridges. The signals of the accelerometers in the front position of the tank show the highest magnified amplitudes for the time after the tank has its most nose up position and the signals of the accelerometers adjacent to the joints of the tank the smallest magnified amplitudes. When the tank goes from nose down to nose up the signals of the rear and the front accelerometers are the biggest of all.

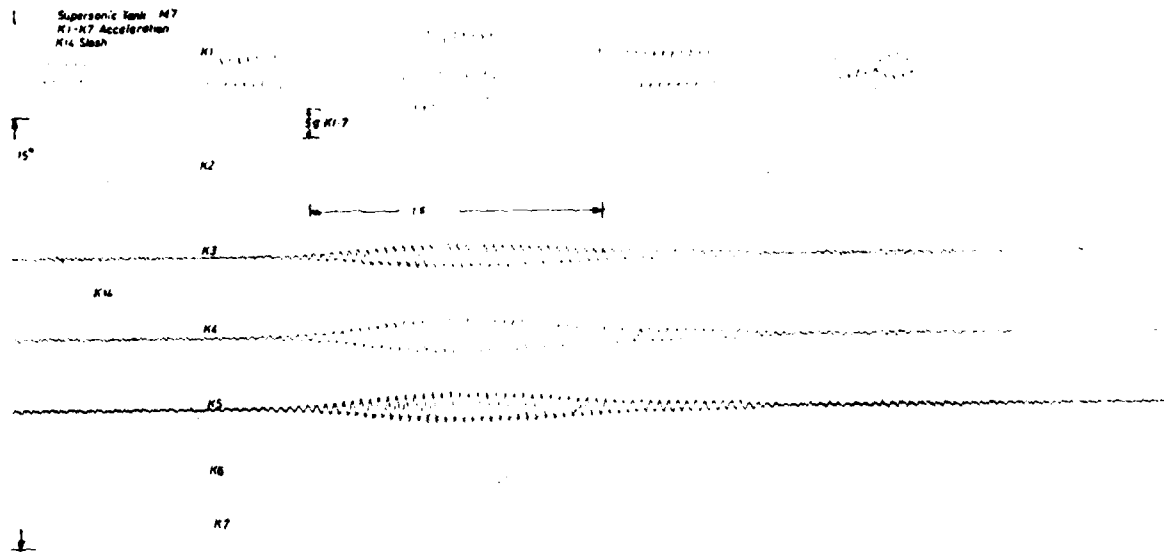


FIG. 8 RECORDED MEASURING RESULTS FOR THE SUPERSONIC TANK

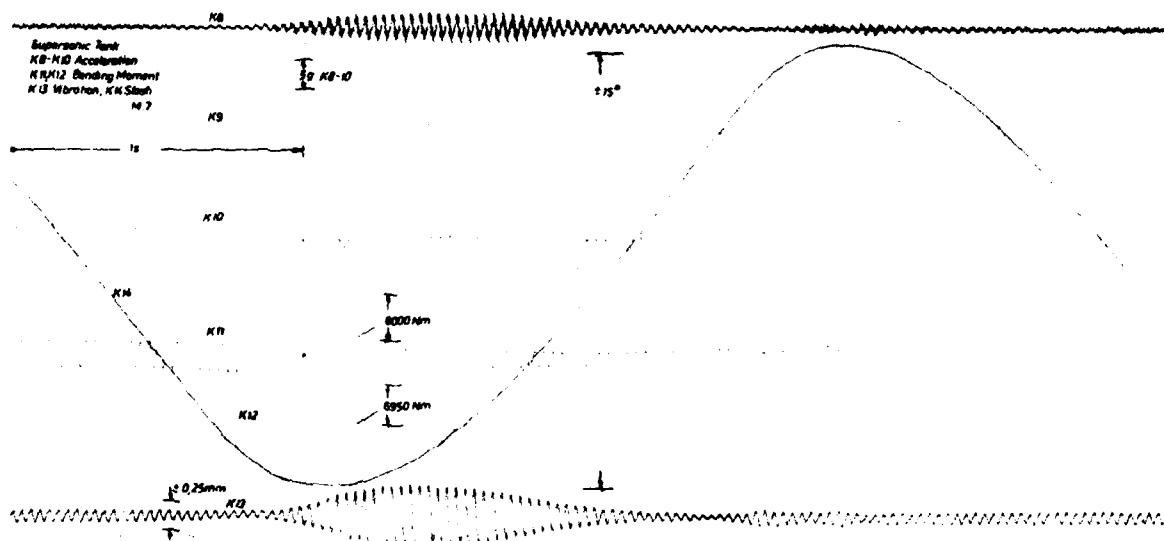


FIG. 9 RECORDED MEASURING RESULTS FOR THE SUPERSONIC TANK

Fig. 8 and 9 show the same recorded signals in a magnified time scale. They show the same behaviour. There exists no phase shift between the signals of the accelerometers K1 to K6. Between the signals of the accelerometers K8, K9 and K10 seems to be a phase shift of nearly 90° . The preceding discussion of the results of the record show clearly that the magnified signals of most of the accelerometers during the sloshing down movement of the tank do not signify, that the tank itself runs in a resonance but that the rig system has a resonance for this arrangement. However, it doesn't seem possible to localize this resonance problem from these records.

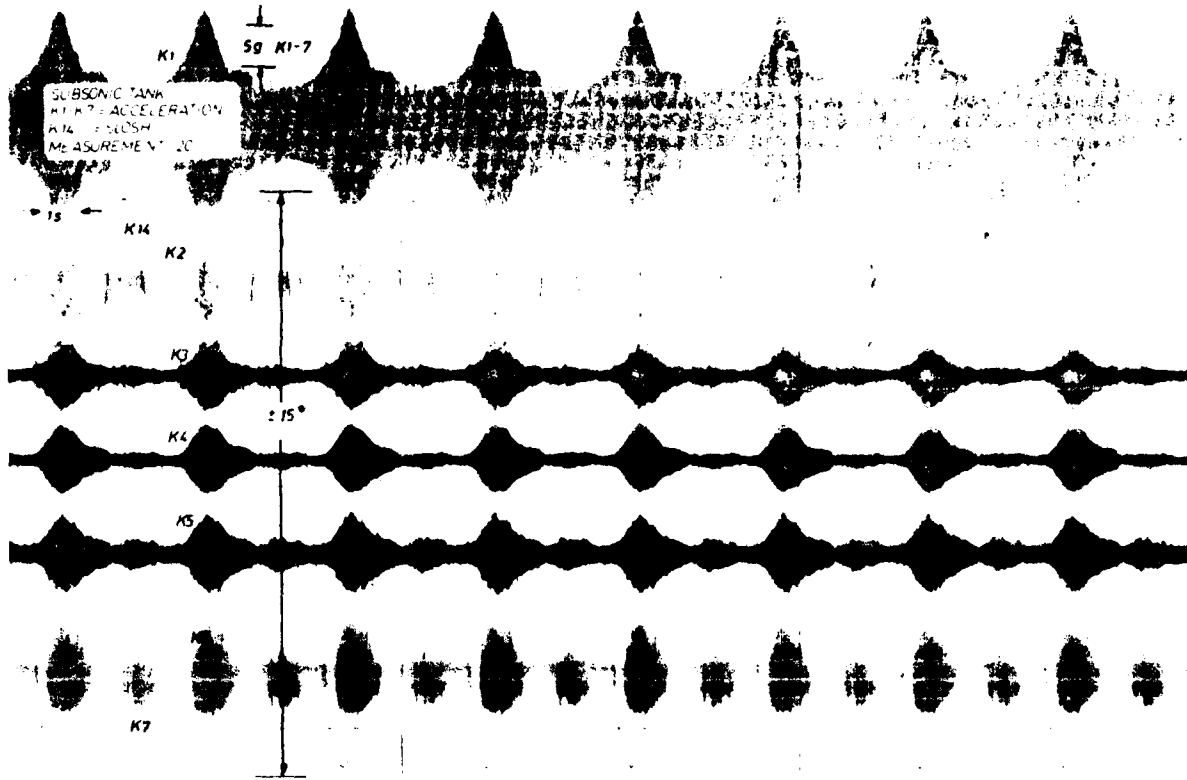


FIG. 10 RECORDED MEASURING RESULTS FOR THE SUBSONIC TANK

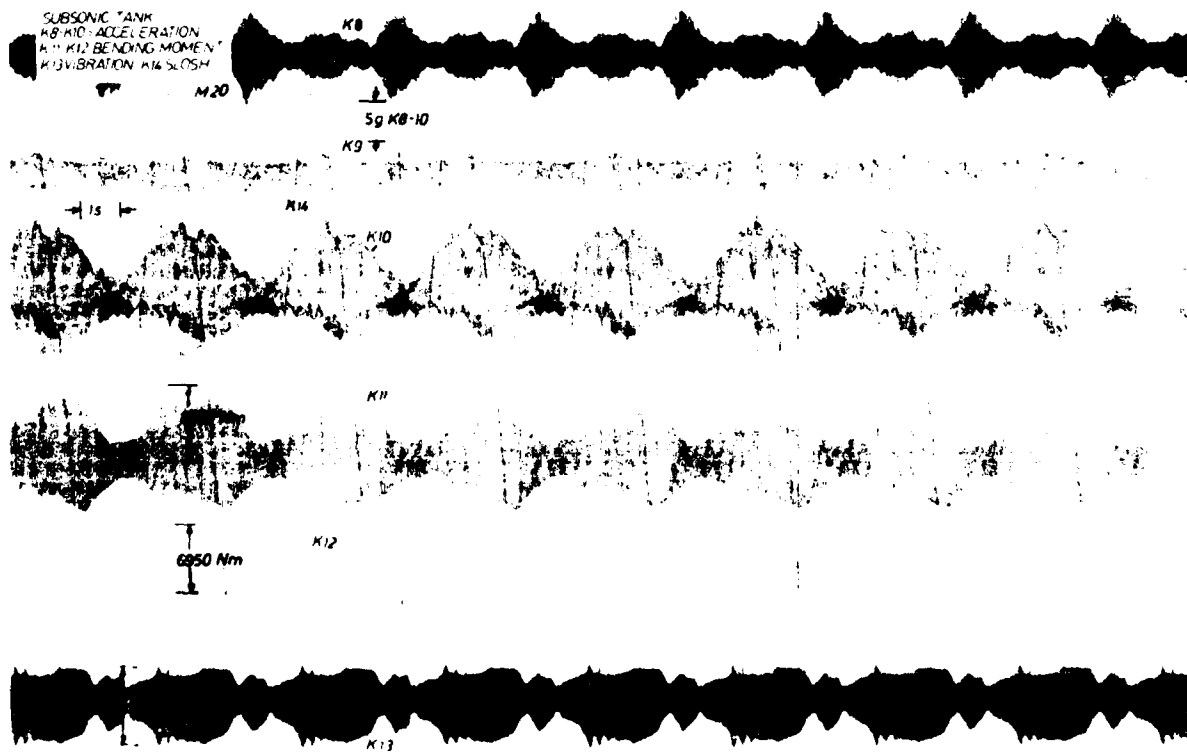


FIG. 11 RECORDED MEASURING RESULTS FOR THE SUBSONIC TANK

Let us now discuss the recorded signals for the subsonic tank. Fig. 10 and 11 show the signals for the accelerometers and the slosh and vibration amplitudes in the same arrangement as for the supersonic tank. After the minimum of the slosh angle (nose up) is reached the signals of all accelerometers except that of the accelerometer at the rear position of the tank show magnified amplitudes. The explanation for this behaviour is the same as for the supersonic tank. There exists a resonance of the rig systems but the tank itself does not have a resonance. Except for the signals of the accelerometers in the front part the signals of all other accelerometers show magnified signals when the sloshing angle is near to the nose down position of the tank. The accelerometer at the most aft position on the tank shows this signal behaviour most strongly. The signals of the strain gauge bridges show more or less the same significant behaviour. This can be an indication, that the tank runs in resonance near the nose down position.

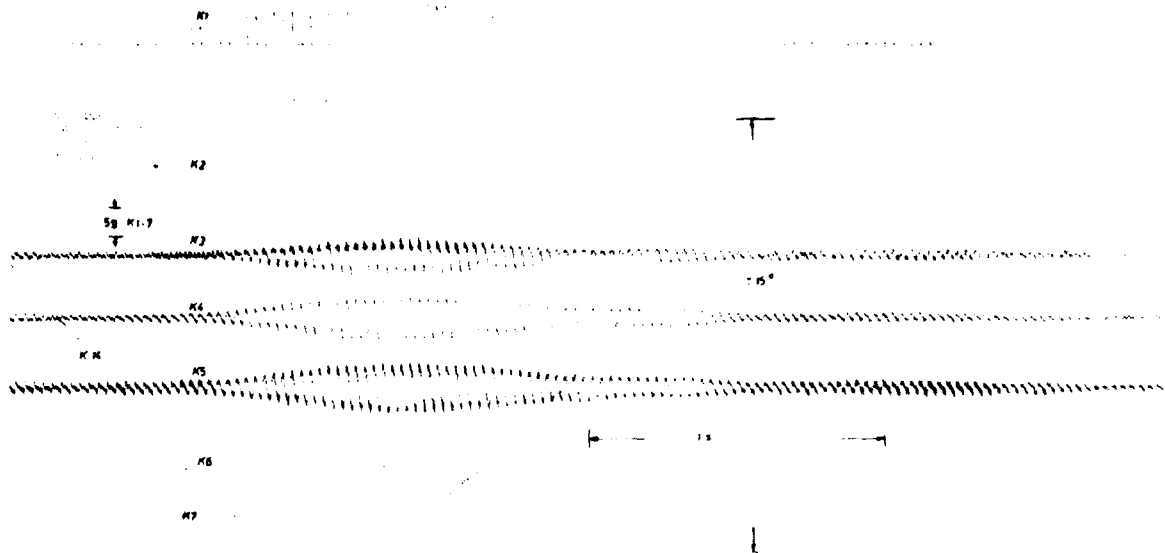


FIG.12 RECORDED MEASURING RESULTS FOR THE SUBSONIC TANK

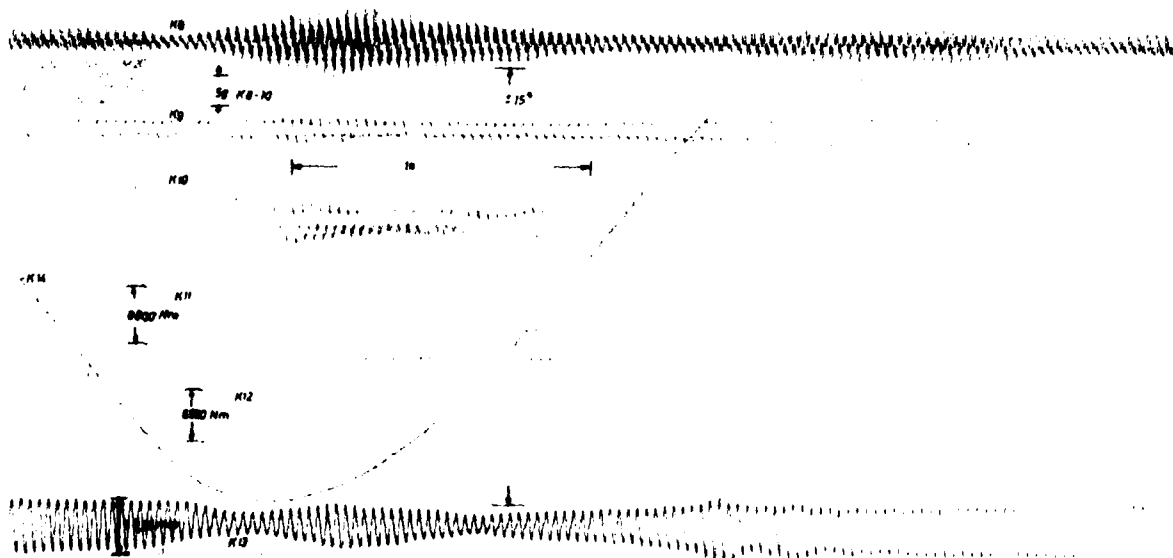


FIG.13 RECORDED MEASURING RESULTS FOR THE SUBSONIC TANK

Fig. 12 and 13 show the same signals as Fig. 10 and 11 but for a magnified time scale. Therefore, they gave no further confirmation that the tank possibly runs in a resonance in the nose down position. An additional indication that for the nose down position of the tank there exists a resonance of the tank is given by measurement results with lower vibration frequencies. There the magnified amplitudes for the accelerometers in the nose down position of the tank disappear.

VI. Eigenfrequency calculation

It seems difficult to accomplish ground resonance tests with the tank in the rig for the different slosh angle position, while the eigenfrequencies of the test rig including the tank colour the measured results. For other external drop tanks attempts to correlate such rig test results with ground resonance test results proved inconclusive. Therefore we tried to calculate the lowest eigenfrequency of the subsonic tank for different suspensions for the tank and different fuel distributions. Fig. 14 gives the results for the different configurations. The rigged tank means that the tank is suspended in a similar way as in the test rig, but without rig stiffnesses. For the nose down and nose up position a mass distribution for the water was used as calculated for the slosh angles of $+15^\circ$ or -15° . The calculation results show that for the horizontal position of the tank and the nose down position the lowest eigenfrequency lies near to the vibration frequency in the test. That is not a confirmation but only an additional indication that the test for the subsonic tank was run near to the eigenfrequency of the tank. But the main acceleration peaks are given by the resonance of the rig.

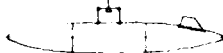




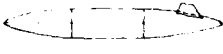


SYSTEM / LOADS		FREQUENCY
RIG		
0°		92,4 Hz
0°		34,9 Hz
0°		26 Hz
-15°		45,2 Hz
+15°		34 Hz
FREE-FREE		
0°		129 Hz
0°		52 Hz
0°		41 Hz

FIG. 14 EIGENFREQUENCIES OF
THE TANK-SYSTEM

VII Experience obtained by the Test

The most significant experiences obtained by these slosh and vibration tests appear to be the following

- It seems difficult to build a test rig which is stiff enough, so that test rig eigenfrequencies in the required frequency vibration range can be prevented, when a simultaneous slosh and vibration test is required.
- For a simultaneous slosh and vibration test the vibration amplitude on the tank cannot be kept constant.
- In spite of the imperfections of the requirements due to the real vibration loads of an external drop tank on the aircraft and the weaknesses of the test rig to keep a nearly constant amplitude with simultaneous slosh and vibration excitation, structural weak points of the tank were discovered during the test.
- Since the requirements for the vibration frequencies and the vibration amplitudes on the tank do not correlate to the frequencies and amplitudes which exist for a real tank configuration on the aircraft, certifying external drop tanks in this way will not necessarily guarantee a proper work of the tank and its equipment on the aircraft.

VIII Recommendations for improvements of the requirements

Normally a fatigue test will be done for an aircraft structure. The load spectra which are used for these endurance tests are composed of the real loads an aircraft structure is exposed to during its life time. For the qualification of an external drop tank a similar procedure must be elaborated. For this a sloshing test similar to the requirements of the Mil-T-7378A seems reasonable. But it must be checked if the amplitude of the loads generated by these tests compare with the most frequently encountered loads on a tank on the aircraft. The frequency of 0,3 Hz for the slosh movement covers the requirement for the time rates for loadings by manoeuvres. The requirement for the frequency of the vibration seems arbitrary. The requirement for a certain excitation amplitude at a certain frequency is justified as long as a correspondance of these frequencies and amplitudes to the frequencies and amplitudes at the corresponding points on the aircraft exists. Requirements for certain differences in the mean amplitudes at the top and the bottom of the bulkheads under the attachment points are difficult to understand. A requirement for certain differences in the mean amplitudes at the top and the bottom means that the stiffer the tank the higher the excitation amplitude necessary - in this way you can destroy everything - or you have to excite in an eigenfrequency of the tank. Therefore, for the excitation frequencies and amplitudes such frequencies and amplitudes must be used which exist at the attachment points of the tanks on the aircraft during flight, landing and taxiing. For the frequencies and amplitudes the real frequency ranges and real amplitudes averaged between the different profile segments must be used.

From the first impression it seems that the requirements for the sloshing movement can be done independent of the aircraft type. The excitation vibration frequency ranges and amplitudes perhaps can be different for different aircraft types. The signals of the accelerometers and the strain gauges have to be used only for monitoring. On the aircraft the low frequency and high frequency loads are superimposed. Therefore a combined slosh and vibration test seems necessary. As we have seen above a combined slosh and vibration test for a tank can lead to an overloading of the tank specimens caused by an eigenfrequency of the test rig in the test frequency range. To prevent such eigenfrequencies in the rig seems very difficult.

The requirement for a vibration test with the full tank after the combined slosh and vibration test with the tank 2/3 full is successfully finished is not clear. The opinion of the Author is, to delete this vibration test for the full tank.

IX Conclusion

Experiences with the qualification tests carried out on the external drop tanks for a fighter aircraft show that the requirements of the Mil-T-7378A for the qualification test should be improved in some points. It is essential that for such qualification tests the input frequencies and amplitudes must correspond to frequencies and amplitudes at the tank attachment points on the aircraft during their profile segments. Furthermore, on the given values for input and output amplitudes must be deleted and it can be deleted by using more realistic frequency and amplitude spectra.

THE STRUCTURAL DYNAMIC INTERFACE
REQUIRED FOR DEVELOPING HELICOPTER
TARGET ACQUISITION SYSTEMS

by

Sam T. Crews
Structures and Aeromechanics Division
Development and Qualification Directorate
ARMY AVIATION RESEARCH AND DEVELOPMENT COMMAND
St. Louis, Missouri 63120

SUMMARY

The paper gives a brief description of the helicopter vibration environment. Two development programs are used as examples to show how vibration sensitive target acquisition systems can be interfaced to the helicopter. The systems are the Target Acquisition Data System/Pilot Night Vision System mounted to the nose of the Army's new Advanced Attack Helicopter and the Stand-Off Target Acquisition System mounted underneath the Army's BLACK HAWK helicopter. The qualification strategy and specific testing performed and to be performed are included.

1. INTRODUCTION

The helicopter presents to the designer of equipment a rather unique vibration environment. This environment can be characterized as complex periodic. The exciting frequencies are very well defined and are directly related to rotating system rotational speeds. "Exciting" amplitudes are a function of the structural dynamic interface between helicopter and equipment. Therefore, "exciting" is really a misnomer. A more appropriate term would be "interface" amplitude. By choosing appropriate structural dynamic properties the helicopter designer and the equipment designer can minimize the interface amplitudes of vibration. It is especially important that they do this for items of equipment whose performance is especially sensitive to vibration. Helicopter target acquisition systems, both passive, with their sensitive electro-optical elements, and active with their long radar reflectors, generally fall into this class of equipment. Therefore, it is extremely important for the Government to structure its development and qualification programs for such systems to allow designers to consider and take advantage of the unique structural dynamic environment the helicopter offers. Two examples of how these programs should be structured are presented. The Department of the Army Materials and Acquisition Readiness Command (DARCOM) was given program management and development responsibility for the Target Acquisition Data System/Pilot Night Vision System (TADS/PNVS). The Program Manager's staff worked out of the Army Aviation Research and Development Command (AVRADCOM) and received technical management support from AVPADCOM. AVPADCOM also formulated the airframe interfacing and airworthiness requirements for the Stand-off Target Acquisition System (SOTAS). Program management of SOTAS was given to the Electronics Research and Development Command (ERADCOM).

2. THE HELICOPTER STRUCTURAL DYNAMIC ENVIRONMENT

Helicopters have fundamentally different vibration environments than fixed wing aircraft. Therefore, helicopter vibration qualification test requirements and structural dynamic interface requirements for equipment mounted on or in helicopters should be quite different than those for fixed wing aircraft. A vibration qualification test spectrum put together from enveloping maximum flight test measurements from the extremes of a store mounted on the F-15 fixed wing fighter (Reference 1) is compared in Figure 1 to a combined set of similar maximum measurements made on a light weight rocket launcher mounted on the AH-1S Cobra helicopter gun ship (Reference 2). The rocket launcher peaks presented are the worst case measurements taken from triaxial accelerometers mounted at the front and rear of the launcher. Flight conditions are worst case taken from eight two hour flights flown to a typical mission profile. Spectrum analyses were performed from 0 to 100 Hz with a 1.0 Hz bandpass. Figure 2 presents a composite spectral plot of maximum accelerations taken from seven triaxial accelerometers mounted on the instrument panel and in the avionics bay of the OH-58 (Bell Kiowa) helicopter. Flights included a wide range of steady state and maneuvering conditions (Reference 3). Spectral data analyses were performed from 0 to 500 Hz with a 1 Hz bandpass. The Cobra is a two bladed helicopter with a main rotor rotational frequency of 5.4 Hz. The OH-58 is a two bladed helicopter with a main rotor rotational frequency of 5.9 Hz. Figures 1 & 2 show that the primary responses on these helicopters occur at integer multiples of the number of blades times the rotor rotational speed. If a rotor's blades are reasonably tracked to run in the same plane and mass imbalance is properly contained, then the only significant loads transferred from the rotating system to the fixed (airframe) system are steady loads and oscillatory loads which occur at integer multiples of the number of blades times rotor rotational speed (Reference 4). This fact and the data presented in Figures 1 & 2 suggest that helicopter vibrations are primarily due to rotor excitation and not due to air stream excitation as in fixed wing aircraft. Oscillatory excitations in helicopters result from loads carried through both the rotor shaft and blade vortex-airframe face interactions.

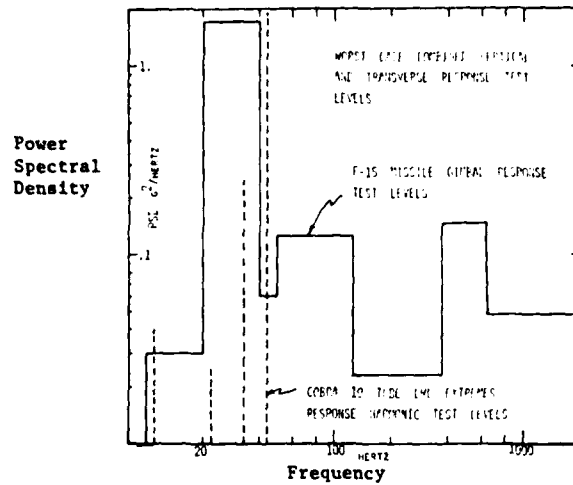


Figure 1 Fixed Wing vs Helicopter External Store Response

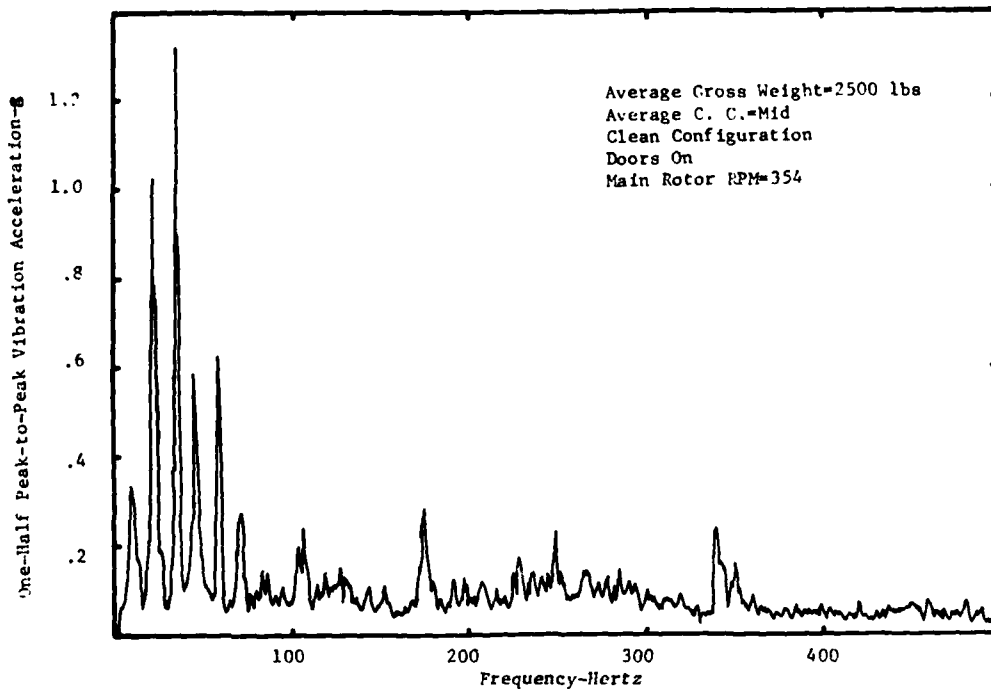


Figure 2 Maximum Vibration Acceleration OH-58A Instruments/Avionics All Axes

Figure 3 shows the sine sweep vibration test spectrum from MIL-STD-810 B & C that is frequently applied, along with sinusoidal resonant dwells, toward qualification of helicopter equipment and also external stores mounted on helicopters. As can be seen from comparison with Figures 1 & 2, this test in no way simulates or resembles a true helicopter vibration environment. This test was originally applied to qualify black boxes, and black boxes which were qualified to this standard have shown good reliability in the field. Therefore, the test gained credibility and consequently was applied to qualify a variety of equipment types, sometimes with very poor results (References 2 & 5).

The test worked well for black boxes because it is in most cases a severe over test. A severe over test produces a weight penalty by requiring more structure than necessary. However, in the case of black boxes this weight penalty is probably quite small. Most dynamics related failures of equipment mounted on helicopters occur because the piece of equipment, as mounted to the helicopter, has a resonance near a major helicopter forcing frequency. Major helicopter forcing frequencies lie between 4 and 60 Hz. Most black boxes have no resonant frequencies below 100 Hz. Thus, even though the MIL-STD-810C test does not force helicopter-equipment compatibility, compatibility does exist for black boxes.

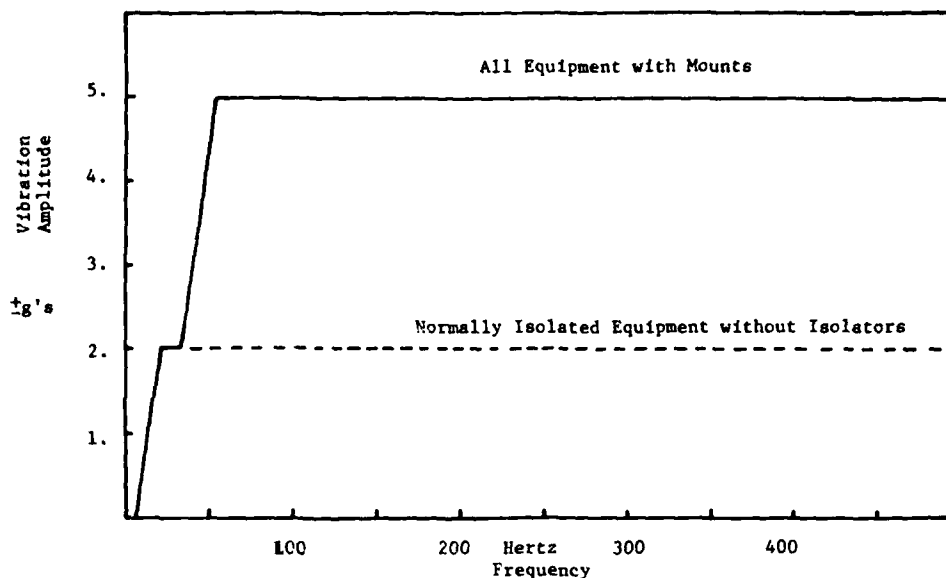


Figure 3 MIL STD-810 B and C Sine Sweep Test

Any item whose performance is structural dynamically sensitive and/or strength requirements/weight sensitive to structural dynamics should receive proper consideration in the design phase to the structural dynamics of the aircraft or aircrafts it will fly on. Qualification to MIL-STD-810C vibration requirements does not do that. In addition such qualification ignores the normal real world flight equipment development cycle of design, test, flight test, redesign, more flight test, production readiness, and then production.

3. THE TADS/PNVS DEVELOPMENT PROGRAM

The Target Acquisition Designation System (TADS) and Pilot Night Vision Sensor (PNVS) are mounted on the nose of the AH-64 Advanced Attack Helicopter (Figure 4). Hughes Helicopters, Inc. (HH) is the prime contractor for AH-64 development and also has system integration responsibility for the AH-64 fire control system. The TADS/PNVS is to be supplied CFE to Hughes. The AH-64 has a four bladed articulated main rotor and a set of 2 two bladed teetering tail rotors. The TADS consist of an optical sensor, a TV sensor, A Forward Looking Infrared Sensor (FLIR), a laser Range Finder Designator and a laser spot tracker all mounted on a closely packed servo controlled four gimbal stabilized platform which isolates these sighting systems from helicopter vibration inputs and compensates for linear and angular motions of the helicopter. The primary structural dynamic design considerations were; the placement of any installed system resonances away from AH-64 forcing frequencies, stabilized platform stiffness to minimize relative displacement between sensors and stabilization servo-system feedback elements, and the avoidance of platform resonances that would impact the stabilization servo system (See Reference 6 for a discussion of the related problem of designing Sights to be mounted above the helicopter rotor).

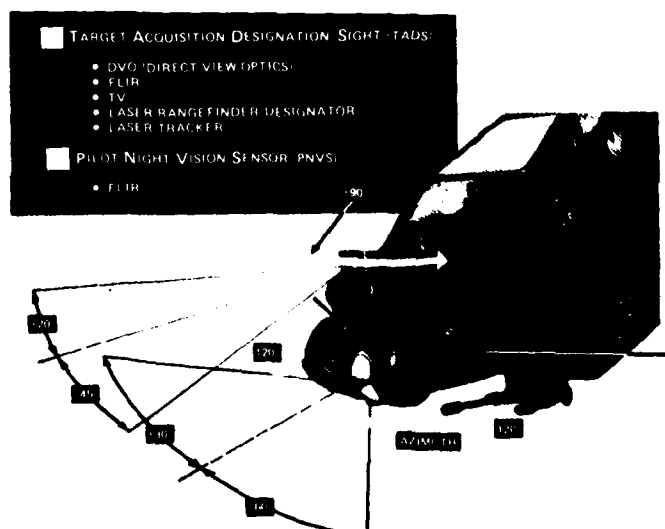


Figure 4 Target Acquisition Designation System/Pilot Night Vision System (TADS/PNVS)

The TADS/PNVS competitive development began in 1977 with Martin Marietta and Northrop as competing contractors. Both were given contracts to build flightworthy systems which would be competitively evaluated in flight tests.

A very limited flight test was conducted on an early AH-64 prototype to define a vibration specification to go into the Prime Item Development Specification (P.I.D.S.), and to which the competing TADS units would be designed to perform to System Level Specifications (target detection, acquisition, and designation ranges). Instrumentation consisted of linear and angular triaxial accelerometers mounted on the nose of the AH-64. A data record was taken at a 130 knot flight condition and spectrum analysis was performed from 0 to 200 Hz with a 10 Hz bandpass. Spectrum based on this analysis were included in the P.I.D.S. (Figure 5). Both AVRADCOM and HH realized that this was not the definitive description of the vibration environment on the AH-64 nose. However, it was considered to be a good design goal since this was an early prototype aircraft with special emphasis to be given during aircraft development to reducing the overall aircraft vibrations, especially at the crew seat and consequently at the aircraft nose. The original contractual requirement for vibration qualification testing of the TADS/PNVS bulkhead mounted equipment was based on Method 514.1 category C of MIL-STD-810B and consisted of both one hour of sinusoidal sweeps per axis and four 30 minute dwells per axis at AH-64 forcing frequencies and 810B levels. This test was to be performed prior to first flights. Early in the competitive program the Army, Hughes Helicopters, and both competing contractors agreed that this particular qualification test was inappropriate because the test did not represent the true helicopter vibration environment and might therefore force unnecessary design changes, some of which might degrade system performance, and "use up" or destroy a useful flight test article. Consequently, the Army constructed a limited environmental vibration qualification test to be conducted prior to first flight that would substantiate system performance and prove airworthiness (Table 1). The 3 waveforms applied as test Level 1, system operational, were based on the P.I.D.S. vibration levels. System Stabilization performance was measured during this part of the test so that specification performance could be evaluated. The Level 2 and nonoperating waveforms were derived from flight test data acquired up to that time on two AH-64's with aerodynamically representative mock ups of the competitor's TADS mounted on each. Level 2 represented the worst case vibration environment under which the TADS could be expected to be used. Stabilization performance was evaluated during the Level 2 portion of the test. The nonoperating levels represented the worst case vibration environment that the units would experience during flight. Performance was evaluated pre and post test. No degradation was allowed. The vibration qualification test of the TADS/PNVS turret was delayed until the single contractor maturity phase of the program.

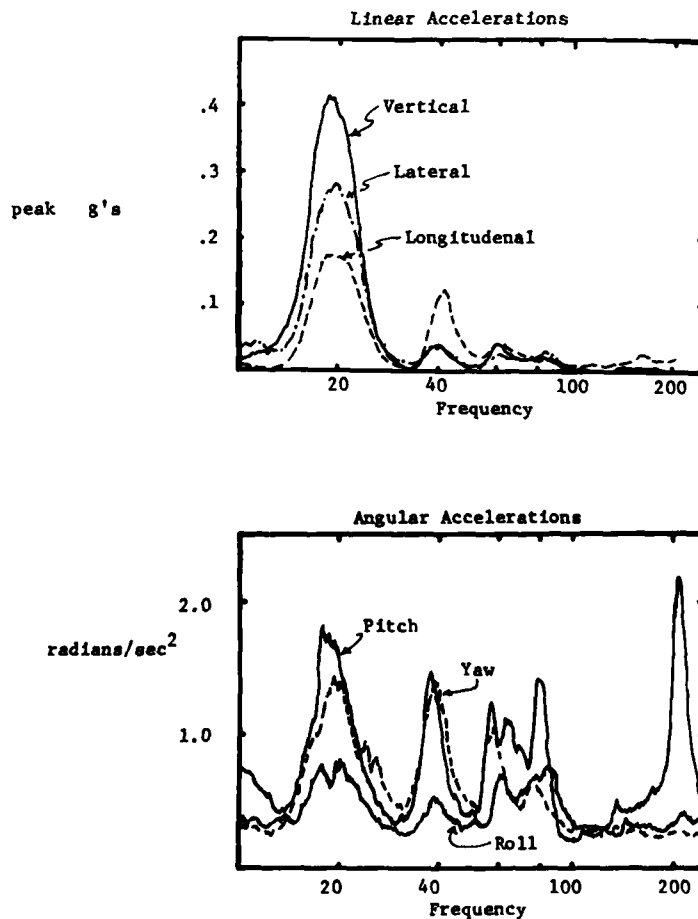


Figure 5 TADS/PNVS Vibration Performance Specification

TABLE I
TADS/PNVS LIMITED ENVIRONMENTAL
VIBRATION TEST

Input Component Frequency	Vertical, g			Longitudinal, g			Lateral, g		
	Level 1 OP.*	Level 2 OP.	Non- OP.	Level 1 OP.	Level 2 OP.	Non- OP.	Level 1 OP.	Level 2 OP.	Non- OP.
4.4 Hz	0.08	0.1	0.35	0.035	0.05	0.15	0.06	0.08	0.26
14.4	--	0.94	0.35	--	0.04	0.15	--	0.07	0.23
19.3	0.42	0.3	1.65	0.18	0.39	0.69	0.28	0.71	1.24
38.5	0.04	0.12	0.53	0.13	0.94	1.64	0.05	0.38	0.66
58.0	0.04	0.06	0.21	0.04	0.12	0.21	0.03	0.09	0.16
77.0	--		0.11	--	0.06	0.11	--	0.06	0.11

*OP Operating

Test duration 15 minutes per axis, each level.

Extensive flight vibration surveys prior to the competitive TADS/PNVS fly-off on the two prototype AH-64's with the associate contractors' TADS installed on their respective aircraft were conducted for the following purposes:

- a) To obtain design information so that the associated contractors could optimize their systems prior to the TADS/PNVS fly-off.
- b) To determine if there were significant differences in the induced vibration environments between the prototypes that would affect the results of the fly-off.
- c) To obtain the vibration information necessary for updating the TADS/PNVS P.I.D.S. for the maturity phase of the TADS/PNVS development.
- d) To obtain the vibration data necessary for constructing a realistic maturity phase environmental vibration test.

Any system whose performance is sensitive to aircraft vibration levels will greatly benefit from such a survey followed by a system optimization period prior to formal systems evaluation. Consequently, if the System Developer Program Manager is technically responsible and/or if the development program is properly structured initially, then the information necessary to construct a realistic vibration qualification test will be available in the development cycle. Guidelines for constructing the qualification test, eventually named the Life Cycle Vibration Qualification Test, were formulated by AVRADCOM and agreed to by both Hughes Helicopters and the two competing associate contractors. These guidelines were based roughly on standard helicopter fatigue methodology (Reference 2). The guidelines were as follows:

The TADS PNVS turret vibration qualification test will be constructed based on the AH-64 System Specification Flight Spectrum (Table II) and flight test measurements. For each important frequency in each direction there will be an agreed to vibration level. The level will be based on the worst case measurement of, or projection for each flight condition or load factor in the table. The following conservative factors will be applied to the agreed to levels:

- a) A quadrupling of spectrum time because only one item will be tested.
- b) A 1.25 multiplier to each level to account for aircraft differences.
- c) A single axis multiplier to each level. This factor being defined as the ratio of the magnitude of the resultant to that of the largest of its vertical, lateral, or longitudinal components and compensates for single axis testing versus multiple axis aircraft excitation.
- d) A Goodman correction in the vertical direction to account for the absence of the load factor induced steady stress during each maneuver.

TABLE II
AH-64 SYSTEM SPECIFICATION FLIGHT
SPECTRUM

Maneuver Spectrum			Level Flight Spectrum		
Load Factor	Minutes at Load Factor	Minutes Gunfire	Flight Condition	Minutes X10 ³	Minutes Gunfire
3.00 g	3		.5 V _H *	6.92	
2.75	10		.6	13.83	
2.50	28		.7	34.59	
2.25	93	1	.8	34.59	
2.00	333	2	.9	34.59	
1.75	1,000	7	1.0	23.06	1,300
1.50	3,333	23	1.2	6.92	
1.25	30,000	540	Sideward & Rearward	16.14	
.75	4,200				
.50	373		HOGE*	53.03	
.25	42		Ground Conditions	6.93	
.00	7				
	<u>657 hrs</u>			<u>3,843 hrs</u>	

V_H Level Flight Speed at Maximum Continuous Power

HOGE Hover Out of Ground Effect

After all levels have been agreed upon and all conservative factors have been applied, the long time low levels can be collapsed to short time higher levels by use of the S/N curve shape of the material in the system with the worst fatigue properties. The time reduction to be applied is based on the sum of the amplitudes of the different frequency components at each condition as shown in Figure 6. Cyclic load application shall be assumed to occur at 19.2 Hz (main rotor 4 per revolution frequency). After appropriate test levels and times have been agreed to the levels will be combined into a complex periodic input such as in Table III where the phase relationships of the different harmonics are constantly changing (Reference 2).

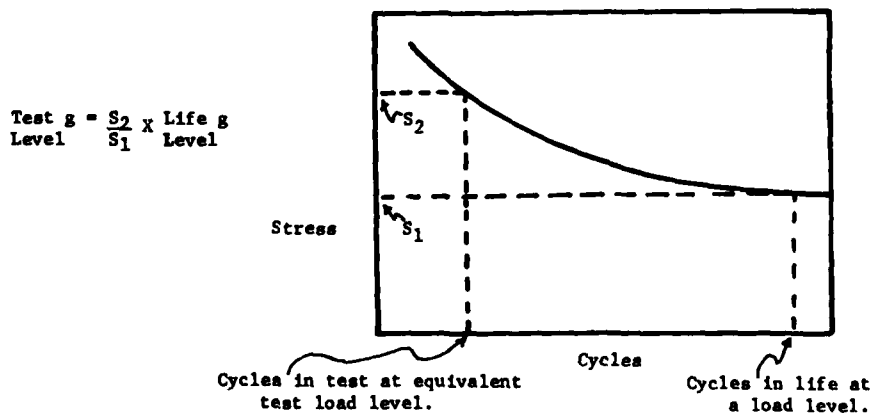


Figure 6 Test Time and g Level Adjustments Using a Typical S/N Curve

TABLE III
TADS/PNVS LIFE CYCLE VIBRATION
QUALIFICATION TEST

Input Component Frequencies	Vertical		Lateral		Longitudinal	
	W/O G.F.	W/G.F.*	W/O G.F.	W/G.F.	W/O G.F.	W/G.F.
MR 1/rev* 4.8 Hz	.32 g	.32	.1	.1	.03	.03
Gunfire 12.0 Hz	-	Pulse	-	Pulse	-	Pulse
MR 3/rev 14.4 Hz	.09	.09	.2	.2	.04	.04
MR 4/rev 19.2 Hz	1.56	1.56	2.02	2.02	.36	.36
TR 1/rev 23.6 Hz	.11	.11	.13	.13	.06	.06
MR 8/rev 38.4 Hz	.46	.46	.16	.16	.37	.37
MR 12/sec 57.6 Hz	.12	.12	.05	.05	.24	.24
Test Time - Hrs.	1.78	1.1	0.45	0.2	1.0	1.4

* G.F. Gunfire

MR 1/rev Main Rotor Rotations per second

MR 4/rev 4 times Main Rotor Rotations per second

TR Tail Rotor

Martin Marietta won the competitive fly-off and was awarded the maturity phase development contract. negotiations have lead to three structural dynamic considerations as follows:

- Vibration levels to which the system was to perform to system level specifications (target detection, acquisition, and designation ranges) were dropped. Instead, Martin agreed to meet system level specifications within the flight operating envelope of the weapon systems. The original P.I.D.S. vibration design levels proved to be quite representative of the vibration levels within the weapons firing envelope and the contractor bettered the stabilization goal in his total error budget by a good margin.
- A reduced version of the Limited Environmental Test (LET) was incorporated into the production verification testing to be performed on every delivered unit. The LET proved to be a valuable aid in ferreting out workmanship defects in the development units prior to installation on the aircraft. Units that underwent LET testing prior to flight test proved far more reliable than those that were flight tested without LET testing.
- Electronic Components not mounted on the AH-64 nose, which consist of "black boxes" mounted in the aircraft avionics bays, were to be qualified to the MIL-STD-810C, 5 to 500 Hz, 5g sweeps.

The Life Cycle Vibration Qualification test for the Stabilized Turret System described in Table III was adopted. The test was developed based on the above AVRADCOM guidelines.

4. THE SOTAS DEVELOPMENT PROGRAM

The Stand-off Target Acquisition System (SOTAS) is designed to detect slowly moving ground or near ground targets such as armored columns or helicopters at long stand-off ranges in a severe radar jamming environment and to provide the target movement information in near real time to battlefield commanders. The system consists of a modified UH-60 BLACK HAWK designated the EH-60C built by Sikorsky Aircraft and a radar antenna with an extension retraction pedestal and an equipment rack built by Motorola (Figure 7). The aircraft main landing gear has been modified to retract a total of 45 inches in-flight. The antenna then extends about 21 inches from its stowed position beneath the belly of the aircraft. The antenna is then free to rotate through a full 360 and perform its target acquisition function. The heart of the antenna is an 18 ft reflector that handles an array of radar feed horns and must allow only small elastic deformations under the influence of aircraft

vibrations in order to achieve the desired anti-jamming performance. The total system error budget allows only .01 inches relative deflection, due to aircraft vibration, across the 18 ft reflector. The mission requires the antenna to perform primarily between 60 and 80 knots airspeed with mild helicopter maneuvers, which is the flight regime where helicopter vibrations are at a minimum.



Figure 7 SOTAS Airborne System Suspended Shake Test

Sikorsky and Motorola were designated as co-equal prime contractors for the airborne equipment with Sikorsky responsible for the helicopter modifications and Motorola responsible for the antenna, pedestal, and equipment rack. AVRADCOM was asked to provide airworthiness requirements for the system and to provide those requirements necessary for a successful interface between the two primes. The AVRADCOM structural dynamic requirements were based on prior helicopter store development program experience (References 2 & 5) and TADS/PNVS experience and include:

- a) A fairly stringent requirement on allowable aircraft vibration at the helicopter floor-pedestal interface that went into the Sikorsky EH-60C specification. This was to make the airframe manufacturer responsible for providing an acceptable operating environment for the radar system.
- b) A requirement in the Motorola specification that the antenna-pedestal and the equipment rack have no as-mounted to the helicopter resonant frequencies of major modes near helicopter forcing frequencies. The helicopter forcing frequencies are usually well defined. Fulfillment of this requirement assures dynamic compatibility between radar and aircraft. It minimizes total system vibration amplitudes and consequently helps the airframe manufacturer meet his vibration requirement and the radar manufacturer meet his system level performance requirements.
- c) A requirement on Motorola that the antenna-pedestal structure have a fatigue life equal to the total life expectancy of the system, in this case, 20,000 hours. The AVRADCOM position was that the SOTAS antenna might well be fatigue critical since it is to operate in both a helicopter induced oscillatory load environment and has its own rotating antenna produced oscillatory loads. This fatigue life requirement was to replace any proposed system level vibration qualification test. Although a fatigue life requirement is much more expensive to comply with than a total system vibration test, (i) it assures structural compatibility between radar and airframe, (ii) it allows for proper structural weight optimization, (iii) it guarantees that the radar structure will last the life of the aircraft system (therefore, perhaps greatly reducing life cycle cost), (iv) and it precludes unnecessary and perhaps counter productive design changes often forced on a contractor who is made to comply with an arbitrary vibration test.
- d) A requirement that all electronic components (black boxes) pass the MIL-STD-810C vibration test.

The airworthiness qualification program was structured to call for close cooperation between contractors and includes:

- a) Interfacing the two contractors' mathematical models (NASTRAN) during the design phase to assure system freedom from improper resonances and also to do forced response studies to evaluate system performance in the specified aircraft vibration environment.
- b) Suspended shake tests of the airborne system to determine actual system structural dynamic properties. The shake test is also the proper place to try out fixes to potential problems prior to flight.

- c) A flight loads and vibration survey of a full scale structural dynamic model of the antenna-pedestal prior to full up radar system flight tests.
- d) A single article antenna-pedestal fatigue test based on flight loads measurements.

5. CONCLUSIONS

The helicopter vibration environment is complex periodic in nature. This provides unique opportunities for the equipment designer to minimize equipment helicopter interface vibration amplitudes and consequently optimize system performance.

Development programs for systems whose performance is sensitive to vibration should be structured to optimize interface dynamics.

Dynamic qualification techniques are available that make this possible. These may include life cycle vibration qualification tests based on early program flight test data or structural fatigue tests and electronics component level vibration testing.

6. REFERENCES

1. Waymon, G.R., Tucker, P.V., Frost, W.C., "Captive Carriage Vibration of Air to Air Missiles on Fighter Aircraft, Journal of Environmental Sciences, Sep/Oct 78
2. Crews, S.T., "Helicopter Component Environmental Vibration Testing - The Poor Man's Fatigue Test-", Presented at 35th Annual Forum of the American Helicopter Society, May 1979
3. Laing, E.J., "Instrument Panel and Avionics Compartment Environmental Survey Production OH-58A Helicopter", AVSCOM Project No. 70-15-1, September 1972
4. Bramwell, A.R.S., "Helicopter Dynamics", Wiley, 1976, pages 345-350
5. Schrage, D.P. and Lutz, R.H., "Environmental Vibration Testing of Helicopter Stores and Equipment to the Procedures Outlined in MIL-STD-810C", May 1978
6. Schrage, D.P., "Review of Helicopter Mast Mounted Sight (MMS) Base Motion Isolation and Line-of-Sight (LOS) Stabilization Concepts", 7th European Rotorcraft and Powered Lift Aircraft Forum, Sep 81

APPROACH IN DYNAMIC QUALIFICATION
OF LIGHT HELICOPTER STORES AND EQUIPMENTS

by

D. Braun and J. Stoppel

Messerschmitt-Bölkow-Blohm GmbH
Postfach 801140
8000 München 80, Germany

SUMMARY

This paper demonstrates problems occurring in connection with the dynamic qualification of equipment and external stores for light military helicopters. Special features of the helicopter vibratory environment are discussed. Some general recommendations for the procedure of dynamic qualification for use with helicopters are given.

An approach in dynamic qualification of relatively heavy equipment is presented using the example of combining the MBB BO 105 helicopter with HOT anti-tank missile launchers. To obtain a basic understanding of the dynamic behaviour of the helicopter with external stores, during the design phase, preliminary dynamic calculations are made for the isolated stores. The results are compared with the qualification requirements, to influence the final design. Shake tests are done with the separated external stores. The experimental results are introduced in the dynamic calculations to obtain more realistic information about natural frequencies and response characteristics of the total system, helicopter plus external stores, with regard to the harmonic main rotor excitation. Flight test vibration measurements conclude the dynamic qualification.

1. INTRODUCTION

The dynamic behaviour of a rotary wing aircraft is characterized - in contrast to a fixed wing aircraft - by the existence of discrete vibration peaks at fixed well known frequencies. This typical vibratory spectrum is caused by the dynamical system of the helicopter, consisting of main and tail rotor, several gearboxes, driveshafts, and engines. All these components rotate with different but nearly constant speeds. The excitation which is responsible for the most severe vibrations has its origin in the main rotor and is conditional upon the helicopter flight principle itself. The nonuniform air flow through the main rotor in forward flight produces periodically variable air loads on the rotor blades leading to sinusoidal excitation forces and moments at the rotor hub. These rotor vibratory loads consist of so-called "number-of-blades" harmonic components with the frequencies $n\Omega$, $2n\Omega$, etc., where n is the number of rotor blades and Ω the rotor rotational speed. In general, the $n\Omega$ harmonic is the predominant helicopter excitation. In consequence, it is an important task for the dynamicist to avoid natural modes of helicopter equipment close to these main excitation frequencies.

Another special feature of the helicopter is that equipment and external stores which are heavy in relation to the structural weight of the fuselage may considerably change existing vibration modes locally or as a whole. Therefore, in many cases, the dynamic qualification for relatively heavy equipment cannot only be treated separately, in particular for light helicopters. On the contrary, additional theoretical as well as experimental work has to be done, with equipment and external stores respectively, as a part of the helicopter structure. The purpose of the present paper is to demonstrate the problems occurring with the dynamic qualification of heavy equipment at the example of the HOT anti-tank missile launchers used with the PAH-1 helicopter.

2. SPECIAL FEATURES OF HELICOPTER VIBRATORY ENVIRONMENT

As mentioned in the introduction, the vibratory loads in a helicopter fundamentally differ from those in other aircraft. In the main, in a rotary wing aircraft, the designer is concerned with severe vibrations at a few significant excitation frequencies below 100 Hz. In Fig. 1 a typical vibration spectrum of the BO 105 helicopter is shown. Naturally, there also exist higher disturbing frequencies, as for example the tooth frequencies of the gear wheels which, however, play a minor part. In most cases, the main problem consists in isolating equipment from high-level low-frequency vibration loads which vary with the individual helicopter types. Due to the extremely light construction of the fuselage, it is easy to understand that rotor excitations are transmitted to various points of the helicopter very differently. Hence, the vibrational loading of equipment depends strongly on the installation place which is nearly always determined by priority operating reasons. Therefore, in many cases special vibration isolating or vibration absorbing provisions have to be taken. As a rule, by applying such precautions, problems which are connected with higher-frequency vibrations are no longer to be expected.

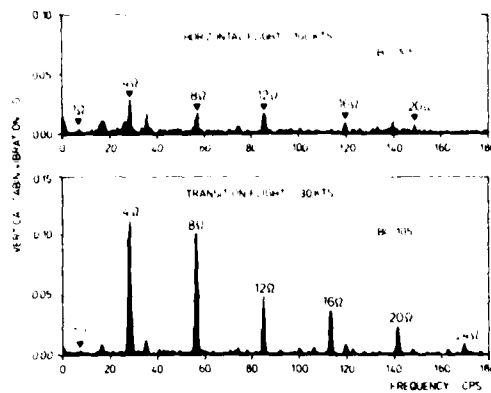


Fig. 1 Typical vibration spectrum of BO 105 helicopter

With respect to the environmental loads which have to be born and thus also with respect to the vibratory loads, equipment which is provided for installation in a helicopter is usually qualified according to well defined standards. Applicable test methods are summarized in sufficiently known prescriptions such as the American MIL-STD-810 or the French AIR NORME. Among others, in these catalogues of test procedures, one requires the simulation of appropriate vibration loadings for the isolated equipment in the laboratory by use of a shaking table. The test conditions and, in particular, the excitation levels depend on excitation frequency, weight of the test specimen, installation position and type of suspension in the aircraft. From our experience, excepting certain restrictions, these standardized qualification methods are well suited for light equipment, such as indicating instruments and other electronic devices. This is particularly valid when vibration isolating suspensions are applied.

It is obvious that devices which are provided for use with helicopters should not have any natural frequencies in the range of the well known main excitation frequencies. However, particularly for relatively heavy built-in or built-on equipment, it is in many cases extremely difficult to fulfil the requirements of the above-mentioned standards within the low-frequency range. In the critical range containing the dominating first "number-of-blades" harmonic excitation, the permitted acceleration values of 2 g are reached or even exceeded in a lot of helicopters, especially at unfavorable installation places. The high-frequency range (frequency range to be tested: 5 - 500 Hz and 5 - 2000 Hz respectively) is essentially relevant only to members, such as plug connections, electronic plate assemblies, etc., where resonance dwell tests, as required among others by MIL-STD-810B and AIR NORME 7304, certainly dictate a severe examination for the test sample. It is open to question, whether resonance dwell tests are sensible in any case or whether, instead of these, dwell tests at the predominant helicopter blade passage frequencies are to be preferred [1]. Compared with edition B, MIL-STD-810C does not include resonance dwell tests for helicopters. In addition, edition C makes a distinction between helicopter built-in equipment and external stores. Dwelling at the helicopter typical excitation frequencies, however, is specified at least for external stores. Often, it would be advisable to perform similar dwell tests with equipment such as a roof mounted sight, for example [2].

Naturally, the dynamic qualification of the isolated equipment by use of a vibration exciter is meaningful, but according to our experience, in many cases not sufficient. For example, installing equipment whose mass amounts to about 5 - 20% of the pure structural weight in a light helicopter is common and frequent practice. Such heavy equipment may significantly change existing vibration modes locally or of the whole fuselage, depending where it is connected to the helicopter structure. In this manner, the severe helicopter specific basic excitation is, in most cases, further increased for equipment and external stores. For these reasons, it may be necessary to perform, in addition to a shake test of the isolated equipment, more extensive theoretical as well as experimental investigations with the combination, equipment and carrier. In the following chapter, a corresponding approach using the example of a pylon for external stores is presented.

3. EXAMPLE OF A DYNAMIC QUALIFICATION PROCEDURE FOR HEAVY EXTERNAL STORES

The problems which the dynamic qualification of relatively heavy equipment raises, in connection with light helicopters, are demonstrated in the following, by the example of the pylons for the HOT missile launchers of the BO 105 P (PAH-1) helicopter. As is seen in Fig. 2, pylons which can be armed with a battery of three HOT anti-tank missiles each, have been attached to both sides of the aircraft. The loaded launchers, originally designed for use on ground restricted vehicles, have a mass of about 150 kg each and weigh therefore, for example nearly twice as much as the engines. The design of the pylons and their hinged mounts in the area of the floor structure of the fuselage has been essentially based on static aspects. It is easy to understand, however, that the attachment of such large masses at such exposed places might influence the vibratory behaviour of the whole helicopter. For this reason, besides the obvious requirement that the isolated launchers have

no resonance points close to the main excitation frequencies, the dynamics of the total system, helicopter plus external stores, have to be considered with care.



Fig. 2 BO 105 P (PAH-1) helicopter

3.1 DYNAMIC QUALIFICATION OF SEPARATED STORES

The dynamical qualification of the launcher itself has been done according to the French AIR NORME 7304. For that, the launcher was fixed on a shaking table in a similar manner to its mounting on the pylon and has been subjected to the tests listed below, in the frequency range between 5 Hz and 500 Hz:

1. Resonance search
2. Sinusoidal cycling (2.5 hrs along each axis)
3. Resonance dwell (20 min along each axis at the most severe resonant frequencies)
4. Noise like excitation.

The excitation for points 2 and 3 has been set according to Fig. 3.

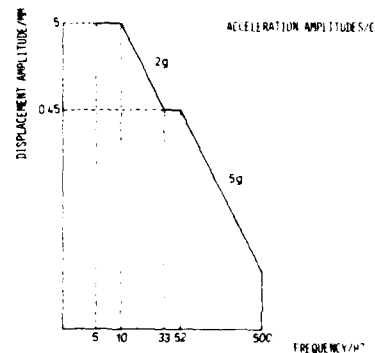


Fig. 3 Vibration test curve (AIR NORME 7304)

3.2 NATURAL MODES OF ISOLATED PYLON AND STORE ASSEMBLY

During the design phase of the pylon a first dynamic structural calculation has been performed for the combination, pylon plus launcher. Complicated structural components require an idealization with correspondingly capacious details. In many cases, however, it is more practical to choose a more simple model for such parts, which is sufficient to enable only the most important deformations to be calculated. The result of this rough estimation was that the natural frequencies for the first modes of the isolated ramp, complete with three HOT missiles, were adequately below the dominant 4/rev excitation frequency, that is, that the design of the pylon could be realized without any modification.

The next step was the manufacture of the first prototype of the pylon. The vibration behaviour of the isolated clamped ramp has been investigated experimentally by shake tests with impulse excitation in the vertical and horizontal plane. The frequency analysis of the measured accelerations yielded natural frequencies of 16.5 Hz for the first vertical vibrational mode and 22.3 Hz for the first longitudinal vibrational mode. These measured values have been used as a base for correcting the input data of the theoretical model of the pylon. Repeated calculations using the same boundary conditions as in the experiment have proved the validity of the assumptions made for the idealization of the ramp (Fig. 4).

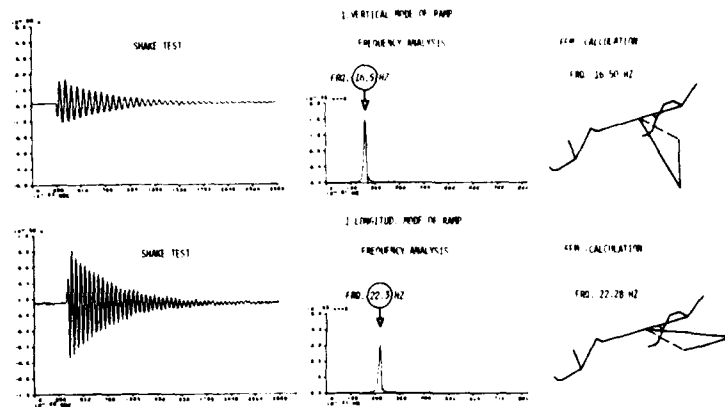


Fig. 4 Shake test and finite element calculation of clamped ramp

3.3 COMBINATION OF EXTERNAL STORES AND HELICOPTER STRUCTURE

Theoretical Model of Helicopter Structure

Fuselage and heavy equipment or external stores form a unit with mutual influences on each other. Therefore, as pointed out previously, it is absolutely necessary to investigate the dynamical behaviour of the launchers attached to the helicopter structure. At first, this was done theoretically by integrating the adapted model of the pylon in the finite-element-model (FEM) of the PAH-1 helicopter.

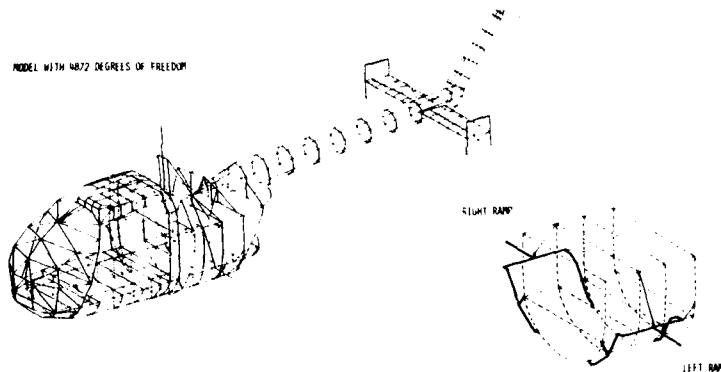


Fig. 5 Finite-element-model of PAH-1 helicopter

The finite-element-model with 4872 degrees of freedom, shown in Fig. 5, considers all the requirements of stress analysis and has been developed for this task. Between this idealization and the hardware exists a nearly one-to-one correspondence. In most cases, such a refinement is not required for dynamic calculations. In our example, the number of degrees of freedom has been reduced to a set of 135 which represents 3% of the original model size. The selection of these degrees of freedom conforms to the natural modes which are of interest in the investigated frequency range. For the proper choice of the analysis set, the possibility that large concentrated masses like the ramps overlaid on a relatively light structure might have a great influence on the complexity of the vibrational modes had to be taken into account.

Here it may be mentioned that the finite element data set used for the PAH-1 helicopter is developed from the data set for the BO 105 helicopter which has been proved experimentally by a modal survey test. Structurally, both helicopters differ only in a few details from each other, such as some modifications of the cabin roof, reinforcement of some fuselage stringers, thickening of the tail boom skin panels, and enlargement of the tail plane. According to our experience, the essential fundamental and higher harmonic modes of the helicopter fuselage can be changed within only narrow limits by structural modifications or installations of additional equipment. Therefore, as a consequence of the structural similarity of the aircraft it is also possible to achieve realistic dynamical results for the PAH-1 helicopter.

A model of this order is only amenable to dynamic calculations by use of special procedures such as the NASTRAN multi-level-substructuring-method (Fig. 6). In our case, the aircraft has been divided into seven substructures or superelements (SE). An additional element has been introduced for the missile launchers. This technique is very effective

for parametric studies of the influences of local structural modifications or locally fastened equipments and external stores on the dynamics of the whole helicopter. After altering a certain device, only the substructures lying in a direct line to the so-called residual structure have to be recalculated (see sketch on the right of Fig. 6). The matrices of the other superelements remain unchanged.

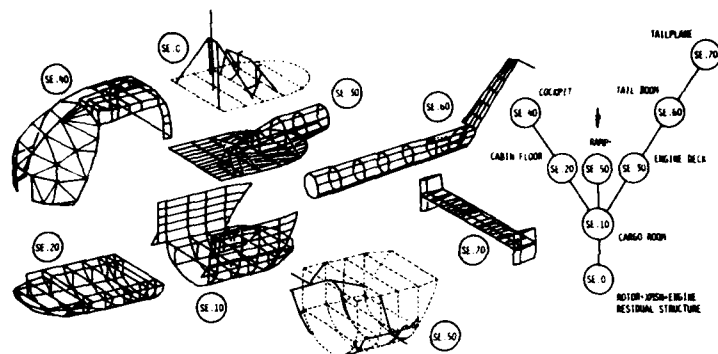


Fig. 6 Substructures of PAH-1 finite-element-model

Vibratory Behaviour of Helicopter Structure in Combination with External Stores

The ramps have been included in the calculation as described above. The natural modes of the pylons coupled with the fuselage structure are shown in Fig. 7. There exist double modes in the vertical as well as in the horizontal plane. These modes where the ramps vibrate in phase and out of phase to each other appear only in connection with the fuselage structure. As a consequence of the flexibility of the attachment points and the elasticity of the fuselage, the natural frequencies have been distinctly reduced in relation to the isolated ramp (Fig. 4).

The next task was to check the positions of the additional modes in the frequency spectrum of the helicopter. In Fig. 8 a survey of the complete natural frequencies and modes respectively up to 30 Hz is given. On the left side, the results of the finite element calculation for the PAH-1 helicopter, with and without ramps, are tabulated. For comparison, corresponding results from calculation and modal survey test for the BO 105 helicopter are recorded on the right side. For more details see [3]. Regarding the table one can see that the fundamental pitching and lateral modes of the fuselage are close to the rotational speed of the main rotor. Higher modes of the fuselage lie near the 4/rev frequency. In between, a set of natural modes appears which are dominated by certain parts of the helicopter, such as engines,

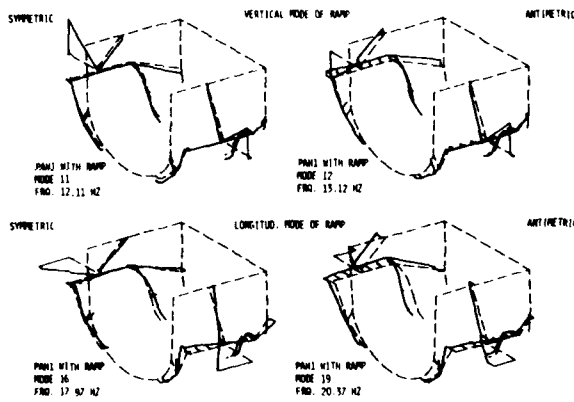


Fig. 7 Natural modes of ramps combined with helicopter structure

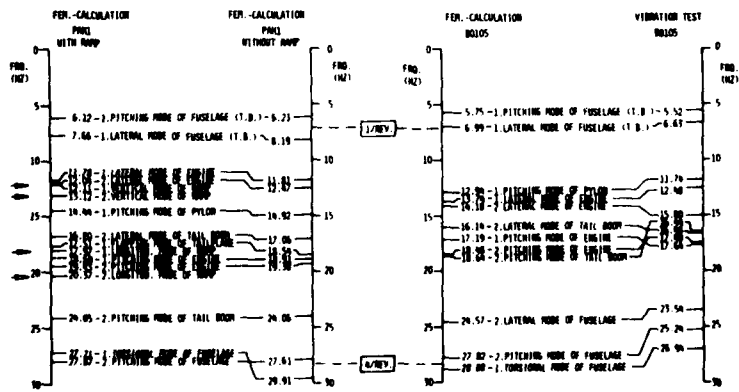


Fig. 8 Natural frequencies and modes of PAH-1 and BO 105 helicopter

rotor-transmission unit, tail boom, stabilizers, and also the missile launchers (marked by arrows).

The modes caused by the ramps are located sufficiently away from the dominant excitation frequencies. From this point of view, any modification of pylon stiffness or mounting attachment was not necessary.

Two normal fuselage modes appear in the most critical region near the dominating 4/rev rotor excitation:

2nd pitching mode of fuselage,
1st torsional mode of fuselage.

These two modes of the PAH-1 helicopter with and without ramps are demonstrated in Figs. 9 and 10. Additionally, a comparison between calculated and measured results for the

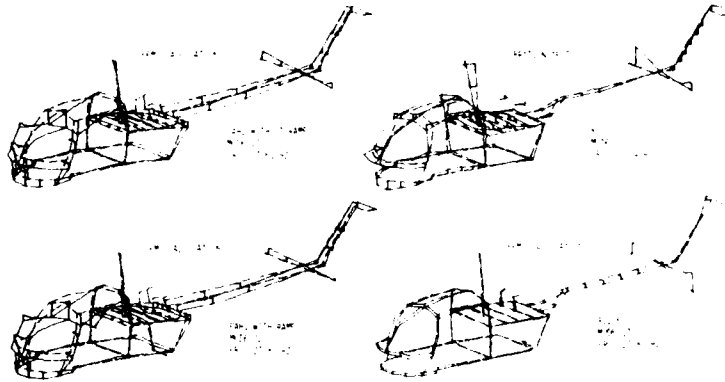


Fig. 9 2nd pitching mode of PAH-1 and BO 105 helicopter

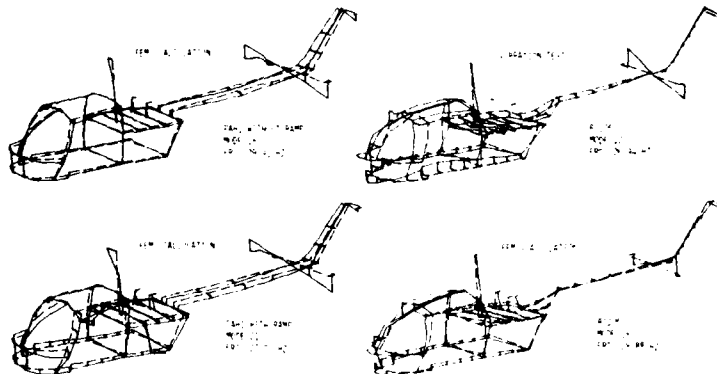


Fig. 10 1st torsional mode of PAH-1 and BO 105 helicopter

BO 105 helicopter is again shown. As expected, good agreement occurs between the mode shapes of the various versions. It is not difficult to understand that the natural frequency for the 2nd pitching mode is hardly influenced by the missile launchers. Due to the outriggering heavy weights of the launchers, however, the calculated natural frequency for the torsional mode has been distinctly shifted towards the 4/rev frequency of the main rotor.

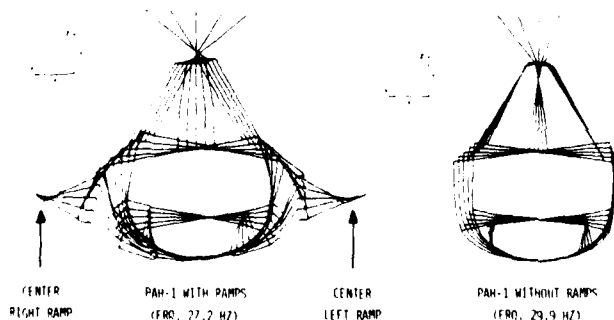


Fig. 11 Cross-sectional mode shapes of PAH-1 helicopter with and without ramps

From Fig. 8 we can learn that for the BO 105 helicopter the measured natural frequencies of the considered modes lie at about 2 Hz below the calculated values. Assuming that this fact is also true for the PAH-1 helicopter the vibratory behaviour of the aircraft with external stores would be more favourable than that of the basic helicopter.

The oscillatory motions in the case of the torsional mode are illustrated in Fig. 11 by means of cross-sections of the fuselage in the ramps area. In both cases, with and without ramps, the helicopter vibrates torsionally about the longitudi-

nal axis. The missile launchers oscillate out of phase to the fuselage which results in a nodal point in the center of each ramp.

At this point, it would have been advisable to examine by a finite element response calculation for several loading configurations of the launchers to what extent these two modes can be excited by realistic 4/rev main rotor forces and moments. In this way, vibration levels at the launchers can be predicted in an early design stage. Because of other than technical reasons we were not able to do such response calculations in the present example.

Vibration Flight Test Results

Concluding the dynamic qualification procedure for the PAH-1 HOT launchers, vibration measurements have been performed at different flight conditions. Some features of the PAH-1 flight tests with ramps in level flight are shown in Fig. 12: amplitudes and phase

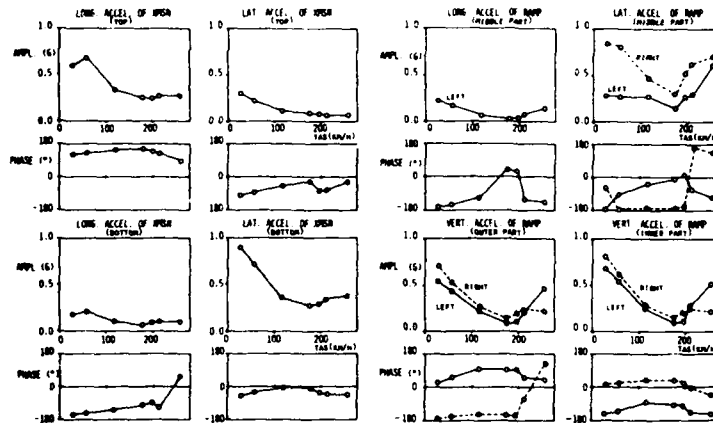


Fig. 12 Flight test vibration measurements for PAH-1 helicopter with ramps

angles of the interesting 4/rev acceleration components at several measuring points of main gearbox and ramps. Maximum vibration levels occur in transition flight (20-30 kts).

In the entire horizontal flight range, the 4/rev acceleration components do not exceed the 1 g limit. Thus, the qualification requirements based on the AIR NORME 7304 have been met. In Fig. 13 an attempt is made to show for the torsional mode a correspondence between the FEM-eigenvalue computation and the flight test measurements by qualitatively contrasting the mode shapes of the fuselage cross-section in the ramps area as a component representation. This is admissible with some restrictions since the natural frequency for the considered mode is located close to the 4/rev excitation frequency. Some correlation has been obtained in particular in the case of the vibratory motion in the vertical plane.

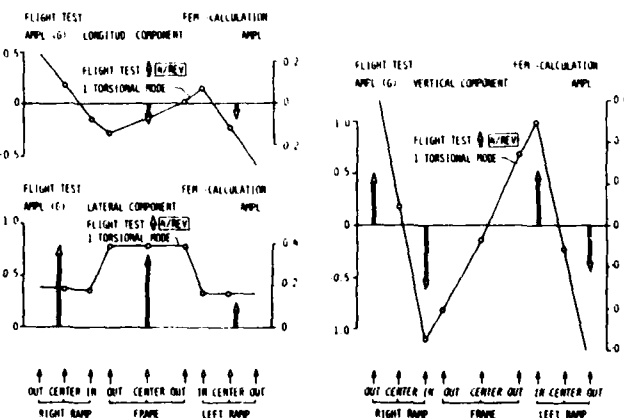


Fig. 13 Fuselage cross-section of PAH-1 helicopter: comparison between flight test and FEM-calculation

4. CONCLUDING REMARKS

The vibratory load in a helicopter is characterized by high-level sinusoidal excitations at a few discrete frequencies. This low-frequency vibration load has its origin in the main rotor and is caused by the nonuniform air flow through the rotor in forward flight. In general, the first "number-of-blades" harmonic is the predominant helicopter excitation. Compared with this harmonic, other existing higher disturbing frequencies are negligible in many cases.

Dynamic qualification by use of sinusoidal cycling, dwell tests, etc., following well introduced standards is a common practice. However, it is often difficult to meet the requirements of these standards within the low-frequency range.

In particular heavy equipment and external stores may significantly influence the vibrational behaviour of the adjoining parts of the structure or even of the whole fuselage. Thus, the severe basic vibratory loading of a helicopter is increased in most cases. In addition to laboratory vibration tests with the separated equipment, more extensive investigations have to be done with helicopter and equipment as a unit.

The presented example of the approach in design and dynamic qualification of the HOT anti-tank missile launchers for the PAH-1 helicopter does not claim to be a universally valid procedure, but it gives at least an idea of the problems which may occur in combining heavy equipment with a light helicopter. In that special case, the requirement for a 2 g acceleration limit for the 4/rev excitation could be met. Fundamentally, for many applications, it would be desirable to increase the admissible vibration levels in the low-frequency range and, in general, to replace resonance dwell tests by dwell tests at the individual main excitation frequencies. With MIL-STD-810C a good step has been made in this direction by allowing a 3 g vibration level for external stores in connection with the UH-1 helicopter.

REFERENCES

1. R.H. Volin, MIL-STD-810C Panel Session.
A. Piersol The Shock and Vibration Bulletin 45, Part 2, June 1975
2. D.P. Schrage, Environmental Vibration Testing of Helicopter Stores and Equipment
R.H. Lutz to the Procedures Outlined in MIL-STD-810C.
Presented at the 34th Annual National Forum of the American Helicopter Society, Washington, D.C., May 1978
3. J. Stoppel, Investigations of Helicopter Structural Dynamics and a Comparison
with Ground Vibration Test.
Presented as Paper 12 at the 6th European Rotorcraft and Powered Lift Aircraft Forum, Bristol, U.K., September 1980

THE DYNAMIC QUALIFICATION OF
EQUIPMENT AND EXTERNAL STORES
FOR USE WITH ROTARY WINGED AIRCRAFT

by
G.M. Venn
Dynamics Department
WESTLAND HELICOPTERS LIMITED
Yeovil
Somerset
BA20 2YB

SUMMARY

The paper outlines the dynamic regime imposed on helicopter-borne stores and equipment, highlighting the differences between the rotary and fixed-wing environments. The need for helicopter requirements to be addressed in particular is discussed.

The influence of a number of contributory factors to the dynamic environment arising from varying military applications covering both land and sea operation is discussed. The interests of, and implications for WEL as a supplier of helicopters to both UK and Overseas customers are outlined.

The dynamic criteria for design and test currently employed by WEL are given, explaining the particular influence of discrete sinusoidal forcing on the helicopter environment. The evolution of these standards and their consolidation through flight and service experience is described.

The paper concludes by offering some views on the future development of dynamic qualification criteria for rotary-winged aircraft.

1. INTRODUCTION

The vibration environment in helicopters differs from that in jet aircraft by one important feature, the existence of discrete peaks of vibration at fixed frequencies. These peaks are generated by the rotating components in the helicopter, such as the main and tail rotors, engines and gear meshing. The rotor speed under normal flight conditions is essentially constant, varying by only about five percent and therefore these vibration peaks have fixed frequencies.

The vibration spectrum in the cockpit of a four-bladed, medium size helicopter (the Lynx) is shown in figure 1 for a steady forward speed of 140 kts. The lower frequency end of this spectrum is dominated by peaks at multiples of the main rotor passing frequency (4R, 8R etc; 4R = four per main rotor revolution). The peaks at the higher frequency end, above about 400 Hz. are generated by the meshing of gears in the gearboxes (principally the main rotor gearbox) and by the various shafts in, and connected to, the engines.

The relative levels of these peaks differ in various regions of the helicopter depending on the proximity of the sources of the various peaks and the geometry of the aircraft construction. However, the vibration in all regions of the Lynx is dominated by vibration at the four per revolution frequency of the main rotor (4R) at about 21.7 Hz. Regions near the engines and main rotor gearbox also experience significant forcings from these two items.

An obvious requirement for helicopter equipment is the avoidance of natural frequencies at or near to the frequencies of the major vibration peaks in the helicopter vibration spectrum. The frequencies of these major vibration peaks are defined as avoid frequencies. Normally, a narrow frequency band is defined to allow for slight variations in rotor speed and aircraft configuration, and to avoid exciting any major but slightly off-resonant modes of vibration in the equipment. Each type of helicopter will have different frequency avoid bands and depending on the relative levels at the various frequencies in the different areas of each aircraft, different avoid bands can be defined for the various regions.

Since the vibration environment of the equipment is dominated by discrete frequency peaks of vibration, it is logical to use some of these frequencies for endurance testing of the equipment. Normally about four frequencies are chosen for the endurance testing.

Vibration qualification to Westland Helicopters (WEL) standards follows the following sequence:

- a) Initial resonance search,
- b) Endurance tests,
 - i) by frequency sweeps,
 - ii) by discrete frequency tests.
- c) Final resonance search.

The above tests are required for full type clearance. For equipment under development, limited type testing may be required before the start of flight tests and this normally includes parts (a), (bi) and a reduced (bii).

Each type of helicopter is different having different numbers of main rotor blades and rotor speeds which gives the need for specific requirements for each type of helicopter. Especially important are the different frequencies of the avoid bands and endurance tests.

2. DEVELOPMENT OF REQUIREMENTS

Over the past 20 years the qualification requirements of WHL have become more specific. Examples of this development are given below for two types of helicopters, followed by a detailed discussion of the Lynx helicopter in the next section.

2.1 Scout and Wasp Helicopters (1962 Specification)

These aircraft are four bladed light helicopters.

The requirement states that the equipment may be subject to vibration in the range of 5 to 150 Hz. with the amplitudes given in figure 2. This amplitude curve is used for the resonance search, but no requirement is given for the frequency sweep rate. Four frequency avoid bands are given covering the first and fourth main rotor orders, and the first, second and third tail rotor orders. A fixed frequency endurance test is defined using three frequencies covering the fourth main rotor order and the first and second tail rotor orders. It is not mandatory for the equipment to operate during the endurance testing but WHL must be consulted. There is no requirement for a final resonance search.

This single test is required for equipment mounted in all regions of the aircraft. No distinction is made for different vibration levels in the various parts of the aircraft.

2.2 Sea King and Commando Helicopters (1966 Specification)

These two helicopters are large five-bladed aircraft.

The specification recognises the existence of different levels of vibration in the various regions of the helicopter. The original specification covered two regions; within and outside of the power unit region. Updates in 1975 brought in two other regions; externally mounted equipment and panel mounted equipment. Different frequency ranges are specified for each region.

A resonance search is required using curve D of figure 3a for equipment within and outside the power unit region (3-500 Hz. and 3-150 Hz. respectively) or the severe flight curve of figure 3b for externally mounted equipment (3-175 Hz.).

The curves in figure 3a are the same as those in Av.P.970 which was taken from measurements on British and American helicopters. Curve D represents the acceptable limit for the more severe vibrations which may occur during short period flying conditions such as maximum speed or maximum engine power. This curve is similar to that used for the Scout and Wasp helicopters described in the previous section.

Isolated panel mounted equipment is tested at a constant amplitude to ± 1.00 inches up to 16 Hz. followed by a constant acceleration of $\pm 2.5g$ to 150 Hz. Testing in three mutually perpendicular planes is required.

Endurance tests are required covering the fifth and tenth main rotor orders and fifth tail rotor orders in all regions of the helicopter, with the addition of a high frequency test at 400 Hz. for equipment in the power unit region. The equipment is required to operate normally during the testing and at completion of testing to have suffered no damage.

Any equipment which is driven mechanically from the aircraft engine, rotor or transmission may be required to be subject to a torsional vibration test at the frequency of the input shafts.

3. THE LYNX HELICOPTER (written in 1977)

The Lynx specification is more detailed than previous specifications and is based upon major international specifications with additions and modifications by WHL.

The first step needed to write the vibration specification is the determination of the major forcing frequencies. Once the design of the aircraft is known, these frequencies can be calculated and listed on a vibration order chart. An abbreviated chart for the Lynx is shown in figure 4. Many of the frequencies on this chart can be correlated with peaks on the vibration spectrum of the Lynx helicopter shown in figure 1.

The majority of the low frequency energy occurs at the main and tail rotor blade passing frequencies. The mid and high frequency peaks are generated by the meshing of gears in the various gearboxes, and the rotation of the major shafts. All regions of the helicopter are dominated by a vibration peak at the four per revolution passing frequency of the main rotor. The other rotor orders are also important, especially the first and eighth.

Components mounted on or close to gearboxes are subjected to excitation at the meshing frequency of the gears and in some cases also at the rotational frequencies of the shafts into these gearboxes. The same applies to components mounted near to the engines.

The aircraft has been divided into several regions and the vibration order sheet enables the forcing frequency bands to be defined for each region. For the Lynx, six regions have been defined. All the regions are subject to main rotor forcing with the addition of extra frequencies from nearby components. These forcing frequency bands are shown in figure 5. Equipment with rotating parts driven by an external source also include the operating frequency of its input shaft as an avoid frequency.

The equipment is subjected to an initial resonance search and for this purpose the various regions of the helicopter have been identified and given a letter code. These are shown in Figure 6. The letter code refers to the amplitude curves shown in figure 7. Note that the curves are similar to those in RTCA DO 160 with some modifications and additions made by WHL.

The various regions reflect the different levels of vibration. The lowest levels are on isolated equipment such as instrument panels and equipment racks (curve P). The main fuselage and non-isolated racks are subject to the general level of vibration in the airframe (Curve N). The extremities of the aircraft, on the tail and undercarriage sponsons are subjected to higher levels at the lower frequencies (Curve V) because of the magnification due to their geometric positions and their relative flexibility.

Externally mounted equipment is tested to slightly higher levels (Curve X) than the extremities of the aircraft. Curve X was derived from vibration measurements taken in-flight of various aircraft.

The high frequency excitation of components mounted on, or near to the engines and gearboxes, is reflected in the higher levels at the high frequency end of Curve W.

These curves are used to define the amplitude of the initial resonance search using a sweep rate not exceeding 1 octave per minute. The test is carried out in three mutually perpendicular directions. The damping(Q) factors of any resonances are recorded.

Any resonances in the avoid bands are either removed by structural modifications, or if this is not practicable and the resonances have low damping an endurance test is carried out at the resonant frequency using the appropriate (measured) input levels.

An endurance test is carried out in two stages by a sweep test and constant frequency endurance test. For the sweep test, the appropriate curve in figure 7 is used for a one hour sweep in each of the three perpendicular directions at a sweep rate of one octave/minute.

Following this, a fixed frequency endurance test is carried out using the frequencies and amplitudes given in figure 8. The times are divided equally between each of the three perpendicular directions.

A final resonance search is then made in the same manner as the initial resonance search to determine if there are any changes in the resonant frequencies.

The next few figures show comparisons of measured vibration levels in the Lynx with the vibration level curves of figure 7. The Lynx has two major versions, the Naval and Utility (Army). The two versions possess very similar vibration levels as figures 9 and 10 show. In these two figures, the vibration levels in the cockpit and cabin are compared with curve N which is the test curve for the main fuselage and non-isolated instrument racks. On these figures, the main vibration at about 22 Hz. can be seen. Very few other frequencies are important except for the gearbox-meshing and engine frequencies at around 500 Hz. especially for the Utility Lynx.

The vibration levels on the starboard engine of a Naval Lynx are shown in fig.11. These levels are compared with curve W. The much higher levels at the engine frequencies can be seen at around 500 Hz.

Two types of external stores are shown in figure 12 which are compared with curve X. The generally higher levels at the lower frequencies can be seen.

The specification of the life of equipment for the Lynx helicopter states that the minimum ultimate life of equipment should be 7000 hours or 100000 duty cycles. The minimum ultimate life is defined as the period of use at the end of which, for any reason (e.g. material fatigue, deterioration or economic reasons) the equipment may no longer be used. Therefore, the vibration qualification of equipment should qualify the equipment for a life of 7000 flying hours.

The main endurance testing of the equipment is carried out at the fixed frequencies and levels shown in figure 8. These are accelerated tests and must be sufficiently rigorous to ensure a life of 7000 hours. The equivalent service life of equipment tested to these levels can be calculated using the method of test acceleration given in BS 3G 100. This standard makes the assumption that for equal fatigue damage at different vibration levels, the test duration varies inversely with the fifth power of the displacement or acceleration level.

Figure 13a shows the endurance testing levels and periods for the various aircraft regions. Using a service life of 7000 hours at the various frequencies, the implied service vibration levels can be calculated by the equal fatigue damage law. This calculation has been made, and the resulting service vibration levels are shown in figure 13b.

Comparing the service levels with the measured levels on figures 9 to 12 shows that the vibration levels experienced for equipment in regions N and X (figure 9, 10 and 12) are lower than the 7000 hr. levels given in figure 13b. Therefore, components in these regions which meet the full specification should have operating lives in excess of 7000 flying hours.

However, equipment in region W, on or near the engines (including the engines themselves, figure 11), are marginally above the 7000 hours vibration levels at 22 Hz. But these components have much shorter overhaul times than the 7000 hours.

The above vibration levels have all been taken from steady forward flight measurements at cruise speeds of around 140 knots. The levels vary with the flight condition, i.e. whether hovering, climbing, aircraft weight and e.g. etc. Generally, for the Lynx the lowest hR vibration in steady forward flight in the cabin occurs at speeds of between 70 to 90 knots with the levels being approximately half those shown in the figures. The levels can also vary with the location in the aircraft. For example the co-pilot of the Lynx (port side) receives a much rougher ride than the pilot by a factor of two or three. The levels at hover are relatively low.

Rotor speed also plays a part giving changes in the lower levels of vibration by factors of up to two or three. The rotor speed can be changed by up to $\pm 5\%$ and the various parts of the airframe are affected differently. In some areas the LR vibration can increase, in others decrease.

Equipment on the aircraft will, for a large proportion of the time, experience vibration levels much lower than those shown on figures 9 to 12, and for very short periods experience higher levels (up to about 50% higher). However, these higher levels do not generally exceed the levels defined by the endurance testing curves.

A final check on the vibration levels experienced by the equipment is sometimes made with the equipment in situ on the aircraft. This is especially important for the larger pieces of equipment whose mass or stiffness may alter the dynamic characteristics of structure of the aircraft to which it is mounted, such as for example, a large piece of avionics equipment mounted into racking.

The checks take the form of a 'bonk test' to determine the resonant frequencies of the equipment and mountings. If any resonances are found close to the major exciting frequencies of, principally, the main rotor orders, then design modifications are made to the mounting to move the resonant frequencies away from the exciting frequencies. The way the equipment is mounted will affect frequencies as will the impedance of the structure to which it is attached. Thus rig tests are only an indication of local equipment problems, and not of rigid-body attachment modes.

4. SPECIFICATIONS OF HELICOPTERS CURRENTLY BEING DESIGNED

Specifications for aircraft which are currently being designed are similar to the Lynx specification described in the previous section. For example, the same vibration level curves as shown in figure 7 are used. Different frequency avoid bands are defined for each new design, and these are used for the fixed frequency endurance tests.

5. RANDOM AND SINUSOIDAL EXCITATION

The object of any specification is to prescribe a series of tests which will show whether the item under test can withstand a vibratory environment for a certain length of time. To achieve this, the test environment must be representative of the service environment and the duration of the test must be related to the time in the service environment.

As shown in the previous sections, the helicopter vibration environment is very different from that of the fixed-wing aircraft. In fixed wing aircraft the vibration is principally a broad-band random spectrum compared with the discrete frequency spectrum found in helicopters. The result of this difference is that in the fixed-wing environment all of the resonances in the applicable frequency band will be excited to some degree. In the helicopter, however, the natural frequencies of the equipment should not be close to the major exciting frequencies because these are defined as frequency avoid bands. For these reasons, the endurance testing for helicopters is carried out in fixed frequencies and for fixed wing aircraft a random vibration test is more appropriate.

There is no definite equivalence between sinusoidal and random vibration. Therefore WHL does not accept equipment tested to a random vibration test such as that specified in BS 3G.100. Further fixed-frequency endurance testing is insisted on, along the lines of the previous sections. It is not always necessary to repeat all of the tests demanded by WHL's own specifications because parts may have already been covered, such as for example the initial and final resonance searches and sometimes the one-hour frequency sweep.

The most important part of the equipment specification is the endurance testing and there is no easy or convenient method of relating the amount of damage incurred under sinusoidal and random excitation. Therefore, any bought-out equipment (i.e. equipment purchased by WHL for fitting to an aircraft for a customer) will not be accepted without being subjected (substantially) to tests specified for that aircraft.

However, much of the equipment will have already been subjected to testing to outside specifications for fitting to other aircraft. The extra testing required by the helicopter user incurs expense for the customer or equipment manufacturer which could be reduced if the need for the extra testing was obviated.

A reliable correlation is required between the damage incurred under sinusoidal and random excitation. At present there are many correlation curves and formulae available, some of which give different comparisons of the damage, implying widely different lives for the equipment. Until this situation is resolved, by extensive experimental work, WHL will continue to require testing to its own specifications.

6. CONCLUDING REMARKS

Dynamic environmental testing required by WHL follows the lines of the major international specifications with resonance searches and endurance testing. The vibration levels of the tests are similar to international specifications with some modifications and additions made by WHL based on their experience. All bought-out equipment must be subjected to testing to the relevant specification.

However, there are cases where the vibration levels required by the specifications are too severe and designing to these levels would incur extra expense or a weight penalty from the increased ruggedness. In these cases, the vibration levels are usually reduced to reflect the lower measured values.

Failure to meet the specification does not necessarily mean rejecting the equipment. The type of failure will be considered and the equipment may be accepted for, say, a shorter life.

If the equipment has been subjected to testing to outside specifications, extra testing is usually required, especially the endurance testing, to fully approve the equipment.

Much of this extra testing could be obviated if reliable correlations could be established between the damage incurred under random and sinusoidal testing.

Specifications for the immediate future seem likely to follow very closely the present specifications.

FIGURES

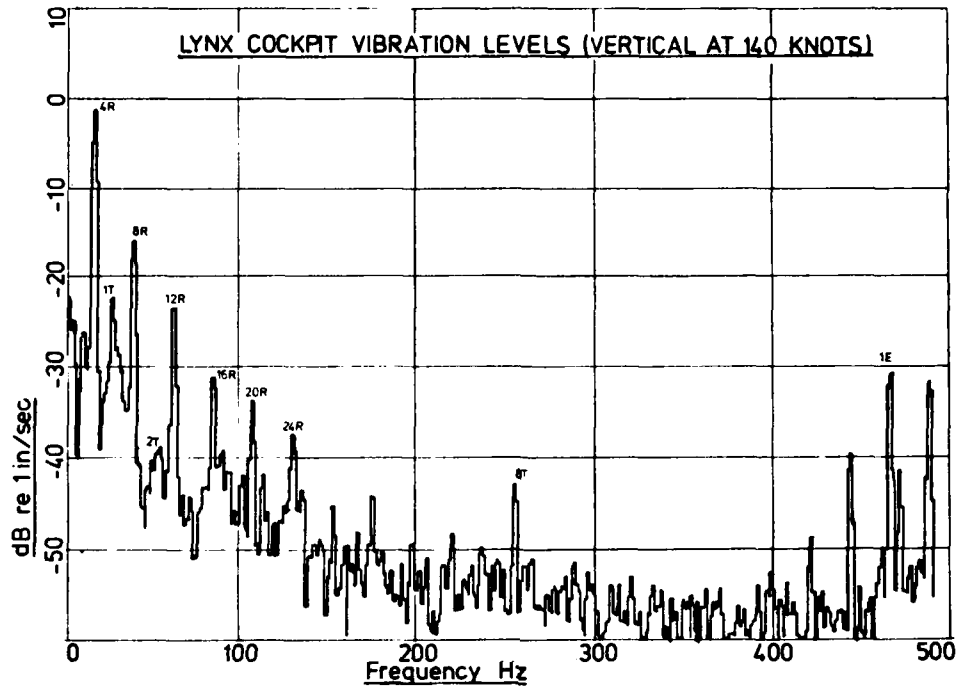


FIGURE 1

VIBRATION TESTING CURVE FOR SCOUT & WASP HELICOPTERS

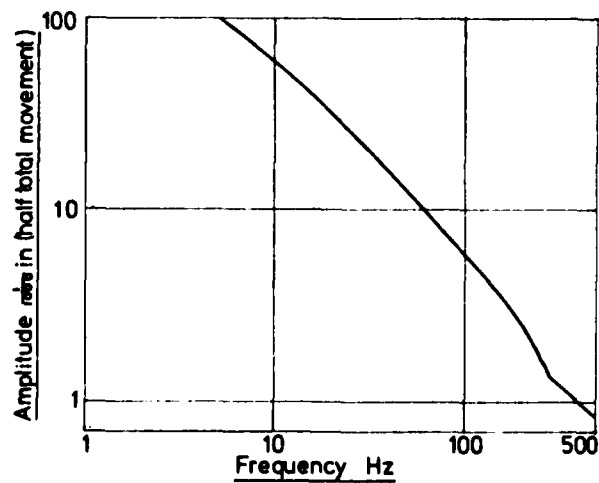


FIGURE 2

VIBRATION TESTING CURVES
SEA KING AND COMMANDO HELICOPTERS
 (within and outside power-unit region)

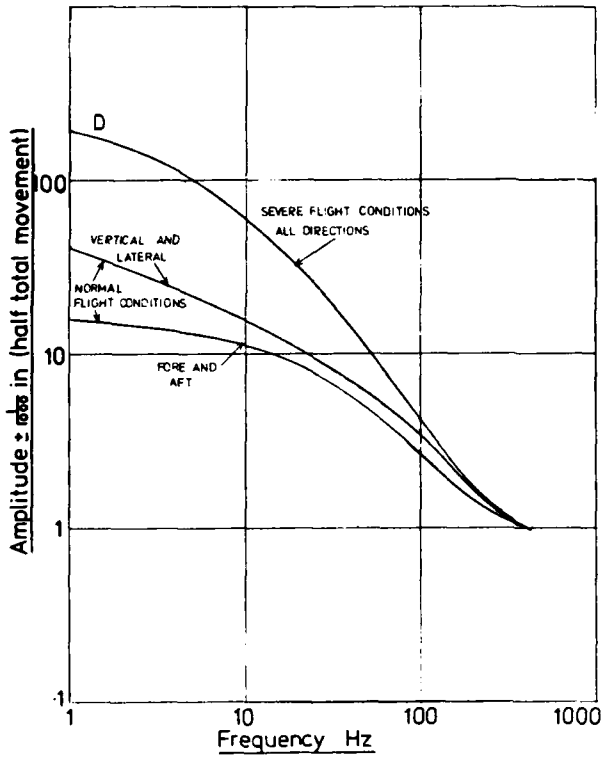


FIGURE 3a

VIBRATION TESTING CURVES
SEA KING AND COMMANDO HELICOPTERS
 (Externally mounted components)

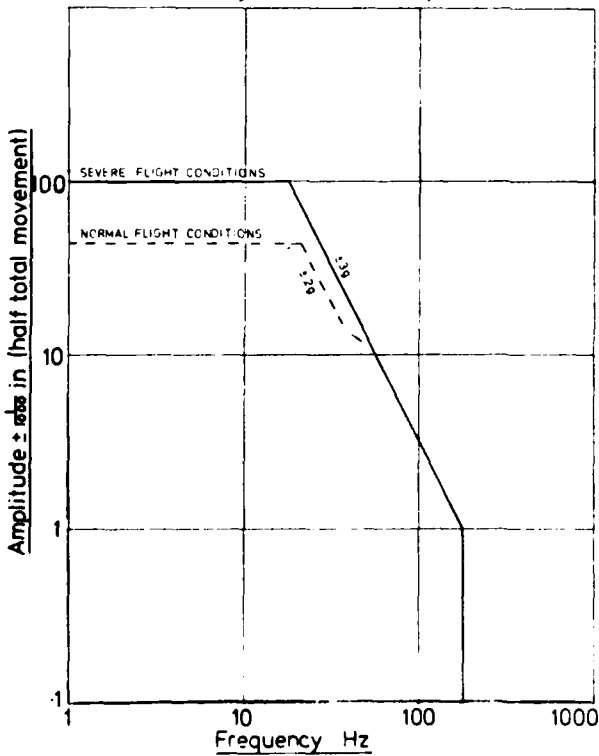


FIGURE 3b

VIBRATION ORDERS	Hz
1R 1st main rotor order.....	5.3
2R	10.6
4R	21.2
1T 1st tail rotor order.....	30.7
8R	42.4
Pylon tail drive shaft.....	59.7
Forward tail drive shaft.....	70.1
Main drive shaft.....	100.0
4T	123.0
8T	245.0
Meshing m.g.b. conforal gears..	446.0
Engine.....	451.0
Meshing tail gearbox.....	1135.0
Meshing intermediate gearbox....	1613.0
Meshing m.g.b. input bevels.....	2110.0

FIGURE 4
VIBRATION ORDERS FOR LYNX

- (a) All regions
- | | | |
|---------------------------|---------|---------|
| 1 x Main rotor shaft (1R) | 5.2 to | 5.9 Hz |
| 2 x Main rotor shaft (2R) | 10.4 to | 11.7 Hz |
| 4 x Main rotor shaft (4R) | 20.8 to | 23.4 Hz |
| 8 x Main rotor shaft (8R) | 41.6 to | 46.8 Hz |
- (b) On or in close proximity to engine
All orders given at (a) plus:-
- | | | |
|------------------------------|---------|----------|
| 1 x Forward tail drive shaft | 68.8 to | 77.4 Hz |
| 1 x Main drive shaft | 98.3 to | 110.8 Hz |
| 1 x Free turbine | 440 to | 590 Hz |
| 1 x Compressor | 490 to | 720 Hz |
- (c) On or in close proximity to main rotor gearbox
All orders given at (a) plus:-
- | | | |
|-----------------------------------|----------|----------|
| 1 x Forward tail drive shaft | 68.8 to | 77.4 Hz |
| 1 x Main drive shaft | 98.3 to | 110.8 Hz |
| 1 x Meshing M.G.B. conforal gears | 438 to | 492 Hz |
| 2 x Meshing M.G.B. conforal gears | 875 to | 985 Hz |
| 1 x Meshing M.G.B. input bevels | 2,070 to | 2,330 Hz |
- (d) Tail cone and tail pylon
All orders given at (a) plus:-
- | | | |
|------------------------------|----------|----------|
| 1 x Tail rotor shaft | 30.1 to | 33.8 Hz |
| 1 x Pylon tail drive shaft | 58.6 to | 66.0 Hz |
| 1 x Forward tail drive shaft | 68.8 to | 77.4 Hz |
| 4 x Tail rotor shaft | 120.4 to | 135.5 Hz |
- (e) Intermediate gearbox
All orders given at (a) and (d) plus:-
- | | | |
|----------------------------------|----------|----------|
| 1 x Meshing intermediate gearbox | 1,583 to | 1,780 Hz |
|----------------------------------|----------|----------|
- (f) Tail rotor gearbox
All orders given at (a) plus:-
- | | | |
|----------------------------|----------|----------|
| 1 x Tail rotor shaft | 30.1 to | 33.8 Hz |
| 1 x Pylon tail drive shaft | 58.7 to | 66.0 Hz |
| 4 x Tail rotor shaft | 120.4 to | 135.5 Hz |
| 1 x Meshing tail gearbox | 1,114 to | 1,253 Hz |
- (g) Equipment with rotating parts driven by an external source shall include the normal operating frequency range of its input shaft as an avoid frequency band.

FIGURE 5

FIGURE 6 TESTING REGIONS OF LYNX

Aircraft Region	Main Fuselage	Instrument Panels and Isolated Racks	Instrument Racks - Not Isolated	On/in close proximity to Engine
Curve (See Fig.1)	N	P	N	W
Aircraft Region	Under-carriage Sponsons	Tail Cone and Tail Pylon	Gearboxes (See Note (i))	Externally Mounted Equipment
Curve (See Fig.1)	V	V	W	X
<p>Note: (i) (a) For equipment mounted on the Tail Rotor and Angle gearboxes a composite curve of V and W shall be used, i.e. Curve V shall be followed from 5Hz until it intersects Curve W and then continued on Curve W.</p> <p>(b) For equipment mounted on the Main Gearbox the vibration envelope does not preclude the possibility of gearbox excited vibration in the range of 3000 Hz to 30,000 Hz.</p>				

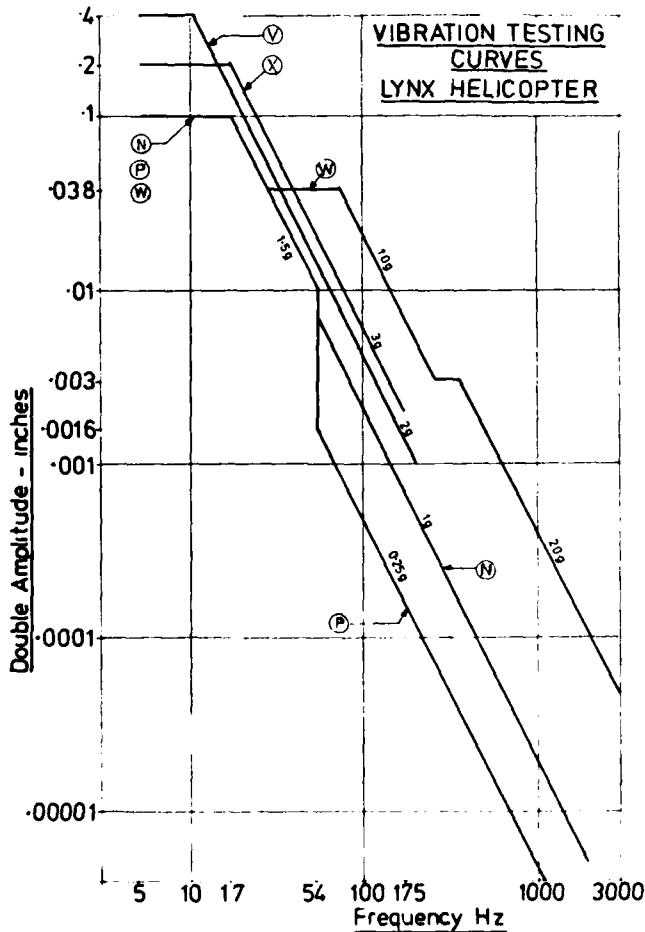


FIGURE 7

- (a) Programme for equipment tested to curves N, P, V or X
 3×10^6 cycles @ 22 Hz = 37.9 hours
 3×10^6 cycles @ 44 Hz = 18.9 hours
 3×10^6 cycles @ 128 Hz = 6.5 hours
- (b) Programme for equipment tested to curve W
 3×10^6 cycles @ 22 Hz = 37.9 hours
 3×10^6 cycles @ 44 Hz = 18.9 hours
 3×10^6 cycles @ 128 Hz = 6.5 hours
 3×10^6 cycles @ 500 Hz = 1.7 hours
- (c) For equipment driven by external means the 128 Hz test of programme (a) or (b) shall be replaced by one of 3×10^6 cycles at its own drive frequency at a level given by the specified test curve.

FIGURE 8

LYNX HELICOPTER ENDURANCE TESTING TIMESNAVAL LYNX - CURVE N (at 140 knots)

- † CO-PILOTS SEAT VERTICAL
- x MID CABIN FORE AND AFT
- MID CABIN LATERAL

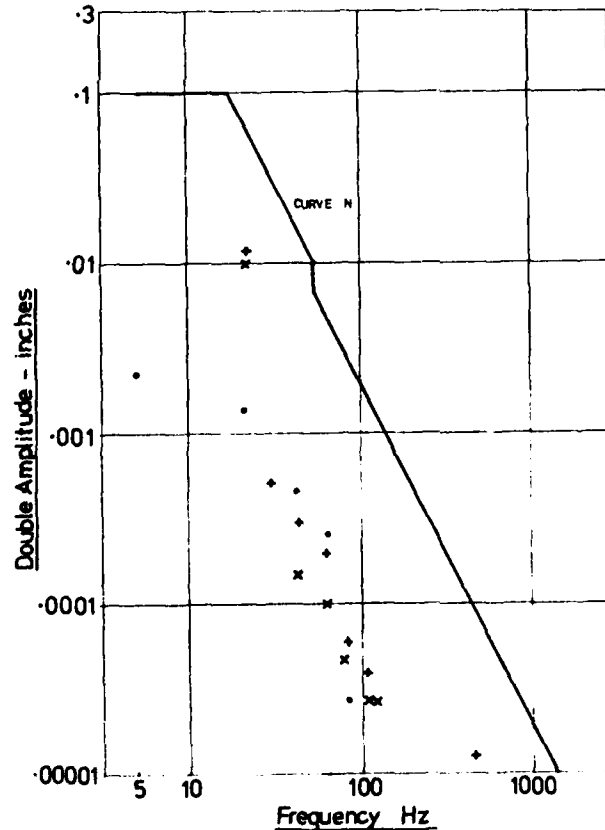


FIGURE 9

UTILITY (ARMY) LYNX - CURVE N (at 140 knots)

- ◆ CO-PILOTS SEAT VERTICAL
- PILOTS SEAT VERTICAL
- ✕ MID-CABIN LATERAL
- MID-CABIN FORE AND AFT

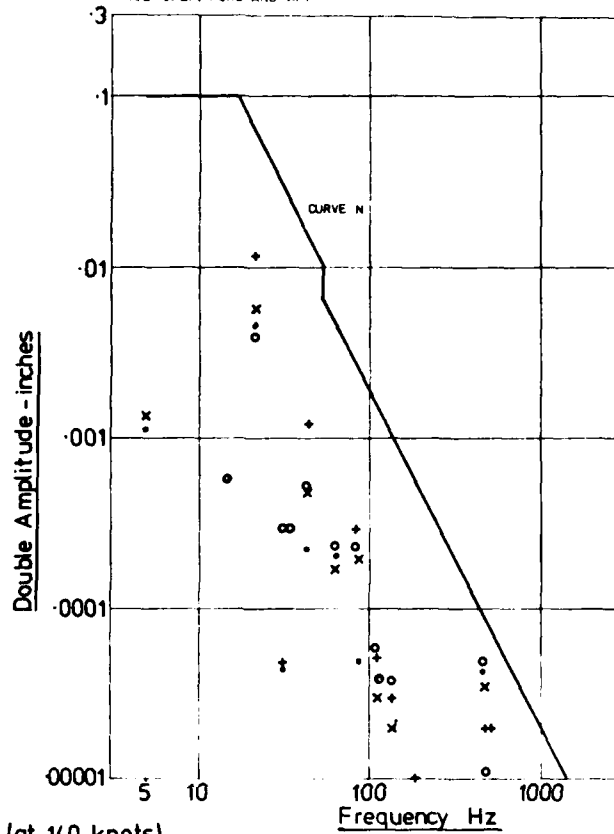


FIGURE 10

NAVAL LYNX - CURVE W (at 140 knots)

- ✕ STARBOARD ENGINE - VERTICAL

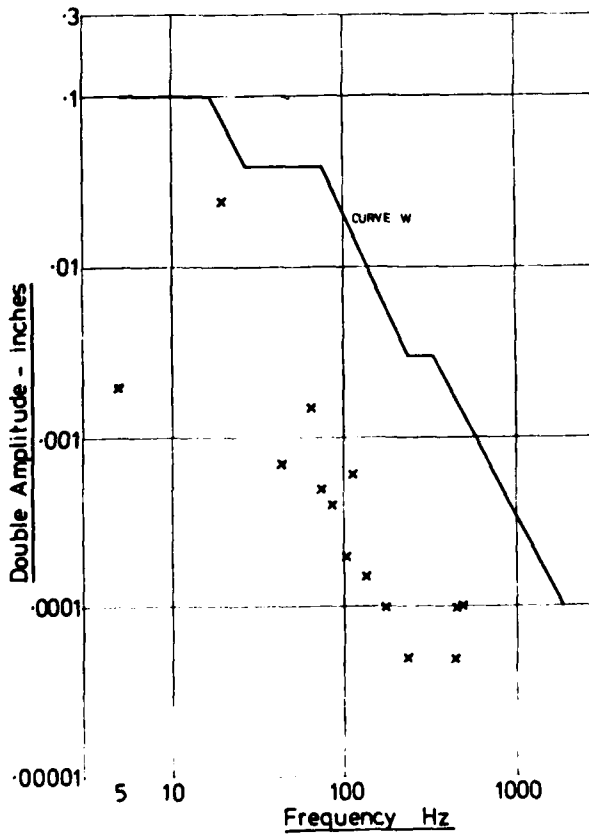


FIGURE 11

NAVAL LYNX - CURVE X (at 140 knots)

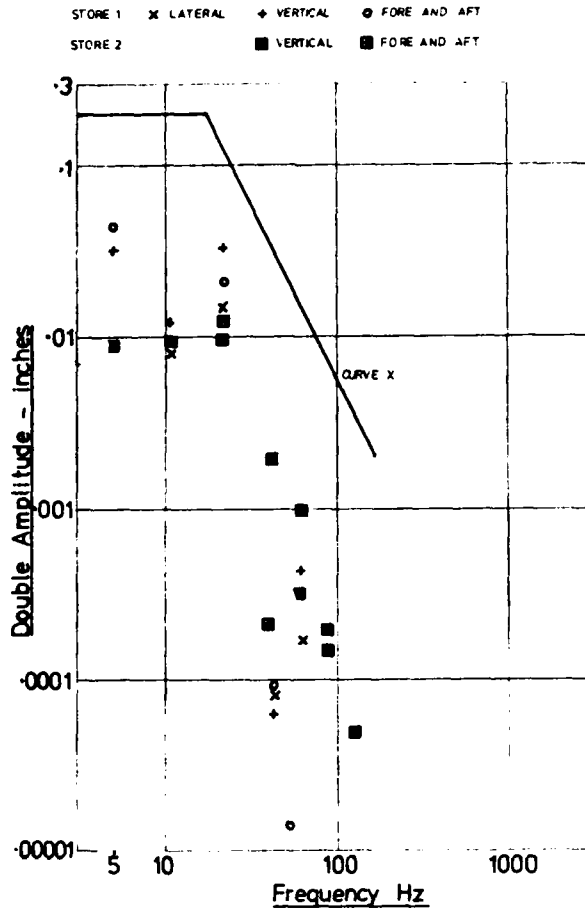


FIGURE 12

CURVE	TESTING LEVELS AT			
	22Hz	14Hz	128Hz	500Hz
N	1.5g	1.5g	1g	-
P	1.5g	1.5g	.25g	-
V	2g	2g	2g	-
X	3g	3g	3g	-
W	1.5g	3.8g	10g	20g

FIGURE 13a

ENDURANCE TESTING LEVELS FOR LYNX

CURVE	SERVICE LEVELS AT			
	22Hz	14Hz	128Hz	500Hz
N	.53g	.46g	.25g	-
P	.53g	.46g	.06g	-
V	.70g	.61g	.49g	-
X	1.1g	.92g	.74g	-
W	.53g	1.16g	2.5g	3.78g

FIGURE 13b

IMPLIED SERVICE LEVELS FOR LYNX

Application of Modal Synthesis Techniques for the Dynamic
Qualification of Wings with Stores

by

E. Breitbach
DFVLR-AVA Goettingen
Institute of Aeroelasticity
Bunsenstr.10, D-3400 Goettingen, Germany

Summary

Dynamic qualification as well as flutter clearance of modern combat aircraft is usually burdened by considerable computational and test effort due to the great variety of different external stores configurations. It is shown that modal synthesis techniques such as modal correction and modal coupling approaches are convenient in substantially reducing the test effort to only a few representative trial configurations which may be taken as a basis for establishing reliable mathematical models of all other configurations. Emphasis is also placed on how to deal with special phenomena due to nonlinearities, in particular combinations of backlash and dry friction, in the connecting parts between wing, pylon and store which may significantly infringe on the validity of the linear mathematical models as used in ground and flight vibration testing.

1. Introduction

Accurate prediction of the flutter and dynamic response behavior of aircraft requires full knowledge of the elastodynamic properties usually determined by extensive dynamic ground and flight testing complemented by thorough numerical analyses. Especially the development of modern combat aircraft is burdened by extremely high test and computational effort due to the great variety of different underwing stores carried within the range of missions. In particular, ground vibration testing would exceed any reasonable cost frame if the number of different external stores configurations would require an equivalent number of ground vibration tests (GVT).

Modal synthesis can help to ease this problem considerably by ground vibration testing only a few representative external stores configurations, whereas the modal characteristics of the much more numerous remaining configurations can be determined in a purely numerical way by means of modal correction or modal coupling procedures. Since the mid-fifties, much fundamental work has been devoted to these techniques, particularly in the USA and UK where some key publications related to modal synthesis originated, see for instance Refs. [1], [2], [3], [4].

In the last decade the capability of modal synthesis has been extended to structures, the dynamic properties of which are given only in terms of measured modal data without any knowledge of the geometrical mass, stiffness and damping distribution, see Refs. [5], [6], [7], [8], [9]. A comprehensive survey of the state of the art in modal synthesis is given in Ref. [10]. All these references may be taken as a useful basis for elaborating modal synthesis techniques for special application to wing-with-stores dynamics.

Ground and flight test experience has shown that many peculiar phenomena are due to structural nonlinearities locally concentrated not only in the connecting parts between wing, pylon and store, but also in the control mechanism and other parts of aircraft structures. Standard structural dynamics methods such as GVT or flight vibration test techniques have structural linearity as a common basis. Consequently, all these approaches fail if applied to nonlinear systems. To overcome this problem, modal synthesis can be employed successfully as an essential part of an overall concept to identify nonlinear systems. This concept consists basically of ground vibration testing, modal synthesis and special approaches to identify the elastodynamic behavior of nonlinear coupling elements. How this concept can be applied to real structures is demonstrated in Ref. [8] for the example of an airplane with nonlinearities in the control system.

Application to other systems such as wing-with-stores combinations raises no additional problems. The main steps towards a complete nonlinear mathematical model may be described as follows:

- Decomposing the nonlinear structure into linear subsystems and nonlinear connecting elements - or, if modal correction is applied, establishing a linearized test configuration with the nonlinear elements replaced by linear ones;
- Ground vibration testing the linearized subsystems (if modal coupling is applied) or the linearized test configuration (if modal correction is applied);
- Experimental identification of the nonlinear connecting elements;
- Setting up the equations of motion of the complete nonlinear system by means of modal synthesis approaches.

Further emphasis has to be placed on the convergence problem due to frequency range truncation and inconsistent boundary or coupling conditions. It will be shown that interface loading is a promising means to ease this problem considerably.

Finally, attention will be drawn to a troublesome phenomenon especially detected in non-linear wing/store connections. It will be shown how this problem can be explained by using the concept of an oscillator with one and one-half degrees of freedom, Ref.[11].

2. Fundamental relations

Before coping with problems involving structural nonlinearities, the basic equations of motion of an elastodynamic system are derived on the simplified precondition of linearity and viscous damping (later on replaced by so-called structural damping defined as the imaginary part of a complex stiffness). Formulation in the time domain in terms of the physical deflections $u(t)$ leads to

$$(1) \quad A \ddot{u}(t) + B \dot{u}(t) + C u(t) = P(t)$$

where

A	mass matrix
B	viscous damping matrix
C	stiffness matrix
P(t)	column matrix of external forces
u(t)	column matrix of the dynamic response to P(t) where $\dot{u}(t)$ and $\ddot{u}(t)$ are first and second order differentials with respect to time t .

Applying to Eq.(1) the modal transformation

$$(2) \quad u(t) = \Phi q(t)$$

where

Φ	modal matrix with the normal mode shapes Φ_r , ($r = 1, 2, \dots, n$) of the conservative undamped system as columns
q(t)	column matrix of the generalized coordinates

and left-hand multiplication by the transposed Φ^T changes Eq.(1) into

$$(3) \quad M \ddot{q}(t) + D \dot{q}(t) + K q(t) = Q(t)$$

where

$M = \Phi^T A \Phi$	diagonal matrix of the generalized masses M_r
$D = \Phi^T B \Phi$	generalized damping matrix, not necessarily diagonal, with the coefficients D_{rs}
$K = \Phi^T C \Phi$	diagonal matrix of the generalized stiffnesses $K_r = M_r \omega_r^2$ with ω_r denoting the (circular) normal frequency
$Q(t) = \Phi^T P(t)$	column matrix of the generalized forces $Q_r(t)$.

In the case of an harmonic excitation

$$(4) \quad Q(t) = Q e^{j\omega t} \quad , \quad j = \sqrt{-1}$$

the structure responds harmonically as well

$$(5) \quad q(t) = q e^{j\omega t}$$

where ω designates the (circular) excitation frequency. Insertion of Eqs.(4) and (5) into Eq.(3) and replacement of the viscous-type damping definition by the complex stiffness definition leads to

$$(6) \quad (-\omega^2 M + jD + K)q = Q \quad .$$

Another fundamental relation repeatedly used in the following sections is a simplified form of Lagrange's equations:

$$(7) \quad \frac{d}{dt} \left(\frac{\partial E_k}{\partial \dot{q}_r} \right) + \frac{\partial E_s}{\partial q_r} = 0 \quad , \quad r = 1, 2, \dots, n$$

where

E_k	kinetic energy
E_s	stiffness or potential energy.

3. Modal correction method

The so-called modal correction method, Refs. [5],[7],[8], has been applied successfully for more than a decade to problems with relatively small changes of mass, damping and stiffness. As far as wing-with-stores problems are concerned modal correction can be used basically to account for changes of the mass inertia properties of stores and of pylon stiffness as well as damping.

3.1 Modal mass inertia correction

Let the difference between the mass inertia properties of two different types of interchangeable underwing stores be represented by changes of mass m , mass moments of inertia $\theta_x, \theta_y, \theta_z$ and the location of the center of gravity (x_{CG}, y_{CG}, z_{CG}) , then the difference between the kinetic energies of the two stores can be expressed by

$$(8) \quad \Delta E_k = E_{k2} - E_{k1}$$

The subscripts 1 and 2 indicate the basic configuration 1 measured in a ground vibration test and any changed configuration 2. The energy terms E_{k1} and E_{k2} can be written as follows:

$$(9) \quad E_{ki} = \frac{1}{2} \dot{u}_i^T I_i \dot{u}_i \quad , \quad i = 1, 2$$

According to Figure 1 the displacement vectors

$$(10) \quad u_i = (u_x^i, u_y^i, u_z^i, \alpha_x^i, \alpha_y^i, \alpha_z^i)^T \quad , \quad i = 1, 2$$

and the mass inertia matrices

$$(11) \quad I_i = \begin{bmatrix} m_i & & & & & \\ & m_i & & & & \\ & & m_i & & & \\ & & & \theta_{xi} & & \\ & & & & \theta_{yi} & \\ & & & & & \theta_{zi} \end{bmatrix}$$

are formulated with respect to the centers of gravity (x_{CG}, y_{CG}, z_{CG}) , $CG=1,2$, where $x_2=x_1+\Delta x$, $y_2=y_1+\Delta y$, $z_2=z_1+\Delta z$.

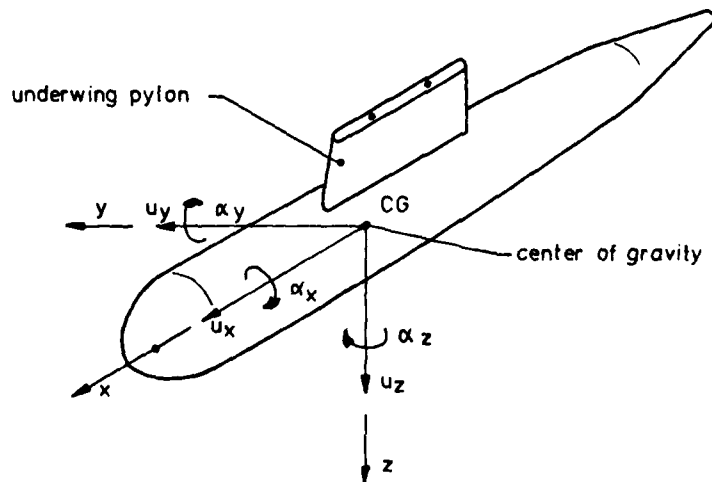


Figure 1: Aircraft underwing store with pylon.

Expressing vector u_2 by vector u_1 leads to the transformation

$$(12) \quad u_2 = T u_1$$

where

$$(13) \quad T = \begin{bmatrix} 1 & & & 0 & \Delta z & -\Delta y \\ & 1 & & -\Delta z & 0 & \Delta x \\ & & 1 & \Delta y & -\Delta x & 0 \\ \hline & 0 & & 1 & & \\ & & & & 1 & \\ & & & & & 1 \end{bmatrix}$$

Then, the change of the kinetic energy is

$$(14) \quad \Delta E_k = \frac{1}{2} \dot{u}_1^T (T^T I_2 T - I_1) \dot{u}_1$$

Applying the modal transformation

$$(15) \quad u_1 = \Phi_1 q$$

and subsequently Lagrange's operation (7) to Eq.(14) results in the modal correction matrix

$$(16) \quad \Delta M = \Phi_1^T (T^T I_2 T - I_1) \Phi_1$$

where the modal matrix Φ_1 contains the measured modal displacements of the underlying store of the basic test configuration as column vectors:

$$(17) \quad \Phi_{1r} = (u_{xr}^1, u_{yr}^1, u_{zr}^1, \alpha_{xr}^1, \alpha_{yr}^1, \alpha_{zr}^1)^T$$

Addition of matrix ΔM to M in Eq.(3) or (6) results in the equations of motion of the changed systems. Then, taking into consideration all changes of mass inertia properties in the changed configuration 2 leads with a number of L stores ($i = 1, 2, \dots, L$) to the equations of motion

$$(18) \quad \left\{ -\omega^2 (M + \sum_{i=1}^L \Delta M_i) + jD + K \right\} q = Q$$

The capability of modal mass inertia correction has been proved successfully for some applications, one of which is described in Ref.[12]. The system investigated is a simple swept back wing model carrying two underwing stores as sketched in Figure 2. The mass inertia properties of the two stores i (inner) and o (outer) are listed in Table 1, giving the masses, the mass moments of inertia, the center of gravity locations (measured from the pylon center line), and the radii of gyration in configurations 1 and 2.

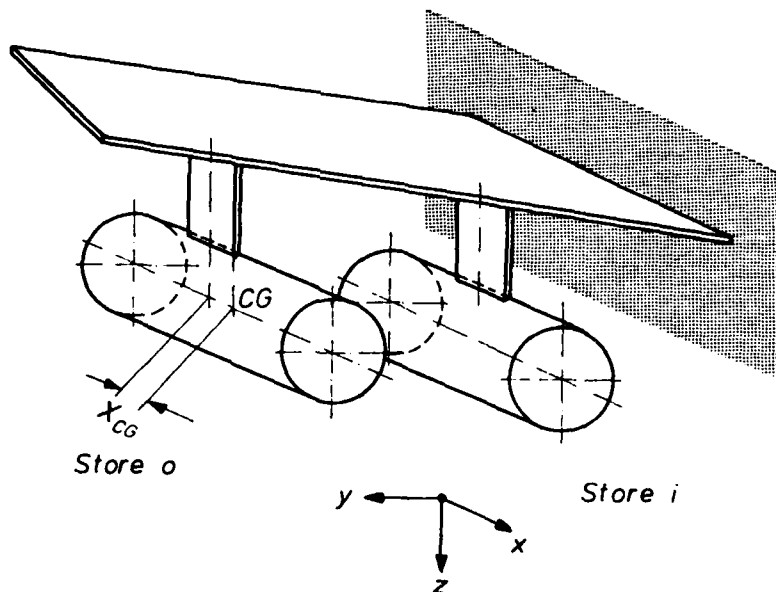


Figure 2: Swept back wing model carrying two underwing stores.

	Configuration 1		Configuration 2	
	Store i	Store o	Store i	Store o
m [kg]	5.003	4.723	5.003	4.723
θ_x [kg cm ²]	21.05	19.79	21.05	19.79
θ_y, θ_z [kg cm ²]	379.83	375.35	379.83	375.35
x_{CG} [cm]	0.23	5	5.23	0
r_G [cm]	8.72	10.22	10.16	8.91

Table 1: Modal correction application to a wing-with-stores model, mass inertia properties of the external stores mass m , mass moments of inertia $\theta_x, \theta_y, \theta_z$, center of gravity location x_{CG} , radius of gyration r_G .

The first and third columns in **Table 2** show the measured normal frequencies of the basic test configuration 1 and the normal frequencies of configuration 2 resulting from a modal correction calculation. The second column contains the measured normal frequencies of configuration 2 validating the modal correction results. The greatest error between the modal correction results and the appertaining test results is 4.2% in mode 5:

Normal mode	Normal frequency [Hz] Config. 1	Normal frequency [Hz] Config. 2	
	measured	measured	calculated (Modal correction)
r=1	7.71	7.64	7.65
2	9.07	10.78	10.86
3	10.65	8.83	8.65
4	12.42	14.73	14.63
5	14.62	11.84	12.34
6	33.53	35.76	35.99
7	48.19	44.97	44.99
8	61.82	62.59	63.14
9	100.46	99.82	102.02

Table 2: Modal correction application to a wing-with-stores model, measured normal frequencies of the basic test configuration 1 and related measured and modal correction results of the changed configuration 2.

3.2 Modal stiffness correction

The modal correction approach can also be used to deal with stiffness changes in underwing store pylons which may occur if alterations of the mission requirements lead to pylon design changes. A quite similar case may arise due to changes of the attachment conditions (fixation forces) at the store/pylon and pylon/wing interfaces.

Let the change of the pylon stiffness be represented by the 12×12 matrix

$$(19) \quad \Delta C = C_2 - C_1$$

where the pylon stiffness matrices C_1 and C_2 are related to the basic test configuration 1 and the changed configuration 2, then the difference between the pylon stiffness energies E_{S1} and E_{S2} can be expressed accordingly by

$$(20) \quad \Delta E_S = \frac{1}{2} u_p^T \Delta C u_p$$

As can be seen from Figure 3 the column vector u_p comprises the arbitrary displacements u_p^A and u_p^B at the interfaces A and B:

$$(21) \quad u_p = \begin{Bmatrix} u_p^A \\ u_p^B \end{Bmatrix}$$

where

$$(22) \quad u_p^i = (u_x^i, u_y^i, u_z^i, \alpha_x^i, \alpha_y^i, \alpha_z^i)^T, \quad i = A, B$$

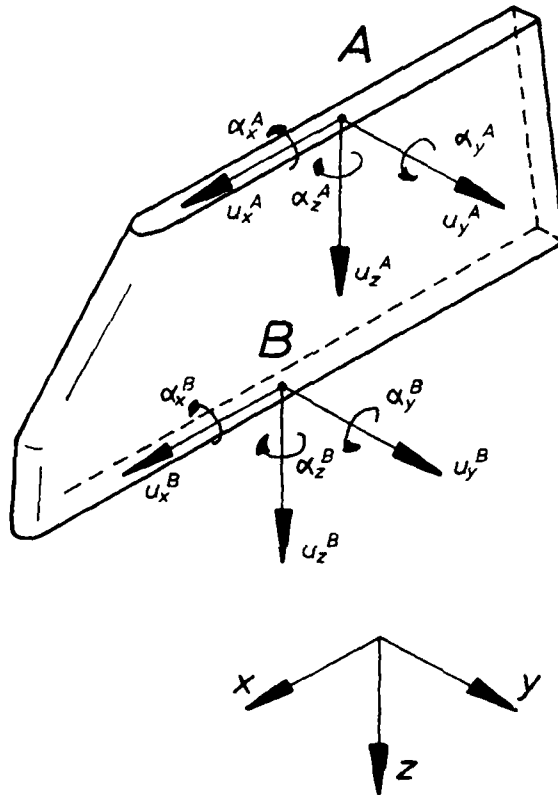


Figure 3: Underwing pylon.

This formulation is based on the approximating assumption that the interface displacements can be described as statically determinate.

By applying the modal transformation

$$(23) \quad u_p = \Phi_p q$$

to Eq. (20), ΔE_S converts to

$$(24) \quad \Delta E_s = \frac{1}{2} q^T \Phi_p^T \Delta C \Phi_p q$$

where matrix

$$(25) \quad \Phi_p = \begin{bmatrix} \Phi_{p1}^A, \Phi_{p2}^A, \dots, \Phi_{pr}^A, \dots, \Phi_{pn}^A \\ \Phi_{p1}^B, \Phi_{p2}^B, \dots, \Phi_{pr}^B, \dots, \Phi_{pn}^B \end{bmatrix}$$

contains the normal mode deflections at the interfaces A and B, measured in a ground vibration test on the basic test configuration 1. Thus

$$(26) \quad \Phi_{pr}^i = (u_{xr}^i, u_{yr}^i, u_{zr}^i, \alpha_{xr}^i, \alpha_{yr}^i, \alpha_{zr}^i)^T, \quad i = A, B$$

Application of Lagrange's operation (7) to Eq.(24) leads to the modal stiffness correction matrix

$$(27a) \quad \Delta K = \Phi_p^T \Delta C \Phi_p$$

which must simply be added to matrix K in Eq.(1) or (6). In the case of more than one pylon stiffness change, the modal stiffness correction matrix Eq.(27a) has to be replaced by

$$(27b) \quad \Delta K = \sum_{l=1}^L \Delta K_l$$

where index $l = 1, 2, \dots, L$ stands for the number of pylons changed.

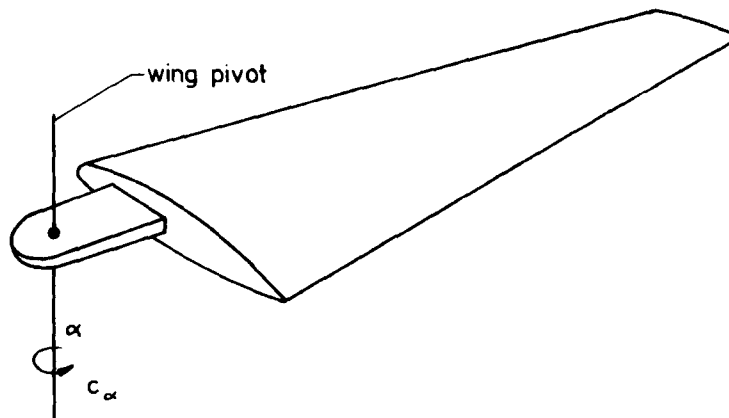


Figure 4: Sweepable wing with pivot stiffness c_α .

To date, there is a lack of experience with practical applications to underwing stores systems and only little experience with other systems. Just to illustrate how successful modal stiffness correction may be, the stiffness change in the wing pivot of a sweepable wing, see Figure 4, is given as an example. An increase of the wing pivot stiffness $c_{\alpha_1} = 646.7 \text{ N-m/rad}$ (basic configuration 1) by $\Delta c = 661.5 \text{ N-m/rad}$ up to $c_{\alpha_2} = 1308.2 \text{ N-m/rad}$ (changed configuration 2) leads to the normal frequencies as given in Table 3. The first column of Table 3 contains the normal frequencies of the basic configuration whereas the two other columns show the results of the modal stiffness correction method compared with validating measured data. The agreement between calculation and test is surprisingly good for such a large stiffness change of more than twice the value of the basic configuration.

Normal Mode	Normal frequencies f_r [Hz]		
	Basic Config. measured	Changed Config.	
		measured	calculated
r=1	3.14	3.32	3.32
2	4.38	4.34	4.39
3	4.65	5.03	4.97
4	6.18	6.76	6.74
5	6.75	7.99	7.45
6	15.4	15.06	15.4

Table 3: Application of the modal correction method to a sweepable wing with the wing pivot stiffness $c_{\alpha 1} = 646.7$ N-m/rad increased by $\Delta c = 661.5$ N-m/rad up to $c_{\alpha 2} = 1308.2$ N-m/rad .

3.3 Some remarks to practical application of modal correction

After derivation of the fundamentals of the modal correction approach in the foregoing sections, some open questions still remain concerning the practical application to real underwing stores problems.

To make proper use of the modal correction approach the following requirements have to be fulfilled:

- The modal deflections Φ_{1r} and Φ_{Dr}^A Φ_{Dr}^B according to Eqs.(17) and (26) are to be measured in the basic test configurations as accurately as possible. Redundant numbers of measuring pickups are recommended;
- The basic test configurations have to be conditioned in such a way that orthogonal sets of normal modes can be measured to guarantee consistent mathematical models such as required for modal correction calculations. Concretely speaking, the ever existent nonlinear effects have to be suppressed for instance by testing at low force levels, thus keeping the nonlinear elements in fairly linear amplitude ranges.
- Unlike the determination of the mass inertia matrices I_1 and I_2 , see Eq.(11), which can be measured easily, the determination of the pylon stiffness matrices C_1 and C_2 requires more attention. They can be determined either by measuring the flexibility matrices C_1^{-1} and C_2^{-1} in static tests or by carrying out dynamic tests on the real store/pylon system clamped with the wingside end of the pylon to a foundation. The foundation has to be rigid except for the backup structure in the vicinity of the pylon fixation which should be a replica of the actual wing/pylon interface. This test could also be carried out with the store/pylon system left on the wing but with the wing kept at rest, which in many cases is not simple to accomplish. On the condition that stores can usually be considered rigid in a frequency range of interest this dynamic test delivers a total of six normal modes Φ_{Rr} , $r=1,2,\dots,6$ collected in the modal matrix Φ_R , and the related normal frequencies ω_{Rr} , generalized masses M_{Rr} and damping loss angles γ_{Rr} . With these data in hand the stiffness matrix C_i , ($i=1,2$), of the pylon can be calculated easily from the modal retransformation

$$(28) \quad C_i = (\Phi_R^T)^{-1} K_R \Phi_R^{-1}$$

where matrix K_R contains the generalized stiffnesses $K_{Rr} = \omega_{Rr}^2 M_{Rr}$ as diagonal elements.

A computer software package for general application of the modal correction approach has been elaborated at the DFVLR in the Institute of Aeroelasticity and published in Ref.[13].

4. Modal coupling

Aside from the modal correction approach modal coupling offers an alternative way to tackle underwing stores problems. The basic relations of this method are described in many publications, for instance in Refs.[5],[6],[8],[9],[10].

One can basically distinguish between three different types of coupling conditions:

- *Rigid coupling*
In the case of coupling two substructures with interfaces which can be considered

approximately rigid, the displacements at the coupling points have to fulfill the compatibility condition;

- *Flexible coupling*
If substructures are coupled together by means of flexible elements, a special coupling approach can be used provided that the elastomechanic properties of the flexible elements are known;
- *Mixed coupling*
It often occurs that a coupling element has to be considered rigid with respect to some of its degrees of freedom whereas the others may be treated as flexible.

By neglecting external forces and structural damping for the sake of simplifying the derivation, the elastodynamic equations of motion of the complete system with the coupling elements removed can be written as follows:

$$(29) \quad (-\omega^2 M + K)q = 0$$

where for the case of two substructures A and B

$$(30) \quad M = \begin{bmatrix} M^A & | & 0 \\ \hline 0 & | & M^B \end{bmatrix}, \quad K = \begin{bmatrix} K^A & | & 0 \\ \hline 0 & | & K^B \end{bmatrix}$$

$$(31) \quad q = ((q^A)^T, (q^B)^T)^T$$

The way in which Eq.(29) must be changed due to rigid, flexible or mixed coupling is discussed in the following sections in a general way before arriving at the special problem of underwing stores configurations. A computer software package comprising these three types of substructure coupling has been worked out at the DFVLR Institute of Aeroelasticity and published in Ref.[14].

4.1 Flexible coupling

The flexible coupling approach, described in Refs.[5],[6],[8] and [9], commences by formulating the stiffness energy of a coupling element between two arbitrary substructures A and B. Thus we obtain

$$(32) \quad E_s = \frac{1}{2} u_F^T C u_F,$$

where C denotes the stiffness matrix of the coupling element and

$$(33) \quad u_F = \begin{bmatrix} u_F^A \\ \hline u_F^B \end{bmatrix}$$

The column vectors u_F^A and u_F^B contain the arbitrary displacements at the coupling points of the substructures A and B, respectively. By developing vector u_F into the modal series expansion

$$(34) \quad u_F = \Phi_F q$$

where

$$(35) \quad \Phi_F = \begin{bmatrix} \Phi_F^A & | & 0 \\ \hline 0 & | & \Phi_F^B \end{bmatrix}$$

Eq.(32) can be transformed into

$$(36) \quad E_s = \frac{1}{2} q^T \Phi_F^T C \Phi_F q$$

The submatrices Φ_F^A and Φ_F^B contain normal mode displacements at the coupling points as part of the normal modes of the uncoupled substructures A and B, respectively.

Application of Lagrange's operation (7) to Eq.(36) results in the modal coupling matrix

$$(37) \quad \Delta K = \Phi_F^T C \Phi_F$$

Adding ΔK to matrix K in Eq.(29) leads to the equations of motion of the substructures A and B coupled by a flexible spring element described by matrix C.

4.2 Rigid coupling

Rigid coupling of two substructures A and B, described for instance in Refs. [4] and [5], requires fulfillment of the compatibility condition in the coupling points

$$(38) \quad u_R^A - u_R^B = 0$$

where column matrices u_R^A and u_R^B contain the displacements at the coupling points of the substructures A and B, respectively. Eq. (38) can be expanded again into a series of the normal mode displacements at the coupling points such as

$$(39) \quad Gq = 0$$

where

$$(40) \quad G = \left[\begin{array}{c|c} \phi_R^A & -\phi_R^B \end{array} \right]$$

By partitioning matrix G into an invertible square matrix $\bar{\Phi}$ and a matrix Φ^* , Eq. (39) can be reordered as follows:

$$(41) \quad Gq = 0 \rightarrow \bar{G}\bar{q} = 0$$

where

$$(42) \quad \bar{G}\bar{q} = \left[\begin{array}{c|c} \Phi^* & \bar{\Phi} \end{array} \right] \begin{Bmatrix} p^* \\ \bar{p} \end{Bmatrix}$$

By using relation (42) the column matrix \bar{p} may be expressed by the column matrix p^* as follows:

$$(43) \quad \bar{p} = -\bar{\Phi}^{-1} \Phi^* p^*$$

so that column vector \bar{q} can be expressed by the relation

$$(44) \quad \bar{q} = T p^*$$

where

$$(45) \quad T = \begin{bmatrix} 1 & & \\ - & - & - \\ -\bar{\Phi}^{-1} \Phi^* & & \end{bmatrix}$$

meaning that matrix $\bar{\Phi}$ must not be singular. Application of the reordering scheme (41) to Eq. (29) and application of transformation (44) leads to the equations of motion of the coupled system

$$(46) \quad T^T (-\omega^2 \bar{M} + \bar{K}) T p^* = 0$$

As to the order of the column matrices \bar{q} , \bar{p} and p^* it has to be mentioned that if n^A and n^B are the numbers of generalized degrees of freedom of the uncoupled substructures A and B and if n_C is the number of constraints, then

$$\bar{q} \text{ is of order } (n^A + n^B) \times 1$$

$$\bar{p} \text{ is of order } n_C \times 1$$

$$p^* \text{ is of order } (n^A + n^B - n_C) \times 1$$

4.2.1 Some remarks to the problem of statically overdeterminate coupling

In contrast to the flexible coupling approach rigid coupling entails in all cases a loss of degrees of freedom due to the compatibility condition at the coupling points. Thus, fulfillment of the compatibility condition as usually expressed by a number of n_C constraints leads to a reduction of the generalized coordinates by the number of constraints. No disadvantage results unless a case of statically overdeterminate coupling is considered. The most extreme situation imaginable may be characterized by

$$(47) \quad n^A + n^B = n_C$$

which no longer makes sense because of a total loss of degrees of freedom. Thus, problems with statically overdeterminate coupling conditions must be treated delicately. The problem may be eased somewhat by

- Using the flexible coupling or mixed coupling approach as far as possible even though the coupling joints are relatively stiff;

- Using more normal modes, i.e. generalized coordinates of the substructures in question, which is not always possible especially if the modal data are experimentally determined.

4.2.2 An approach to establish independent coordinates

The determination of the transformation matrix T , Eq.(45), can be seriously hampered by the requirement that a square matrix $\bar{\Phi}$ be found which may be inverted. This process can be facilitated considerably by means of the so-called "zero eigenvalue theorem" published in Ref.[15] where a comprehensive proof is given. The mathematical background of this approach is also described for instance in Ref.[16] especially aiming at a method to determine the rank of a matrix by considering the well-known Gram's determinant.

With special view to the rigid coupling method described above, the mathematical problem can be characterized as follows: a transformation matrix T has to be determined so that transformation (44) relates the dependent coordinates \bar{q} to a set of independent coordinates p^* . The following steps must be performed to attain this aim:

- Calculate a matrix

$$(48) \quad E = G^T G$$

then E will be symmetric of order $(n^A + n^B) \times (n^A + n^B)$ and positive semi-definite;

- Determine the eigenvalues λ_i , ($i = 1, 2, \dots, n^A + n^B$) of matrix E and corresponding modal matrix H the columns of which represent the eigenvectors H_i of matrix E .
- Identify the columns of H which correspond to the zero eigenvalues of matrix E . This step requires special attention as to calculation round-offs which can affect the rigorous distinction between the finite eigenvalues and the zero eigenvalues to be identified.
- Arrange the eigenvectors H_i corresponding to the zero eigenvalues in a matrix which is the required transformation matrix T of order $(n^A + n^B) \times (n^A + n^B - n_C)$. The number of constraints n_C is equivalent to the number of positive eigenvalues.

4.3 Mixed coupling

As is well known, coupling conditions sometimes occur which cannot be categorized clearly as purely rigid coupling or purely flexible coupling. This special type of coupling is termed mixed coupling which can best be explained with the example of a wing-with-stores system. As is evident from Figure 3, the flexible coupling conditions are the ones related to the displacements $u_y^A, u_y^B, \alpha_x^A, \alpha_x^B, \alpha_z^A, \alpha_z^B$. The coupling stiffnesses related to the degrees of freedom within the pylon symmetry plane are usually much higher by more than one order of magnitude, so that these connections can be considered rigid. Due to this fact, coupling between a wing and an underwing store by means of a pylon can be carried out in good approximation by satisfying the compatibility conditions

$$(49) \quad \begin{Bmatrix} u_x^A \\ u_z^A \\ \alpha_y^A \end{Bmatrix} - \begin{Bmatrix} u_x^B \\ u_z^B \\ \alpha_y^B \end{Bmatrix} = 0$$

In such a case of mixed coupling conditions, the equations of motion can be formulated as follows:

$$(50) \quad T^T (-\omega^2 \bar{M} + \bar{K} + \Delta \bar{K}) T p^* = 0$$

where matrix T accounts for the rigid coupling conditions. Matrix $\Delta \bar{K}$ relating to the flexible coupling conditions is basically equivalent to Eq.(37) but reordered in accordance with Eq.(41).

4.4 Exemplary application of the mixed coupling approach

To give an impression of how the modal coupling approach works, the swept back wing model with two underwing stores as shown in Figure 2 was subjected to the first application of this approach, see Ref.[5]. The model was decomposed into the clean wing (stores removed) and the two stores as substructures. The modal data of the clean wing system were determined in a GVT. The two stores can be considered rigid with mass inertia properties as listed below

$$\begin{aligned} m &= 8.14 \text{ kg} & \theta_x &= 132.1 \text{ kg cm}^2 \\ X_{CG} &= Y_{CG} = Z_{CG} = 0 & \theta_y &= \theta_z = 895 \text{ kg cm}^2 \end{aligned}$$

The measured normal frequencies of the clean wing substructure are given in Table 4. The stiffness matrices of the pylons were determined by measuring the flexibility matrix as described in Section 3.3.

Normal mode	r=1	2	3	4	5	6
Normal frequency [Hz]	11.6	66.06	97.52	163.20	183.87	288.03

Table 4: Normal frequencies of the clean wing.

Application of the mixed modal coupling approach resulted in a list of normal frequencies of the coupled system given in Table 5 together with a set of corresponding normal frequencies measured in a GVT.

Normal mode	Normal frequency [Hz]	
	calculated	measured
r=1	6.85	7.51
2	6.86	7.74
3	8.20	8.36
4	21.37	20.46
5	21.48	20.66
6	27.86	27.44

Table 5: Normal frequencies of the coupled wing-with-stores system.

Agreement between the measured and the modal coupling results is fairly good with maximum errors of about -10% for the first two values, which is probably due to mismeasurements of the pylon yaw stiffness whereas the other values show much better agreement. The agreement is not nearly as good at higher frequencies which may have been caused by improper loads at the substructure interfaces and frequency range truncation. These problems will be discussed in the following section.

4.5 Convergence problem

Whether a modal coupling calculation results in a satisfactory description of the elasto-dynamic behavior of the complete system depends on the conditions under which the different substructures have been tested. First of all, for every substructure only a limited number of normal modes can be measured. This truncation of the frequency range may result in convergence problems. Even more difficult to cope with is the problem arising from the requirement that the dynamic load distribution in the substructure GVT must be closely representative of the dynamic load distribution in the complete system. In other words, the normal modes of the substructures must contain dynamic load distributions, a superposition of which rapidly converges to the dynamic load distribution in the complete system. This load conditioning problem may best be illustrated by the example of a halfwing with one underwing store as sketched in Figure 5.

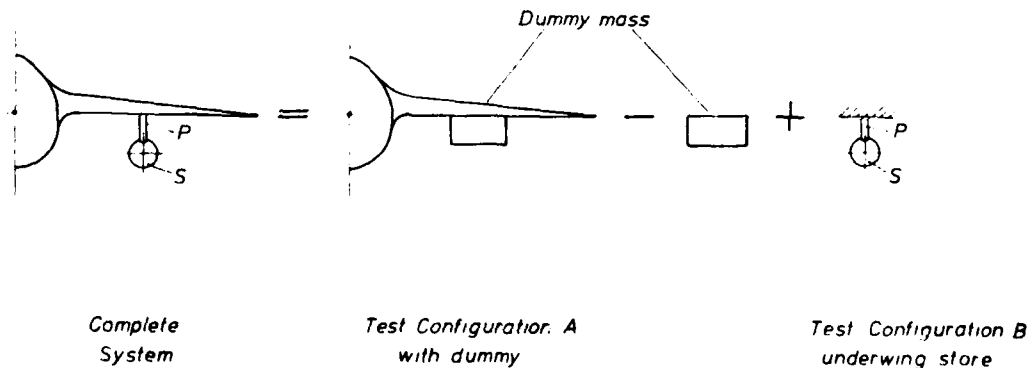


Figure 5: Wing-with-store system.

In the general case of an aircraft with various interchangeable stores, it proves convenient to decompose the complete system into two types of different substructures conditioned in such a way that they can serve as basic GVT configurations of type A (clean wing aircraft) and B (stores). For the simple wing-with-store system depicted in Figure 5, configuration A consists of the clean wing structure with the pylon/store system replaced by a nearly rigid dummy mass, approximately representing the mass inertia properties of the store. The dummy is rigidly coupled to the wing, i.e. without any flexible interface elements.

Test configuration B consists of the pylon/store unit fixed to a heavy seismic block at the wingside end of the pylon. As for the fixation mechanism and the GVT to be carried out on this configuration, the same conditions as recommended in Section 3.3 have to be fulfilled. The result is a set of six normal modes Φ_{Er}^B with the pertaining normal mode characteristics M_{Er}^B , f_{Er}^B and γ_{Er}^B ($r = 1, 2, \dots, 6$).

According to Figure 5 the main steps to be conducted in establishing the mathematical model of the complete system may be described as follows:

1. GVT on configuration A (clean wing plus mass dummy);
2. GVT on configuration B (store/pylon system);
3. Removal of the dummy mass from configuration A by means of a modal correction calculation (by subtracting a modal correction matrix ΔM^A from matrix M^A);
4. Coupling of subsystem B to the clean wing system by means of rigid coupling.

There are no serious problems in carrying out steps 1, 2 and 3. However, step 4 entails a special problem deserving closer consideration. It is obvious that coupling substructure B rigidly to the clean wing aircraft involves not only the above-mentioned set of six elastic normal modes Φ_{Er}^B but also the rigid body modes Φ_{Or}^B of the store/pylon system in free-free condition. Due to the various boundary conditions these two mode sets Φ_{Er}^B and Φ_{Or}^B are not mutually orthogonal. This inconsistency generally results in off-diagonal elements in the generalized mass matrix

$$(51) \quad M^B = (\Phi^B)^T A^B \Phi^B = \begin{bmatrix} M_O^B & & M_{OE}^B \\ & \ddots & \\ M_{EO}^B & & M_E^B \end{bmatrix}$$

where

$$(52) \quad \Phi^B = \begin{bmatrix} \Phi_O^B \\ \vdots \\ \Phi_E^B \end{bmatrix} \quad \begin{array}{l} \text{positive definite mass matrix of the store/pylon system;} \\ \end{array}$$

and

$$M_O^B = (\Phi_O^B)^T A^B \Phi_O^B \quad \begin{array}{l} \text{diagonal matrix of the generalized masses } M_{Or}^B \text{ corre-} \\ \text{sponding to the rigid body modes } \Phi_{Or}^B \text{ of the store/pylon} \\ \text{system in free-free condition;} \end{array}$$

$$M_E^B = (\Phi_E^B)^T A^B \Phi_E^B \quad \begin{array}{l} \text{diagonal matrix of the generalized masses } M_{Er}^B \text{ corre-} \\ \text{sponding to the elastic normal modes } \Phi_{Er}^B \text{ of configura-} \\ \text{tion B;} \end{array}$$

$$M_{OE}^B = (\Phi_O^B)^T A^B \Phi_E^B \quad \begin{array}{l} \text{matrix fully occupied due to the nonorthogonality of the} \\ \text{normal modes } \Phi_{Or}^B \text{ and } \Phi_{Er}^B, M_{OE}^B = (M_{EO}^B)^T. \end{array}$$

As experience has shown, a mass matrix A^B stemming for instance from finite element analysis is fairly correct and usually much closer to the physical reality than the complementary analytical stiffness matrix C^B can be. Thus, matrix M_{OE}^B can be determined easily on the basis of the normal modes Φ_{Er}^B and Φ_{Or}^B and the mass matrix A^B .

The generalized stiffness matrix can be written as follows:

$$(53) \quad K^B = (\Phi^B)^T C^B \Phi^B = \begin{bmatrix} K_O^B & & K_{OE}^B \\ & \ddots & \\ K_{EO}^B & & K_E^B \end{bmatrix}$$

where, because $(\Phi_O^B)^T C^B = 0$ with C^B semi-definite,

$$(54a) \quad K_O^B = (\Phi_O^B)^T C^B \Phi_O^B = 0$$

$$(54b) \quad K_{OE}^B = (\Phi_O^B)^T C^B \Phi_E^B = 0$$

$$(54c) \quad K_{EO}^B = (K_{OE}^B)^T$$

Furthermore

$$(55) \quad K_E^B = (\Phi_E^B)^T C^B \Phi_E^B$$

is a diagonal matrix comprising the generalized stiffnesses $K_{Er}^B = (\omega_{Er}^B)^2 M_{Er}^B$ with ω_{Er}^B denoting the r-th circular normal frequency.

Thus, Eqs. (51) through (55) show that the mathematical model of the store/pylon system can be established despite the nonorthogonality of the normal modes Φ_{Or}^B and Φ_{Er}^B in a relatively simple way without any information on the stiffness distribution of the store/pylon unit. The only store/pylon data required are:

- A complete set of modal data related to the rigid body degrees of freedom (diagonal matrix M_O^B and normal mode shapes Φ_{Or}^B);
- A complete set of modal data measured in a GVT in configuration B (diagonal matrix M_E^B , normal mode shapes Φ_{Er}^B and normal frequencies ω_{Er}^B);
- A reliable mass matrix A^B to calculate matrix $M_{OE}^B = (M_{EO}^B)^T$.

Setting up the mathematical model of the complete wing-with-store system requires also the knowledge of the elastic normal modes and the related modal data of configuration A and, in the case of rigid coupling, the transformation matrix T .

5. Effects of localized nonlinearities

The world of structural dynamics is not always as linear as described in the foregoing chapters, though a great many problems can be solved quite successfully on such a simplified linear basis. In the past decade, it has become increasingly evident that a total disregard of nonlinear effects may in a considerable number of cases lead to severe mispredictions of the real elastodynamic behavior of aircraft structures and also to misinterpretations of ground and flight test results. The effects of structural nonlinearities on the dynamic and aeroelastic behavior of aircraft has been dealt with in numerous publications, see for instance Refs. [17], [18], [19], which place special emphasis on locally concentrated nonlinearities in the control mechanism.

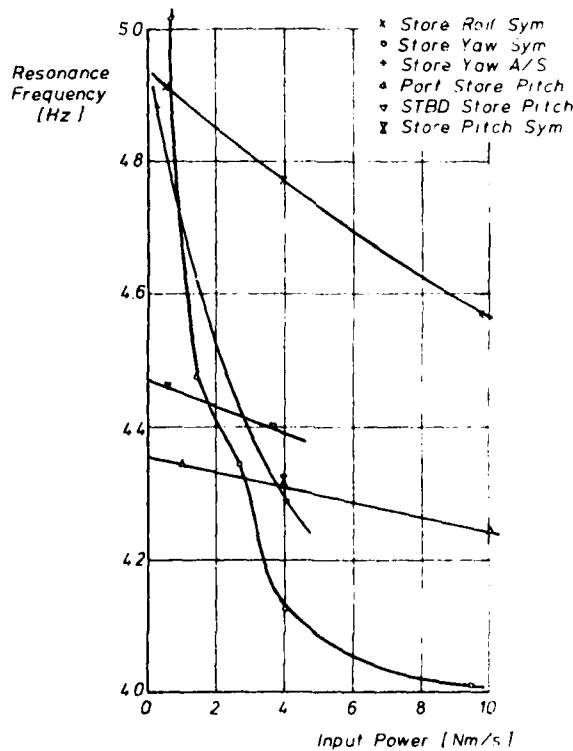


Figure 6: Resonance frequencies of low-frequency store modes versus input power.

There are also a few publications, Refs. [20], [21], [22], concerned with nonlinearities in wing-with-stores configurations. Measurements on a sweepable wing aircraft with underwing stores illustrate impressively how seriously the dynamic behavior of the store modes may be inflicted by backlash-friction (hysteresis-type) nonlinearities such as occur in wing/store connections, Ref. [20]. Thus, Figure 6 shows the variation of store roll, yaw and pitch mode frequencies versus input power. Not only a drop of the yaw mode frequency versus input power and frequency crossing incidents between the yaw and the pitch mode but also strong asymmetry effects have been identified. In particular Ref. [21] focusses on the influence of an hysteresis-type nonlinearity in the store yaw degree of freedom on the flutter behavior of the same type of sweepable wing aircraft. That aircraft with fixed wing can also be seriously affected by nonlinearities in the pylon connections between stores and wing was clearly found in the course of developing an active flutter suppression system for the F-4F aircraft, Ref. [22]. Figure 7 shows measured frequency versus airspeed plots for the wing bending mode and the store roll mode indicating a significant frequency jump due to differences in the vibration amplitude level. It is obvious that this kind of nonlinearity may severely hamper not only the evaluation of ground and flight vibration tests but also analytical flutter prediction and the design of optimum control laws for active flutter suppression.

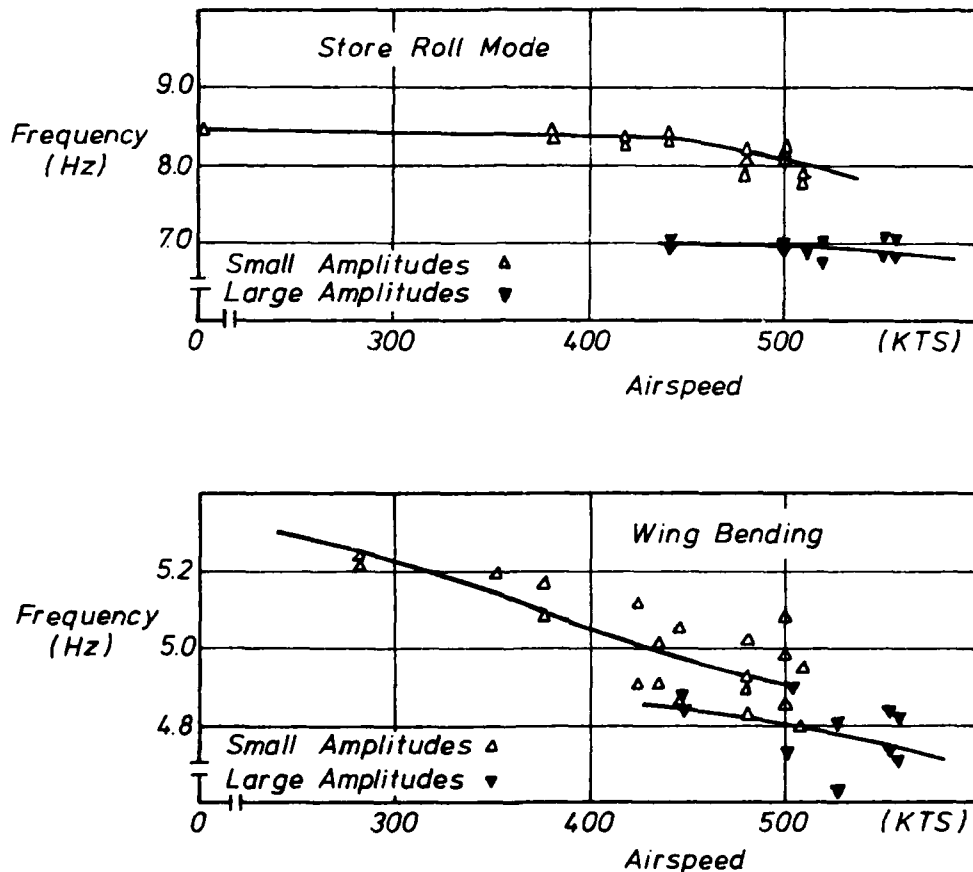


Figure 7: Frequency discontinuity due to structural nonlinearities.

5.1 Application of modal synthesis to nonlinear systems

To overcome these problems the methods of analytical flutter prediction and also ground and flight vibration testing techniques have to be extended to systems with localized nonlinearities. A promising concept for attaining this goal may be elaborated on the basis of the above-described modal synthesis approaches in combination with methods to identify nonlinear joints and connecting elements.

With special regard to aircraft wing-with-stores configurations, such a concept may essentially consist of two parts no matter whether modal correction or modal coupling is applied.

AD-A112 533

ADVISORY GROUP FOR AEROSPACE RESEARCH AND DEVELOPMENT--ETC F/G 1/3
DYNAMIC ENVIRONMENTAL QUALIFICATION TECHNIQUES.(U)
DEC 81

UNCLASSIFIED

AGARD-CP-318

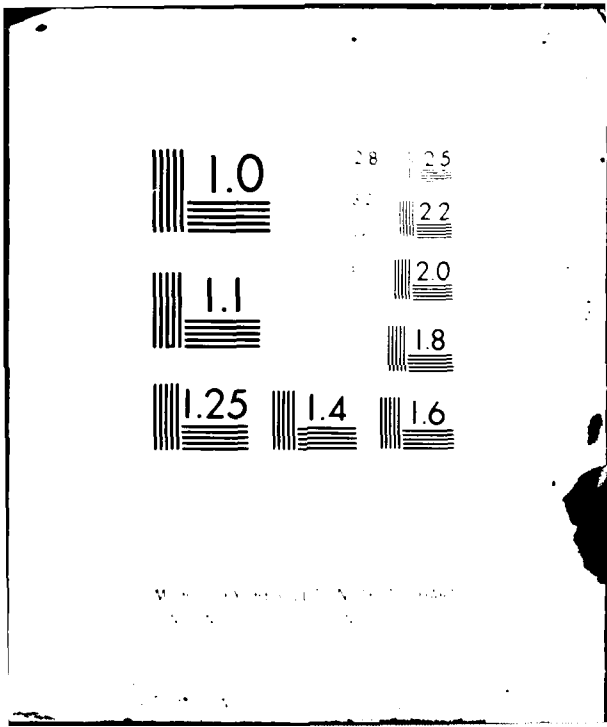
NL

3 of 3

AD-A
112533



END
DATE
FILMED
104-82
DTIC



Resolution Test Chart
1963

5.1.1 Nonlinear modal correction concept

- Determination of the modal data of a test configuration artificially linearized by replacing the nonlinear elements by linear and slightly damped dummy devices. Alternatively, linearization can also be attained approximately by keeping the test forces for all normal modes within the range where nonlinearities behave nearly linearly. This may be at low exciting forces (as suggested in Section 3.3) before damping forces reach the transition point between "static" and "gliding" friction or, far beyond this point, at higher force levels asymptotically converging to another nearly linear force deflection range;
- Identification of the nonlinearities in the connecting parts between wing, pylon and store as to allow simple formulation of the nonlinear equations of motion on the basis of the modal data of the artificially linearized test structure with nonlinear modal correction matrices accounting for the nonlinearities.

5.1.2 Nonlinear modal coupling concept

- Decomposition of an aircraft with underwing stores into the clean wing system and the different stores as largely linear substructures and the pylons as nonlinear connecting elements. Measurement of the substructure modal data in GVT;
- Identification of the pylon connection nonlinearities in the same way as described for the nonlinear modal correction concept.

5.2 Identification and mathematical modelling of nonlinear connecting elements

The elastodynamic behavior of localized nonlinearities such as those typically occurring in aircraft control mechanisms or in the connecting parts between wing and underwing stores can be determined with good approximation based on the principle of *energetic equivalence* in terms of equivalent amplitude-dependent stiffness and damping values.

Let $F(\beta, \dot{\beta})$ be the force deflection diagram of a nonlinear joint either in measured or analytical form, then the equivalent stiffness and damping can be calculated by means of

$$(56) \quad C_e'(B) = \frac{1}{\pi B} \int_{\varphi=0}^{2\pi} F(B \cos \varphi, -\omega B \sin \varphi) \cos \varphi \, d\varphi$$

and

$$(57) \quad \gamma_e(B) = \frac{1}{C_e'(B) \pi B} \int_{\varphi=0}^{2\pi} F(B \cos \varphi, -\omega B \sin \varphi) \sin \varphi \, d\varphi$$

where $F(\beta, \dot{\beta})$ is the periodic force function in response to an harmonic displacement function

$$(58) \quad \beta = B \cos \varphi$$

and where

$$(59) \quad \varphi = \omega t$$

is the integration variable with the circular frequency ω and time t . According to Eq. (57) the equivalent damping coefficient is defined as damping loss angle.

Fortunately, F is for a preponderant number of aeroelastic problems merely a function of deflection β , i.e. $F = F(\beta)$, which holds true especially for underwing stores problems. This property features not only a simpler solution of the integrals (56) and (57) but also less test effort.

The integrals (56) and (57) can be solved analytically if function $F(\beta)$ can be approximated sectionwise by a number of straight lines. As may be seen from Ref. [18] such a solution becomes more complicated the greater the number of different straight line sections necessary to obtain a curve fitting sufficiently close to the nonlinear force deflection diagram. This situation is even more aggravated for cases with force deflection diagrams changing shape from amplitude to amplitude, thus requiring an individual curve fitting for every amplitude level. The shortcomings of such a sectionwise analytical integration can be avoided by an experimental approach characterized by simplicity, greater accuracy and broader general applicability.

5.3 Determination of the equivalent stiffness and damping values by means of an experimental approach

A closer look at the integrals (56) and (57) reveals the fact that $C_e'(B)$ is merely the real part J_1' of the first harmonic J_1 of the periodic force F divided by B . In the same way $\gamma_e(B)$ can be interpreted as the imaginary part J_1'' of J_1 divided by

$C_e'(B)B$:

$$(60a) \quad C_e'(B) = \frac{J_1'}{B}$$

$$(60b) \quad \gamma_e(B) = \frac{J_1''}{C_e'(B)B} = \frac{J_1''}{J_1'}$$

For this reason it is obvious that the terms $C_e'(B)$ and $\gamma_e(B)$ can be determined by co-quad¹ analysis which is well known from the GVT technique. This analysis can be carried out either by means of a digitized time series analysis or by applying a more conventional analogue circuit, the block diagram of which is shown in Figure 8. It consists of two parts each of which is identically composed of a multiplier M_1 , an extreme low-pass filter LP and a second multiplier M_2 . The following operations are consecutively executed:

- Multiplication of the periodic force function $F(\delta)=F(B \cos \varphi)$ with the reference voltage $\cos \varphi$ in phase with the harmonic deflection function $\delta = B \cos \varphi$ which can be written as

$$(61) \quad F(\delta) \cos \varphi = \cos \varphi \sum_{n=1}^{\infty} (J_n' \cos n\varphi + J_n'' \sin n\varphi) \quad ;$$

- Filtering out all the time-variant components from the output of multiplier M_1 leads to the time-invariant term $1/2 J_1'$ which after multiplication with $2/B$ results in the equivalent stiffness in accordance with Eq. (60a).

Furthermore, the second part of the circuit delivers the term $1/2 J_1''$ which after multiplication with $2/C_e'(B)B$ results in the equivalent damping loss angle $\gamma_e(B)$ as defined in Eq. (60b).

This procedure requires a special displacement-controlled excitation, forcing the nonlinear test specimen to carry out an harmonic deflection $B \cos \varphi$. In reaction to this requirement the exciting force becomes periodic and may be measured by commercial force gauges. Moreover the excitation frequency must be extremely low (quasi-static) to avoid disturbing effects due to inertia forces.

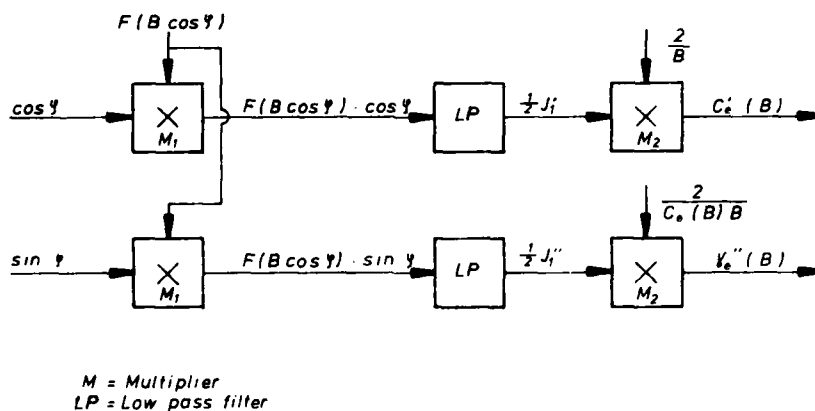


Figure 8: Block diagram to determine the equivalent stiffness and damping values of nonlinear elements.

In extending this procedure to measurements at higher frequencies with mass inertia forces thus having the same order of magnitude as the equivalent stiffness forces, we insert into Eq. (61) not only the quasi-static periodic force $F(\delta)$ but also the additional mass inertia force. Let the test setup for measuring the equivalent stiffness and damping coefficients $C_e'(B)$ and $\gamma_e(B)$ of a nonlinear element be represented by a longitudinal single-degree-of-freedom oscillator. Then forcing the system to an harmonic vibration $\delta = B \cos \varphi$

¹ Co(incidence)-quad(rature) analysis is identical to a vector component analysis delivering real and imaginary parts of the first harmonic of a periodic signal in relation to a given phase reference.

with a finite frequency results not only in damping and stiffness forces but also in a mass inertia force $m\ddot{B} = -m\omega^2 B \cos \varphi$ which is added to $F(B)$ in Eq.(61).

After low-pass filtering the product

$$(62) \quad (F(B) - m\omega^2 B \cos \varphi) \cos \varphi$$

we obtain in accordance with Eqs.(60) and (61)

$$(63) \quad J_1' = B(C_e'(B) - \omega^2 m)$$

as the first harmonic of the periodic dynamic force $F(B) + m\ddot{B}$. By keeping the deflection amplitude $B = \text{const}$ at two different frequencies ω_1 and ω_2 we measure two different values of J_1' :

$$(64a) \quad J_1'(\omega_1) = B(C_e'(B) - \omega_1^2 m)$$

$$(64b) \quad J_1'(\omega_2) = B(C_e'(B) - \omega_2^2 m)$$

Under the condition of m being invariant with respect to frequency changes, the equivalent stiffness value $C_e'(B)$ can be determined from Eqs.(64) as follows:

$$(65) \quad C_e'(B) = \frac{J_1'(\omega_1)\omega_2^2 - J_1'(\omega_2)\omega_1^2}{B(\omega_2^2 - \omega_1^2)}$$

Mass inertia forces have no effect on the determination of J_1'' because low-pass filtering of the expression

$$(66) \quad (F(B) - m\omega^2 B \cos \varphi) \sin \varphi$$

results in

$$(67) \quad J_1'' = \gamma_e(B) C_e'(B) B$$

which is equivalent to Eq.(60b).

5.4 Experimental verification

To get an idea of the accuracy and limitations of the approach just described, verification tests were performed on a simple one-degree-of-freedom oscillator with nonlinear stiffness. The system was harmonically excited at several amplitude levels for each of which both the resonance frequency and the corresponding input energy were measured by means of the phase resonance criterion. With these data and the correct mass inertia properties in hand the equivalent stiffness and damping coefficients were recalculated.

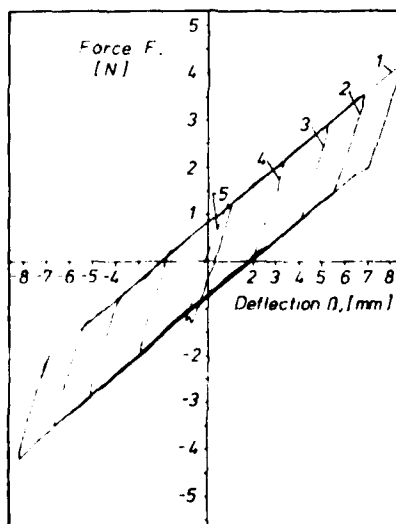


Figure 9: Nonlinear force deflection diagram.

The test specimen in question is characterized by the force deflection diagram plotted in Figure 9. The related equivalent stiffness (in terms of resonance frequency) and damping values are given in Figure 10 as functions of deflection amplitude B showing good agreement between the results of the equivalent linearization approach and the dynamic verification measurements thus justifying the procedure suggested in Section 5.3.

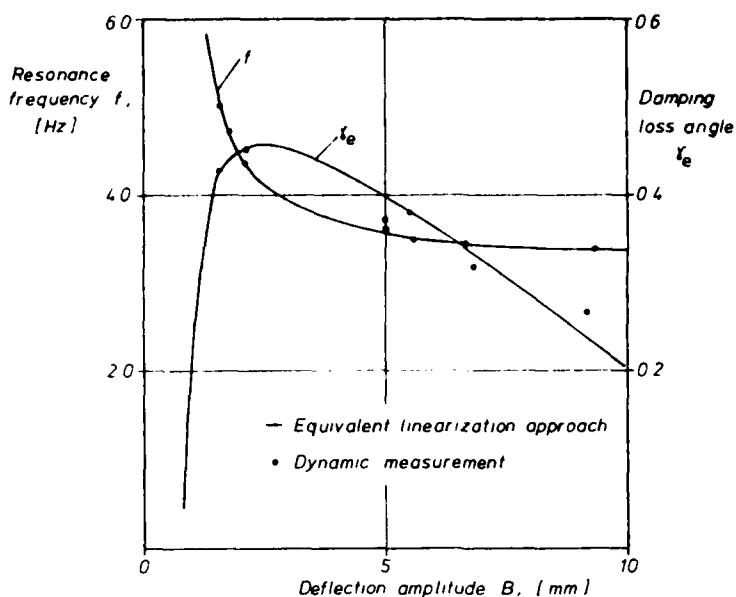


Figure 10: Equivalent stiffness (in terms of resonance frequency) and damping coefficients of an hysteresis-type nonlinearity.

5.5 Integration of nonlinearities into the equations of motion

Once the modal data of the linearized basic system (in the case of modal correction) or subsystems (in the case of modal coupling) and the dynamic behavior of the nonlinear connecting elements are determined, the nonlinear equations of motion can be formulated according to Ref. [8]:

- For the case of nonlinear modal stiffness correction by adding to matrix K in the equations of motion (3) or (6) of the linearized basic test structure a nonlinear modal correction matrix

$$(68) \quad \Delta K = \Delta K_{NL} - \Delta K_L$$

where in accordance with Eq. (27a)

$$(69) \quad \Delta K_L = \Phi_P^T C_L \Phi_P$$

and

$$(70) \quad \Delta K_{NL} = \Phi_P^T C_{NL} \Phi_P$$

Matrix C_L accounts for the pylon connection stiffness in the linearized test configuration whereas matrix C_{NL} contains the nonlinear stiffness properties of the pylon connection as determined on the basis of the energetic equivalence, see Section 5.3.

- For the case of nonlinear modal (flexible) coupling by adding to matrix K in the equations of motion (29) of the uncoupled linearized substructures in accordance with Eq. (37) a nonlinear modal coupling matrix

$$(71) \quad \Delta K = \Phi_F^T C_{NL} \Phi_F$$

where matrix C_{NL} accounts for the nonlinear pylon connection stiffness as determined on the basis of the energetic equivalence, see Section 5.3.

In order to enable a consistent experimental determination of matrix C_{NL} , Eqs. (70) and (71), the reference axis for the pylon connection should be chosen in such a way that no coupling between the different degrees of freedom (see Figure 3) is present, i.e. off-diagonal elements of matrix C_{NL} should be zero as far as possible.

5.6 Effects of pylon nonlinearities in the light of the "one and one-half degrees-of-freedom oscillator"

Recent windtunnel flutter tests on a halfwing model with sweepable wing and an underwing store and with nonlinearities in both the store/pylon connection and the wing sweep mechanism produced rather poor agreement between the test results and corresponding nonlinear

flutter calculations. Further inquiry disclosed a physical phenomenon which may be explained by differences in the excitation energy transport due to various exciter positions. Thus, in other words, aircraft with underwing stores show different dynamic responses depending on whether they are excited from the wingside or from the pylonside. This behavior has been confirmed by a number of ground and flight vibration tests on aircraft external stores configurations.

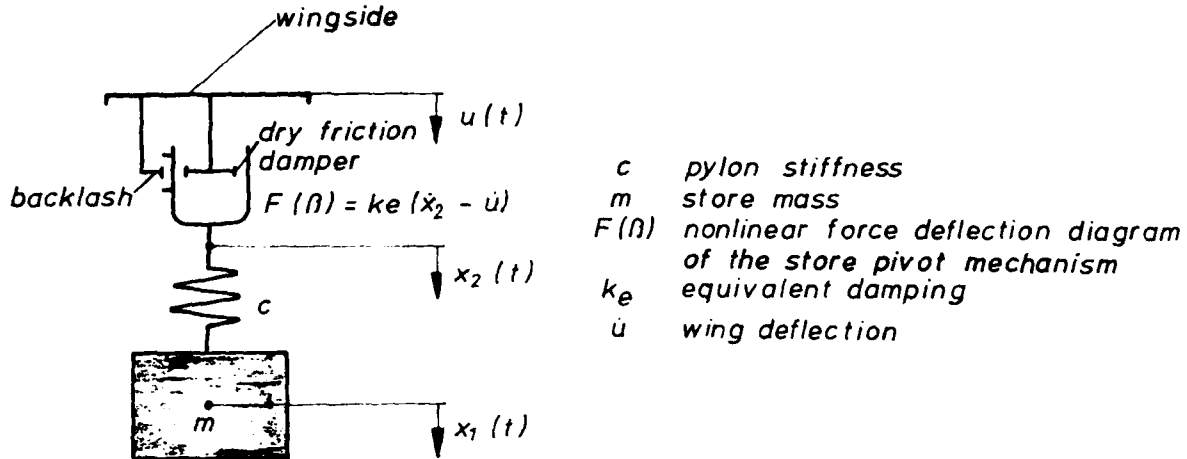


Figure 11: Sketch of an oscillator with one and one-half degrees of freedom.

The physical background of this phenomenon can best be illuminated by studying a largely simplified oscillator, see Figure 11, consisting of a mass m , linear stiffness c and nonlinear backlash friction-type damping represented by the equivalent damping term k_e . The coefficients m and c stand for the store mass inertia and the pylon stiffness, respectively. The elements k_e and c are connected to each other in a series arrangement. With direct excitation $P(t)$ at the store and with the wingside kept at rest, each of the two third-order differential equations, see Ref. [11], written in terms of x_1 and x_2 describes the vibration behavior of the oscillator:

$$(72a) \quad \ddot{x}_1 + \frac{c}{k_e} \dot{x}_1 + \frac{c}{m} x_1 = \frac{1}{m} \dot{p} + \frac{c}{k_e m} p$$

$$(72b) \quad \ddot{x}_2 + \frac{c}{k_e} \dot{x}_2 + \frac{c}{m} x_2 = \frac{c}{k_e m} p$$

In the case of harmonic excitation $p = P e^{j\omega t}$ the relation between the deflection amplitudes X_1 and X_2 of the harmonic responses $x_1 = X_1 e^{j\omega t}$ is defined by

$$(73) \quad \frac{X_1}{X_2} = 1 + j \frac{k_e \omega}{c}$$

Let the system be excited from the wingside by a wing vibration $u(t)$ then the vibration behavior is defined again by each of the two third-order differential equations written in terms of $y_1 = x_1 - u$ and $y_2 = x_2 - u$:

$$(74a) \quad \ddot{y}_1 + \frac{c}{k_e} \dot{y}_1 + \frac{c}{m} y_1 = -\frac{c}{k_e} \dot{u} - \ddot{u}$$

$$(74b) \quad \ddot{y}_2 + \frac{c}{k_e} \dot{y}_2 + \frac{c}{m} y_2 = -\frac{c}{k_e} \dot{u}$$

which in the case of an harmonic wing vibration $u = U e^{j\omega t}$ leads to the relation

$$(75) \quad \frac{X_1}{Y_2} = j \frac{k_e}{\omega m}$$

It turns out that by keeping k_e in Eqs. (73) and (75) (wingside and storeside excitation) at the same constant value and thus equating the relative motions X_2 and Y_2 in the damped element, the vibration behavior varies completely with the way the system is excited.

6. Conclusion

The modal coupling methods as well as the modal correction approach constitute a promising tool to deal with problems arising especially in conjunction with flutter clearance and dynamic qualification of combat aircraft with numerous underwing stores configurations. As is shown, all these methods can be employed without any information of the stiffness distribution. A reliable mass model attained for instance from a finite element analysis, the elastodynamic properties of the store/wing connections and the modal data (generalized masses, normal frequencies and normal mode shapes) of the different substructures (in the case of modal coupling) and of a basic test structure (in the case of modal correction) are the only prerequisites to set up the equations of motion of the coupled system. Consequently, all these approaches can be employed largely on the basis of measured data. Moreover, some emphasis has been placed on the convergence problem due to frequency range truncation and inconsistent boundary or coupling conditions. It has been shown that interface loading is a convenient tool to ease this problem considerably.

Finally, attention has been drawn to increasingly troublesome problems due to localized nonlinearities in the wing/pylon/store connections. An experimental approach based on the well-known idea of the *energetic equivalence* was presented turning out to be a useful means to identify the dynamic behavior of nonlinear joints and connecting elements in a way conveniently adapted to establishing nonlinear equations of motion of an aircraft with external stores.

7. References

- [1] Hurty, W.C. Dynamic Analysis of Structural Systems by Component Mode Synthesis. Techn.Memorandum No.32-530, Jet Propulsion Laboratory, Pasadena, Calif. (1964).
- [2] Gladwell, G.M.L. Branch Mode Analysis of Vibrating Systems. *Journ. Sound Vibration*, Vol.1, pp.41-59 (1960).
- [3] Goldman, R.L. Vibration Analysis by Dynamic Partitioning. *AIAA Journ.* 7(6), pp.1152,1154 (1969).
- [4] Hu, S.N. Review of Modal Synthesis Techniques and New Approach. *Shock and Vibr.Bul.* 40(4), pp.25-30 (1969).
- [5] Breitbach, E. Investigation of Spacecraft Vibrations by Means of the Modal Synthesis Approach. ESA-SP-121 (1976).
- [6] Bertram, A. Dynamic Qualification of Large Space Structures by Means of Modal Coupling Techniques. Proc. XXX Int'l Astronaut.Congress, Munich, W.Germany (1979).
- [7] Küssner, H.G. Breitbach, E. Bestimmung der Korrekturglieder der Bewegungsgleichungen bei Änderung eines elastomechanischen Systems. AVA Report 69 J 101 (1969).
- [8] Breitbach, E. Treatment of the Control Mechanisms of Light Airplanes in the Flutter Clearance Process. NASA CP 2085, Part II, pp.437-466 (1979).
- [9] Breitbach, E. Modal Synthesis. Modal Correction - Modal Coupling. Lecture held in the course "Identification of Vibrating Structures." at CISM, Udine, Italy, Oct.20-24, 1980.
- [10] Bertram, A. Degener, M. Freymann, R. Development of Modal Techniques Using Experimental Modal Data. DFVLR Report IB 253-77 C 05 (1977).
- [11] Meirovitch, L. Elements of Vibration Analysis. McGraw-Hill Book Co., New York (1975).
- [12] Freymann, R. Structural Modifications on a Swept Wing Modal with Two External Stores by Means of Modal Perturbation and Modal Correction Methods. ESA-TT-463 (Translation of DLR-FB 77-21) (1978).
- [13] Freymann, R. Development of Modal Techniques Using Experimental Modal Data. Work Package 1 - Small Modifications of Structural Configurations. Users' and Programmers' Manual for the Computer Program DIMOC. DFVLR Report IB 253-78 C 02 (1978).
- [14] Bertram, A. Development of Modal Techniques Using Experimental Modal Data. Work Package 2 - Users' and Programmers' Manual for the Computer Program MODAC. DFVLR Report IB 253-79 C 07 (1979).
- [15] Walton, W.C. Steeves, E.C. A New Matrix Theorem and its Application for Establishing Independent Coordinates for Complex Dynamical Systems with Constraints. NASA TR R-326 (1969).
- [16] Courant, R. Hilbert, D. Methods of Mathematical Physics. Volume 1. Interscience Publishers, Inc., New York (1953).

- [17] Breitbach, E. Aircraft Flutter Simulation by Means of the Electronic Analogue Computer with Special Regard to Structural Nonlinearities. ESRO-TT-121, (Translation of DLR-FB 73-30) (1974).
- [18] Breitbach, E. Effects of Structural Nonlinearities on Aircraft Vibration and Flutter. AGARD Report No.665 (1977).
- [19] Breitbach, E. Flutter Analysis of an Airplane with Multiple Structural Nonlinearities in the Control System. NASA TP 1620 (1980).
- [20] Haidl, G. Non-Linear Effects in Aircraft Ground and Flight Vibration Tests. AGARD Report No.652 (1971).
- [21] De Ferrari, G.
Chesta, L.
Sensburg, O.
Lotze, A. Effects of Nonlinearities on Wing Store Flutter. AGARD Report No.687 (1980).
- [22] Sensburg, O.
Hönlinger, H. Active Flutter Suppression on an F-4F Aircraft with External Stores Using already Existing Control Surfaces. AIAA Proceedings of the 21st Structures, Structural Dynamics and Materials Conference, May 12-14, 1980.

STOL AIRCRAFT STRUCTURAL VIBRATION
PREDICTION FROM ACOUSTIC EXCITATION

by

B. F. Dotson
Chief Structural Dynamics
The Boeing Military Airplane Company
P.O. Box 3707 (MS 41-10)
Seattle, Washington 98124
U.S.A.

and

J. Pearson
Project Engineer
U.S. Air Force Wright Aeronautical
Laboratories (F18G)
Dayton, Ohio 45433
U.S.A.

SUMMARY

A method was developed to improve environment vibration prediction methods, particularly in the lower frequency range where high acoustic excitation is expected on STOL aircraft. A rigorous mathematical spectral analysis approach was used which simulated the structure with finite element models (FEM) and used measured and calculated acoustic input data for the forcing function. Calculated and measured vibrations levels were compared on a medium sized Upper Surface Blowing (USB) STOL aircraft.

The development of a method for prediction of the external acoustic environment of USB flap-type STOL aircraft was also accomplished. The method compares favorably with actual measurements and represents a significant improvement in acoustic prediction methods for aircraft with USB type flaps. The method includes scaling factors for engine size, thrust, aircraft size, and other parameters.

Finally, noise and vibration levels were predicted on a small STOL aircraft and later compared to measured data.

I. INTRODUCTION

Short-takeoff-and-landing (STOL) aircraft usually have more severe vibration and acoustic environment in which the crew and equipment operate compared with conventional aircraft. The direct impingement of engine exhaust gases on flaps of upper surface blowing (USB) and lower surface blowing (LSB) configurations poses a potential problem of intense flap vibration. In addition, STOL engines are large and usually placed close to the fuselage, which increases even more the expected intensity of the external noise field to which the fuselage is subjected. As a result of potential transmitted flap vibration and the more intense external noise field, STOL aircraft interior vibration levels are expected to be substantially higher than for conventional aircraft, especially at lower frequencies.

Traditionally environmental vibration prediction has been accomplished by statistical energy methods (SEA). Statistical energy methods provide meaningful answers when many closely spaced modes are involved. At the lower frequencies of fundamental aircraft modes, this requirement is not satisfied and SEA breaks down. Also, a second very common approach to environmental vibration prediction is to use scaling methods in which the characteristics of existing aircraft having known vibration levels are scaled to new similar aircraft. Himmelblau, Fuller, and Scharton give a good summary of these methods (Reference 1). For this study, with the concern for low frequencies and the desire for more accurate vibration prediction capability, it was decided to use classical methods of modal analysis to predict vibration levels.

There has been considerable research conducted by acoustic engineers on structural excitation and its effect on noise transmission and internal noise. The paper by E. H. Dowell "Master Plan for Prediction of Vehicle Interior Noise" (Reference 2), has an excellent bibliography with 171 titles. Many of these papers have a direct relationship to the aircraft vibration prediction problem. From a review of several of these papers, it was decided to try two approaches, one using periodic structure theory and one using a finite element analysis (FEA) approach to develop modal analyses for predicting vibration levels.

The plan followed in this study to develop a more rigorous approach to aircraft vibration prediction was to study the noise and vibration characteristics of the Boeing YC-14, a medium sized STOL transport (gross weight 104,300 kilograms). Specifically, the following steps were taken:

- 1) Develop an acoustic field prediction method as a function of engine size, distance from fuselage, thrust, temperature, etc., so that parameter studies could be done on various aircraft configurations.
- 2) Compare predicted YC-14 noise data with measured YC-14 noise data.

- 3) Analyze a YC-14 USB flap and fuselage section using FEA and periodic structure theory and finite element methods and then predict structural vibration levels using measured YC-14 noise data.
- 4) Compare the predicted to the measured YC-14 acceleration response data, and select one approach.
- 5) Then, if the comparisons were acceptable, predict noise and vibration levels on a small STOL aircraft and compare with measured data.

The work which is summarized in this paper was accomplished under contract with the U.S. Air Force Wright Aeronautical Laboratories, Dayton, Ohio.

II. ACOUSTIC FIELD PREDICTION METHOD

The method used to predict the acoustic field was developed under U.S. Air Force and NASA contracts. Reference 3 gives a detailed description of this method.

This prediction method provides one-third octave band estimates of fluctuating pressures on USB STOL aircraft surfaces primarily aft of the nozzle exit plane, and in direct view of the engine exhaust field. Predictions can be made in terms of engine size, distance from fuselage, thrust, low velocity and temperature, and flap impingement effects. The method was developed by studying YC-14 measured noise data. For example, Figure 1 shows how the exterior fuselage noise spectra varies during takeoff. Figure 2 shows how fuselage noise spectra varies with USB flap angle. All sound pressure levels (SPL) presented in this paper are given in dB, namely:

$$\text{SPL (in dB)} = 10 \log_{10} \frac{\text{Pressure}}{\text{Ref. Pressure}}$$

where the reference pressure is 200 pico-bars or 200×10^{-7} Newtons per square meter.

The method estimates the following separate noise spectra and is summed to give the total noise.

- o Jet mixing noise in the presence of a scrubbed wing/flap system with or without vortex generators
- o Near-nozzle noise
- o Trailing-edge noise
- o Noise associated with (partial) separation of the exhaust flow from flaps
- o Turbulent boundary layer noise
- o Exhaust shock noise

Figure 3 shows a typical general arrangement of the component noise spectra making up the total noise estimates.

Comparisons of Measured vs Estimated Acoustic Data

Measurements were taken on the flap and on the fuselage during takeoff and flight and with various extensions of the flaps. In general the comparisons were fairly good with the predictions being slightly conservative. Figure 4 shows noise data at a point on the wing in the exhaust flow during STOL approach. Figure 5 is a point on the flap, and Figure 6 shows a point on the fuselage during takeoff.

III. PREDICTION BY PERIODIC STRUCTURE THEORY

In this approach the structural response is predicted by first calculating the frequency response functions of the periodic structure and then calculating the Power Spectral Density of the structural response due to broadband random excitation. This broadband random excitation is the measured or predicted convected random pressure field resulting from jet noise. A detailed mathematical description of this method is contained in References 4 and 5 and will not be repeated here. Proponents of this method point out that it simulates the effects of structural discontinuities provided by fuselage frames and stringers, and at the same time limits the computer storage requirement to that necessary for modeling only a single periodic unit. For an unpressurized fuselage, such as the Boeing YC-14 prototype (Figure 7), two structural models are required to cover frequencies below 250 Hz: a periodic skin-stringer model (Figure 8), and a periodic frame-stiffened cylinder (Figure 9). In both the skin-stringer panel model and the frame-stiffened model, the structure is assumed to be infinitely long. This assumption is used in the analysis because it leads to great simplification in formulating and solving the problem numerically, but is not essential (Reference 6).

The periodic method was used to estimate vibration response of a section of fuselage structure. Comparisons with test data is discussed later in this paper.

IV. PREDICTION BY FINITE ELEMENT METHODS

In the FEA method a finite element computer program is used to calculate the influence coefficients of a structure. Then, with the structural mass the resonant modes of the structure are calculated:

$$[[I] [M] - \left[\frac{1}{\omega} \right]] \{\delta\} = 0 \quad (1)$$

where

- [I] = influence coefficient matrix from FEA
- [M] = mass matrix
- ω = resonant frequency
- \{\delta\} = structural deflections

The eigenvectors from the solution of Eq. (1) are used to form generalized coordinates:

$$\{\delta\} = [\phi] \{q\} \quad (2)$$

where

- [\phi] = matrix of eigenvectors
- \{q\} = generalized coordinates

The equations of motion of the structure are then

$$[(\phi' M \phi)_{ij}] \{q\} + (1 + 2i \xi) [\omega_i^2 (\phi' M \phi)_{ij}] \{q\} = [\phi]' \{F\} \quad (3)$$

where

- [(\phi' M \phi)_{ij}] = generalized mass matrix (diagonal)
- ξ = percent of critical damping
- [\omega_0^2 (\phi' M \phi)_{ij}] = generalized stiffness matrix (diagonal)
- \{F\} = sinusoidal forces due to unit pressures as a function of frequency

Equation (3) is then used to develop frequency response functions of a structure.

The output power spectrums are calculated as follows:

$$\phi_i(\omega) = [H]_i [\text{CPSD}] \{H\}_i \quad (4)$$

where

- \phi_i[\omega] = output power spectrum at station i
- [H]_i = frequency response functions at each station due to excitation at station .

- $\{H\}_i$ = conjugate transpose of $[H]_i$
- [CPSD] = Matrix of power spectral densities and crosspower spectral densities due to sound pressure levels at various locations on the structure.

The root mean square response for each station are calculated as follows:

$$A_i = \left[\int_0^{\infty} \phi_i(\omega) d\omega \right]^{1/2} \quad (5)$$

where

A_i = root mean square response at Station i

The above-described finite element approach was used to calculate flap response and fuselage response using the same section of fuselage that was analyzed using the periodic structures theory.

V. FLAP STRUCTURE VIBRATION PREDICTION

The USB flap which lies in the exhaust of the YC-14 engine is 240 inches by 60 inches and weighs 1150 pounds (522 kilograms). A simple 27-node finite element plate model was developed and the first ten frequencies ranged from 32 Hz to 281 Hz.

One of the major difficulties in vibration prediction when using the modal method or the periodic method is estimating structural damping. As an indication of the importance of structural damping, RMS acceleration for two accelerometers were calculated for structural damping values of $g = 0.3, 0.06, 0.09, 0.12,$ and 0.15 , see Figure 10. As one can see, the effect of damping is significant and when compared to YC-14 test data, a value of 0.15 gives the best comparison. The measured and calculated power spectrum density of two accelerometers are shown in Figures 11 and 12. As can be seen, fairly good results can be obtained using simple models.

All acceleration power spectral densities presented in this paper are given dB, namely:

$$\text{Acceleration PSD (in dB)} = 10 \log_{10} \frac{\text{Acc. PSD}}{\text{Ref. Acc. PSD}}$$

where the reference acceleration PSD is $1 G^2/\text{Hz}$, and G is the acceleration of gravity.

VI. FUSELAGE STRUCTURE VIBRATION PREDICTION USING FEA

Finite Element Modeling

In order to simplify the modeling and at the same time cover a broad frequency range (25 to 1000 Hz), three models were developed: one for the low frequency range (25 to 100 Hz), one for the intermediate frequency range (100 to 300 Hz), and one for the high frequency range (above 300 Hz). Figures 13 to 15 show how these models relate to actual fuselage structure.

All the models used beam and plate elements. The low frequency range model used 66 nodes and the nodes were located at the intersections of every third frame and every fourth stringer. The section of fuselage used was 10 frames and one-half of fuselage circumference.

The intermediate frequency range model used 35 nodes. The nodes were located at the intersections of each frame and stringer as well as on each stringer midway between frames. The nodal density was 24 times that of the low frequency range model. The section of fuselage used was four frames and five stringers.

The high frequency model used 81 nodes and were contained between two frames and four stringers. The nodes were distributed in seven rows between the frames and between the first and fourth stringers. The nodal density was 8 to 16 times that of the intermediate frequency model.

Modal Analysis

Twenty modes (13 to 117 Hz) were calculated for the low frequency range model; eight modes (60 to 354 Hz) were calculated for the midfrequency range model; and twenty modes (269 to 987) were calculated for the high frequency range model. The modal frequencies for the models are listed in Figure 16.

Vibration Prediction

Measured acoustic data was used to calculate structural response. Figure 17 shows the microphone locations for acoustic data measurement from which the data was interpolated for the model acoustic loading. The measured noise level shown in Figure 9 is an example of noise data taken with maximum engine thrust during ground run-up.

At the same time the noise data was being taken, fuselage response data was being taken. The response of three accelerometers are shown in Figures 18, 19 and 20. One is on a stringer, one on a frame, and one on a skin panel. Also shown in these figures are the predicted responses for the low and intermediate range frequency models.

Figures 21 and 22 show the same noise data and the predicted response using the high frequency range model for a stringer and a skin panel. For this frequency range fuselage frames have little effect on structural response.

The comparisons appear reasonable, however, the vibrations are somewhat overpredicted at low frequencies.

VII. FUSELAGE VIBRATION PREDICTION USING PERIODIC STRUCTURE THEORY

Two models of the YC-14 fuselage were developed for use with the periodic structure theory (see Figures 2 and 3). The frame-stiffened cylinder model was expected to predict responses up to 150 Hz and the skin-stringer model above 150 Hz. The noise excitation was based on one microphone and the acceleration response was on the fuselage skin near the microphone. The comparison between measured and predicted is shown in Figure 23. The frame-stiffened cylinder model did not seem to predict the low frequency response very well. Although further work might have shown the reason for the difference, it was decided to use the FEA method for verifying the vibration prediction technique on a small STOL aircraft.

VIII. STRUCTURAL VIBRATION PREDICTION--SMALL STOL AIRCRAFT

The QSRA (Quiet Short Range Aircraft) airplane was chosen for the study of a small STOL Aircraft. The QSRA is a 50,000-pound (22,680 kilograms), four-engine, over-the-wing blowing, STOL airplane which was converted from a DeHaviland Buffalo for NASA by The Boeing Company (Figure 24). The vibration prediction analysis was done on this airplane before the airplane was delivered to NASA and before vibration and noise measurements were made by NASA.

QSRA USB Flap

A 31-node FEA model of the USB flap using beam and plate elements was developed for calculating modes. The flap was 52 by 76 inches (1.32 by 1.93 meters). The first 20 modal frequencies ranged from 150 Hz to 1048 Hz.

The acoustic input was calculated using the method described in Section IV of this paper. The resulting vibration at one point on the QSRA USB flap is shown in Figure 25. Also shown on this figure is measured data taken by NASA at the flap actuator attachment. The calculated values are somewhat higher than the measured values, however, one would expect the accelerations to be lower at the flap attachment than on the flap itself.

QSRA Fuselage

The QSRA FEA fuselage model was a 77-node beam and plate model representing skins, frames, and stringers of the upper quarter of the fuselage aft of the USB flaps. In the conversion of the Buffalo to the QSRA, the skin panels at this part of the fuselage were replaced with bonded aluminum and honeycomb panels as a protection from sonic fatigue. The FEA model represented the skin panels as flat plates.

The first 20 modal frequencies ranged from 165 Hz to 761 Hz. The acoustic input was calculated according to the method discussed in Section IV of this paper. The resulting vibration prediction at one point on the fuselage is shown in Figure 26, along with measured data. A comparison between predicted and measured shows fairly good agreement.

IX. CONCLUSIONS

Methods used in the past for predicting environmental vibration levels have proven to be very useful, for example, scaling methods where configurations are similar, and statistical energy methods where structural modes are closely spaced. These methods have not been very successful at low frequencies and when modes are widely spaced. This was of particular concern due to the high energy noise at low frequencies for STOL aircraft.

In this study it has been shown that finite element analyses and classical modal methods can also be useful in predicting environmental vibrational levels. In addition, it is a more powerful method useful over a wide range of frequencies including those areas where SEA breaks down.

With the noise prediction method described in this study for USB STOL aircraft the FEA modal analysis approach is a feasible technique during preliminary design when structural details are being configured and equipment specifications are being written. It requires, however, that one has the knowledge of the level of structural damping to be expected from different kinds of structure.

REFERENCES

1. Himelblau, Fuller, and Scharton, "Assessment of Space Vehicle Aeroacoustic-Vibration Prediction, Design and testing," NASA CR-1596, July 1970.
2. Dowell, E. H., "Master Plan for Prediction of Vehicle Interior Noise," presented at the AIAA 5th Aeroacoustic Conference, Seattle, Washington, March 1979.
3. L. M. Butzel, A. J. Bohn, R. Armstrong and J.B. Reed, "Noise Environment of Wing, Fuselage and Cabin Interior of a USB STOL Airplane," NASA CR-159053, July 1979.
4. SenGupta, G., "Natural Frequencies of a Periodic Skin-Stringer Structure, using a Wave Approach," J. Sound and Vibration, Vol. 16, No. 4, 1971.
5. Comparisons of the Predicted and Measured Structural Response of a Fuselage to a Broadband Random Excitation, H. H. Nijim and G. SenGupta, presented at the AIAA 5th Aeroacoustic Conference, Seattle, Washington, March 1979.
6. Mead, D. J., "Vibration Response and Wave Propagation in Periodic Structures," ASME Paper No. 70-WA/D3-3, Winter Annual Meeting of ASME, N.Y., November 29 to December 3, 1970.

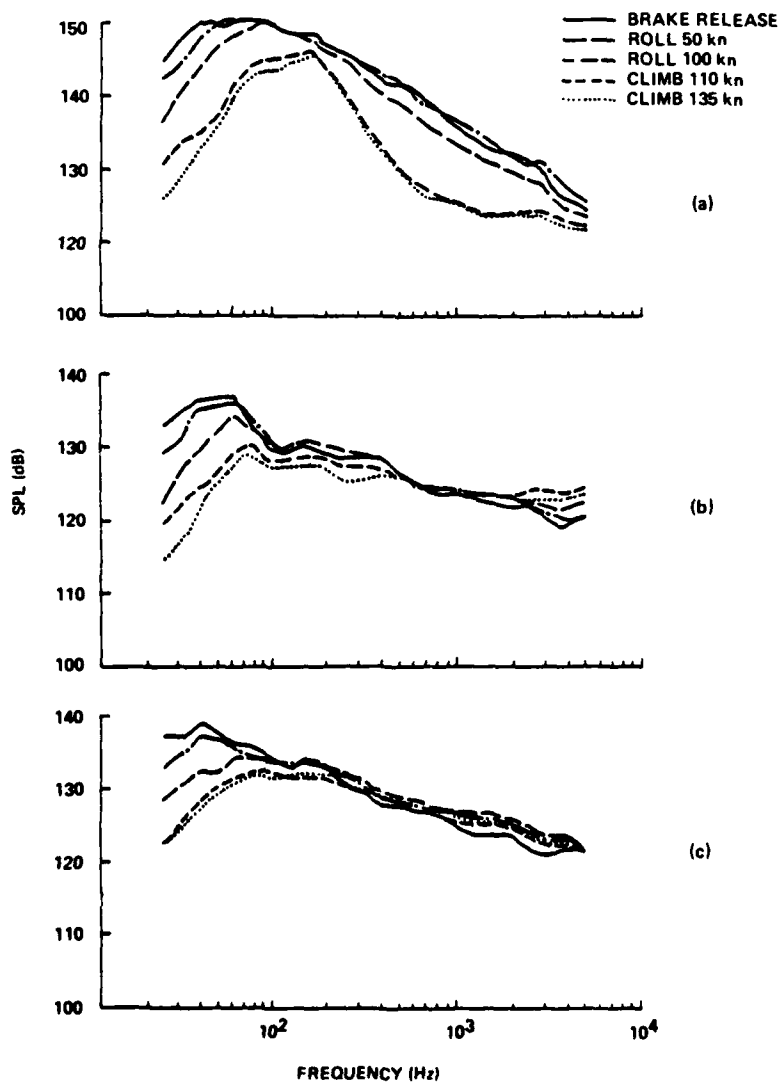


Figure 1. Variation in Exterior Fuselage Noise Spectra during Takeoff at Three Separate Fuselage Locations

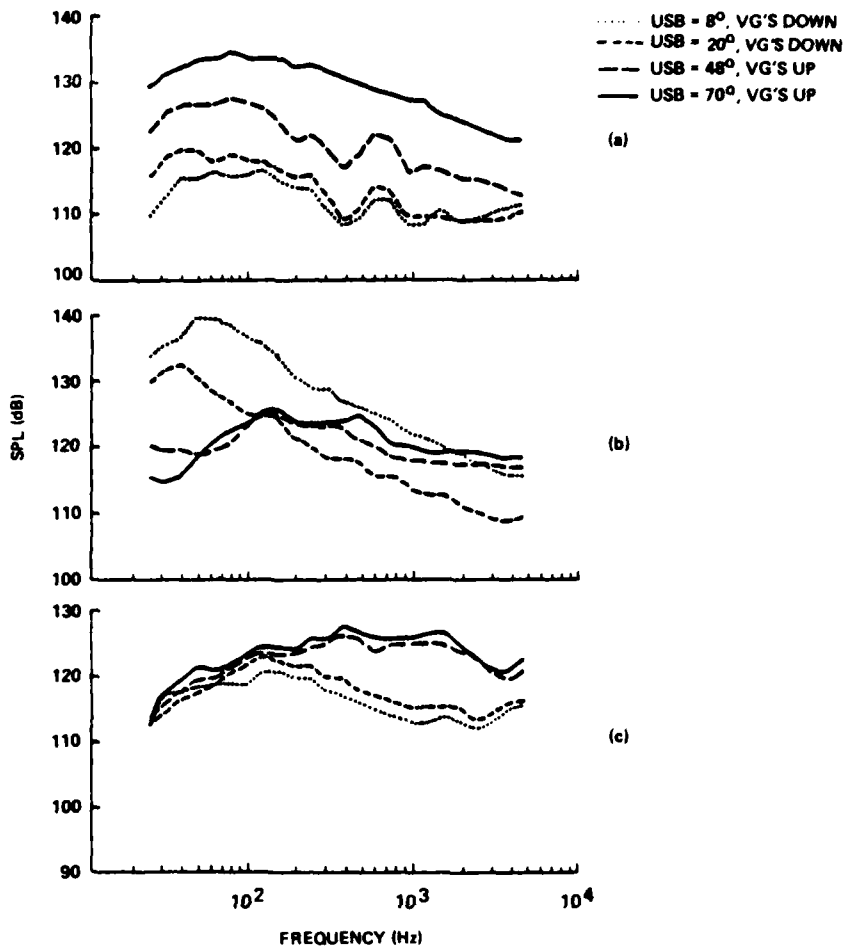


Figure 2. Effect of USB Flap Position on Exterior Fuselage Spectra at Three Separate Fuselage Locations

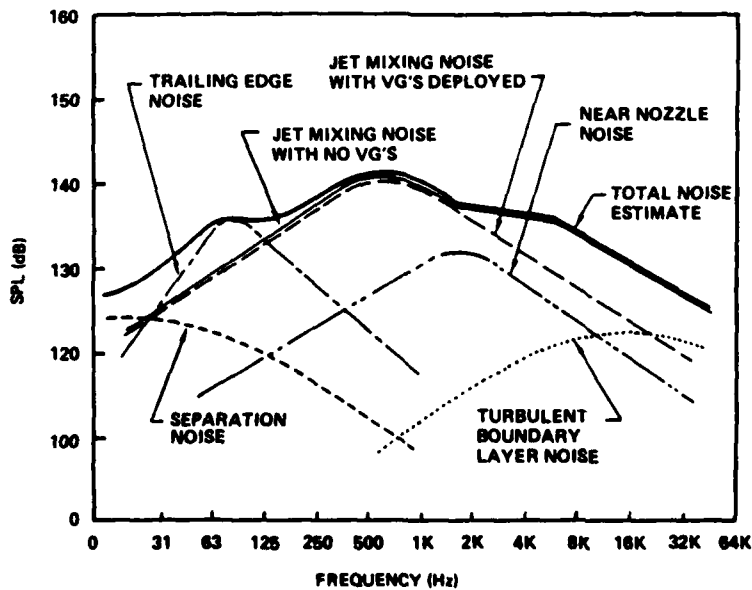
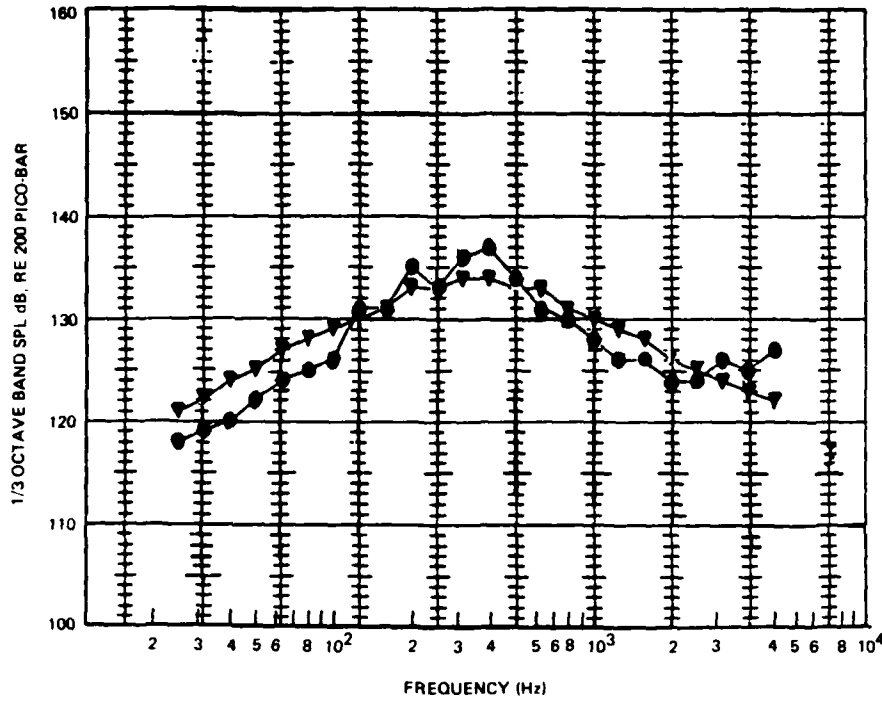


Figure 3. General Arrangement of Component Noise Source Estimates making up Total Noise Estimates (Typical Climbout Condition)

PREDICTION PROCEDURE DEMONSTRATION

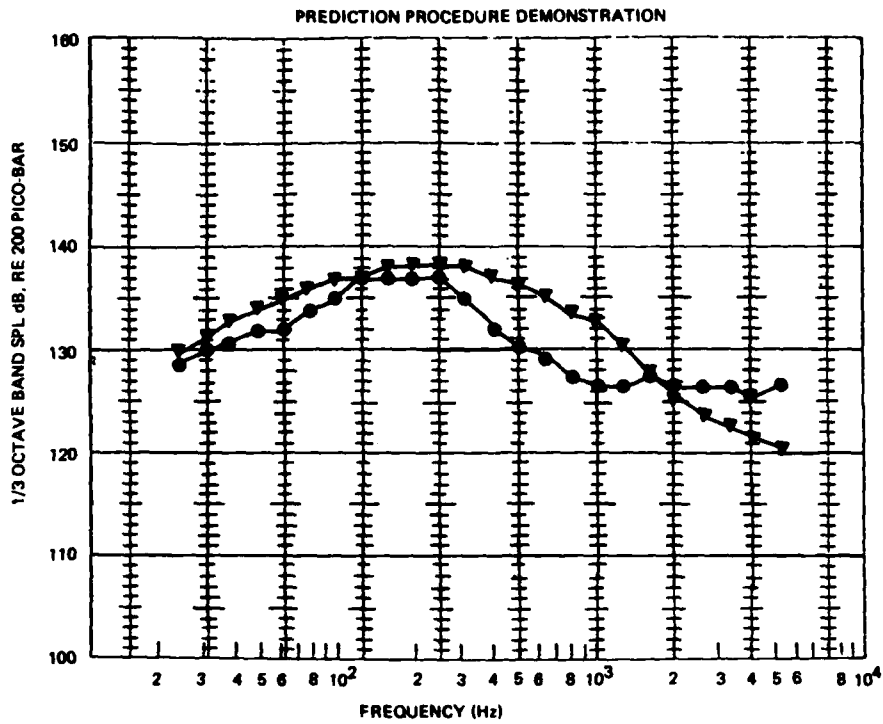


PLOT SYMBOL	X-DUCER NO	COND NO	ALT (FT)	SPEED (FPS)	N1 (RPM)	VMIX (FPS)	USBFA (DEG)	OVERALL (dB)
●	M33	3160	7650	204	2463	674	60	144
▼	M33	3160						144

NOTES

- MEASURED TOTAL NOISE
- ▼ PREDICTED TOTAL NOISE

Figure 4. Results for a Point on Wing in Exhaust Flow

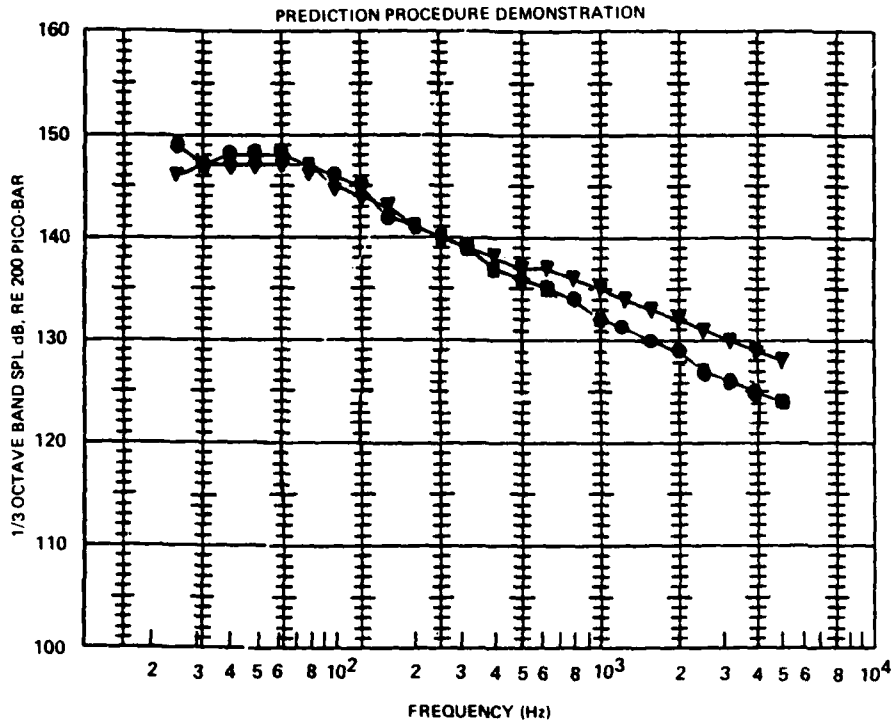


PLOT SYMBOL	X-DUCER NO	COND NO	ALT (FT)	SPEED (FPS)	N1 (RPM)	VMIX (FPS)	USBFA (DEG)	OVERALL (dB)
●	M38	3160	7660	204	2463	674	60	148
▼	M38	3160						148

NOTES

- MEASURED TOTAL NOISE
- ▼ PREDICTED TOTAL NOISE

Figure 5. Results for a Point on the USB Flap



<u>PLOT SYMBOL</u>	<u>X-DUCER NO</u>	<u>COND NO</u>	<u>ALT (FT)</u>	<u>SPEED (FPS)</u>	<u>N1 (RPM)</u>	<u>VMIX (FPS)</u>	<u>USBFA (DEG)</u>	<u>OVERALL (dB)</u>
●	M16	7132	0	42	3640	1100	0	157
▼	M18	7132						156

NOTES

- MEASURED TOTAL NOISE DATA
- ▼ PREDICTED TOTAL NOISE

Figure 6. Results for a Point on the Fuselage

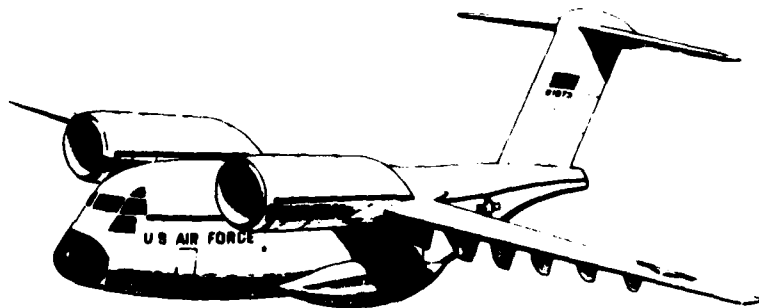


Figure 7. YC-14 Prototype

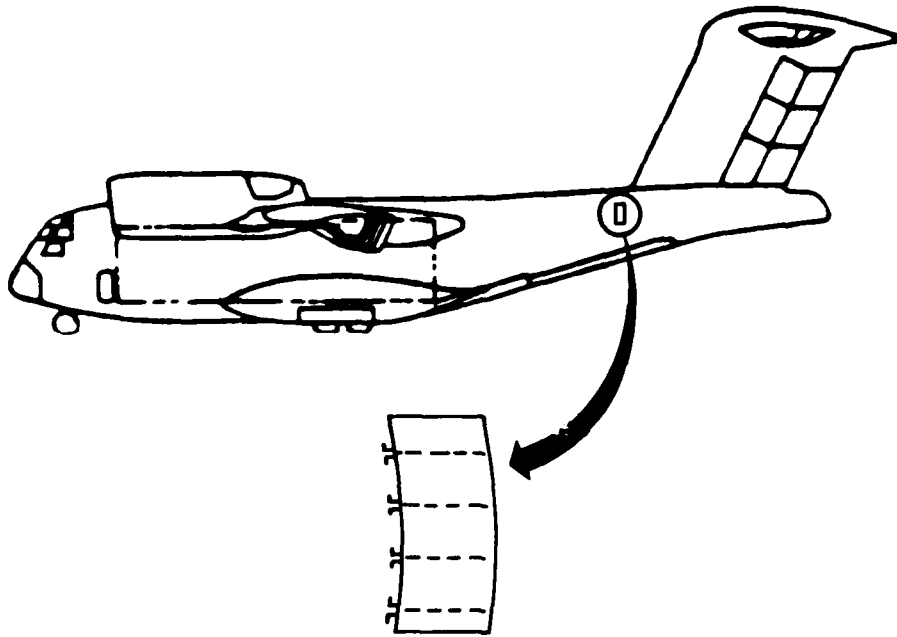


Figure 8. Periodic Skin Stringer Model

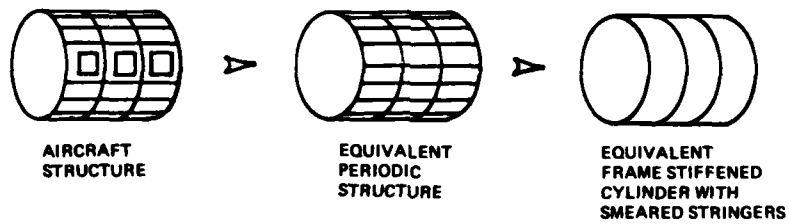


Figure 9. The Periodic Frame-Stiffened Cylinder

ACCELERATOR NUMBER	STRUCTURAL DAMPING					FLIGHT TEST YC-14
	0.03	0.060	0.090	0.120	0.150	
1421	1.67	1.180	0.968	0.846	0.783	0.716
1417	2.56	1.821	1.511	1.334	1.217	1.200

Figure 10. RMS Acceleration Values in G's for YC-14 USB Flap for Frequency Range 20-200 Hz

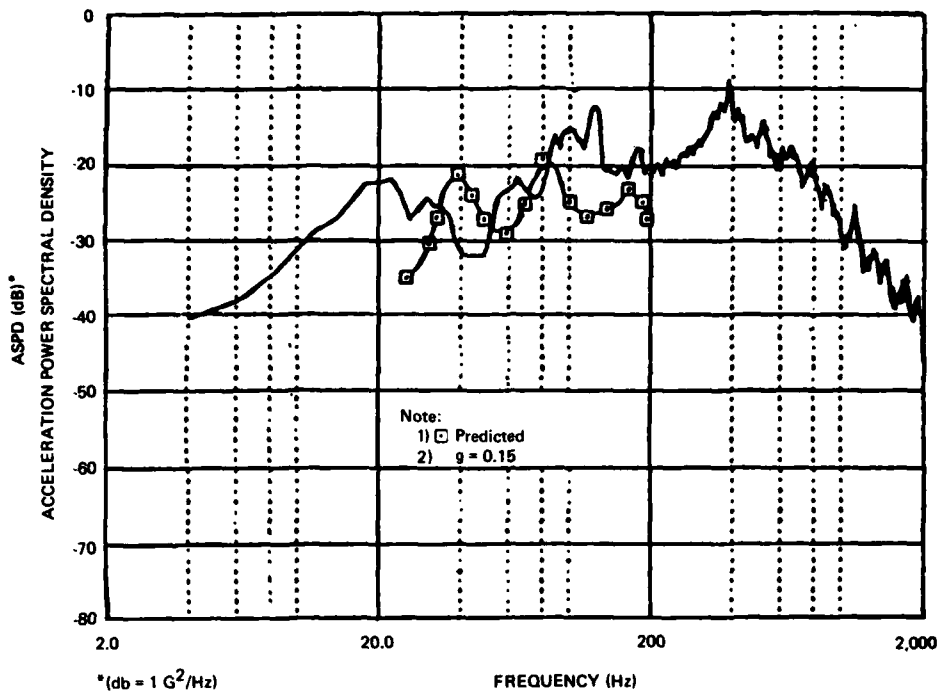


Figure 11. USB Flap Response Comparison with Prediction, Accelerometer 1421

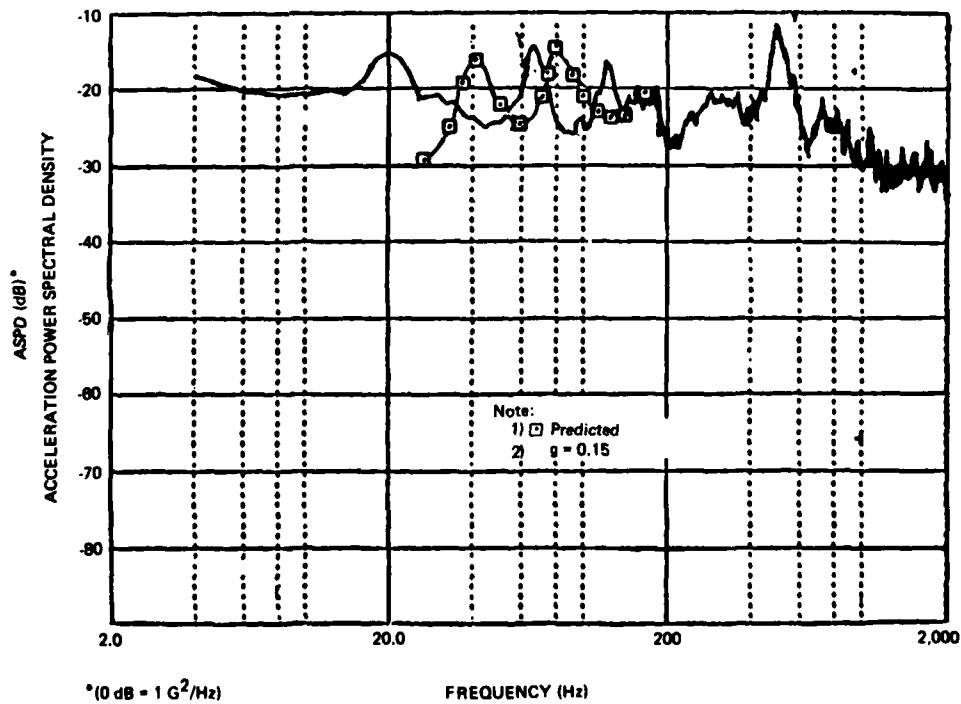


Figure 12. USB Flap Response Comparison with Prediction, Accelerometer 1417

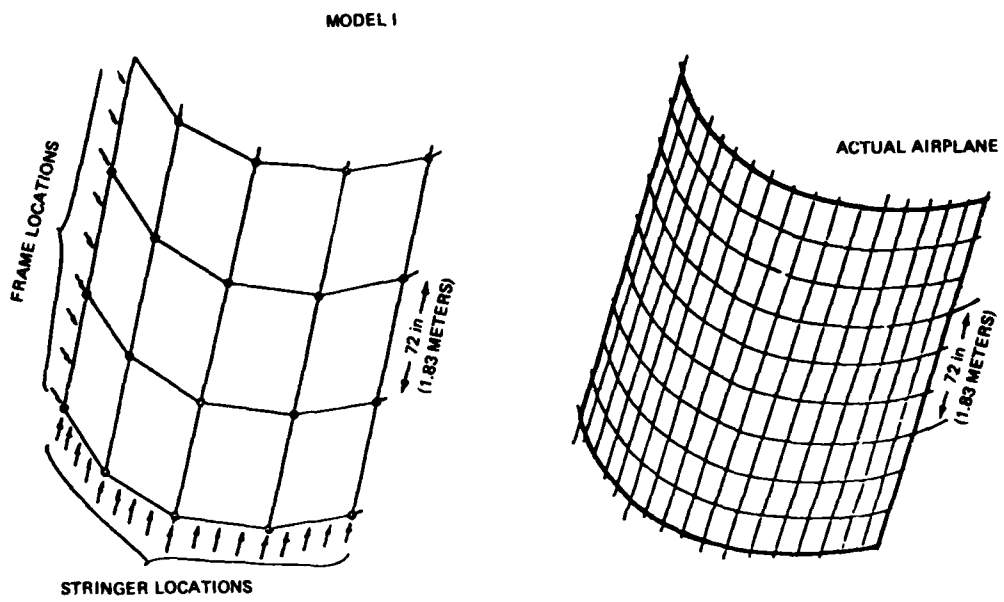


Figure 13. Low Frequency Fuselage Model I

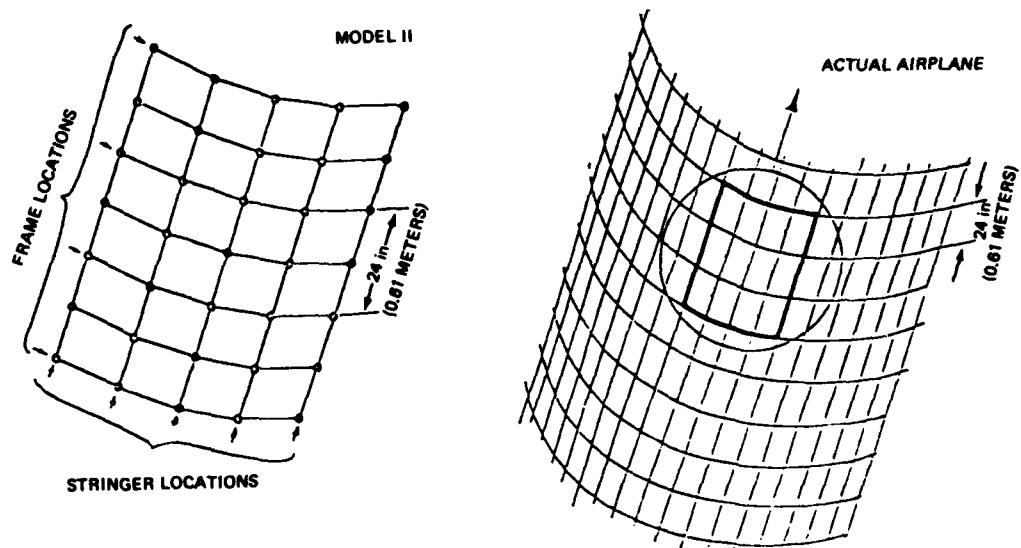


Figure 14. Mid-Frequency Fuselage Model II

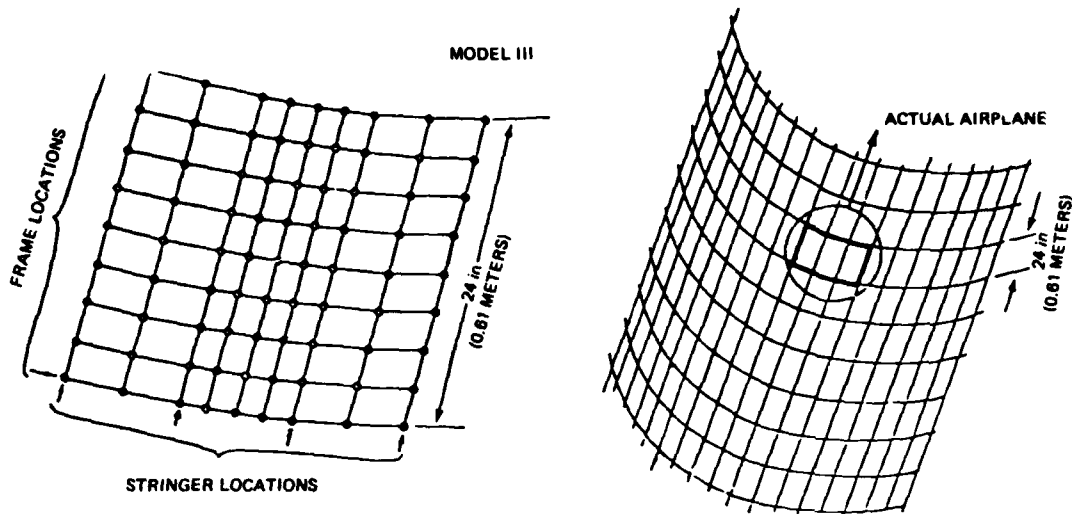


Figure 15. High Frequency Fuselage Model III

MODE NUMBER	FREQUENCIES, Hz		
	LOW FREQUENCY RANGE	INTERMEDIATE FREQUENCY RANGE	HIGH FREQUENCY RANGE
1	13	60	270
2	25	146	326
3	39	190	376
4	52	235	388
5	61	284	431
6	62	336	488
7	73	342	523
8	77	354	553
9	84		634
10	89		742
11	90		748
12	93		800
13	100		830
14	101		840
15	105		848
16	108		868
17	109		908
18	110		964
19	113		983
20	117		987

Figure 16. Modal Frequencies

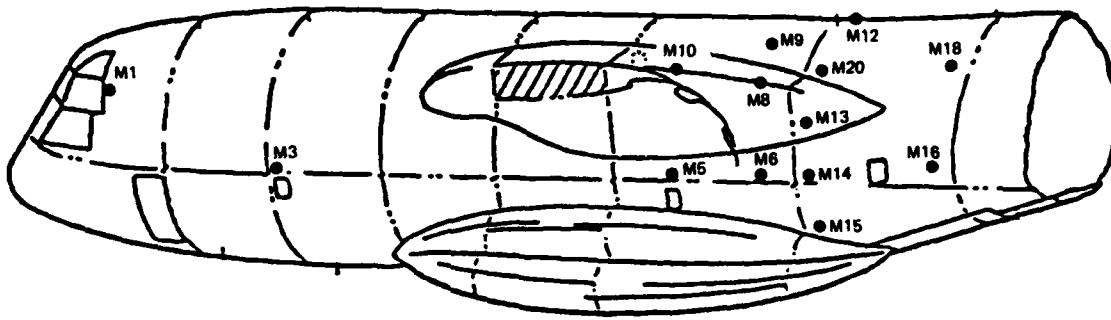


Figure 17. YC-14 Microphone Locations for Fuselage

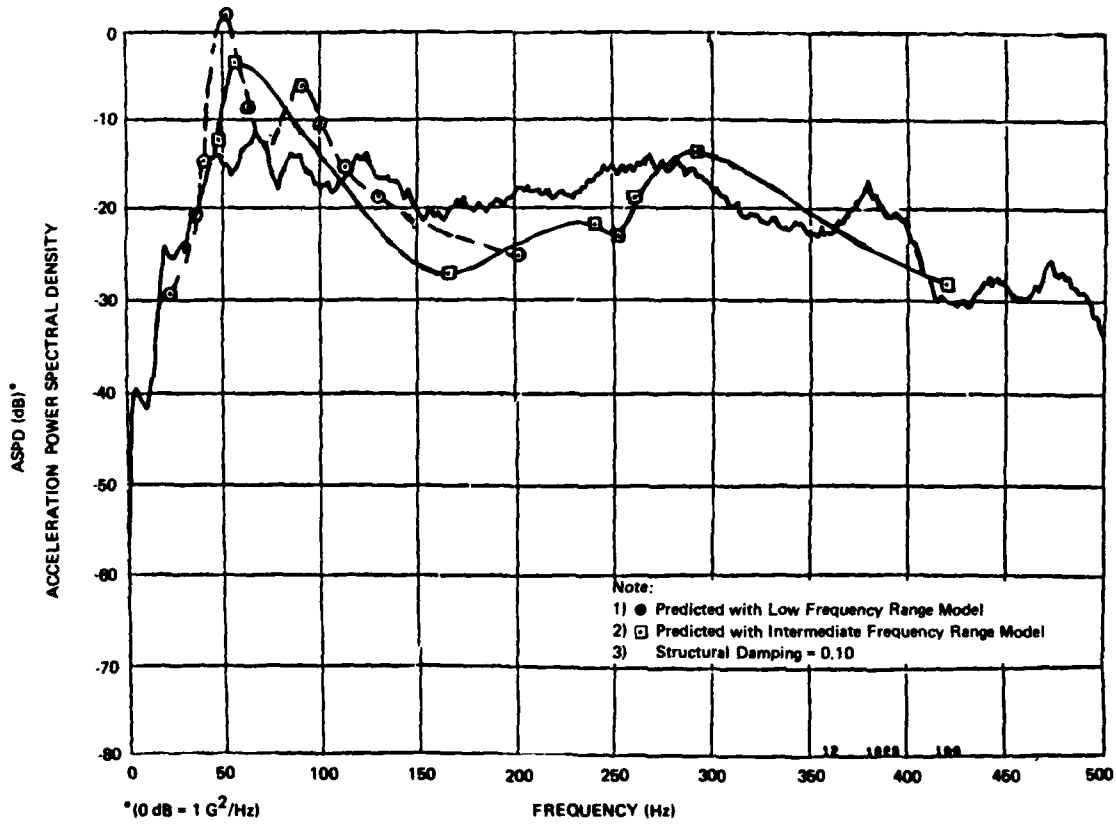


Figure 18. Measured and Predicted Fuselage Response for Accelerometer 1474 Mounted on a Stringer

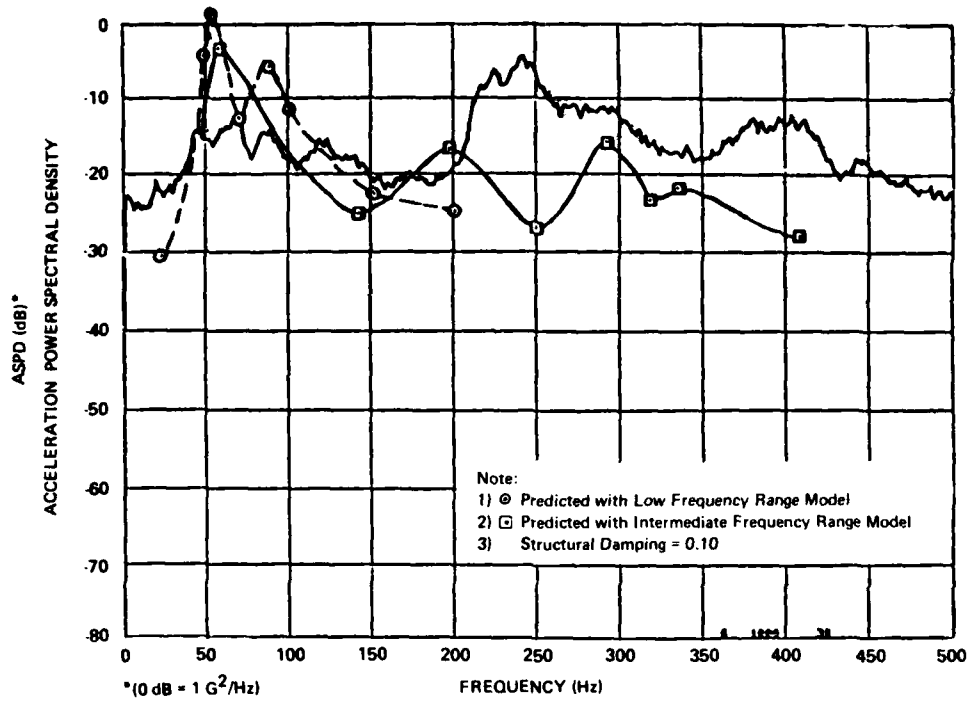


Figure 19. Measured and Predicted Fuselage Response for Accelerometer 1481 Mounted on the Skin

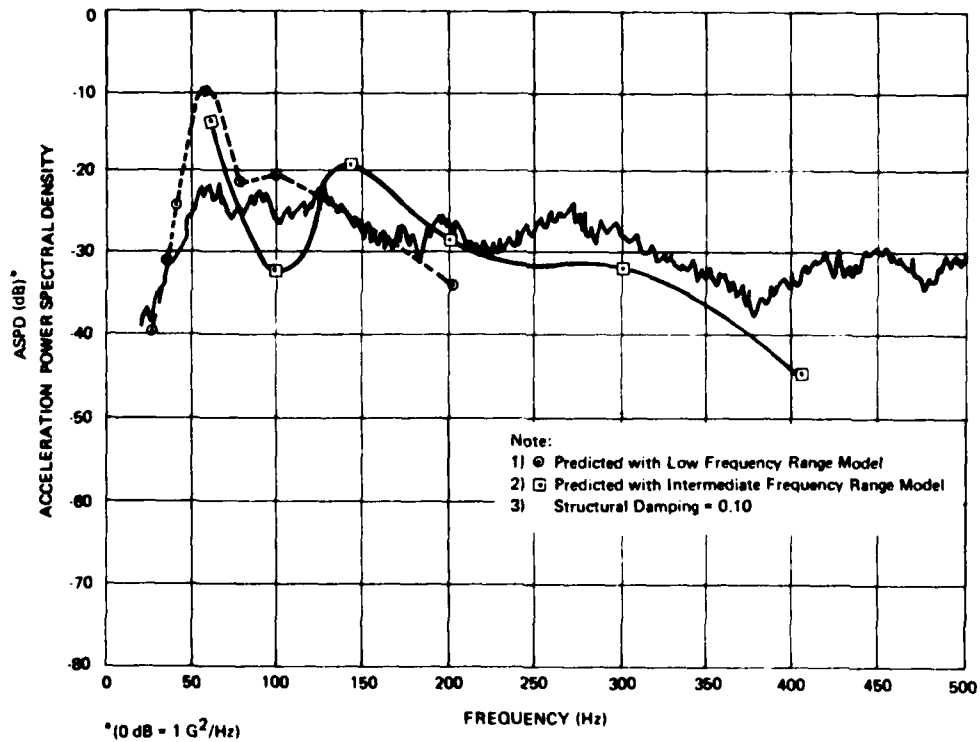


Figure 20. Measured and Predicted Fuselage Response for Accelerometer 1474 Mounted on a Frame

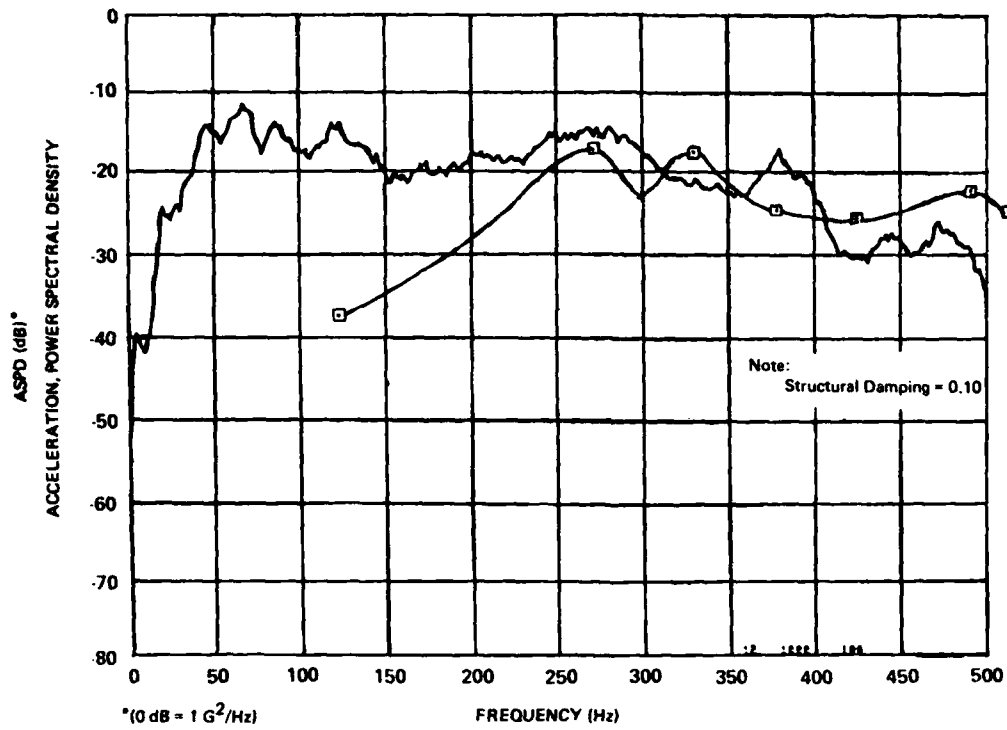


Figure 21. Measured and Predicted Fuselage Response for Accelerometer 1474 Mounted on a Stringer, High Frequency Model

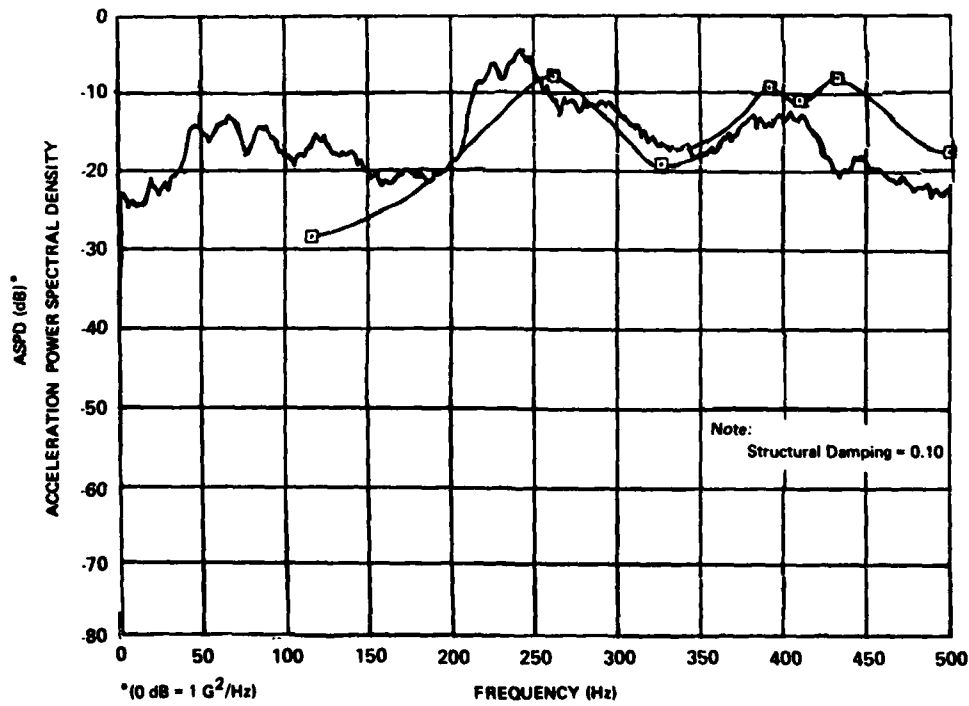


Figure 22. Measured and Predicted Fuselage Response for Accelerometer 1481 Mounted on a Skin Panel, High Frequency Model

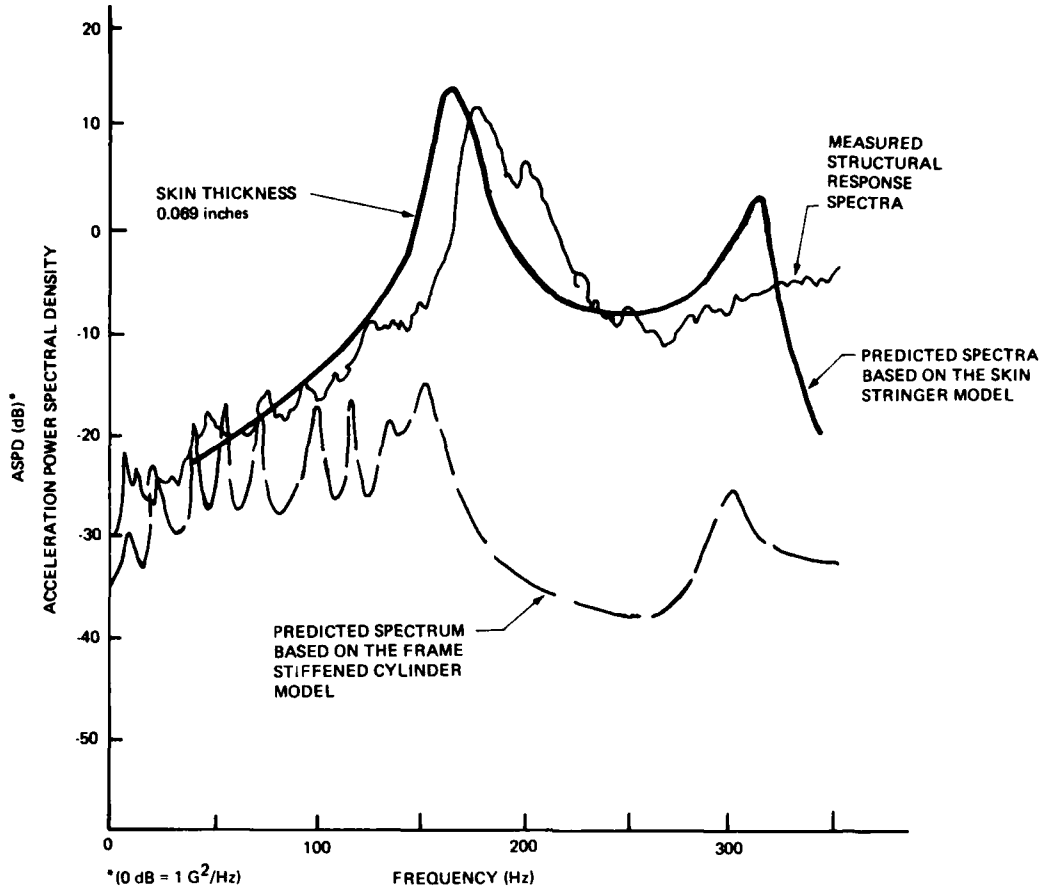


Figure 23. Measured and Predicted Fuselage Response for Accelerometer 1481 Mounted on a Stringer

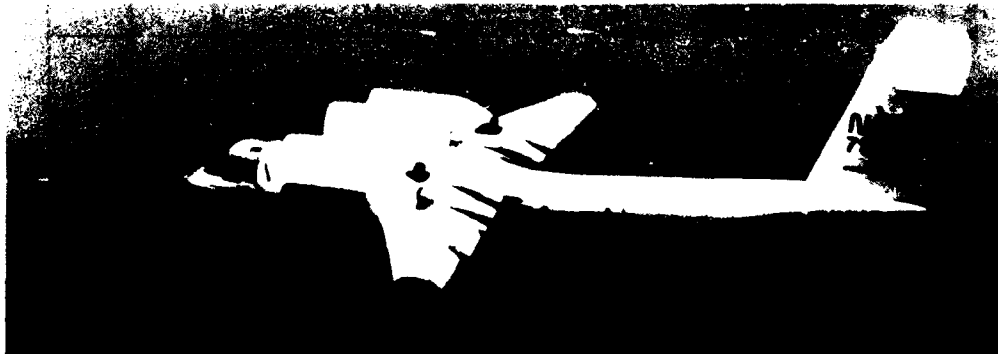


Figure 24. Quiet Short Range Aircraft (QSRA)

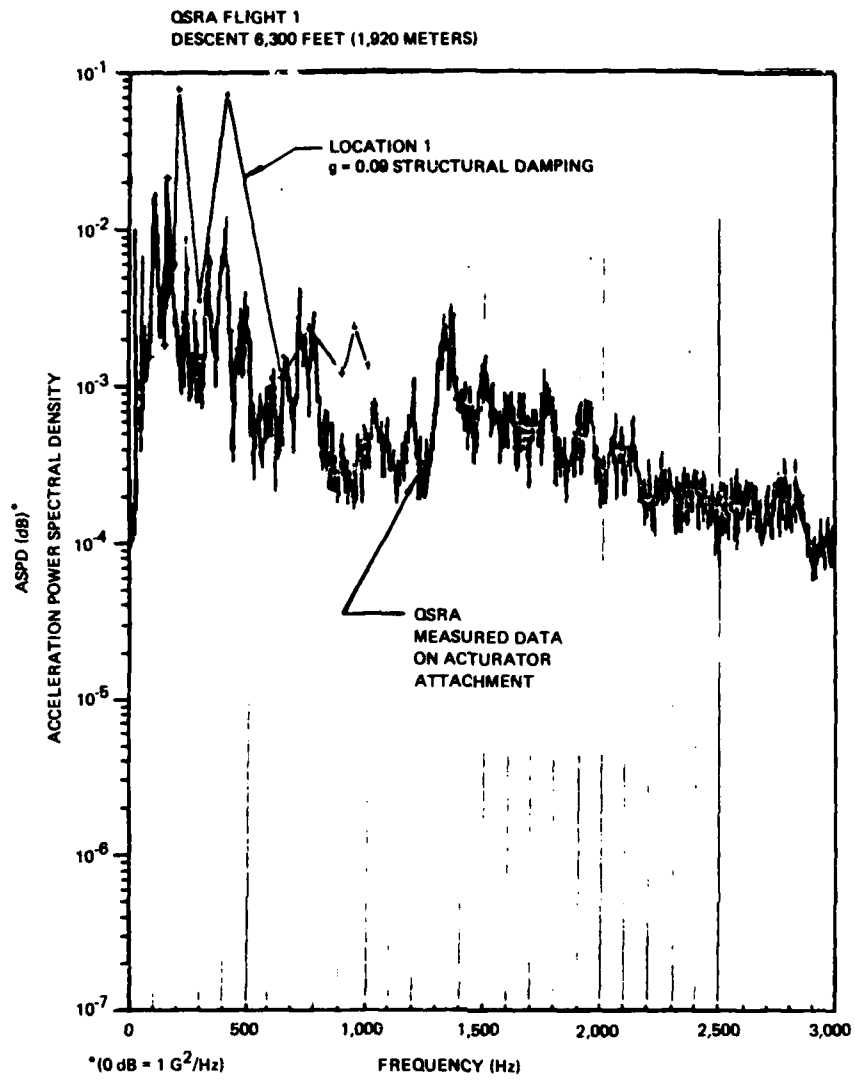


Figure 25. Comparison of USB Flap Prediction to Flight Test Data

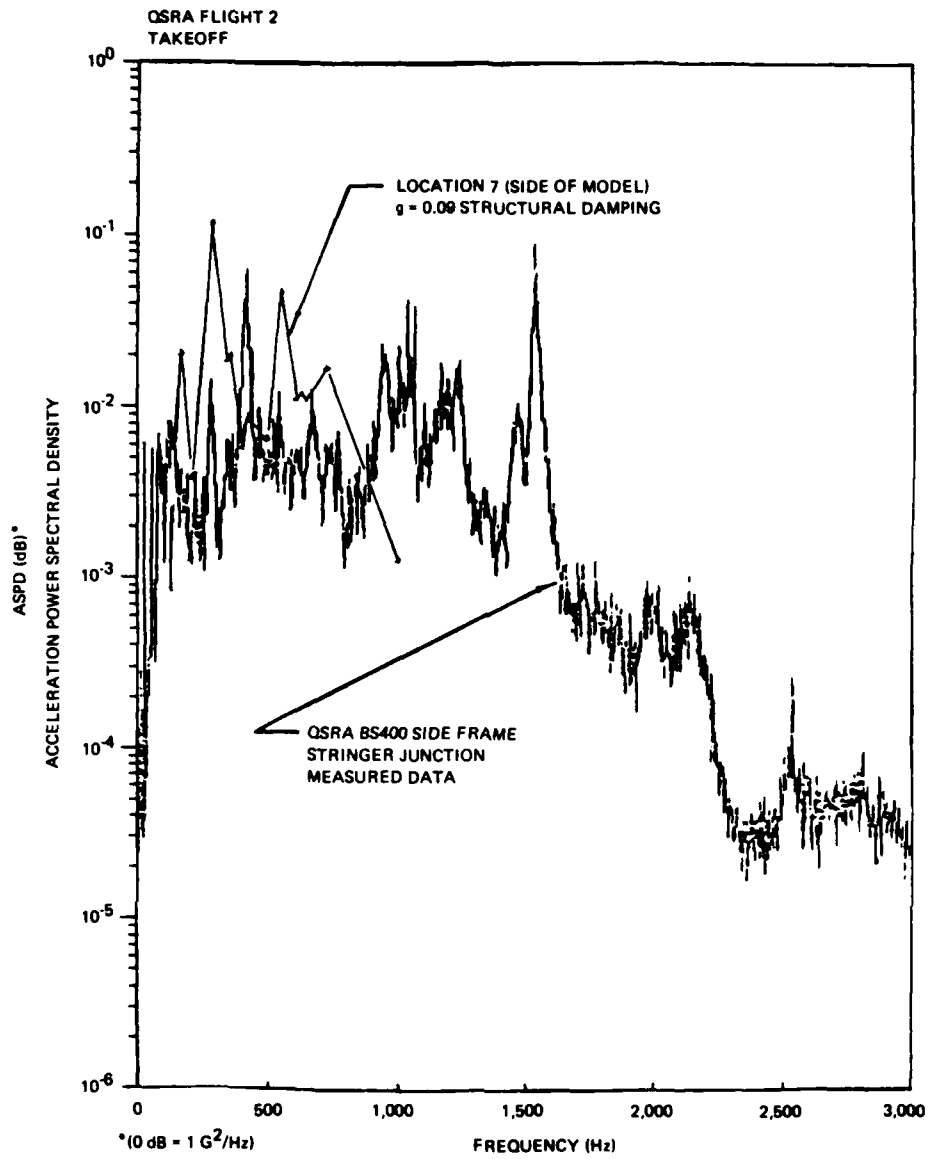


Figure 26. Comparison of OSRA Fuselage Response with Predicted Values, Location 7

GUNFIRE BLAST PRESSURE PREDICTIONS

by

R.M.Munt, A.J.Perry and S.A.Moorse
 Aerodynamics Department
 Royal Aircraft Establishment
 Farnborough, Hampshire GU14 6TD
 England

SUMMARY

A scheme for predicting the blast pressures from aircraft guns is presented which extends existing theory. The predictions correlate well with some experimental measurements of gun blast pressures in free space. Blast pressures were also measured experimentally on a surface in the vicinity of the muzzle of a 7.62 mm rifle but these could only be satisfactorily predicted in regions where the classical theory of regular reflection of shock waves could be applied. These results are discussed in relation to the surface blast pressures from aircraft mounted guns.

LIST OF SYMBOLS

a_e	speed of sound in the propellant at the muzzle
a_0	speed of sound in the ambient gas
a_r	speed of sound in the propellant at ambient conditions
c	calibre of gun
c''	stretched calibre
f	angular distribution parameter
I	total impulse behind blast wave
I_+	positive impulse behind blast wave
K	is a constant for a given explosive
$m(t)$	mass of expelled propellant
M_e	muzzle exit Mach number
M_1	Mach number of incident blast front
p	peak pressure within blast wave
P_e	muzzle pressure
P_0	ambient pressure
P_1	peak pressure within incident blast wave at a surface
P_2	peak pressure within reflected blast wave at a surface
P_s	peak pressure within Mach stem
R	radial distance from muzzle
R'	radial distance from x_0
r_s	radius of hypothetical charge
r'_s	radius of hypothetical charge accounting for forward speed of gun
r''_s	distance from detonation point to surface of hypothetical charge
t	time from instant the projectile leaves muzzle
t_s	time (t) of arrival of blast front
U	forward velocity of the gun
W	excess energy driving the blast wave

x	axial distance from muzzle ($x > 0$ is direction of fire)
x_0	axial distance to apparent gun blast origin
x_D	axial distance to Mach disc
y	lateral distance from gun axis
z	height of gun from surface parallel to gun axis
α	index expressing dependence of overpressure on R/c
α_e	critical angle of incidence
α_0	angle of incident blast wave at a surface
α_2	angle of reflected blast wave at a surface
γ	ratio of specific heats in the ambient gas
γ_e	ratio of specific heats in the propellant gas
ϵ	specific energy of propellant relative to ambient conditions
θ	angle from gun axis with origin at the muzzle
θ'	angle from gun axis with origin at x_0
ξ_0	= p_0/p_1 , incident pressure ratio
τ	duration of positive overpressure blast phase

1 INTRODUCTION

There are various operating situations in which the blast from guns is a cause for concern. For instance the blast can be a hazard to the personnel who operate the guns or, for guns installed on aircraft, it may cause a variety of malfunctions from faulty behaviour of instruments to aero-engine surge. In this paper the main interest is in the prediction of blast pressures due to firing guns in military aircraft and on determining the blast loading on nearby surfaces such as the aircraft fuselage where the fatigue life of the structure could be affected.

A description of the blast from a gun can be found, for example, in the papers by Schmidt and Shear¹ and Klingenberg². From a single shot two blast fields are produced, as depicted in Figs 1 and 2. The first is the precursor field which is created when the accelerating projectile forces the air ahead of it out of the barrel. The second is a consequence of the sudden expansion of the propellant gas after the projectile leaves the muzzle. Both flow fields exhibit the supersonic underexpanded jet characteristic^{3,4} of a 'shock bottle', formed by the intercepting shock and Mach disc. The precursor flow field, with its muzzle pressure of around 10 to 20 bar, is quickly enveloped by the more intense propellant field, whose initial muzzle pressures are typically 400 to 600 bar. Consequently it is usual to ignore the precursor in the theoretical modelling of gun blast, as this assumption is only likely to lead to significant errors in the initial stages of the propellant flow field development⁵.

In addition the propellant flow is affected by the projectile until it draws clear of the contact surface; in particular the presence of the projectile initially inhibits the forward motion of the Mach disc (see Figs 3c, 3d and 4). Eventually the projectile, which moves at approximately constant speed, overtakes the expanded gas and emerges with its own shock system. At some stage after this happens the Mach disc reaches its limiting forward position and for a while remains stationary with almost steady conditions within the shock bottle before moving inwards as the barrel empties.

There are several papers⁶⁻¹³ which discuss numerical solutions to the propellant flow field. Erdos and Del Guidice⁶ have extended Oswatitsch's⁷ spherically symmetric model to include a translating origin but ignore the projectile. They use a combination of the method of characteristics and McCormack's finite difference procedure¹⁴ to determine the field along the axis of symmetry. On the other hand other authors⁸⁻¹³ adopt a cylindrically symmetric model and take account of the projectile. Some of these⁸⁻¹¹ use particle-in-cell finite differences¹⁵ whilst Traci *et al*¹² use the slightly faster fluid-in-cell technique¹⁶. Taylor and Lin¹³ use a finite-difference method with time-steps chosen in accordance with Godunov's stability theory¹⁷ and spacial coverage by means of sweeping in alternate directions, *ie* the ADI ('alternate directions implicit') procedure. For the cylindrically symmetric model the cheapest computer code is claimed by Taylor and Lin and is at least an order of magnitude faster than the rivals⁸⁻¹². None of these papers provide convincing overall agreement with experiment although Taylor and Lin and Erdos and Del Guidice illustrate good comparisons with experiment for the time histories of the axial positions of the shock fronts. However all the techniques exhibit poor accuracy in determining the blast front pressures because of numerical shock smoothing.

The propellant blast front is created in much the same way as the blast from detonating an explosive charge although, because of choked conditions at the muzzle, for a gun the energy deposition is at more-or-less constant rate rather than being instantaneous, as is assumed for conventional spherical charges. There are a few papers^{5,18-20} which employ this resemblance to derive scaling rules for guns. Westine¹⁸ assumes similarity with a conventional explosive to derive a variation on Hopkinson's scaling rule. But the correlations he obtains do not take account of the variation of blast pressures with angle to the gun axis. This variation is modelled by Smith^{19,20} who draws on an analogy with a moving explosive releasing energy at a constant rate. Schmidt *et al*⁵ have applied the same distribution function as that derived by Smith but assume the distance from the muzzle to the Mach disc, x_D , to be the fundamental scaling length rather than calibre. They obtain good correlation over a wide range of muzzle velocities. Indeed since the shock bottle represents the source region for the blast it would seem natural to use a scale based on x_D . In addition we might expect to find the apparent blast origin to be located within the shock bottle, at say $x_D/2$, rather than at the muzzle.

In the present paper we have adopted a similar model to Smith's but assume an origin positioned on the gun axis between the muzzle and Mach disc, instead of at the muzzle. These models are characterised by a parameter f first used by Thornhill²¹ who suggested that the net linear momentum in the blast field of a gun could be simulated by taking an equivalent fixed spherical charge and detonating it off-centre; see Fig 5. This would generate the strongest blast in the direction of most explosive (as seen from the detonation point) which would be chosen as the direction in which the gun pointed. Then f is the ratio of the off-centre distance of the detonation point divided by the true radius of the sphere of explosive; further analysis is given in the Appendix. The value proposed later is $f = 0.5$ rather than $f = 0.8$ used by Smith and this reduction leads to a weaker directionality in the blast field, which is shown later to improve substantially the correlation with experiment.

Our interest is in determining the reflected blast pressures at a surface. Smith²² and Mabey and Capps²³ obtained experimental data from which they reach the puzzling conclusion that the blast pressure is factored by 2 or less at a nearby surface. This may be true of weak blast waves where acoustic theory can be applied to give pressure doubling but for the strong blasts involved here we would expect, from shock reflection theory, that a factor of 3 or 4 would be more appropriate. Indeed Yagla²⁴ has reasonable success in applying classical reflection theory to the problem of predicting Naval gun blast overpressures on a ship deck. Therefore in order to establish whether shock reflection theory can be applied to gun blast interactions with a surface near to the muzzle we have carried out experiments, which are described in section 2.

2 EXPERIMENTAL DETAILS

Two experiments were performed with a NATO rifle of calibre, c , of 7.62 mm using standard L2A2 ammunition. One was designed to measure the blast pressure field in a reflection-free environment and the other was arranged to measure the pressures on a large flat surface. In both experiments the measurements were recorded on a 14 track tape recorder with a bandwidth of 40 kHz.

2.1 Free-field measurements

In the first experiment measurements were made using four standard $\frac{1}{4}$ inch microphones and seven blast gauges manufactured by the Atomic Weapons Research Establishment (AWRE) comprising 2 of type B19 and 5 of type B21. The B19 and B21 gauges, illustrated in Fig 6, have a nominal sensitivity of 2000 pico coulomb/bar and were used in the near-field to measure pressures in excess of 0.03 bar.

The experimental configuration is shown in Fig 7. Pressure measurements were made in the same horizontal plane as the rifle which was mounted 1.5 m (200 calibres) above the ground. The $\frac{1}{4}$ inch microphones and the directional B19 gauges were used to measure pressures along radial lines from $\theta = 0^\circ$ to 150° in increments of 30° , where the $\theta = 0^\circ$ radial is along the gun axis in the direction of fire, and at radial distances of R/c from 100 to 800. The omnidirectional B21 gauges were arranged in an array parallel to the gun axis at stand-off distances of $z/c = 11.5, 21.5, 30$ and 60 and at axial distances of x/c from -70 to 126 .

Far-field pressure measurements below 0.05 bar were made with the $\frac{1}{4}$ inch microphones; these were mounted vertically (with reference to Fig 7) on low-frequency wire supports with the microphone diaphragms at grazing incidence to the blast wave. The time at which the round left the muzzle was assessed from a strain gauge bridge designed to measure the hoop stress near the end of the barrel and from a pressure probe mounted externally at 1 cm to the rear of the muzzle.

In Fig 8 a comparison is made between the pressure-time histories measured simultaneously by a $\frac{1}{4}$ inch microphone and a B19 gauge; both positioned at $R/c = 200$, $\theta = 90^\circ$. The traces are almost identical and agree to within about 6% for the measured peak overpressure. This is typical of the agreement obtained with all the gauges and $\frac{1}{4}$ inch microphones and gave confidence in the measured results. Also to ensure that ground reflections did not contaminate the measurements appropriate nearby areas of the ground were covered with acoustic foam wedges, each 300 mm high with a base of 150 mm square, having effective attenuation down to about 200 Hz. The ground treatment is shown to have been effective by the comparison made in Fig 8.

2.2 Measurement on a surface

For the second experiment the rifle was mounted above a large horizontal rectangular plate, of dimensions 1.113 m x 0.914 m x 0.013 m, which could be offset from the gun axis by vertical displacements of $z/c = 6.5, 11.5, 16.5$ and 21.5 . The general arrangement, as shown in Figs 9 and 10, consists of eight pressure transducers mounted flush with the surface of the plate at axial positions $x/c = -14, 0, 14, 28, 42, 56, 70$ with $y/c = 0$ and at the lateral position $x/c = 0, y/c = 14$. Typical pressure-time histories are shown in Fig 11. These clearly show the precursor wave being overtaken by the propellant blast and later the appearance of the sonic boom of the projectile, which is only visible in the most distant recording taken.

3 PREDICTION SCHEME

We propose to use the theory of Smith^{19,20} for predicting the blast pressures about a gun, but with significant modifications to improve the fit with experimental results. Smith noted that, in the middle distance, the blast from a gun is similar to that of a moving explosive with a steady release of energy. An approximation to the effects of forward motion had been derived by Thornhill²¹ for an explosion with an instantaneous energy release and Smith modified Thornhill's transformation to take account of a slower release of energy. It should be observed that in the middle-distance no exact solution exists to the equations describing a stationary blast and therefore Thornhill's and Smith's theories are methods of interpreting experimentally derived data. Smith assumes that the main difference between the blast distributions about similar guns arises through variations in the momentum of the propellant gas exhausts. Once the effects of this momentum are accounted for all similar guns (i.e. guns having about the same muzzle velocity and thermodynamic properties) can be related to the same hypothetical static explosive, having a constant rate of energy release. These steps, which are implicit in Smith's theory, enable him to derive relations first for the blast pressure as a function of the effective radial distance in a static spherical explosive with a constant rate of energy release and then for the ratio of effective distance to true radial distance from a gun as a function of a distribution parameter f and angle θ . There is, however, some uncertainty about the centre from which these distances are measured; this was arbitrarily assumed by Smith to be the muzzle but for the reasons given below we feel something more accurate is needed. We accordingly use a slightly different approach although the principle is the same, and we can thus work back from a measured blast distribution to an effective distance and hence to the properties of the hypothetical static explosive. The technique for obtaining these properties, in the form of standard non-dimensional curves, is discussed later in this section.

From inspection of Fig 3a it will be observed that the almost spherical blast contours appear to originate from a non-stationary point, x_0 , on the axis of the gun. Within the timescale depicted in Figs 3a and 3b analysis suggests that x_0 settles down to around $x_D/2$, where x_D is the axial distance to the Mach disc. During the following period, which is that of interest in the present work, the trajectory of the Mach disc closely follows the location of the Mach disc for a corresponding steady jet⁴ taken to have the same nozzle exit conditions as the instantaneous muzzle conditions. It is assumed that this value of x_D represents a satisfactory approximation to the observed value and is given by

$$x_D/c = 0.7 M_e (\gamma_e p_e / p_0)^{1/2}$$

where M_e is the exit Mach number (typically unity in this case), p_e is the muzzle pressure, p_0 is the ambient pressure and γ_e is the ratio of specific heats of the propellant exhaust. We shall assume that the blast origin is at the point $x_0 = x_D/2$ instead of Smith's assumption of an origin at the muzzle. Polar co-ordinates (R, θ) at the muzzle are simply related to polar co-ordinates (R', θ') at x_0 through

$$R' = \left\{ R^2 + x_0^2 - 2Rx_0 \cos \theta \right\}^{1/2} \quad (3-1)$$

and
$$\theta' = \tan^{-1} \left\{ R \sin \theta / (R \cos \theta - x_0) \right\}. \quad (3-2)$$

The blast pressures about a gun are strongest to the front and weakest to the rear as a consequence of the forward momentum possessed by the propellant. This can be simulated by stretching the calibre, c , to give an effective calibre, c'' , which is increased and reduced in the positive and negative x directions respectively; viz

$$\frac{c''}{c} = \left(\frac{\epsilon + \frac{1}{2}U^2 + a_e U}{\epsilon} \right)^{1/2} \left[f \cos \theta' + (1 - f^2 \sin^2 \theta')^{1/2} \right] \quad (3-3)$$

This is derived from equations (A-4) and (A-5) of the Appendix by assuming that the radius of the blast source is proportional to calibre. Here the distribution parameter, f , satisfies

$$\frac{a_e + u}{a_0} = \frac{K}{a_0} \left(\epsilon + \frac{1}{2} U^2 + a_e U \right) f(1 - f^2/5) \quad (3-4)$$

and the specific energy of the propellant relative to ambient conditions is

$$\epsilon = \frac{a_e^2}{2} + \frac{a_e^2 - a_r^2}{\gamma_e (\gamma_e - 1)} \quad (3-5)$$

where a_e is the acoustic speed at the muzzle,

a_0 is the acoustic speed in ambient conditions,

a_r is the acoustic speed in the propellant gas at ambient temperature and pressure,

U is the forward velocity of the gun

and K is a constant for a given explosive such that if $V(\theta, t)$ is the mean velocity of the explosion products within a conical element $\delta\theta$ of a stationary explosion of energy ϵ , $V(\theta, \infty) = K\epsilon/a_0$. Values of the parameters for the 7.62mm rifle, can be found in Table 1. In the following discussion the forward velocity, U , of the gun will be assumed to be zero.

The non-dimensional constant K is thus related to the asymptotic value of the blast momentum in a completely spherical blast system as $t \rightarrow \infty$. To determine K , Smith first assumes that the close-in similarity solution of Rogers²⁵ for a stationary explosion at a constant rate of energy release will apply in the middle-distance for guns; thus

$$\frac{p - p_0}{p_0} \propto \left(\frac{c''}{R} \right)^4 \quad (3-6)$$

where $(p - p_0)/p_0$ is the non-dimensional peak overpressure within the blast wave*. Then from experimental measurements of the variation of $(p - p_0)/p_0$ with R/c'' Smith uses relation (3-6) to determine the distribution of c'' around the gun at a distance of $R/c = 20$. Smith found that, with the origin at the muzzle, $f = 0.8$ gave the best fit to the data for a 7.62 mm rifle and from the expression (3-4) he derived the value $K = 0.166$. If the same assumptions are made and K is derived from measurements at $R/c = 20$, then the same value would be obtained from the experiments described in section 2. However the derivation gave cause for concern since it appeared inappropriate to evaluate the asymptotic constant K from values taken so close to the muzzle. As a result, although theory and experiment agreed well in the region of $R/c = 20$, poor correlation was obtained with experiment at larger distances from the muzzle and was especially noticeable at the extreme angles, $\theta \approx 0^\circ$ and 180° .

Strictly speaking the evaluation of K is only valid after the time when the propellant flow ceases to influence the blast front. Then the blast from guns and explosives begins to behave in a similar fashion. However analysis of experimental results suggests that this is not likely to occur before the blast front reaches $R'/c = 100$. At this stage the weak blast wave theory of Bethe²⁶ can be expected to apply; then

$$\frac{p - p_0}{p_0} \propto \left(\frac{c''}{R'} \right) \left(\log \frac{R'}{c''} \right)^{-\frac{1}{2}} \approx \left(\frac{R'}{c''} \right)^{-\alpha} \quad (3-7)$$

where $\alpha = 1.17$ for $R'/c'' = 100$.

In Fig 12 we have displayed the overpressure distribution about x_0 as a function of θ' at $R'/c = 30, 60, 100, 300$ and 800 . These correspond to the experimental measurements for a 7.62mm rifle and we have assumed $x_0/c = 8$ from noting, in Fig 4, that $x_p/c \approx 16$ is the maximum forward position of the Mach disc. One of the effects of choosing an origin at x_0 rather than at the muzzle is that there is a weaker angular dependence close-in to the blast; for instance at $R'/c = 30$, where we have applied relation (3-6), the best fit is obtained with $f = 0.6$. At the other radial distances relation (3-7) was applied and in these cases the value of f giving the 'best fit' varied between 0.6 at $R'/c = 60$ to 0.5 at $R'/c = 800$. This is consistent with our expectation that K will increase with time as the mass of the propellant exhaust \dot{m} increases. (The similarity solution with steady release of energy has momentum $\sim t^5$ whereas mass $\sim t$ so that to satisfy the momentum equation per unit mass, equation (3-4), K must increase with time.) For $f = 0.5$ we find $K = 0.245$ and this is the value we propose using in the prediction scheme.

To determine the reference blast characteristics of the equivalent stationary explosive we note from equation (3-3) that there is an angle θ' for which there is no

* Rogers' solution strictly applies to p/p_0 rather than $(p - p_0)/p_0$ which is not a similarity parameter, but since it is implicit that p_0 is negligible the form (3-6) also holds in the region of validity.

stretching of calibre (i.e. $c'' = c$) to account for the propellant momentum. For a static gun with $f = 0.5$ this is $\theta' = \cos^{-1}(0.25) \approx 75^\circ$. From the experimental measurements of a 7.62mm rifle the non-dimensional parameters

$$\frac{p - p_0}{p_0}, \quad \frac{t_s a_0}{c}, \quad \frac{t a_0}{c} \quad \text{and} \quad \frac{I_+ a_0}{p_0 c}$$

have been evaluated in the direction $\theta' = 75^\circ$ and are plotted as a function of R'/c in Fig 13. Here t_s is the time of arrival of the blast wave measured from the instant when the round leaves the barrel, t is the duration of the positive blast phase and I_+ is the positive impulse. The curves differ from those originally derived by Smith, partly through having a different origin and partly through being based on a different way of evaluating the experimental data; i.e. not using filtering techniques.

It is presumed that these curves will apply to all guns with about the same muzzle velocity and thermodynamic properties as the 7.62mm rifle and that $K = 0.245$. To estimate the blast pressures about a different gun, details of the propellant muzzle conditions and velocity of the gun are needed to determine f using equation (3-4). Then the apparent change in calibre can be calculated from equation (3-3) and used instead of c to interpret the standard curves of Fig 13.

The effect of altitude can also be estimated from the scaling rule suggested by Smith; viz

$$p_0 a_0 c^2 \propto \frac{dm}{dt} \quad (3-8)$$

where p_0 is the ambient pressure, m is the mass of propellant and a_0 is the local speed of sound. He then obtains the relationship

$$\frac{\hat{c}}{c} = \left\{ \frac{p_0 a_0}{\hat{p}_0 \hat{a}_0} \right\}^{1/2} \quad (3-9)$$

where the accents denote values at altitude. This should be used in conjunction with equation (3-3), multiplying the calibre ratios together, and used to interpret the standard curves. The validity of this scaling rule has been demonstrated by Mabey and Capps²³.

4 FREE-FIELD COMPARISONS

In Figs 14 and 15 comparisons are made between theoretical predictions and experimental measurements of the blast pressure distribution about a 7.62mm rifle. Included in these comparisons is the prediction from Smith's original scheme. It will be observed that the latter generally overpredicts the pressures at low values of θ and underpredicts those at high values of θ . In general the current predictions, based on an origin at x_0 and a different distribution parameter ($f = 0.5$), give reasonable agreement with the experimental measurements. The predictions are shown for $x_0/c = 6$ and $x_0/c = 8$. It is difficult to discern which of the two predictions, either that with $x_0/c = 6$ or $x_0/c = 8$ produces the better correlation with the experimental data. Indeed, as expected, only in the regions close to the muzzle (at say $R/c < 40$) is a significant difference observed between the predictions. Now we noted earlier that the apparent origin, x_0 , seemed to be related to the Mach disc position, x_D , through $x_0 = x_D/2$. However it should be observed from Fig 4 that by the time the Mach disc reaches its maximum forward position ($x_D/c \approx 16$) the blast front has already propagated out to $R/c = 40$. Thus at early times, where the Mach disc has not reached its maximum forward position and the blast wavefront is within the range $R/c < 40$, the smaller value of x_0 , $x_0/c = 6$, might be expected to be more appropriate. Strictly speaking our model should include a moving origin since at these early times both the Mach disc and apparent origin are rapidly varying with time as is clearly seen from the time of arrival curves illustrated in Fig 3. As a compromise the fixed value $x_0/c = 6$, rather than $x_0/c = 8$, will be used in the prediction scheme and this fits the data reasonably well down to $R/c = 10$.

Deviations of the current predictions from the experimental results are most significant to the rear of the gun where the measured pressures are lower than predicted. This apparent shadow region could be related to the limiting angle of Prandtl-Meyer expansion at the muzzle.

It is also interesting to note that in Fig 14, for $\theta = 0^\circ$, the blast wave initially decays very slowly near the muzzle. Here the linear injection of momentum and energy tend to dominate the blast-wave propagation at the expense of spherical symmetry.

An overpressure scaling, $c^2(p - p_0)/W$, proposed by Westine¹⁸ for $\theta = 90^\circ$ has been used in Fig 16 to compare some aircraft guns. Here

$$W = E_p - \frac{m_s v_s^2}{2}$$

where E_p is the propellant energy, l is the length of the barrel, m_s is the mass of projectile and V its velocity. Relevant data for the various guns are given in Table 1 together with Westine's scale parameter. The experimental data collapse well according to the scaling, being in general bounded above and below by our predictions for the 27mm and 7.62mm gun, respectively. Westine's correlations for army and naval guns are also included in this figure and it should be observed that aircraft guns have a substantially different correlation.

Westine's scaling is less successful at 0° and 180° for which some data are presented in Fig 17. It produces some collapse at 0° with scatter about our prediction for the 27mm gun but produces no collapse at 180° . This is perhaps not so surprising because Westine's scaling in effect makes an allowance for the energy addition due to the moving propellant gases but none for their momentum and this discrepancy should be most significant along the gun axis while having little significance at 90° .⁵ The discrepancies are not resolved by applying the correlation proposed by Schmidt *et al*.⁵

5 INTERACTION OF GUN BLAST WITH A SURFACE

A gun mounted on the side of the fuselage of a military aircraft is likely to produce much more severe blast loading of the aircraft structure than a gun located in remote areas such as on the wings or nose of the aircraft. In the latter situations the blast can be considered as though initially propagating into free space. On the other hand for a gun installed on the side of the fuselage the blast wave will be affected from early times by interactions with the adjacent fuselage surface.

In this section we shall be concerned with predicting the blast pressures on a surface in close proximity to the muzzle. A cross-sectional view of the developing blast wave as it interacts with an unyielding surface is illustrated in Fig 18. The view is in the plane of the muzzle looking down the barrel.

The presence of the unyielding surface introduces additional shocks into the system which are associated with the reflection of the incident blast wave at the surface. In theoretical terms the situation can be modelled by the familiar source and image system with a blast field having the characteristics of that produced by two guns firing simultaneously. Along the surface line the blast wave may be reflected either as a regular reflection or as a Mach reflection. Discussion of the properties of reflection of shocks and blast waves can be found in Refs 27 to 30.

5.1 Regular reflection

Regular reflection of blast waves occurs in much the same way as the reflection of acoustic waves, with the incident and reflected wavefronts merging at a single point on the surface as illustrated in Fig 18. However for oblique incidence the angle of reflection only equals that of the incident wave in the acoustic limit of a weak blast wave.

Since the reflected wave moves into a gas which is preheated and compressed by the incident wave it travels faster than the latter. There is a critical angle ($\alpha_0 = \alpha_e$, where α_0 is defined in Fig 18) beyond which part of the reflected wave catches up with the incident wave and merges with it to produce a single shock. This is the second reflection process called Mach reflection. The single merged shock is often called the Mach stem and is indicated in Fig 18.

Below the critical angle of incidence regular reflection prevails. On the surface the coincidence of the two shocks will give rise to larger overpressures than would be observed in free space. For instance at normal incidence the peak instantaneous reflected overpressure is given by

$$p_2 - p_0 = 2(p_1 - p_0) + (\gamma + 1)\left(\frac{1}{2}\rho u^2\right)_1 \quad (5-1)$$

where $\left(\frac{1}{2}\rho u^2\right)_1$ is the dynamic pressure immediately behind the incident wave front, $p_1 - p_0$ is the peak incident overpressure, $p_2 - p_0$ is the peak reflected overpressure and γ is the ratio of specific heats in the ambient gas. For weak blast waves approaching the acoustic limit of $(p_1 - p_0)/p_0 \ll 1$ the dynamic pressure can be neglected in (5-1), since $\left(\frac{1}{2}\rho u^2\right)_1 \approx (p_1 - p_0)^2/p_0(\gamma + 1)$, and the familiar pressure doubling of acoustic waves is then obtained. However at high incident overpressures the dynamic pressure cannot be neglected and then, for $\gamma = 1.4$, reflected overpressures approaching the asymptotic value of eight times the incident wave are predicted. Such a magnification is unlikely to be experienced for the pressures involved in gun blast but factors of around 4 have been measured.

It should be noted that oblique reflection can result in stronger reflected overpressure ratios than at normal incidence, as is shown in Fig 19, although this only occurs at relatively weak shock overpressures.

For oblique incidence the reflected overpressure can be expressed in terms of the incident overpressure in the usual way, by applying the Rankine-Hugoniot relations, and it can be shown²⁸ that:

$$\frac{(1 - \xi_0)t_0}{1 + \mu\xi_0 + (\xi_0 + \mu)t_0^2} = \frac{(\xi_2 - 1)t_2}{1 + \mu\xi_2 + (\xi_2 + \mu)t_2^2} = \beta \quad (5-2)$$

$$\text{and } \beta^2(1 - \mu)^2(t_0 - t_2) + \beta\{(1 - \mu)^2 - (t_0 - t_2)^2 - (\mu + t_0 t_2)^2\} - (t_0 - t_2) = 0 \quad (5-3)$$

where $\xi_k = p_k/p_1$, $t_k = \tan(\alpha_k)$, and $\mu = (\gamma - 1)/(\gamma + 1)$. Here the suffix k takes the value 0 for the incident wave and the value 2 for the reflected wave. From the angle of the incident wave, α_0 , equation (5-2) is used to calculate β and equation (5-3) to calculate the angle of the reflected wave, α_2 , and finally equation (5-2) is applied again to obtain ξ_2 . Equation (5-3) is a quadratic in t_2 and therefore there are two solutions for regular reflection at a surface. Only the solution with the smaller angle, α_2 , is of physical relevance since this is the only solution providing continuity with the solution (5-1) at normal incidence ($\alpha_0 = 0$).

As the angle of incidence, α_0 , is increased we find that for fixed incident pressure ratio, ξ_0 , a stage is reached when the two roots to the quadratic become imaginary. At this and higher angles there is no solution to regular reflection. The extreme wave angle, α_e , satisfies a cubic relation²⁹ and the solution is shown in Fig 20 as a function of the incident pressure ratio. It is around 40° for a strong shock but increases as the shock is weakened and approaches 90° in the acoustic limit. Above this extreme angle of incidence Mach reflection occurs.

The above analysis is possible because for the reflection of a plane shock at an infinite wall with $\alpha_0 < \alpha_e$ coordinates can be found which move with the point of contact between the shock and the wall, in which a steady solution exists. This is no longer possible when $\alpha_0 > \alpha_e$ since the point of contact has already been engulfed by the waves from earlier reflections which form the Mach stem, and this reflection pattern is known as Mach reflection.

5.2 Mach reflection

In the region of Mach reflection approximate techniques need to be used to calculate the overpressure across the Mach stem. Kinney³⁰ suggests that an adequate approximation can be obtained by assuming the Mach stem is straight and at right angles to the reflecting surface. Then provided the properties of the Mach stem are slowly varying, the Mach number M_s of the stem (i.e. the velocity of the stem front divided by the speed of sound in the ambient air) can be approximated by $M_1/\sin(\alpha_0)$. Here α_0 is to be understood as the angle at which the incident blast wave would have intercepted the boundary in the absence of a Mach stem and M_1 is the Mach number of the incident blast wave. M_1 is related to the incident overpressure through the expression

$$\frac{p_1 - p_0}{p_0} = \frac{2\gamma}{\gamma - 1} (M_1^2 - 1) \quad (5-4)$$

which is derived from the Rankine-Hugoniot relations for normal shocks. A similar equation, with suffix 1 replaced by suffix s, can be applied to determine the peak overpressure, $p_s - p_0$, within the Mach stem shock.

5.3 Predicted and measured surface pressures

To determine the peak reflected overpressure on a surface it is necessary to have details of (i) the overpressure across the incident wave and (ii) the angle of the blast wave front with the surface. The first of these, the incident overpressure, can be determined from the prediction scheme outlined in section 3. Comparisons between the predicted and measured free-field blast pressures at surface positions are shown in Fig 21 for a 7.62mm rifle.

The angle of incidence, α_0 , between the blast front and a surface parallel to the gun axis can be deduced from the theory of section 3 and satisfies

$$\cot(\alpha_0) = \tan(\theta') \left\{ \frac{n(1 - f^2 \sin^2 \theta')^{\frac{1}{2}} - (1 - n)f \cos \theta'}{n(1 - f^2 \sin^2 \theta')^{\frac{1}{2}} - (1 - n)f \sin \theta' \cos \theta'} \right\} \quad (5-5)$$

where the index n is associated with the relationship $(t_s a_0/c^n) \propto (R'/c^n)^n$ and is

determined from the standard curves in Fig 13. If $\alpha_0 < \alpha_e$ then the equations (5-2) and (5-3) for regular reflection should be applied or alternatively if $\alpha_0 > \alpha_e$ then the approximations for Mach reflection can be used.

In Fig 22 the predicted and measured peak overpressures on a large flat plate, parallel to the gun axis, are compared at two gun heights, $z/c = 11.5$ and 21.5 , for the 7.62mm rifle. Where regular reflection is applicable reasonable agreement is obtained between the predicted and measured overpressures. However less satisfactory correlation is obtained in the region of Mach reflection at $z/c = 11.5$, where the measured overpressures for positive x are considerably greater than those predicted. The poor correlation for Mach reflection probably arises through violation of the initial assumptions in the approximation; specifically the Mach stem may grow much faster than permitted. Indeed if the gun is very close to the surface the incident and reflected waves may quickly fuse into a single blast wave everywhere. Then a distant observer would appear to measure the blast field of two coincident guns; or, equivalently, that of a single gun with twice the blast energy. Such behaviour is often referred to as a surface burst.

The surface burst behaviour can be accounted for in the theory of section 3 by simply factoring the calibre by $\sqrt{2}$. This follows from the scale rule (3-8) and the requirement of a doubling of the blast energy. Calculations from such considerations should only be applicable in the distant field for a gun very close to a large flat surface.

The predicted peak overpressures for a surface burst are shown in Fig 22 for a 7.62mm rifle and these compare favourably with the experimental measurements at extreme locations; although for interest the prediction has been extended into the near field. Surface burst calculations are also presented in Fig 17 for the 27mm gun. It should be noted that a significant proportion of the experimental data for a 27mm gun on a representative fuselage is bracketed by the free-field and surface burst predictions.

6 CONCLUSIONS

A method is described for determining the blast pressures about the muzzle of a gun from properties of the propellant exhaust. The technique is based on Smith's^{19,20} analogy of gun blast with an explosive releasing energy at a constant rate and having strong directional effects due to the momentum of the propellant gas flow. A distribution function is derived by a method similar to that used by Smith²⁰ but including a modification which allows the apparent centre of the explosion to be in the shock bottle at a distance $x_0/c = 6$ from the muzzle. In addition the parameter f is assigned a value 0.5 instead of 0.8; f gives a measure of the contribution of the linear momentum to the blast field arising from the fact that the gases are fired out of the gun barrel. The calculated value of f is not constant and falls with increasing distance; $f = 0.5$ approximates to the asymptotic value for large distance.

Pressure predictions based on this model agree well with experimental data for a 7.62mm rifle and a 27mm aircraft gun. For other guns a reasonable correlation is obtained with Westine's¹⁸ scaling at 90° to the gun axis. The latter scaling does not apply on the gun axis and specifically at 180° there appears to be a strong shadow region for some guns.

Gun blast measurements were also obtained experimentally on surfaces near to the gun muzzle and it is shown that these can be predicted with reasonable accuracy if regular reflection occurs, although in the region of Mach reflection there is still considerable room for improvement. The indications are that better results can be obtained by means of surface burst predictions (*ie* where the incident and reflected waves are assumed to coalesce) and this is recommended for the distant field of a fuselage-mounted gun.

REFERENCES

- 1 Schmidt, E.M. and Shear, D.D. 'Optical measurements of muzzle blast.' AIAA Journal 13, 1086-1091 (1975)
- 2 Klingenberg, G. 'Investigation of combustion phenomena associated with the flow of hot propellant gases. III: Experimental survey of the formation and decay of muzzle flow fields and of pressure measurements.' Combustion and Flame 29, 289-309 (1977)
- 3 Adamson, T.C. and Nicholls, J.A. 'On the structure of jets from highly underexpanded nozzles into still air.' Journal of Aero/Space Sciences, 26, 16-24 (1959)
- 4 Lewis, C.H. and Carlson, D.J. 'Normal shock locations in underexpanded gas and gas-particle jets.' AIAA Journal 2, 776-777 (1964)
- 5 Schmidt, E.M., Kahl, G.D. and Shear, D.D. 'Gun blast: its propagation and control.' AIAA 6th Aeroacoustics Conference, June 4-6, 1980, Hartford, Connecticut
- 6 Erdos, J.I. and Del Guidice, P.D. 'Calculations of muzzle blast flowfields.' AIAA Journal 13, 1048-1055 (1975)
- 7 Oswatitsch, K. 'Intermediate ballistics.' DVL Report 358, Aachen, June 1964

- 8 Moore, G.R. 'Projectile environment during intermediate ballistics.' Proc. TTCPW-2 Meeting Valcartier, Canada, June 1974, pp.251-264
- 9 Maillie, F.H. 'Projectile environment during intermediate ballistics.' Proc. First Int. Symp. Ballistics, II, 1-18 (1975)
- 10 Soo Hoo, G. 'Finite difference calculations of the free-air blast field for an 8"/36 gun.' Naval Weapons Laboratory Technical Report TR-3122, June 1974
- 11 Zoltani, C.K. 'Analysis of the initial development of the intermediate ballistic region of a small arm.' Journal Ballistics 2, No.1 (1978)
- 12 Traci, R.M., Farr, J.L. and Liu, C.Y. 'A numerical method for the simulation of muzzle gas flows with fixed and moving boundaries.' BRL-CR-161, US Army Ballistic Research Laboratory, Aberdeen Proving Ground, June 1974
- 13 Taylor, T.D. and Lin, T.C. 'A numerical model for muzzle blast flow fields.' AIAA Journal 19, 346-349 (1981)
- 14 MacCormack, R. 'The effect of viscosity in hypersonic impact cratering.' AIAA Paper 69-354, Cincinnati, Ohio (1969)
- 15 Harlow, F.H. 'The particle-in-cell computing method for fluid dynamics.' Methods in Computational Physics, Vol.3, p.319, Academic Press, New York (1964)
- 16 Gentry, R.A., Martin, R.E. and Daly, B.J. 'An Eulerian differencing method for unsteady compressible flow problems.' J. Computational Physics 1, 87-118 (1966)
- 17 Godunov, S.K. 'A difference method for the numerical calculation of discontinuous solutions of hydrodynamic equations.' Mat. Sbornik, 47, No.3, 271-306 (1959), translated by US Joint Publications Research Service as JPRS 7226, November 1960
- 18 Westine, P.S. 'The blast field about the muzzle of guns.' Shock and Vibration Bulletin 39, 139-149 (1969)
- 19 Smith, F. 'A study of gun blast in relation to that from a moving explosion.' RARDE Memorandum 28/70 (1970)
- 20 Smith, F. 'A theoretical model of the blast from stationary and moving guns.' First International Symposium on Ballistics, Orlando, Fla., November 13-15, 1974
- 21 Thornhill, C.K. 'A stationary model of the explosion from a moving spherical charge.' ARDE Report (B) 11/57 (1957)
- 22 Smith, F. 'Loads on surfaces due to gun blast.' RARDE Memorandum 29/70 (1970)
- 23 Mabey, D.G. and Capps, D.S. 'Blast from moving guns.' AIAA J. Aircraft 14, 687-692 (1977)
- 24 Yagla, J.T. 'Analysis of gun blast phenomena for naval architecture, equipment and propellant charge design.' Third International Symposium on Ballistics, Karlsruhe, Germany (1977)
- 25 Rogers, M.H. 'Similarity flows behind strong shock waves.' Quart. J. Mech. and Appl. Math. 11, 411-422 (1958)
- 26 Bethe, H. 'Blast wave.' Los Alamos Sci. Lab. Tech. Series, Vol.7, Part 2, August 1947
- 27 Von Neumann, J. 'John von Neumann: collected works.' Vol.6, Ed: A.H. Taub, Pergamon Press (1963)
- 28 Courant, R. and Friedrichs, K.O. 'Supersonic flow and shock waves.' Interscience (1948)
- 29 Polachek, H. and Seeger, R.J. 'Shock wave interactions.' Fundamentals of Gas Dynamics, Vol.III, Ed: H.W. Emmons, Oxford University Press (1958)
- 30 Kinney, G.F. 'Explosive shocks in air.' Macmillan (1962)
- 31 Pennelegion, L. and Grimshaw, J.F. 'The diffraction of the blast wave emerging from a conical nozzle driven by compressed gas.' Proc. 12th International Symposium on Shock Tubes and Waves, Jerusalem, July 16-19, 1979
- 32 Wong, W.F. 'Experimental results of a gun gas induced shock wave study and a method to suppress the shock strength.' Northrup NOR 69-167, September 1969
- 33 Dixon, S.L. 'The reduction of blast pressures from an Aden gun.' RAE Technical Note ARM 589, August 1956
- 34 Mabey, D.G. 'Some measurements of gun blast on a Lightning aircraft.' RAE Technical Memorandum Structures 922 (1978)

35 Glasstone, S. 'The effects of Nuclear weapons.' Chapter 3, US Department of Defense, Atomic Energy Commission (1962)

Table 1
GUN PARAMETERS

Calibre, c	(mm)	30	27	20	7.62	5.56
Barrel length, l/c	(calibre)	42.8	71.8	76	70.7	84.5
Mass of propellant, m_p	(kg)	0.046	-	0.0389	0.002851	0.001782
Mass of projectile, m_s	(kg)	0.219	-	0.098	0.0093	0.003506
Muzzle velocity, V_s	(m/s)	780	-	1006	846	945
Propellant exit velocity, a_e	(m/s)	-	-	900	980	-
Propellant acoustic speed, a_r at ambient temperature (298 K)	(m/s)	-	-	-	300	-
Propellant temperature at exit	(K)	-	-	2577	-	2500
Ratio of specific heats, γ_e for the propellant		1.25	-	1.25	1.286	1.24
Initial muzzle pressure	(Pa)	-	-	235	670	600
Specific impulse, I_p of propellant	(J/kg)	955000	-	955000	955000	986400
Excess energy, W	(J)	109100	211900	99008	6250	5465
Westine's scale, $c^2 l/W$	(Pa ⁻¹)	1.058×10^{-8}	6.675×10^{-9}	6.14×10^{-9}	5.00×10^{-9}	2.66×10^{-9}

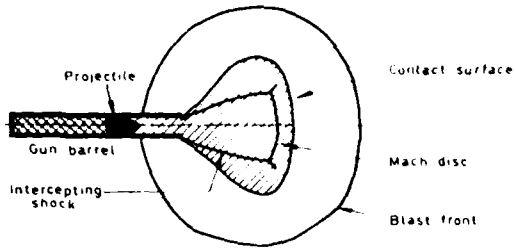


Fig 1 Precursor blast field

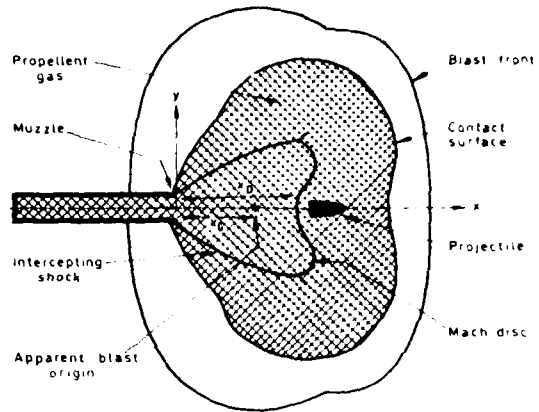


Fig 2 Propellant blast field

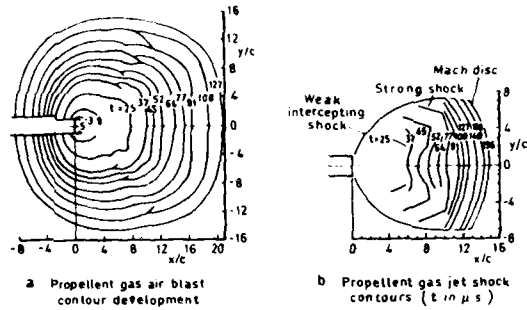


Fig 3a-d Details of the developing propellant field for an M16 rifle (Ref 1)

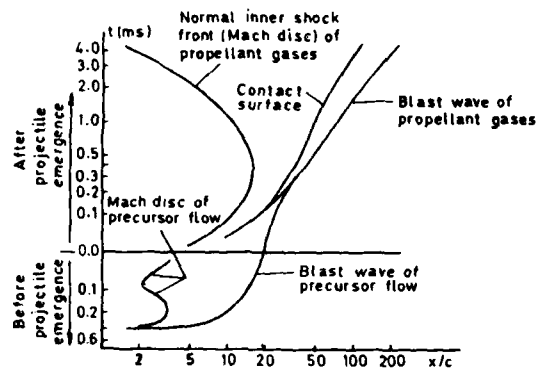


Fig 4 Axial trajectories of the developing field of a 7.62mm rifle (Ref 2)

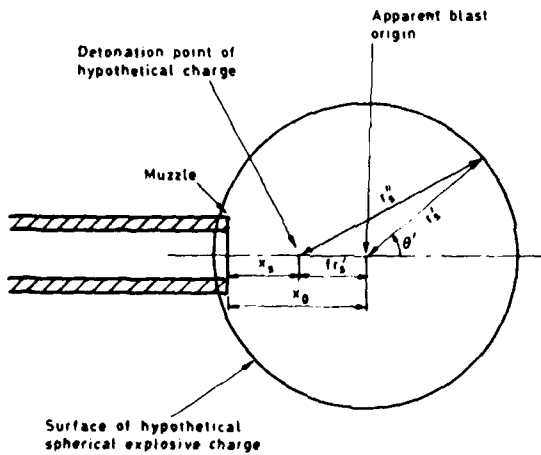


Fig 5 Spherical charge model for gun blast

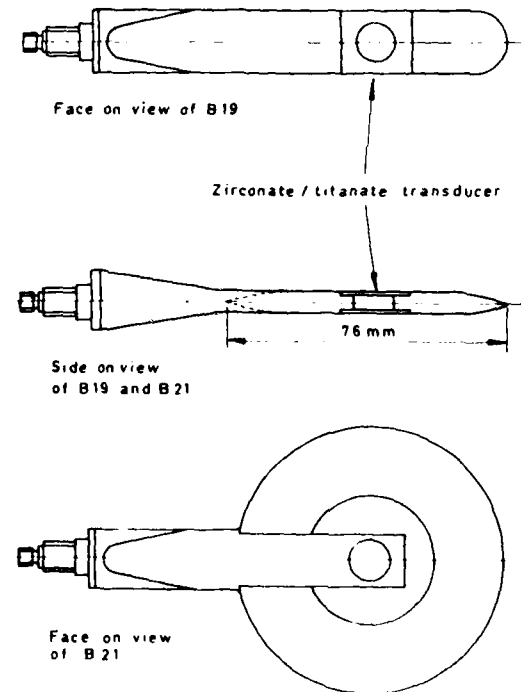


Fig 6 Atomic Weapons Research Establishment B19 and B21 piezoelectric blast gauges

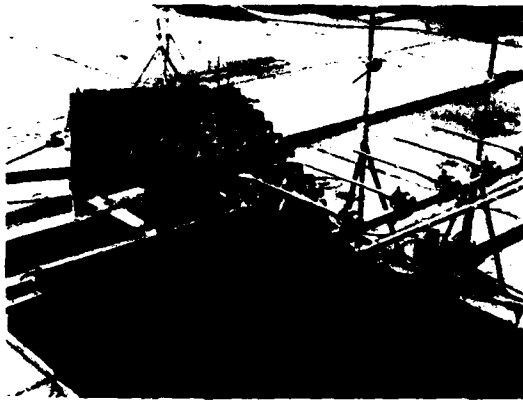


Fig 7 Experimental configuration to measure the field gun blast pressures



Fig 10 Main components of experiment to measure gun blast pressures on a nearby surface

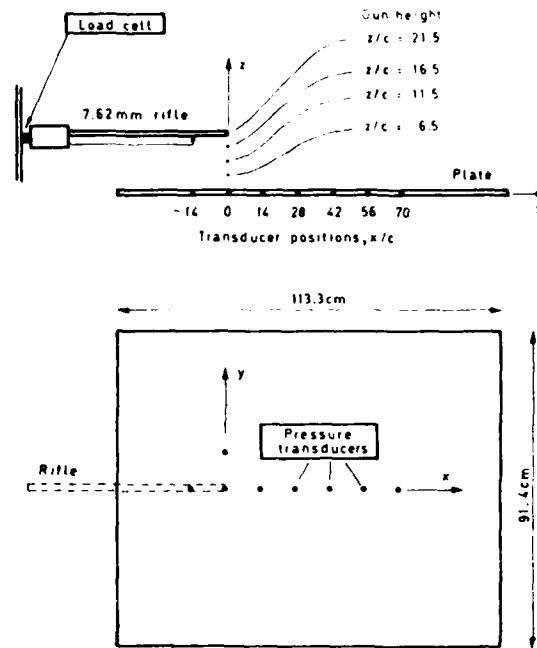


Fig 9 General arrangement of gun blast experiment to measure reflected overpressures

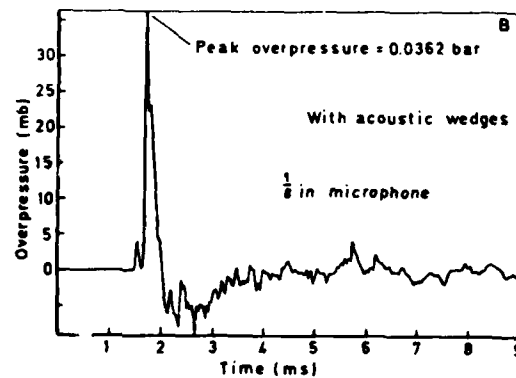
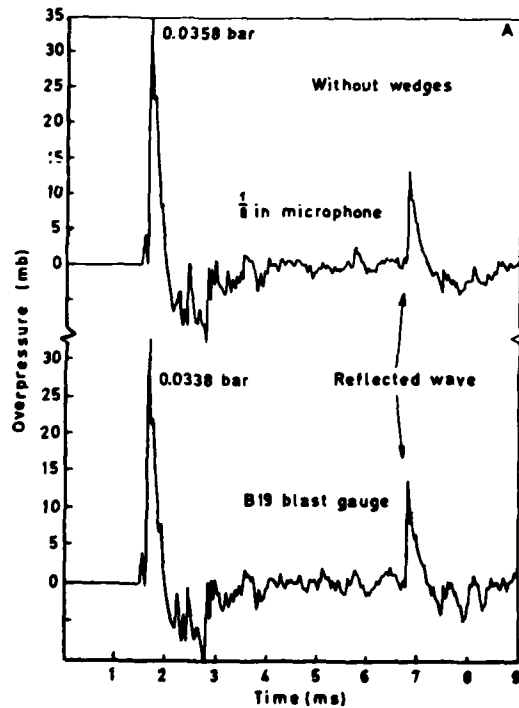


Fig 8 Pressure-time histories measured at 200 calibres to the side of the muzzle of a 7.62mm rifle mounted at a height of 200 calibres above ground. (A) Comparison of a B19 blast gauge with an 1/8 inch microphone. (B) Effect of ground treatment, using acoustic foam wedges

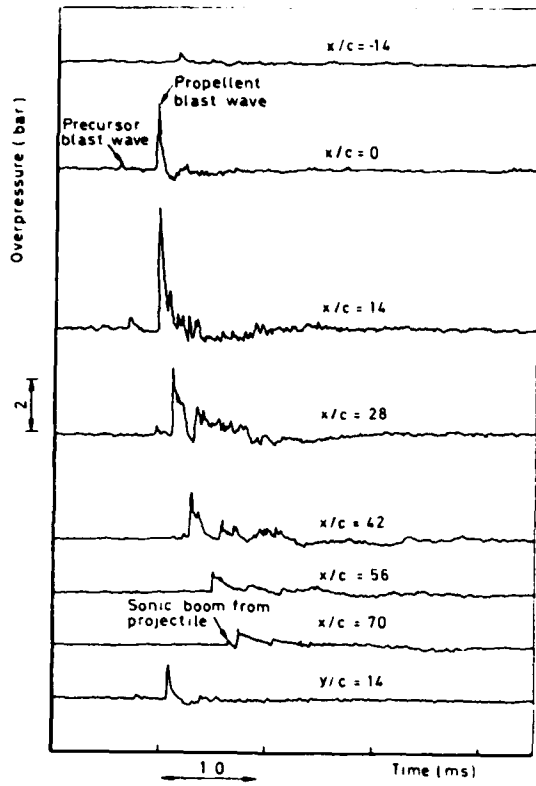


Fig 11 Pressure-time histories on plate at gun height of $z = 11.5$ calibres. Parameters: x = axial distance, y = lateral distance

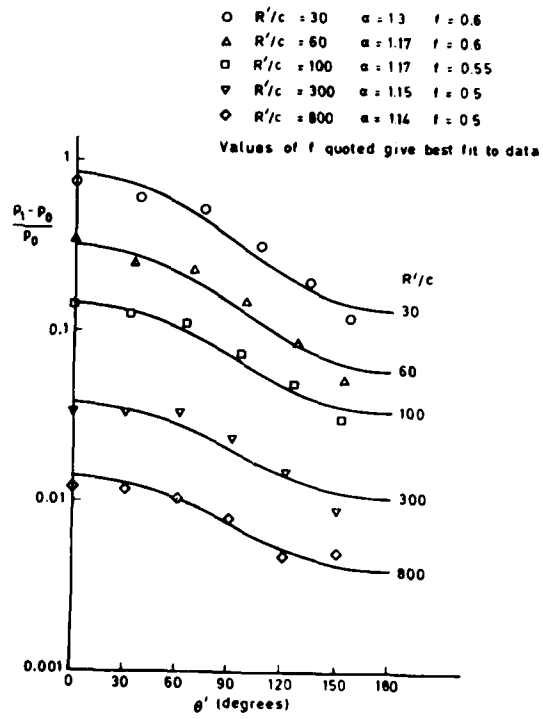


Fig 12 Angular distribution of peak overpressure about a 7.62mm rifle. Blast origin at $8c$

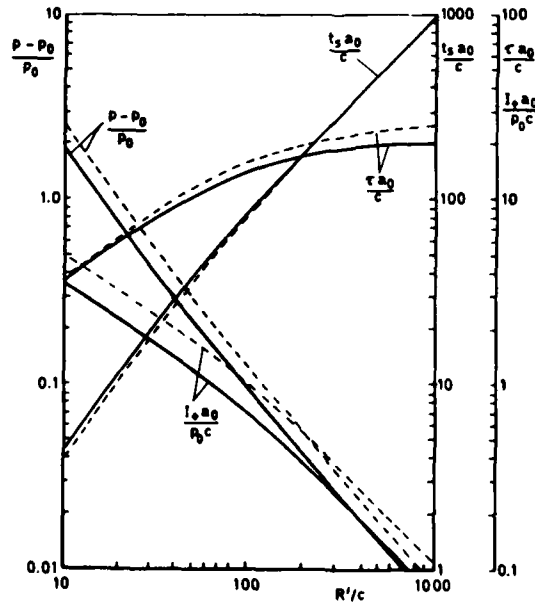


Fig 13 Standard curves, without momentum, for 7.62mm rifle
 — Current calculation (with $x_0 = 8c$)
 - - - - - Smith (with $x_0 = 0$)

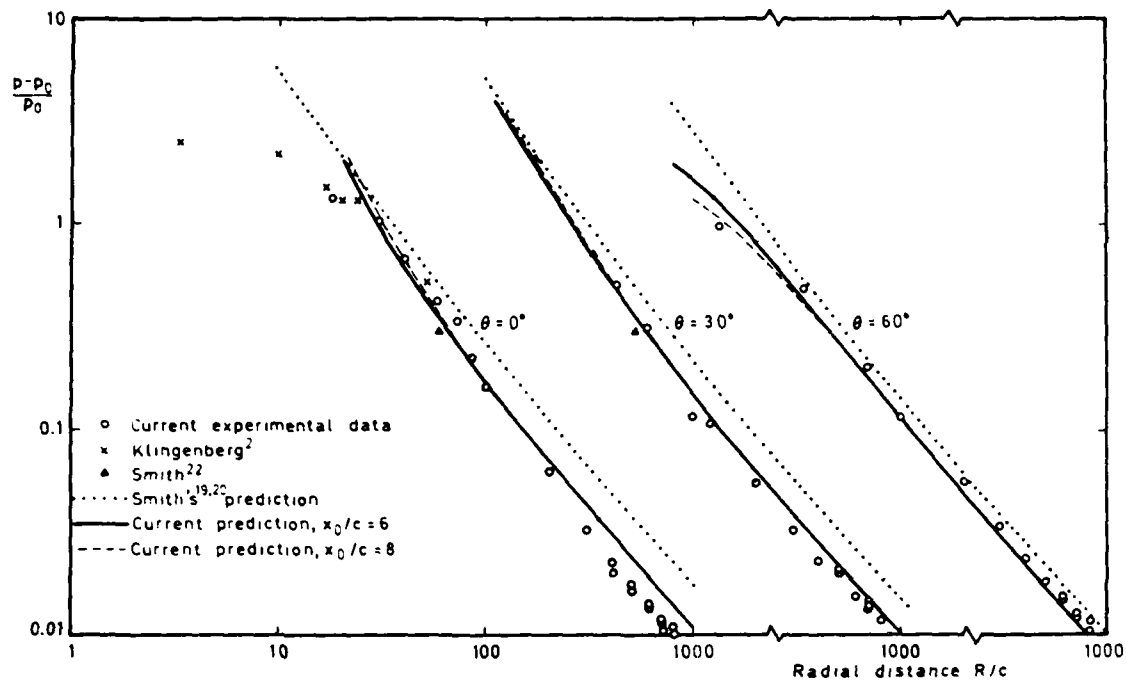


Fig 14 Comparison of current predictions with experiment for the radial distribution of maximum overpressure at $\theta = 0^\circ$, 30° and 60° for a 7.62mm rifle

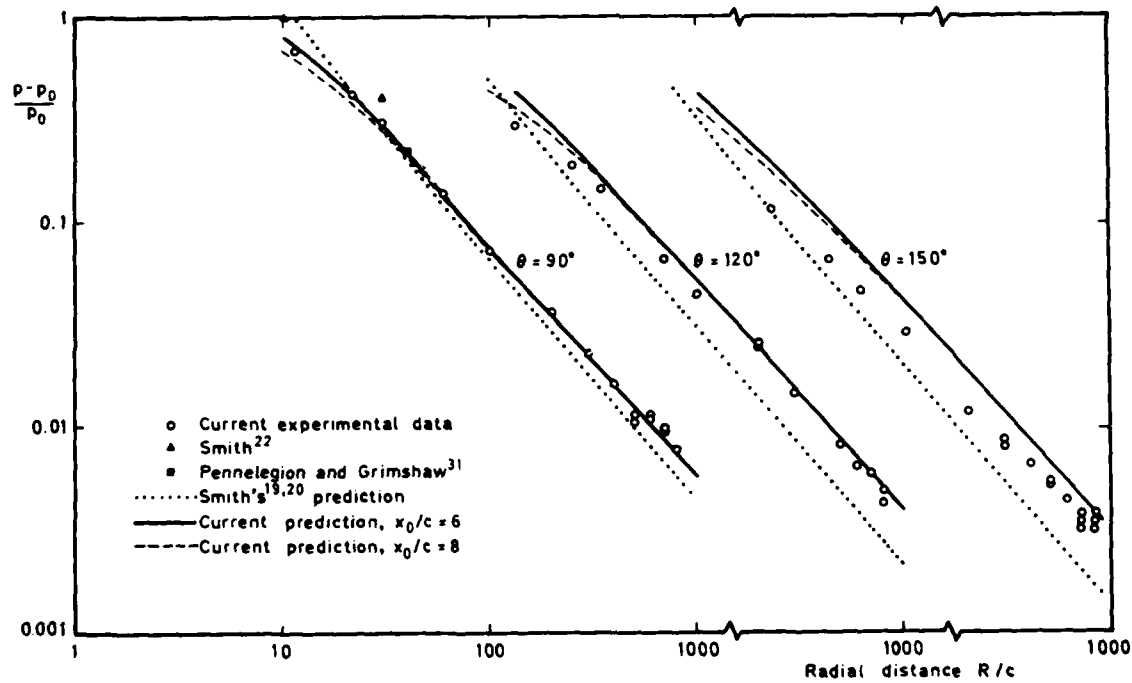


Fig 15 Comparison of current predictions with experiment for the radial distribution of maximum overpressure at $\theta = 90^\circ$, 120° and 150° for a 7.62mm rifle

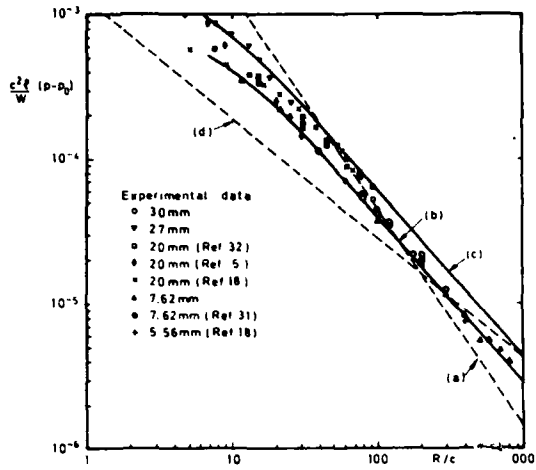
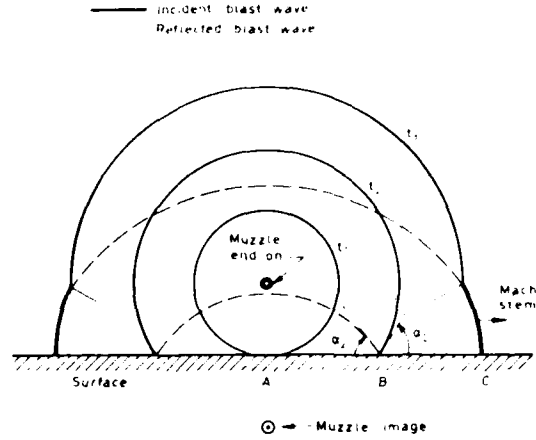


Fig 16 Scaled maximum overpressure versus R/c at 90° to gun axis, after Westine (Ref 18)
 - - - Westine's correlation for (a) Army guns and (d) Naval guns
 - - - Current predictions for (b) a 7.62mm rifle and (c) a 27mm cannon ($x_0/c = 6$)



Pt A - normal reflection
 Pt B - regular reflection
 Pt C - Mach reflection

Fig 18 Reflection of gun blast from a flat surface at successive times t_i

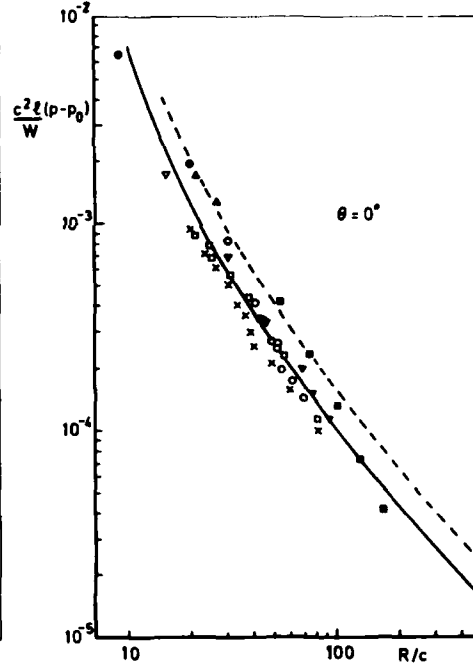
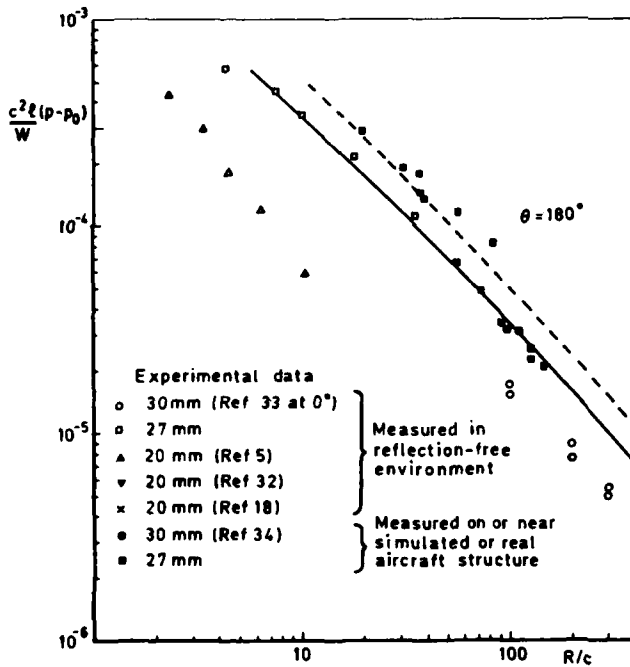


Fig 17 Scaled maximum overpressure distribution about aircraft guns compared with predictions for a 27mm gun: — Free-field; - - - Surface burst ($x_0/c = 6$)

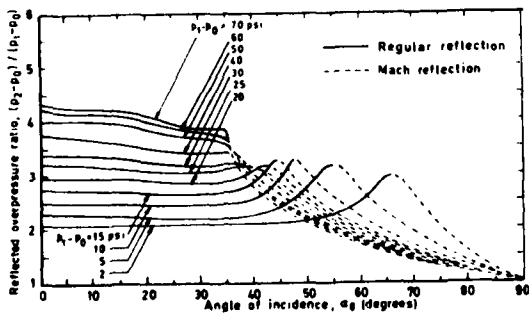


Fig 19 Plane shock reflected overpressure ratio as a function of angle of incidence for various incident overpressures (Ref 35)

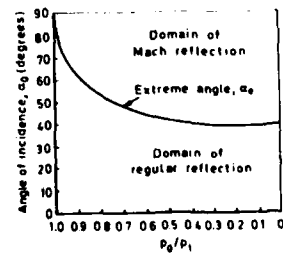


Fig 20 Extreme angle for regular reflection as a function of the pressure ratio p_0/p_1 (Ref 28)

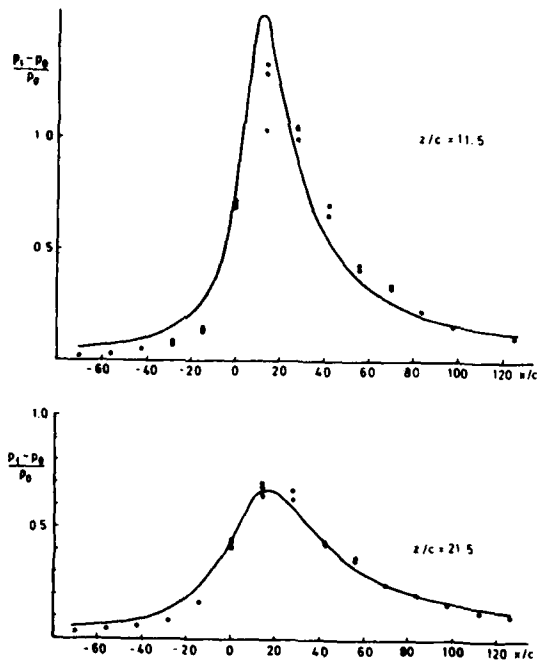


Fig 21 Overpressure distribution in free-field along axial direction at lateral displacements $z/c = 11.5, 21.5$
 o Experimental measurements
 — Current prediction ($x_0/c = 6$)

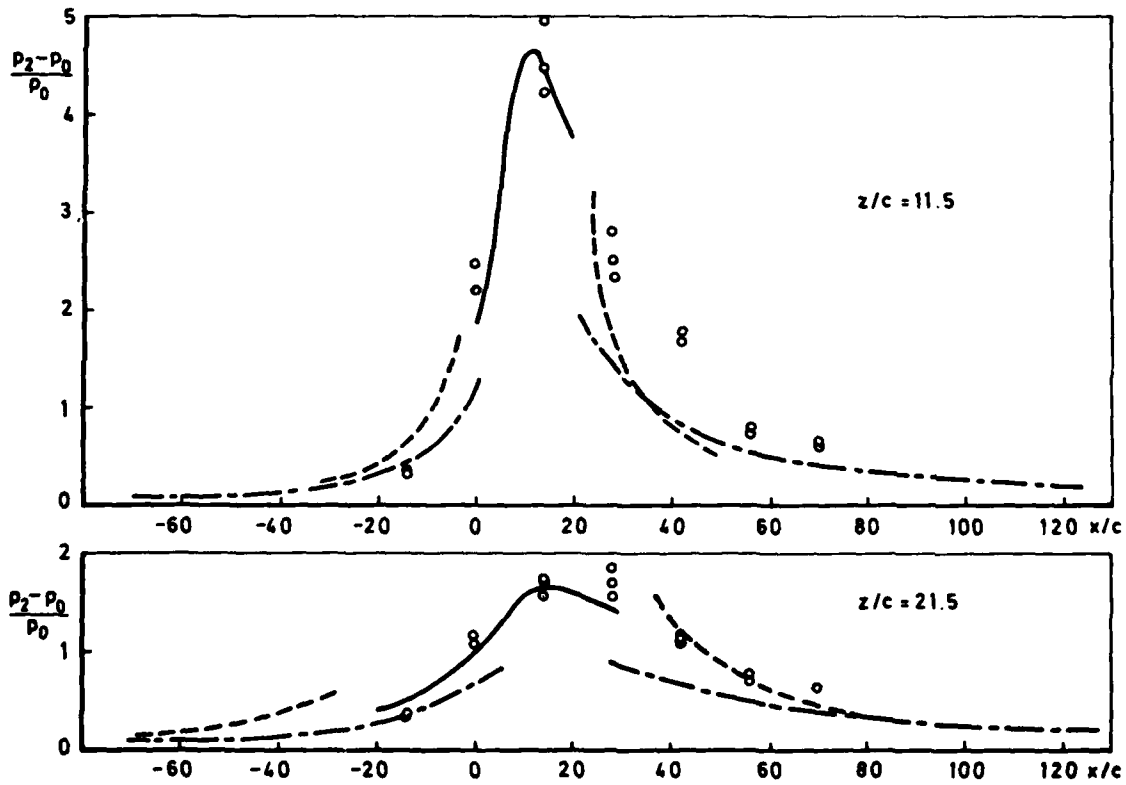


Fig 22 Overpressure distribution on large flat plate at gun heights $z/c = 11.5, 21.5$
 o Experimental measurements
 — Prediction for regular reflection
 ---- Approximation for Mach reflection
 -.- Far-field surface burst prediction

Appendix

THEORETICAL DISCUSSION OF GUN BLAST MODEL

In this Appendix we shall follow the theoretical arguments of Thornhill²¹ and of Smith^{19,20} to derive the theoretical results used in our model, section 3, for predicting the blast from guns. The basic concept adopted by Thornhill is to assume that if a sphere of explosive charge is detonated at its centre while in motion, the blast distribution will be approximately the same as if an identical spherical stationary charge had been detonated off-centre. The principle here is that the linear momentum of the moving charge must be preserved in the blast field, which would not occur for a centrally-detonated stationary charge. When a fixed stationary charge is detonated off-centre, however, it may be deduced that the amount of momentum in a given direction will vary in accordance with the amount of explosive within a cone radiating in that direction from the detonating point. There will thus be a net component of linear momentum in the direction from the detonation point to the charge centre, which should then coincide with the direction of the gun barrel. The concept must be understood in a hypothetical sense. In an experiment in which a spherical charge is detonated off-centre in free space, no net linear momentum would accrue so that the charge must be thought of as fixed in some way with the reaction force generating the linear momentum. Even so, there would be no extra energy supply and the 'energy excess' would be cancelled by expansion waves; these too must be disregarded as they are in the conical model. Details of the blast field can then be determined from those of a stationary charge.

Let us assume that at time t the mass $m(t)$ of exhausted propellant is contained within a sphere centred a distance x_0 from the muzzle in the direction of fire and on the gun axis. Suppose for the moment that there is no net forward momentum of the exhausting gases; this will be included later. Consider a cone with semi-angle ϕ and apex x_0 extending outwards to the spherical shock front at a radius $r = R(t)$. The mass of propellant within this cone is $\frac{1}{2}m(t)(1 - \cos \phi)$. A radial velocity $V(\phi, t)$ is then defined such that the total momentum of the system within the cone is $\frac{1}{2}m(t)(1 - \cos \phi) \times V(\phi, t)$.

Conservation of momentum for the system within this cone can be expressed as

$$\frac{1}{2}(1 - \cos \phi) \frac{\partial}{\partial t} [m(t)V(\phi, t)] = 2\pi \sin^2 \phi \int_0^{R(t)} (p - p_0) r dr$$

where p is the gas pressure and the suffix 0 denotes ambient conditions. Then integration of this expression results in

$$m(t)V(\phi, t) = 8\pi \cos^2\left(\frac{\phi}{2}\right) \int_0^t \int_0^{R(t)} (p - p_0) r dr dt$$

which, on changing the order of integration, can be rewritten as

$$m(t)V(\phi, t) = 8\pi \cos^2\left(\frac{\phi}{2}\right) \int_0^{R(t)} r I(r) dr \quad (A-1)$$

where

$$I(r) = \int_{T(r)}^{\infty} (p - p_0) dt$$

is the total impulse per unit area and $T(r)$ is the time at which the blast front reaches r . Non-dimensionalising (A-1) and taking the limit as $\phi \rightarrow 0$, $t \rightarrow \infty$ we obtain

$$m(\infty)V(0, \infty) = 8\pi \frac{p_0 L^3}{a_0} \int_0^{\infty} \left\{ \frac{r}{L} \right\} \left\{ \frac{I a_0}{p_0 L} \right\} d\left(\frac{r}{L}\right) \quad (A-2)$$

where L is a typical length and a_0 is the speed of sound in the ambient gas.

The mass of propellant $m(t)$ increases linearly with t at early times but must eventually reach a constant value equal to the total propellant mass that was originally in the barrel; i.e. $m(\infty) = \text{constant}$. This is typically reached within 1 ms of shot emergence. Thus $I(r)$ must decay sufficiently rapidly for $V(0, \infty)$ to be bounded at large times. We therefore assume

$$\int_0^{\infty} \left\{ \frac{r}{L} \right\} \frac{I a_0}{P_0 L} d\left(\frac{r}{L}\right) = \frac{K}{8\pi} ,$$

is a finite quantity and thus

$$m(\infty)V(0,\infty) = K \frac{P_0 L^3}{a_0} . \quad (A-3)$$

This represents an asymptotic expression for the momentum in any direction within an explosive system which has no net momentum. We now create a model based on the above to produce a system having net momentum appropriate to the exhausting gases of static and moving guns.

The propellant gases emerge from the gun at local sonic speed a_e and gain this velocity at the expense of the internal energy of the gas. The excess energy is $\epsilon m(t)$, where

$$\epsilon = \frac{a_e^2}{2} + \frac{a_e^2 - a_r^2}{\gamma_e (\gamma_e - 1)}$$

and a_r is the speed of sound in the propellant gas at ambient temperature and γ_e is the ratio of specific heats for the propellant gas. If in addition the gun moves with velocity U the total excess energy relative to the free stream is

$$m(t) \left[\frac{(a_e + U)^2}{2} + \frac{a_e^2 - a_r^2}{\gamma_e (\gamma_e - 1)} \right]$$

which reduces to $m(t) [\epsilon + (U^2/2) + a_e U]$. A new propellant mass $m'(t)$ is defined by

$$m'(t) = m(t) \left(\frac{\epsilon + (U^2/2) + U a_e}{\epsilon} \right) \quad (A-4)$$

so that the new system has the same specific energy, ϵ , as the stationary blast system.

Consider now the effective origin to be displaced towards the muzzle by a fraction f of the source radius r'_s (or radius of equivalent spherical charge) to the point x_s so that $x_0 - x_s = r'_s f$ (see Fig 5) where $r'_s = r_s \left\{ \frac{\epsilon + (U^2/2) + U a_e}{\epsilon} \right\}^{1/2}$ and r_s is the radius that the actual charge would have if spherical. It is assumed that the propellant contained within two rigid right circular cones with infinitesimally displaced semi-angles θ' , $\theta' + d\theta'$ will produce a blast wave element which is identical to that of a zero-net-momentum source with radius

$$r_s'' = r'_s \left[f \cos \theta' + (1 - f^2 \sin^2 \theta')^{1/2} \right] . \quad (A-5)$$

The mass of propellant within the cones separated by $d\theta'$ is

$$\frac{3m'(t)}{4\pi (r'_s)^3} \int_0^{r'_s} 2\pi r \sin \theta' r dr d\theta'$$

and therefore in the limit of $t \rightarrow \infty$ the momentum equation in the axial direction is

$$m'(t) (a_e + U) = \int_0^{\pi} V(0,\infty) \cos \theta' \left[\frac{3m'(t)}{4\pi (r'_s)^3} \int_0^{r'_s} 2\pi r \sin(\theta') r dr \right] d\theta' .$$

Performing the integrations we obtain

$$a_e + U = V(0,\infty) f \left(1 - \frac{f^2}{5} \right) \left(\frac{\epsilon + (U^2/2) + U a_e}{\epsilon} \right) . \quad (A-6)$$

Since in the distant field the blast from a gun is similar to that from an instantaneous explosion we can apply the combined Hopkinson and Sach's rule $p_0 L^3 = m v$ to (A-3) together with (A-6) to give

$$\frac{a_e + U}{a_0} = K \left(\frac{\epsilon + (U^2/2) + U a_e}{a_0^2} \right) f \left(1 - \frac{f^2}{5} \right) . \quad (A-7)$$

To use these results in a prediction scheme it is assumed that the source radius r_s is proportional to the calibre c and that K is a constant for all similar guns. For a specific static gun ($U = 0$) the value of K can be determined from the value of f which provides the best fit of (A-5) to the experimental data. (Details of this procedure can be found in section 3.) The radial line $\theta' = \cos^{-1}(f/2)$ corresponds to the direction of zero momentum and it is assumed that experimental data taken along this line will be applicable to all similar guns. These data form the non-dimensional standard curves given in Fig 13. At other angles these curves are interpreted in terms of the stretched calibre $c'' (= cr_s''/r_s)$ instead of c . For differences in propellant flow and forward speed f is determined from (A-6) and c'' is evaluated from (A-5).

DEVELOPMENT OF A TAPED RANDOM VIBRATION TECHNIQUE
FOR ACCEPTANCE TESTING

by

John Devitt, Richard Pokallus, Joseph Popolo & Eugene Baird
Grumman Aerospace Corporation
Bethpage, New York
11714
U.S.A.

SUMMARY

The use of random vibration as a screen for latent workmanship problems normally found in avionic equipment, has proven to be significantly more effective than the sinusoidal form of excitation normally employed. This has been demonstrated and is now required for acceptance testing by various DoD agencies.

The paper describes the results of a program to develop an economical technique for generating random vibration utilizing an audio tape deck.

The results indicate that compensating factors can be developed to account for the variations that exist in generically identical equipment. Using these factors synthetic random tapes were generated.

BACKGROUND

The benefits of random vibration as a quality screening test for avionics equipment has now been extensively documented and is utilized by most major aerospace manufacturers. Unfortunately, smaller equipment manufacturers and suppliers have been unable or unwilling to implement random vibration screening programs because of the expense of random test equipment. To adapt a sinusoidal vibration system to random capability costs between \$40,000 and \$60,000 today. To help solve this problem, we undertook a program for the Navy to develop an inexpensive method of performing random screening tests using a tape cassette recorder, with the presumption that most small manufacturers already possess electrodynamic shaker systems and sinusoidal vibration control equipment.

A technique was developed to permit manufacturers to safely perform random acceptance tests without the addition of expensive random control equipment and high-skill technicians.

TAPED RANDOM METHOD

The use of a prerecorded random signal on a tape cassette to perform random vibration tests on a routine basis requires that the dynamic characteristics of all the system components, i.e., the tape cassette, tape deck, shaker system, and the test article, remain relatively constant over the long term of the production run. Each of these factors was extensively examined in this study.

Three tape decks were evaluated in the program, all being good quality stereo cassette A.M. recorders and priced in the \$500 range. The tape cassettes were standard low-noise types, recommended by the recorder manufacturer. No problems in the day-to-day operation of the cassette decks were encountered and their frequency response characteristics remained invariant. It should be noted that none of the tape decks tested had completely flat response characteristics over the frequency range of the random test (20 to 2000 Hz). The drop in output at low frequencies (in the range of -4 dB) was compensated during the development of the synthesized random tape.

No significant deviations were noted in the day-to-day characteristics of any of the shaker systems used in the program. However, care must be taken to assure that any variables, such as shaker field current, amplifier plate voltage, etc., are the same for each test run.

The final system component, i.e., the test article, may be different for each run in a production screening program and while production techniques should assure that each product is mechanically identical, minor variations due to manufacturing and assembly tolerances can be expected. How these minor variations will affect the dynamic characteristics of the shaker system is dependent to a great extent on the mass ratio between the test article and the shaker armature and fixture. As would be expected, a 10 oz. realy package fastened to a 60 lb. fixture and armature is not going to significantly affect the acceleration at the package interface with the fixture. In this study, eight different products ranging in weight from 20 to 60 lbs. were evaluated, and the ratio of test article mass to fixture/armature mass was in the range of 1:2. The evaluation was made by comparing the system transfer function ratio E/g (input voltage to the shaker power amplifier ÷ acceleration measured at the control accelerometer) for 1.0 g sinusoidal sweeps on several samples of a particular test article. The results can be summarized as follows:

- (1) Variations in Amplitude
 - o 1 dB in non-resonant frequency ranges
 - o 3 dB at resonance or anti-resonance frequencies
- (2) Variation in Frequency of Resonances and Anti-Resonances
 - o $\pm 3\%$ in range of 20 to 1000 Hz
 - o $\pm 5\%$ in range of 1000 to 2000 Hz

These variations can be compensated for when preparing the random tape by reducing voltage peaks and widening voltage valleys so that the net result to the test article is the desired input.

PREPARING THE RANDOM TAPE

There are two essential elements in the preparation of a random tape:

- (1) The dynamic characteristics of the test system must be analyzed.
- (2) A random noise equalization and analysis system must be used for synthesizing the random spectrum. Since the small manufacturer with limited test equipment cannot readily supply either of these two elements, the procedure was tailored to permit the manufacturer to use an outside facility (major contractor, commercial test lab, or random taping service) to accomplish this task.

The actual implementation of the procedure consists of the following:

- (1) The manufacturer configures his shaker system with the test article installed in the manner used for all production acceptance tests. He then runs a normal servo controlled sine sweep at 1.0 g acceleration while recording (on the tape cassette) the control acceleration and the input voltage to the shaker power amplifier (e.g., the test system signature (See Fig. 1). This tape cassette is then delivered to the outside facility to prepare the random tape.
- (2) The random tape facility plays the manufacturer's tape through a spectral analyzer to determine the system transfer function (See Fig. 2). This transfer function is modified to reflect the required test spectrum (See Fig. 3) and any compensation factors required (i.e., for tape recorder characteristics, variance and non-linearities in the test article) and a synthetic random voltage spectrum is analytically derived (See Fig. 4). This random voltage spectrum is used to generate a random voltage time history which is recorded on the tape cassette. The finished tape cassette is then returned to the test article manufacturer.

TESTING WITH THE RANDOM TAPE

The tape is played directly into the shaker power amplifier with the amplitude adjusted by a simple gain control and the control accelerometer monitored with a true rms meter (See Fig. 5). The simplicity of this system leads naturally to the question of test safety as well as spectrum verification. We will discuss the latter question of spectrum verification first, since it is integrally concerned with test safety.

The lack of a spectrum analyzer by the small manufacturer using the tape makes the verification of the random spectrum impossible to perform directly during the random vibration test. However, before performing the random test, the system transfer characteristics are verified by playing the original system signature sine sweep recording through the test article manufacturer's shaker system. The recorded sine voltage should produce a 1.0 g sine sweep on the shaker system if the sine characteristics are unchanged. The acceleration is monitored on the rms meter and any significant deviations from 1.0 g are noted. The study showed that most of these problems were associated with improper test fixturing and were readily detected during the low level sine sweep. These problems can and must be corrected prior to running the random vibration tests on the production unit.

After verifying the system transfer function, a verification of the actual random acceleration spectrum can be performed if desired. To accomplish this, the output acceleration during the acceptance test on the first test article is recorded on tape. This tape is then sent to a facility having a spectral analyzer, and the result is compared with the desired acceptance test spectrum.

The question of test safety is often brought up when discussing "open-loop" testing such as this tape system employs. "Open-loop" testing refers to the fact that there is no automatic amplitude control of the acceleration level as there is in the conventional "closed-loop" servo system.

It is the authors' conclusion that this "open-loop" system is inherently a safer system for steady-state random tests than most of the "closed-loop" automatic analog random systems in use today. These closed-loop systems typically have 80 individual servo systems automatically adjusting the spectral energy of the shaker. An opening in the feedback loop or a malfunction of any of these servo systems will automatically drive the system output higher in one or all frequency bands until noticed by the operator who then halts the test. With the tape system the operator adjusts the gain only once at the start of the test to the required amplitude. An opening in the accelerometer path will not alter the test level. And since the spectrum shape is prerecorded, no changes in the drive spectrum can occur.

A further benefit of open-loop testing is realized in the case of a structural failure in the test article. In an automatic random system, the servos will automatically adjust the input spectrum to compensate for a change in voltage requirements (such as that caused by the failure of one of the four attachment fasteners of a test article). This often promotes progressive failures because of the servos' blind attempt to maintain the test level. However, with the "open-loop" tape system, the failure of a test article attachment fastener causes a change in the dynamic characteristics of the system, resulting in an abrupt change in the Grms (since the pre-recorded spectrum voltage is improperly shaped for this "three-attachment" configuration). The test operator thus noticing the change can easily shut down the system before any further damage occurs.

CONCLUSIONS

The study program clearly indicates that the tape cassette approach to random vibration screening tests is a viable low-cost alternative to the conventional automatic equalization system approach. It can be readily implemented by any manufacturer with a sinusoidal vibration system to provide true random (Gaussian probability distribution with 30 peaks) test spectrums under controlled tolerances. While there may be complicated test setups and spectrums that do not lend themselves to this method, the authors in their continuing use of the taped random method have not encountered any significant problems with test articles as large as 350 lbs. tested on a 30,000 force-pound shaker system.

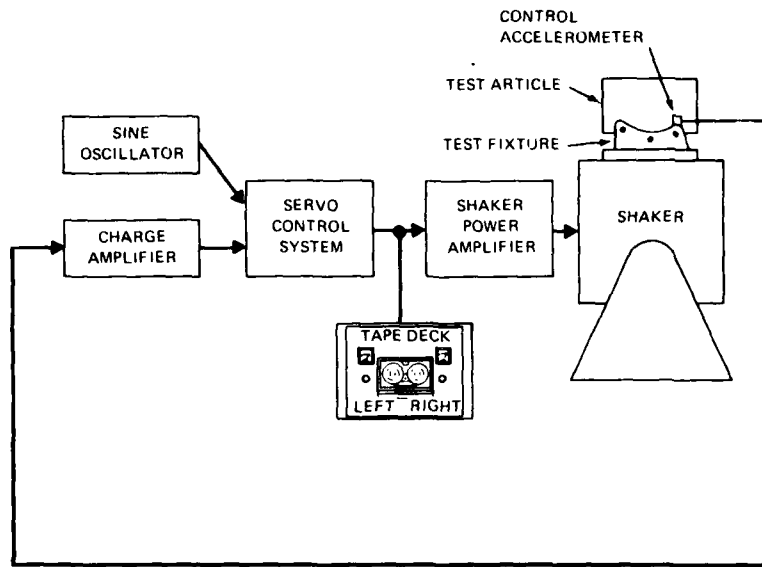


Fig.1 System transfer characteristics determination

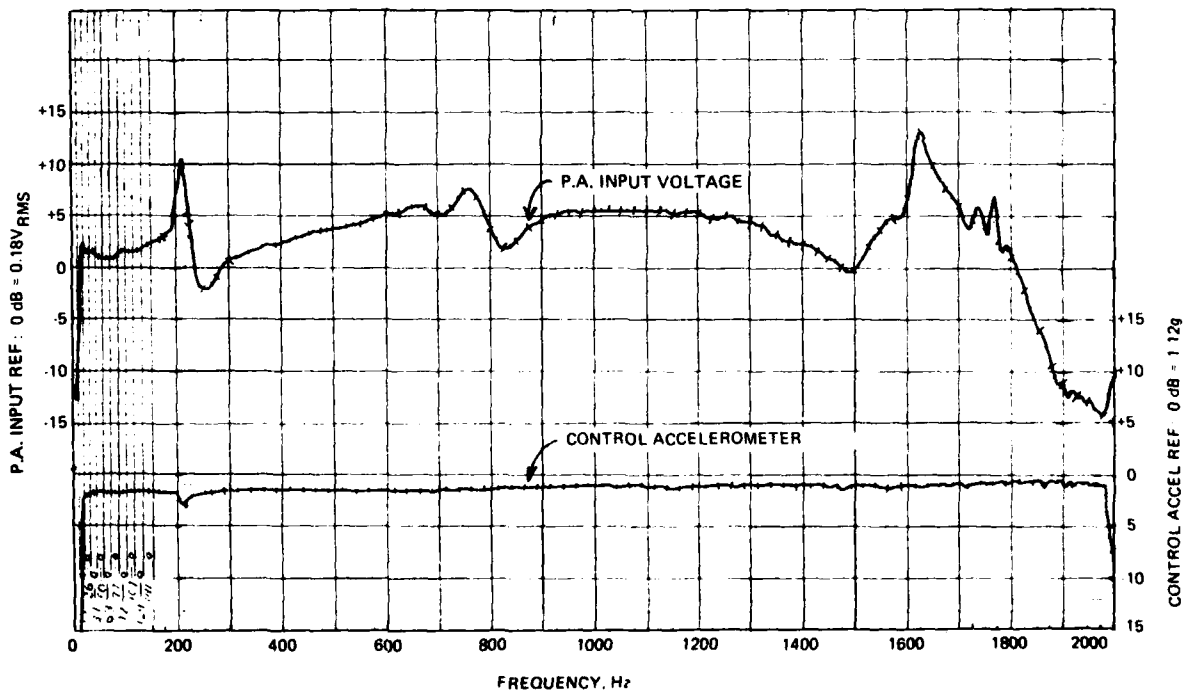


Fig.2 P.A. input voltage and acceleration

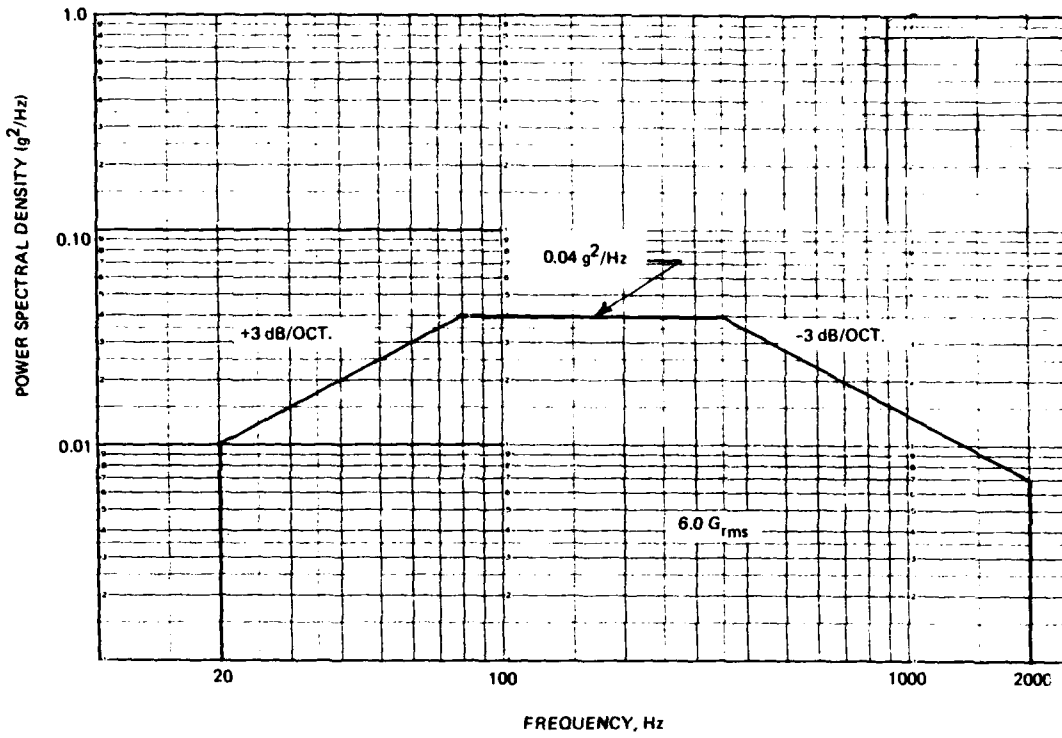


Fig.3 Required random test spectrum

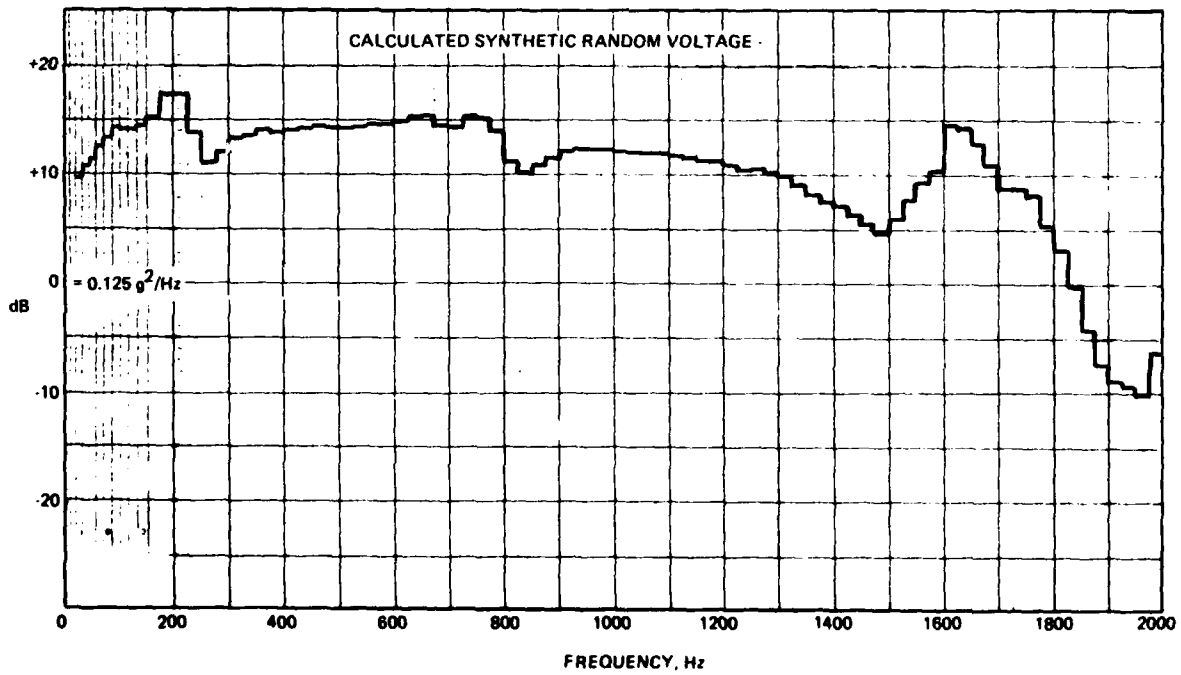


Fig.4 Synthetic random voltage

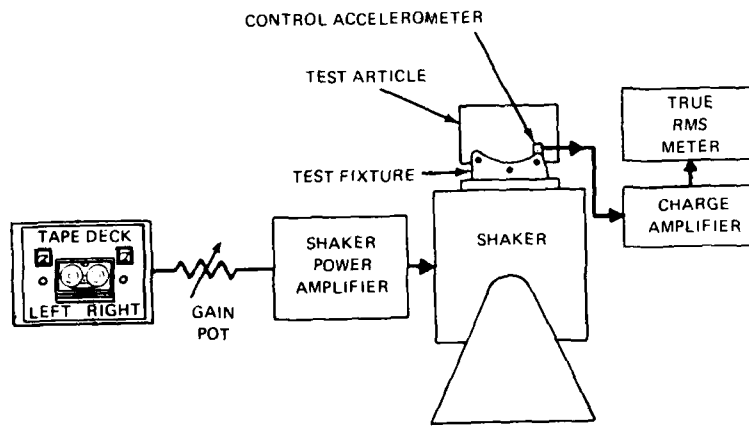


Fig.5 Testing with taped synthetic random

REPORT DOCUMENTATION PAGE											
1. Recipient's Reference	2. Originator's Reference	3. Further Reference	4. Security Classification of Document								
	AGARD-CP-318	ISBN 92-835-0306-6	UNCLASSIFIED								
5. Originator	Advisory Group for Aerospace Research and Development North Atlantic Treaty Organization 7 rue Ancelle, 92200 Neuilly sur Seine, France										
6. Title	DYNAMIC ENVIRONMENTAL QUALIFICATION TECHNIQUES										
7. Presented at	the 53rd Meeting of the AGARD Structures and Materials Panel in Noordwijkerhout, the Netherlands on 27 September-2 October 1981.										
8. Author(s)/Editor(s)	Various		9. Date December 1981								
10. Author's/Editor's Address	Various		11. Pages 254								
12. Distribution Statement	This document is distributed in accordance with AGARD policies and regulations, which are outlined on the Outside Back Covers of all AGARD publications.										
13. Keywords/Descriptors	<table border="0"> <tr> <td>Military aircraft</td> <td>Dynamic structural analysis</td> </tr> <tr> <td>External stores</td> <td>Dynamic tests</td> </tr> <tr> <td>Helicopters</td> <td>Test procedures</td> </tr> <tr> <td>Dynamic response</td> <td>Vibration</td> </tr> </table>			Military aircraft	Dynamic structural analysis	External stores	Dynamic tests	Helicopters	Test procedures	Dynamic response	Vibration
Military aircraft	Dynamic structural analysis										
External stores	Dynamic tests										
Helicopters	Test procedures										
Dynamic response	Vibration										
14. Abstract	<p>The Meeting reviewed the state-of-the-art of dynamic qualification techniques and test methods for military aircraft with external stores, including consideration of the rationale and interpretation of existing standards. The determination of environmental inputs from various sources and their application to specific aircraft and store configurations, including helicopters, was covered. Presentations were also given on the development of vibration analysis techniques and the evaluation of possible improvements in prediction methods and establishment of criteria.</p>										

<p>AGARD Conference Proceedings No.318 Advisory Group for Aerospace Research and Development, NATO DYNAMIC ENVIRONMENTAL QUALIFICATION TECHNIQUES Published December 1981 254 pages</p> <p>The Meeting reviewed the state-of-the-art of dynamic qualification techniques and test methods for military aircraft with external stores, including consideration of the rationale and interpretation of existing standards. The determination of environmental inputs from various sources and their application to specific aircraft and store configurations, including helicopters, was covered. Presentations were also given on the development of</p> <p>P.T.O.</p>	<p>AGARD-CP-318</p> <p>Military aircraft External stores Helicopters Dynamic response Dynamic structural analysis Dynamic tests Test procedures Vibration</p>	<p>AGARD Conference Proceedings No.318 Advisory Group for Aerospace Research and Development, NATO DYNAMIC ENVIRONMENTAL QUALIFICATION TECHNIQUES Published December 1981 254 pages</p> <p>The Meeting reviewed the state-of-the-art of dynamic qualification techniques and test methods for military aircraft with external stores, including consideration of the rationale and interpretation of existing standards. The determination of environmental inputs from various sources and their application to specific aircraft and store configurations, including helicopters, was covered. Presentations were also given on the development of</p> <p>P.T.O.</p>	<p>AGARD-CP-318</p> <p>Military aircraft External stores Helicopters Dynamic response Dynamic structural analysis Dynamic tests Test procedures Vibration</p>
<p>AGARD Conference Proceedings No.318 Advisory Group for Aerospace Research and Development, NATO DYNAMIC ENVIRONMENTAL QUALIFICATION TECHNIQUES Published December 1981 254 pages</p> <p>The Meeting reviewed the state-of-the-art of dynamic qualification techniques and test methods for military aircraft with external stores, including consideration of the rationale and interpretation of existing standards. The determination of environmental inputs from various sources and their application to specific aircraft and store configurations, including helicopters, was covered. Presentations were also given on the development of</p> <p>P.T.O.</p>	<p>AGARD-CP-318</p> <p>Military aircraft External stores Helicopters Dynamic response Dynamic structural analysis Dynamic tests Test procedures Vibration</p>	<p>AGARD Conference Proceedings No.318 Advisory Group for Aerospace Research and Development, NATO DYNAMIC ENVIRONMENTAL QUALIFICATION TECHNIQUES Published December 1981 254 pages</p> <p>The Meeting reviewed the state-of-the-art of dynamic qualification techniques and test methods for military aircraft with external stores, including consideration of the rationale and interpretation of existing standards. The determination of environmental inputs from various sources and their application to specific aircraft and store configurations, including helicopters, was covered. Presentations were also given on the development of</p> <p>P.T.O.</p>	<p>AGARD-CP-318</p> <p>Military aircraft External stores Helicopters Dynamic response Dynamic structural analysis Dynamic tests Test procedures Vibration</p>

<p>vibration analysis techniques and the evaluation of possible improvements in prediction methods and establishment of criteria.</p> <p>Papers presented at the 53rd Meeting of the AGARD Structures and Materials Panel in Noordwijkerhout, the Netherlands on 27 September-2 October 1981.</p> <p>ISBN 92-835-0306-6</p>	<p>vibration analysis techniques and the evaluation of possible improvements in prediction methods and establishment of criteria.</p> <p>Papers presented at the 53rd Meeting of the AGARD Structures and Materials Panel in Noordwijkerhout, the Netherlands on 27 September-2 October 1981.</p> <p>ISBN 92-835-0306-6</p>
<p>vibration analysis techniques and the evaluation of possible improvements in prediction methods and establishment of criteria.</p> <p>Papers presented at the 53rd Meeting of the AGARD Structures and Materials Panel in Noordwijkerhout, the Netherlands on 27 September-2 October 1981.</p> <p>ISBN 92-835-0306-6</p>	<p>vibration analysis techniques and the evaluation of possible improvements in prediction methods and establishment of criteria.</p> <p>Papers presented at the 53rd Meeting of the AGARD Structures and Materials Panel in Noordwijkerhout, the Netherlands on 27 September-2 October 1981.</p> <p>ISBN 92-835-0306-6</p>

DATE
ILME